

UNIVERSITY OF
OXFORD

Development of Small-Molecule P21-Activated Kinase (PAK1) Activator

Management of Heart Failure and Cardiac Hypertrophy

James S.H. Bae



Linacre College

Department of Pharmacology

A thesis submitted to the University of Oxford for the degree of Doctor of Philosophy (D.Phil.)

Trinity Term 2018

Table of Content

Abstract 5

List of Figures 7

List of Tables 12

List of Acronyms 13

Declaration and Copyright 15

CHAPTER 1: INTRODUCTION TO PAK1 DRUG DISCOVERY 17

1.1 Cardiovascular Disease (CVD) 18

1.2 The Burden of Cardiovascular Diseases 20

1.3 Current Treatment of CVDs 22

1.4 Cardiovascular Drug Discovery 25

1.5 P21-Activated Kinase 1 (PAK1) 27

1.6 P21-Activated Kinase 1 (PAK1): Therapeutic Target 30

1.7 PAK1: Overview Structure 34

1.7.1 PAK1 Auto-Inhibitory Domain (AID) 35

1.7.2 PAK1-CDC42 Interactions 37

1.7.3 PAK1 Kinase Domain (KD) 38

1.7.4 PAK1 Protein Binding Motifs 40

1.8 Development of PAK1 Activators 43

1.8.1 Sphingosine-1-phsophate & FTY720 (Fingolimod) 43

1.8.2 PAK1 Activating Peptide (PAP) 47

1.9 Aim of Thesis: Small-molecule PAK1 Activator 50

CHAPTER 2: *IN SILICO* DRUG DISCOVERY: PAK1 ACTIVATORS.....52

2.1 Background Overview.....53

2.2 Structural Based Virtual Ligand Screening (SBVLS).....56

2.3 Discovery of PAK1 Activator: Virtual Ligand Screening Overview.....59

2.4 In-silico Program: ICM-Pro VLS, Molsoft.....61

2.4.1 ICM-Pro VLS: PAK1 Receptor Preparation.....62

2.4.2 ICM-VLS Pro: Virtual Ligand Screening.....65

2.5 Secondary Screening: AutoDock Vina.....68

2.6 Hit Validation: Discovery of JB01.....73

2.7 Summary & Concluding Remarks.....76

CHAPTER 3: VALIDATION OF PAK1 ACTIVATORS.....78

3.1 Background Overview.....79

3.2 Physiochemical Guideline.....82

3.3 Optimization of JB compounds: in silico.....83

3.4 In silico optimization: Mcule.com.....86

3.5 Optimization of JB compounds: in vitro, ADP-GLO™ Kinase Assay.....88

3.6 Optimization of JB compounds: Rapid-Fire™ Mass-Spectrometer Kinase Assay.....95

3.6.1 Rapid-Fire™ Mass-Spectrometer Kinase Assay Methods.....97

3.6.2 Rapid-Fire™ Mass-Spectrometer Kinase Assay: JB01 Validation.....99

3.6.3 Rapid-Fire™ Mass-Spectrometer Kinase Assay: JB Compounds.....102

3.7 Summary & Concluding Remarks.....108

CHAPTER 4: CLINICAL TRANSLATION - PAK1 ACTIVATORS.....110

4.1 Background Overview.....111

4.2 Anti-arrhythmic effect of JB79 on ISO-induced adult cardiomyocytes.....113

4.3 Anti-arrhythmic effect of JB79 on Induced Pluripotent Stem Cells (IPSC).....116

4.4 Ex-Vivo Heart: Anti-arrhythmic effect of JB79 on PES-induced arrhythmia 118

4.5 Ex-Vivo Heart: Anti-hypertrophic effect of JB79 on TAC-induced Cardiac Hypertrophy 122

4.6 Potential Roles of PAK1 in Cancer 125

4.7 Effects of JB79 on human umbilical vein endothelial cells (HUVECs) 129

4.8 Effects of JB79 on Malignant Cancer Cells: HOP-92 & MDA-MB-231 133

4.8.1 Effects of JB79 on Cancer Cells: Resazurin Proliferation Assay 133

4.8.2 Effects of JB79 on Cancer Cells: Spheroids invasion assay in 3D collagen matrix 135

4.8.3 Effects of JB79 on Cancer Cells: Wound Healing Scratch Essay 136

4.8.4 Effects of JB79 on Cancer Cells: Boyden Chamber Invasion Essay 138

4.9 Summary & Concluding Remarks 140

CHAPTER 5: MOLECULAR INSIGHT INTO PAK1 ACTIVATORS 143

5.1 Background Overview 144

5.2 PAK1 activators: binding at the Auto-inhibitory domain 145

5.3 Characterization and comparative analysis of fragment-based binding 151

5.4 Mechanism of inhibitory effect of PAK1 Activators at high concentrations 157

5.4.1 Mechanism of inhibition: Non-specific binding at the kinase domain 158

5.4.2 Mechanism of inhibition: Covalent modifications 159

5.4.3 Mechanism of Inhibition: Compound Coagulations 165

5.5 Co-crystallography: Understanding the activate site of PAK1 activators 169

5.6 Summary & Concluding Remarks 177

CHATER 6: MECHANISM ACTION OF PAK1 ACTIVATORS 179

6.2 Background Overview 180

6.2 Optimization of JB compounds 182

6.3 Ligand Binding Study: Photoaffinity Labeling (PAL) – MS 191

6.4 Co-crystallography: Process update 203

6.5 Catecholaminergic polymorphic ventricular tachycardia (CPVT) 208

6.6 Summary & Concluding Remarks 213

CHAPTER 7: FUTURE STUDIES AND CONCLUSIONS 216

7.1 Additional Functional Studies for Clinical Indication 217

7.2 PAK1 Molecular Signaling Map 218

7.3 Ligand expansion search for small molecule PAK1 activators 219

7.4. X-ray Co-crystallography 221

7.5. IS: another potential allosteric site for PAK1 activators 223

7.6 Conclusions 225

REFERENCE 228

APPENDIX 241

Appendix 1. Experimental Methods 242

Appendix 2. *In silico* Virtual Ligand Screening Software 250

Appendix 3. JB Compounds Overview 253

Appendix 4. Physiochemical Properties & Efficacies of JB Compounds 261

Appendix 5. PAK1 Co-Crystallgraphy Report (prepared by Proteros) 307

Abstract

P21-activated kinase (PAK1), a serine/threonine protein kinase, has significant homeostatic functions in the myocardium. PAK1's activation of protective signaling in cardiac pathways has been reported to modulate cardiac hypertrophy and associated ventricular arrhythmias. Clinical significance of PAK1 has been emphasized by the growing evidence on the protective role of PAK in the myocardium, which offers important implications for therapeutic targeting. Based on this evidence, we designed the PAK1-activating peptide (PAP) to establish whether disrupting the auto-inhibitory domain (AID) of PAK1 would stimulate PAK1's activation through preventing the inhibitory mechanism. The results showed that PAP both considerably stimulated PAK1 activation and had an anti-hypertrophic effect in cardiomyocytes, proving to be a viable method of regulating PAK1 activation with important therapeutic benefits.

For clinical translation, the PAK1-activating peptide was successfully redesigned into a small-molecule PAK1 activator that can directly stimulate PAK1 activity. Computational *in silico* methods were used to perform virtual ligand screening in the AID of PAK1. Compounds with high negative energy scores were synthesized, and their efficacy in PAK1 activation was tested using *in vitro* kinase assays. To acquire an in-depth understanding of the active site, we used the structure-based drug discovery for drug optimization. Such detailed understanding of the active site would be necessary to comprehensively understand the protein-ligand interactions and to design novel ligands with improved selectivity, efficacy, and physiochemical profiles. The lead compounds showed a 3-fold stimulatory effect on PAK1 with significantly enhanced physiochemical properties.

The interaction between protein-ligands was also biophysically examined using photoaffinity labelling coupled with mass spectrometry (PAL-MS). Based on the results, we identified that the compounds were binding at the interface between the kinase inhibitory segment of AID and the kinase domain, i.e. the domain where the interaction is crucial for kinase activity regulation. Such mechanisms of kinase activation have not been demonstrated in previous research. Furthermore, along with discovering small molecules with significant stimulatory effects on the kinase activity, the present study is the first to demonstrate that enzymatic regulation can be achieved through hindering the inhibitory mechanism of enzymes. In future

research, these mechanisms of action can be applied to other drug discoveries, which can then be used as a footprint to design other kinase activators. In addition, previous therapeutic targets regulating beneficiary signaling pathways can now be targeted for drug discovery and activated to confer clinical elevation in various pathological conditions.

In order to gain further insight into the physiological effect of PAK1 activation, selected lead compounds were tested in functional studies. First, the results of immunohistochemical staining in isolated cardiomyocytes of PAK1 activator revealed a significant increase in fluorescence, indicating an increased PAK1 activation (phospho-PAK1). Second, a rapid perfusion of JB compound on isolated ventricular myocytes was found to have an antagonizing effect on isoprenaline-induced hypertrophy and arrhythmia. Third, the results of examining JB79's cardio-protective effect against programmed electrical stimulation (PES)-induced arrhythmia in an *ex vivo* whole heart model, with the specific focus on PVC and VF, showed that a sufficient activation of PAK1 signaling at the concentration of 10mg/kg considerably increased the voltage tolerance for PES-induced VF and PVC, thereby reducing the incidence of cardiac arrhythmia. These results were further supported by our findings on PAK1 activators' effect on the catecholaminergic polymorphic ventricular tachycardia (CPVT). After 25-minute PAK1 activator treatment, the damaged heart from isoprenaline-induced fibrillation and arrhythmia exhibited a significant overall improvement in contractility. Finally, the results of our functional study on the TAC-induced cardiac hypertrophy model demonstrated that prolonged treatment of PAK1 activator also provides significant protection against pressured overload cardiac myopathy. Taken together, the results of the present study demonstrate that PAK1 activators are a potential novel therapeutic strategy for both prophylactic and therapeutic measures involving cardiac hypertrophy and arrhythmia.

List of Figures

CHAPTER 1: INTRODUCTION TO PAK1 DRUG DISCOVERY 17

Figure 1.1.1 Progress of cardiovascular disease development.....19

Figure 1.5.1 Distribution of PAK1 in hearts.....28

Figure 1.5.2 Representation of PAK1 cardiac signaling pathway.....30

Figure 1.6.1 Electrophysiological studies between PAK1 and $PAK1^{cko}$ 32

Figure 1.6.2 $PAK1^{cko}$ gross heart anatomy and histology comparison to WT 33

Figure 1.6.3 Transverse Aortic Constriction (TAC) on $Pak1^{CKO}$ mice 34

Figure 1.7.1 Diagram representation of a PAK1 structure.....35

Figure 1.7.2 Comparison between PAK1 KD (inactive) vs. PAK1 KD (active).....37

Figure 1.7.3 Interaction site between CDC42 and PAK1 38

Figure 1.7.4 Structure of PAK1 Kinase Domain.....39

Figure 1.7.5 ATP Binding of PAK1 Kinase Domain 40

Figure 1.8.1 Effects of Sphingosine on PAK1.....44

Figure 1.8.2 Effect of FTY720 on PAK1 activation 46

Figure 1.8.3 *In silico* prediction of PAK1 activating biopeptides (PAPs) on PAK1 48

Figure 1.8.4 PAP attenuates stress-induced hypertrophy and fibrosis 49

CHAPTER 2: *IN SILICO* DRUG DISCOVERY: PAK1 ACTIVATORS.....52

Figure 2.1 Summary of Virtual Ligand Screening (VLS) Strategies.....55

Figure 2.2 Schematic of PAK1: functional domains and auto-phosphorylation sites.....57

Figure 2.3 Diagram representation of PAK1 structure.....59

Figure 2.4.1 PAK1 (PBD: 1F3M) setup for Virtual Ligand Screening (VLS).....63

Figure 2.4.2 VLS protein pocket set-up 64

Figure 2.4.3 *In silico* ligand screening at the PAK1 auto-inhibitory (AI) domain....66

Figure 2.4.4 ICM-VLS Pro Chemical Property Monitor....68

Figure 2.5.1 PAK1 receptor set-up for AutoDock Vina using MGL-Tools 70

Figure 2.5.2 Command prompt view of the Autodock Vina program 71

Figure 2.5.3 The crystal structure of PAK1 using MGL Tools 72

Figure 2.6.1 Overview of PAK1 activator in silico screening filteration....73

Figure 2.6.2 Dose response curve of JB01 on PAK1 activation 74

Figure 2.6.3 Physiochemical Properties of JB01 75

CHAPTER 3: VALIDATION OF PAK1 ACTIVATORS 78

Figure 3.1 Key propertis relevant for rational drug discovery....79

Figure 3.3.1 JB01 Chemical Properties....84

Figure 3.4.1 Chemical availability using Mcule.com....86

Figure 3.4.2 Similar compound screening using Mcule.com....87

Figure 3.5 The dose-response curve of JB compounds on PAK1 activation 91

Figure 3.6.1 RF-MS result integration analysis....96

Figure 3.6.2 RF-MS Kinase Assay: Staurosporine inhibits PAK1 activity....97

Figure 3.6.3 RF-MS Kinase Assay: CDC42 stimulates PAK1 activity....98

Figure 3.6.4 Rapid-Fire mass spectrometry PAK1/CDC42 kinase assay 100

Figure 3.6.5 Effect of JB compound actvation on PAK1/CDC42 105

CHAPTER 4: CLINICAL TRANSLATION - PAK1 ACTIVATORS 110

Figure 4.2 Calcium transient recording of cardiomyocte 114

Figure 4.3 Representative Ca2+ transients recorded from human iPSCs showing the effects of 100nM isoprenaline and 20μM JB79....117

Figure 4.4.1 Electrocardiography under PES with different indications of arrhythmia .119

Figure 4.4.2 Effect of JB79 on the VF voltage threshold 120

Figure 4.5.1 Transverse Aortic Constriction (TAC) on mice heart 122

Figure 4.5.2 Effect of JB79 on TAC-induced hypertrophy.....123

Figure 4.6 Regulation of cancer cels: main cell signaling pathways 128

Figure 4.7.1 Dose response test of JB79 on HUVEC proliferation effect.....129

Figure 4.7.2 Effect of JB79 20uM on the motility of HUVECs.....130

Figure 4.7.3 Effect of JB79 20uM on the actin organization on HUVECs.....131

Figure 4.8.1 Resazurin assay results of HOP-92 & MDA-MB-231 (JB79 treatment) 134

Figure 4.8.2 3D Tumor Spheroid Invasion Assay results of HOP-92 & MDA-MB-231 (JB79 treatment) 135

Figure 4.8.3 Effect of JB79 on cancer cell migration 137

Figure 4.8.4 Effect of JB79 on cancer cell membrane invasive properties.....138

CHAPTER 5: MOLECULAR INSIGHT INTO PAK1 ACTIVATORS 143

Figure 5.2.1 Comparative kinase activities using RF-MS Kinase assay 148

Figure 5.2.2 Comparative kinase activities under different modulators 149

Figure 5.3.1 Time Dependent Kinase assay on JB01, JB79 and JB81 152

Figure 5.3.2 General compound formular for PAK1 activator 153

Figure 5.3.3 Fragment Drug Discovery 154

Figure 5.3.4 Dose-response curve of JB99 & JB100 on PAK1 activation.....154

Figure 5.3.5 Time Dependent RF-MS Kinase assay on JB79 Fragments 155

Figure 5.4.1 Inhibitory effect of JB53 & JB120 at high concentration 157

Figure 5.4.2 Covalent modification of JB08 and JB79 on PAK1 160

Figure 5.4.3 Covalent modification of JB08 and JB79 on PAK1 (Presence of CDC42).163

Figure 5.4.4 MS results of JB106 overnight incubation 165

Figure 5.4.5 Chemical breakdown of JB106 compound 166

Figure 5.4.6 Mechanism of intramolecular coagulation 167

Figure 5.5.1 Westernblot results of purified PAK1 for crystsallography 172

Figure 5.5.2 Crystallography structure of PAK1 174

Figure 5.5.3 Observed difference in density in PAK1 Co-Crystallography 176

CHATER 6: MECHANISM ACTION OF PAK1 ACTIVATORS 179

Figure 6.2.1 Comparative analysis of MW vs cLogD, PSA, and PAINS 183

Figure 6.2.2 PAINS and Micheal acceptors in JB compounds 184

Figure 6.2.3 Structure activity relationship (SAR) of JB79 and its analogs 186

Figure 6.2.4 Structure activity relationship (SAR) of JB79 compound Overview 188

Figure 6.2.5 Effects of core group changes on PAK1 activators 190

Figure 6.2.6 Optimization results of JB79 191

Figure 6.3.1 Photoaffinity labelling ligands of JB120 193

Figure 6.3.2 DRT on PAK1 activity by PAL probes 194

Figure 6.3.3 PAL-MS workflow using JB122 196

Figure 6.3.4 Analysis of PAL-MS peptide with JB122 197

Figure 6.3.5 Analysis of PAL-MS peptide with JB122 and CDC42 198

Figure 6.3.6 Overview map of PAL bound peptides 200

Figure 6.3.7 Proposing mechanisms of JB compound's PAK1 activation 202

Figure 6.4.1 DRT of PAL probes on PAK1 (Proteros) 204

Figure 6.4.2 DRT of PAL probes on PAK1 (Oxford University) 204

Figure 6.4.3 Validation of FL-PAK1(Evotec): CDC42 and JB compound 207

Figure 6.5.1 Electrocardiography of ex vivo CVPT heart recording 209

Figure 6.5.2 ECG of ex vivo CVPT heart recording (JB131 Treatment) 211

CHAPTER 7: FUTURE STUDIES AND CONCLUSIONS 216

Figure 7.3.1 Activation-inhibition pattern found in kinase activation by sphingosine ...220

Figure 7.4.1 DLS analysis of FL-PAK1 (Evotec) and PAK1 Δ-70 PAK1 (OU).....221

Figure 7.4.2 Proposing PAK1 construct for co-crystallography 222

List of Tables

Table 1.2 Number of deaths related to cardiovascular disease in UK.....21

Table 1.7 Mutagenesis studies of PAK1.....41

Table 2.2 Drugs derived from structure-based approaches.....58

Table 2.3 List of docking software for *in silico* studies.....61

Table 3.2 Lipinski's Rule of Five and its extensions.....82

Table 4.6 Development of PAK1 inhibitors by various pharmaceutical companies.....127

Table 5.1 Examples of catecholamine receptor agonists and antagonists.....145

List of Acronyms

AKT	Protein kinase B (PKB)
ADP	Adenosine diphosphate
AID	Auto inhibitory domain
ATP	Adenosine triphosphate
BAD	Bcl-2-associated death promoter
BSA	Bovine serum albumin
CA-PAK1	Constitutively-active PAK1
CaMKII	Calcium calmodulin-dependent protein kinase II
cAMP	Cyclic adenosine monophosphate
CDC42	Cell division control protein 42
CF_3	Trifluoromethyl
CTN1	Cardiac troponin
cTnC	Cardiac calcium binding troponin C
CVD	Cardiovascular disease
DAD	Delayed after depolarization
EAD	Early after depolarization
EC_{50}	Effective concentration at 50% response
ECM	Extracellular matrix
eNOs	Endothelial nitric-oxide synthase
ERK	Extracellular signal-regulated kinase
FITC	Fluorescein isothiocyanate
FR18024	ERK1/2 selective inhibitor
FTY720	2-amino-2-[2-(4-octylphenyl)ethyl]propane- 1,3-diolhydrochloride
GPCR	G-Protein coupled receptor
GRB2	Growth factor receptor-bound protein 2
GTP	Guanosine 5'-triphosphates
HIV	Human immunodeficiency virus
HPLC	High performance liquid chromatography
I/R Injury	Ischemia/reperfusion Injury
IC_{50}	Concentration giving half-maximal inhibition
IPA3	1,1'-Dithiodi-2-naphthtol
IPSC	Induced peripotent Stem cells
ISO	Isoprenaline
JNK	c-Jun N-terminal kinases
KI	Kinase inhibitory
LB-CADD	Ligand-based computer-aided drug discovery
LTCC	L-type calcium channel

MALDI	Matrix-assisted laser desorption/ionization
MAP	Monophasic action potential
MAP2K1	Mitogen-activated protein kinase
MKK4	Mitogen-activated protein kinase kinase
MLCK	Myosin light chain kinase
mTOR	Mammalian target of rapamycin
MYBP-C	Myosin-binding protein C
NRVM	Neonatal rat ventricular myocytes
PAK1	P21-activated kinase
$PAK1^{CKO}$	PAK1 knock-out mice
PAP	P21 activating peptide
PAL	Photoaffinity labeling
PES	Programmed electrical stimulation
PI3K	Phosphatidylinositol 3-kinase
PIX	PAK interacting exchange factor
PKC	Protein kinase C
PLN	Phospholamban
PP1	Protein phosphatase 1
PP2A	Protein phosphate 2
RAC	Rho family of GTPases
RAC1	Ras-related C3 botulinum toxin substrate
RLU	Relative luminescence unit
RF-MS	Rapid-Fire™ Mass-Spectrometer
Roc1	Ring box protein 1
RTK	Receptor tyrosine kinase
RyR	Ryanodine receptor
S.E.M	Standard error of the mean
S1P	Sphingosine-1-phosphate
$S1PR_{(1-3)}$	Sphingosine-1-phosphate receptors (1-3)
SAN	Sino-atrial node
SERCA2a	Sarcoplasmic reticulum calcium ATPase 2a
SphK	Sphingosine kinase 1
SAR	Structure-Activity Relationship
SR	Sarcoplasmic reticulum
TAC	Transverse aortic constriction
TAT	Trans-activator of transcription
TGFβ	Transforming growth factor β
Tris	Tris(hydroxymethyl)aminomethane
V_{max}	Maximum velocity
WT	Wild type

Declaration and Copyright

I confirm that all the research and findings presented in this thesis are my own work unless otherwise indicated through the use of a clear referencing system. The author of this thesis (including any appendices and/or schedules to this thesis) owns any copyright in it. He has given the University of Oxford the rights to use Copyright for any administrative, promotional, educational and/or teaching purposes. The ownership of any patents, designs, trademarks, and any other intellectual property rights except for the copyright and any reproductions of copyright works, for example graphs and tables, which may be described in this thesis, may not be owned by the author and may be owned by third parties. Such intellectual property rights and reproductions cannot and must not be made available for use without prior written permission of the owner of the relevant intellectual property rights.

CHAPTER 1

INTRODUCTION TO PAK1 DRUG DISCOVERY

Summary Points

- Cardiovascular diseases (CVDs) are the world's leading cause of death. The burden of CVDs persists as a global challenge and raises concern for the public health.
- Despite increasing research funds on the drug discovery field, the rate of approval for new cardiovascular drug therapies have significantly declined. The lack of novel therapeutics as an effective treatment for CVDs brings about doubt for prospective CVD treatments.
- Recent findings on PAK1's roles in the myocardium demonstrate the gene to be essential in maintaining cardioprotective mechanisms, as well as in regulating cardiac signal pathways for homeostasis.
- Dysregulations in PAK1's activity have been implicated in various physiological and pathological conditions, suggesting it to be a strong therapeutic target for novel drug therapy.
- The detailed accounts of PAK1's structure, as well as its mechanism of activation, provide to be valuable information in facilitating PAK1 drug discovery.
- PAK1 activating Peptide (PAP), containing complementary sequence, was designed in order to demonstrate whether the disruption at the PAK1 dimerization would induce stimulation.
- Having verified significant activation of PAK1 through PAP, we concluded that a small molecule could also potentially stimulate PAK1 through disrupting its inhibitory mechanism.

1.1 Cardiovascular Disease (CVD)

Cardiovascular disease (CVD) is a class of disease characterized by abnormalities within the heart and vascular circulations. It is a progressive condition that consist of multiple stages of disease classifications, often termed: "Stages of Heart Failure".

In the early phase of cardiovascular complications, before any physiological or morphological changes occur inside the myocardium, high heart rate and blood pressure are often indicative of the disease's pathological initiation. Causal factors of these symptoms arise from a variety of areas, including genetic, epigenetic, lifestyle, and hormonal dysregulation. Chronically raised blood pressure (hypertension) or frequently increased heart rate are the most prominent risk factors that lead to an adaptive response of hypertrophic growth. This adaptive response may further develop into cardiac hypertrophy (CH). Subsequently, the deterioration of endothelial functions and build-up of cholesterol-containing deposits, lipids, and platelets (known as cholesterol plaques) can narrow the coronary artery and thereby reduce blood flow to the cardiac tissues, limiting the delivery of nutrients and oxygen. If left untreated, this can bring about blockages of coronary arteries (coronary artery disease, CAD) and thrombosis. Acute thrombosis most often occurs due to the rupture of coronary artery atherosclerotic plaque, leading to ischemic heart damage and myocardial infarctions. Complications of ischemic heart disease manifestations include ventricular arrhythmia and post-infraction fibrinous pericarditis, where the myocardium loses its ability to contract properly (Ajijola and Shivkumur, 2013).

Eventually, the disease can progress to later stages of heart failure – including cardiac remolding and ventricular dilations. Cardiac pump dysfunction, congestion/low perfusion, and low inotropic contraction may proceed to end-stage heart failure where the heart functions become significantly compromised and the organ is unable to pump efficiently enough to support blood flow. End-stage heart failure patients are reported with the highest mortality rate; 38% of patients will die within the first year of diagnosis of heart failure, while another 60% will die within five years (Scarabelli et al., 2015).

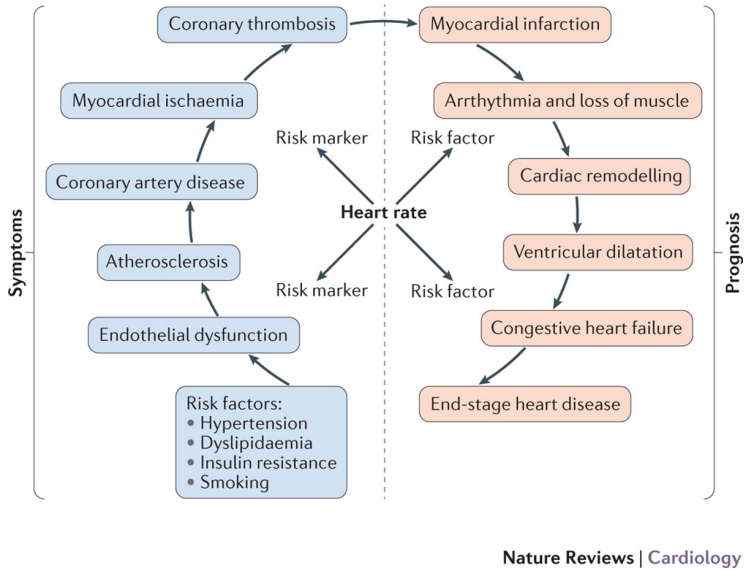

Figure 1.1.1 *Progress of cardiovascular disease development.* Excessive exposure to various risk factors/unhealthy lifestyles can lead to damages in myocardium and can deviate from the optimal cardiac functions. Chronic cardiac hypertrophy along with atherosclerosis can induce cardiac ischemia and myocardial infraction. If left untreated, loss of muscle and disruption of cardiac contraction rhythms (arrythmias) can lead to cardiac remodelling and heart failures – end stage heart disease. (Figure derived from Ferrari and Fox, 2016).

Extensive studies have indicated a strong association between various, distinct pathologies and those of cardiovascular diseases. Diabetics, hypercholesterolemia, hypertension in pregnancy, rheumatoid arthritis, air pollution, and low social economic status (SES) are only a few examples suggesting a substantial linkage with increased prevalence of CVDs (Navab et al., 2011, Clark et al., 2009, Baccarelli and Gosh, 2013) Genetic, ethnicity, and familial factors also play into the predisposition to CVDs. For instance, genome-wide association studies (GWAS) have indicated numerous gene variants loci that are strongly associated with CVDs. Amongst the many, CDKN2B-AS1 loci have scored the highest in its association with high blood pressure in multiple studies (Shunkert et al., 2011; Lu et al., 2012; Nikpay et al., 2015; Nelson et al., 2017). Environmental factors have also been highlighted to have strong associations in contributing to cardiovascular complications (Napoli, 2011; Chang and Bruneau, 2012; Sun et al., 2013). Other risks factors such as unhealthy lifestyles (e.g. ill dietary habits such as high cholesterol; tobacco; and poor physical activity) have now been well documented to be strong causal factors that accelerate disease development (Ross R, 1999; Steinberg, 2005; Blumenthal et al., 1989; Kramsch et al., 1981; Rao et al., 1998; Nuslund et al., 1996). These numerous physiological symptomatic risk factors, along with the varying disease stages, further the

difficulty in elucidating the CVDs development and its pathophysiological progress. Developing an effective treatment for CVDs would therefore require an extensive understanding of the disease and consideration of the treatment from inter-disciplinary perspectives (holistic manner), while examining one's behavioral and lifestyle changes.

1.2 The Burden of Cardiovascular Diseases

Cardiovascular complications have been the single leading cause of death worldwide - predicted to rise to 23.3 million deaths by 2030 (WHO. Int, 2015). The estimated death from cardiovascular diseases (CVDs) in 2015 was 17.7 million, accounting to 31% of all global death (WHO., 2017). The two most predominant diseases are coronary heart disease (7.4 million deaths) and stroke (6.7 million deaths) (WHO., 2017). From 1990 to 2010, the age-standardized death rate from CVDs have continuously decreased, yet this progress has slowed over the years. In 1990, there were about 393 deaths for every 100,000 people from CVD globally. However, over the next five years, we observed only a slight decrease to 286 deaths per 100,000, despite vast progress in various diagnostics modalities, as well as surgical and therapeutic interventions (American College of Cardiology, 2017). Furthermore, such a decrease in CVDs mortality trend is predominantly found in high income countries. Countries with low or middle incomes are exhibiting a rising tide of CVDs and other non-communicable diseases (Flaherty et al., 2013). As of today, the disease still prevails as the number one killer in the world (Roth et al., 2015). It is therefore demanded with great urgency that innovative and effective measurements for managing CVDs – whilst maintaining low-cost – are developed.

In the United Kingdom (UK), CVD remains to be a substantial burden, both in terms of health and economic costs. As observed from the health surveys of England and Scotland 2003-2013, there is a growing prevalence of CVD, coronary heart disease, and stroke – demonstrating them to be the second leading cause of death in the UK (Bhatnager et al., 2016). According to the Cardiovascular Disease Statistics 2018 report, cardiovascular diseases present a significant burden in the UK – contributing to be the cause for 26% of the deaths (BHF-UK, 2018), which is an estimated 150,000 deaths each year. Currently, 7 million people are living with

cardiovascular diseases in the UK, yet with an aging, growing population, these numbers are expected to increase over the years. Among deaths from cardiovascular causes, hypertrophy and cardiac arrhythmias account for more than half, associated with important morbidity and mortality related to stroke, ischemia, embolism, and heart failure (Jackson et al., 2015). Coronary heart disease is the most common type of CVD, currently affecting 2.3 million people and is responsible for over 66,000 deaths annually in the UK (NHS prevalence data, 2017). In between 2012 and 2013, more than 1.6 million patients have been diagnosed with episodes of cardiovascular related diseases in NHS hospitals. This was translated to be about £9 billion spending on CVD treatment alone (Bhatnagar et al., 2015).

Nation	Number of people dying from CVD	Number of people (<75 years old) dying from CVD	Estimating number of people living with CVD
England	124,615	33,812	5.9 million
Scotland	15,131	4,644	685,000
Wales	8,655	2,495	375,000
N. Ireland	3,629	1,070	225,000
United Kingdom	152,465	42,311	7 million+

Deaths BHF/University of Birmingham analysis from latest official statistics (ONS/NISRA/NRS)

Table 1.2 Number of deaths related to cardiovascular disease in UK. The number of deaths from heart and circulatory disease and the number of people living with heart and circulatory disease across the UK.

Susceptibility to CVDs are generally due to a combination of several risk factors, including detrimental medical factors and harmful lifestyles. Medical risk factors such as hypertension is shown to increase the risk of developing CVDs by three times, and nearly 30% of adults in the UK are currently affected by the disease (Heart UK, 2019). Other risk factors such as high blood cholesterol and diabetes are also reported to have a significant impact in the risk of CVD; nearly observing a 2-fold increase in potentially developing a CVD if complicated with Type II diabetes (British Heart Foundation, 2018). An unhealthy lifestyle – including alcohol, smoking, or inactivity - may also considerably increase the risk of CVD. Alcohol consumption in moderate amount has been shown to have a cardio protective effect (Ronksely et al. 2011), however irregular heavy drinking showed a significant rise in the risk of ischemic heart disease

by 154% (Roerecke and Rehm, 2009). Furthermore, 30% of all annual deaths caused by coronary heart disease (CHD) in the United States are attributable to cigarette smoking, with the risk being strongly dose-related (Ockene and Miller, 1997). About 39% of UK adults are failing to meet government-recommended amount of physical activity, estimating around 11.8 million women and 8.3 million men being inadequately active (British Heart Foundation, 2017). Considering these aspects, strategic approaches in managing behavioural and lifestyle risk factors – in addition to medical interventions - are imperative to prevent CVDs.

1.3 Current Treatment of CVDs

Between 1991 and 2014, the number of prescriptions for diseases of the circulatory system increased by around 243 million or 78% in England (CPRD GOLD database, 2014). Current standard pharmacological intervention for treating CVDs can vary from one to another, and the vast number of disease subtypes adds further levels of complexity that cannot be all described in this literature review. Only the CVDs that are of relevance to the thesis topic (PAK1 drug discovery) are selected, with their pharmacological interventions highlighted as follows:

Cardiac hypertrophy (CH) is an adaptive response to increases in either acute or chronic biomechanical stress. These include pressure overload, increased volume stress, mutations of sarcomeric proteins (genetic disorder such as hypertrophic cardiomyopathy), aortic valve stenosis, or dysfunctional ion channels – all of which are essential in maintaining cardiac contractility. The stress mechanism causes the heart to undergo hypertrophic growth to normalize ventricular wall stress. However, continuous response to these detrimental stimuli will eventually cause decompensated remodeling such as chamber dilation, reduced contractile function, interstitial fibrosis, myocyte loss, and subsequent heart failure – eventually leading to cardiac hypertrophy (Ke et al. 2012). The defining features of hypertrophy are an increase in cardiomyocyte size, enhance protein synthesis, and higher organization of sarcomere (Frey and Olson, 2003). Unfortunately, CH remodelling is considered to be irreversible, and most current therapeutic methods are only involved in managing the symptoms. These methods include

ACE inhibitors, ARBs, calcium channel blockers, diuretics, and beta blockers - of which are mainly targeted to maintain optimal blood pressure and thereby reduce stress. As CH is considered a hallmark of heart failure, drugs that can provide prophylaxis measurement against CH progression are highly sought for in clinical settings. Given the multitude of redundant signaling pathways capable of promoting pathological cardiac hypertrophy, it is hypothesized that increased efficacy can be obtained with therapies that target long-term suppression of cardiac hypertrophy. In effort to develop these therapeutic interventions, novel small molecule drugs inhibiting CH are currently being studied. Recently, Reid and his colleagues have screened 3,241 distinct small molecules – of those considered as either non-toxic or pre-existing as approved drugs – to evaluate their effects on cardiovascular diseases (Reid et al., 2016). Amongst these compounds, artesunate (anti-malaria drug) was shown to block left ventricular hypertrophy (LVH) and improve cardiac function on TAC-induced mice heart (Reid et al., 2016). Whether such screening methods will allow us to find another potential therapeutic intervention for CH still remains to be seen.

Coronary artery disease (CAD) arises from a lack of blood supply to the heart (ischemia) due to atherosclerosis lesions that forms asymmetric focal thickening of the artery. As a consequence of this blood supply blockage, it may cause abnormal repolarization and excitation wave conditions patterns in the tissue, leading to myocardial infractions, cardiac arrhythmia and even sudden death. In patients with mild or early signs of ischemia, medications such as aspirin, nitrates, cholesterol lowering medications (e.g. statin) are used to improve blood flow and to provide prophylactic measurements against plaque formations. Other medications include beta blockers, calcium channel blockers, ACE inhibitors and potassium channel blockers are used to help relax blood vessels and reduce cardiac tissue overload. If the symptoms do not improve by these medications, surgical interventions such as coronary angiography/stent are often practice in patients with more aggressive symptoms.

Cardiac arrhythmia occurs when the electrical signals to the heart that coordinates heartbeat are not in a synchronized rhythm, leading to irregular electrical conductions and cardiac contractions. Major antiarrhythmic drugs are classified into 4 major classes, based on

their mechanism of actions, influencing major intracellular ion concentrations. The first class of drugs (Class 1) consists of mainly the ones that modulate Na^+ channels and reducing action potentials (AP, phase 0) slope and affecting the AP durations. A few examples of class 1 antiarrhythmic drugs include quinidine, flecainide, and ranolazine – which are often prescribed for ventricular tachycardia. Class II drugs comprises of subclass drugs that targets the β-adrenergic, muscarinic (M_2) or adenosine A receptors and thereby eliciting either increase or reduction in sino-atrial node (SAN) pacing rates and atrioventricular node (AVN) conductions. In different types of tachycardia, for example, non-selective beta blockers (e.g. propranolol) and M_2 receptor inhibitors (e.g. atropine) are often prescribed in order to reduced SAN automaticity and re-entry. Class III are mainly the K^+ channel blockers that increases in AP recovery time and thereby slowing the overall rate of contractions. Amiodarone, sotalol, dofetilide are a few examples of Class III potassium channel blockers that are used in patients with ventricular tachycardia. Finally, Class IV drugs (verapamil, propafenone, flecainide, and bepridil) are involved in modulating intracellular calcium level and shown to reduce AVN conductions. Although current antiarrhythmic drugs are classified into these four, there seems to be a constant emergence of novel anti-arrhythmic drugs that cannot be classified into current classes due to their unique mechanism of action. Recent review paper by Huang et al. have introduced new classes 5, 6, and 7 which corresponds to drugs that acts on mechanosensitive channels, connexin-associated channels, and upstream modulatory targets (Huang et al., 2018). This has provided new insight into current and perspective therapeutic targets for treating different types of cardiac arrhythmias.

Catecholaminergic polymorphic ventricular tachycardia (CPVT) is a subset condition of arrythmia which is characterized by episodic syncope occurring during acute motion. Individuals with CPVT contains mutations in either RYR2 or CALM1 that causes onset of fast ventricular tachycardia due to their inability to regulate intracellular calcium levels correctly (Napolitano et al., 2004). Tachycardia may recover spontaneously, but in some cases, it can further degenerate into atrial fibrillation and cardiac fibrosis, leading to further deterioration of the disease condition. Current method of CPVT management is suggested to

be beta-blockers (Rosso et al., 2007); although the level of therapeutic effect seems to be only moderate or limited (Priori et al., 2015). If untreated, sudden death may be the first manifestation of the disease, being highly lethal. An estimate of 30% of affected individuals experience at least one cardiac arrest and upto 80% experience one or more syncopal spells (Napolitano et al., 2004). A new therapeutic method of attaining optimal calcium level inside cardiac tissue is, therefore, strongly urged in the clinical field.

Heart failure (HF) is the final common stages of many underlying CVDs and is associated with the highest morbidity and healthcare expenditure amongst cardiovascular complications (Public Health England, 2019). Pharmacological agents for HF include diuretics, angiotensin-converting-enzyme inhibitors (ACEIs), beta-blockers, angiotensin-receptor blockers (ARBs), and aldosterone antagonists. Although the anti-anginal effect of β-blockers (such as metoprolol and bisoprolol) and calcium-channel blockers (such as verapamil and diltiazem) have been proven effective in alleviating the increased heart rate, these classes of drugs exert other side-effects such as low blood pressure for β-blockers and dilatation of the coronary arteries for calcium-channel blockers, which may impair patients' quality of life. For end stage HF patients, hydralazine dinitrate and digoxin can be prescribed. However, their short duration of action, narrow therapeutic index, along with its significant increased risk in arrhythmogenesis, make these drugs of last resort (Young and Worthley, 2004)

1.4 Cardiovascular Drug Discovery

Despite major advancement in drug development, cardiovascular disease still remains leading cause of death worldwide, and the burden of CVDs clearly remains both a major public health worries and growing global challenge. What's more concerning is the declined research in the development of CVD drugs (Husten, 2016). Approval for new cardiovascular drug therapies have significantly declined in comparison to the prior decade. The study revealed an approximate 33% reduction in new marketing applications – seeking approval for new molecular entities (NME) for cardiovascular drugs, while the approval for several other therapeutic areas, including oncology, have risen (Kaitin et al., 2011). Part of this is due to a

shift in focus within marketing strategies for many pharmaceutical companies. Their incentive to develop cardiovascular agents has been reduced significantly by increasing clinical development costs associated with high risk of failure. This can be attributed to the unprecedented nature of the promising drug targets and an increasingly challenging regulatory environment. In addition, the scientific advancements in these fields have been too stimulating due to several reasons, including the demanding nature of the disease, the high risks associated with high failure rate, the complexity of clinical trials, and the potential for side effect complications (Prashant, 2017). Future directions of CVD therapies therefore exhort reason for concern.

At the enormity of this issue, incidents of cardiovascular disease are only increasing, and the identification of the mechanisms responsible for untimely deaths, along with the development of safe and effective therapies, remain elusive. Developing innovative medicine to meet critical public health demands is a priority, and much effort has been expended in finding prophylactic measures and pharmacological approaches for disease management. The search for new therapies in the emerging field of cardiac signaling during recent decades has prompted extensive research on myocardial remodeling in cardiac hypertrophy (CH) and HF. Full understanding of the pathophysiology of fundamental disease mechanisms is still required to successfully translate laboratory knowledge into clinical applications. Despite much effort in understanding hypertrophic signaling mechanisms, these understandings have only yielded few clinical strategies to prevent or to treat HF.

Recent studies have shown that PAK1 – a key cellular process regulator in cardiomyocytes – are observed to provide cardio-protection and to be essential for ion channel activity, intracellular Ca^{2+} handling, and cardiac contractility. Alternating the activity of PAK1 has been shown to impact performance of the myocardium under both physiological and stress conditions. Dysregulation of PAK1 activity is associated with various cardiac diseases (e.g. cardiac hypertrophy, arrhythmias, fibrosis, and heart failure) and suggested to be a vital intracellular protein important for maintaining homeostasis within cardiac functionality. These evidences suggest that stimulating PAK1 may provide to be an effective measurement against cardiac abnormalities and highlight PAK1 as a valuable therapeutic target.

1.5 P21-Activated Kinase 1 (PAK1)

The function of myocardial cells during heart contraction relies on strictly regulated rhythm and signaling mechanisms (Pando et al. 2001). This is achieved through a timely, controlled spread of electrical potentials, generated by the movement of ions through transmembrane ion channels, and mediated by signaling messengers. For example, multiple trans-membrane (e.g., ion channels) and intracellular proteins (e.g., Ca^{2+} handling and sarcomeric proteins) work to ensure that the signaling pathways involved in generating action potential are tightly regulated. Amongst various signaling molecules involved in this process, P21 activated kinase 1 (PAK1), serine/threonine protein kinase, demonstrated to be an essential nodal signaling kinases; specifically, in maintaining homeostatic functions in cardiac SA node and ventricular myocytes (Lei et al., 2007).

PAK1 is one of PAK sub-families divided into two groups. Group 1 consists of PAK1-3 containing GTPase binding domain, where GTPases such as CDC42 and RAC1 bind to stimulate the kinase activation. Group 2 (PAK4-6) on the other hand, differ from Group 1 PAKs in their mode of kinase regulation. PAK4-6 do not contain CDC42 binding site, and their intracellular localization and binding partners differ from those of Group 1 PAKs (Zhao and Manser, 2012). However, recent research on PAK4 and PAK5 of Group II family have shown evidence of interacting with CDC42 (Ha et al., 2012; 2018). In addition, both families of PAK have been reported to have similar roles in cardiac homeostatic functions. For example, inhibition of PAK2 and PAK4 using kinase inhibitors have been shown to decrease the rate of cardiomyocyte proliferation/dedifferentiation and significantly reduce cardiovascular regenerations (Peng et al., 2016). These findings suggest that the regulatory mechanisms between the two families of PAKs may be more similar and conserved than previously suspected.

Both groups of PAKs contain highly conserved kinase domain, N-terminal regulatory domain residues, and auto-inhibitory domain in controlling the kinase activity. Upon binding with GTP-ligand forms of CDC42 and Rac1, PAKs dimers dissociate and form monomeric conformation where the kinase domain is exposed, enabling activation via phosphorylation at

T423 (Yu et al., 1998; Gatti et al. 1999). The interaction with small GTPase to the regulatory region releases monomers from the auto-inhibited PAK1 homodimer and allows activation via phosphorylation at T423 (Yu et al., 1998; Gatti et al. 1999). The resulting activation of PAK1 leads to modulations in various downstream pathways and has been recognized as an important modulator in regulating cytoskeletal dynamics, growth signaling, apoptosis, motility, and management of oxidative stresses in myocardial cells (King et al., 2000). One prominent activated PAK1 pathway in maintaining cardiac homeostasis within the cardiac tissue is through activating protein phosphatase 2A (PP2A), which reduces both the phosphorylation effect of protein kinase A (PKA) and thereby the activity of L-type Ca^{2+} and ryanodine receptor (RyR) (both of which are PKA dependent). The mentioned calcium channels have been previously studied to be crucial in mediating currents in ventricular myocytes and often dysregulated in cardiac hypertrophy and arrhythmia (Sheehan et al., 2009; DeSantiago et al., 2013; Wang et al., 2015).

Within cardiac tissue, expression of PAK1 exhibit an overall high profile in all regions of the heart, including the sino-atrial node (SAN), atria, and ventricles (Ke et al., 2008). Other than the cardiovascular aspect, PAK1 has been indicated to be expressed in the brain and blood vessels, where it holds an essential role in neurodevelopment, neuroplasticity, and neonatal cardiac development (Kichina et al., 2010; Kothet al., 2014; Kumar and Li, 2016). Particularly in the peripheral nodal cells, immunocytochemical staining revealed that PAK1 was evenly distributed in a striated pattern, suggesting its functional importance in cardiac myocytes (Ke et al., 2004; Ke et al., 2007

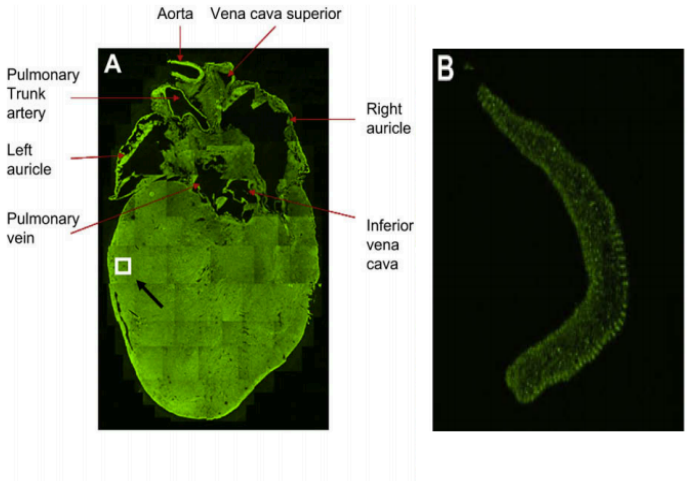

Figure 1.5.1 *Distribution of PAK1 in hearts.* **A)** PAK1 expression in a mouse heart section. The magnification of objective is 10x and sliced at 10 um sections. Stained with rabbit PAK1 antibody (primary) and detected by FITC conjugated antibody (secondary). **B)** PAK1 expression pattern in a SAN cell detected through confocal microscopy. (Figures derived from Ke et al. 2007; Ke et al. 2008).

The activation of PAK1 has also been involved in regulating microtubules and actin-myosin dynamics – effects essential for regulating cytoskeletal dynamics. Monasky *et al.* demonstrated through co-immunoprecipitation studies that PAK1 and cardiac troponin T (cTnT) are directly associated with each other and may indicate PAK1's role in mediating actin and myosin interaction (Monasky et al., 2012). Furthermore, PAK1's interaction with PP2A may augment the calcium sensitivity in myofilaments through dephosphorylation of cardiac inhibitory troponin (cTnI). Genetically modified mice with constitutive activated PAK1 (CA-PAK1) expressed an attenuated beta-adrenergic-stimulated (isoprenaline) phosphorylation of cTnI (Sheehan et al., 2009; Ke et al., 2010), which is supportive of PAK1's antihypertrophic effects. PAK1's involvement in microtubule formations has also been highlighted for its importance in maintaining transverse (T) tubular structures. DeSantiago and his group have shown preliminary evidence that ventricular myocytes lacking PAK1 ($PAK^{-/-}$) will result in decreased cell capacitance, as well as delayed rise time (DeSantiago et al., 2013). They have also observed a decrease in calcium transient amplitude, with less coupling between LTCC-mediated Ca^{2+} influx and RyR2-mediated Ca^{2+}–induced Ca^{2+} release (CICR). These observations are consistent with the central role of T-tubules in triggering and synchronizing excitation-contraction coupling (DeSantiago et al., 2013). Other additional downstream targets of PAK1 include mitogen-activated protein kinase (MAPK), mitogen-activated protein kinase kinases (MKK) and c-Jun N-terminal Kinase (JNK), which are essential in mediating the hypertrophic stress effect (Davies et al., 2014; Cuenda et al., 2000; Wang et al., 2007; Wang et al., 2018). Further details of these pathways and consequences from dysfunctions are described in the following therapeutic section.

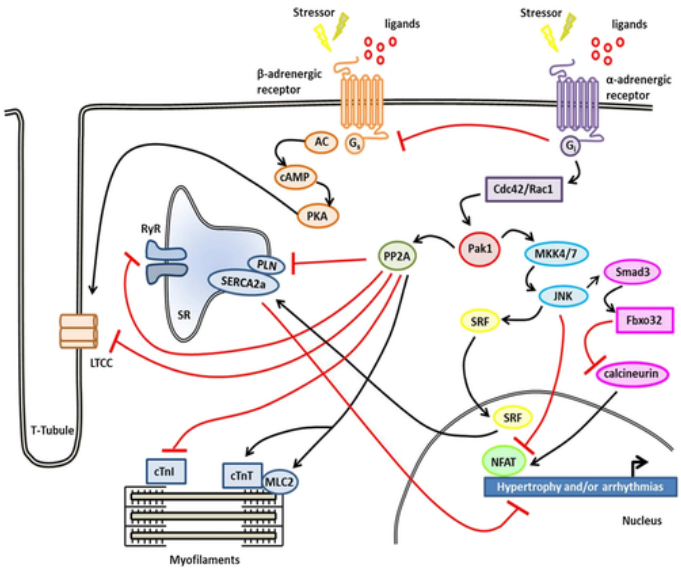

Figure 1.5.2 *Representation of PAK1 cardiac signaling pathway.* Downstream of stress signal activates Cdc42/Rac1, which further activates PAK1 cardiac signaling pathway. PAK1 provides calcium handling through activation of PP2A, which allows dephosphorylation of phospholamban, cTnI, RyR and LTCC and phosphorylation of cTnT and MLC2 – reducing overall beta-adrenergic stress stimulations. PAK1 also provides cardio-protective mechanisms by activating SRF and transcriptionally regulating SERCA2a through the MKK4/7/JNK pathway. Black arrows indicate stimulation/phosphorylation/activation; red lines indicate inhibition/dephosphorylation. (Figure derived from Wang et al., 2018)

1.6 P21-Activated Kinase 1 (PAK1): Therapeutic Target

Recent studies have well-recognized PAK1 to have various protective roles in cardiovascular systems, particularly in the prevention of cardiac hypertrophy, hypoxic, and ischemic injuries (Eroume et al., 2010; Ke et al. 2015; Wang et al. 2014; Liu et al. 2011; Wang et al., 2018). Particularly, PAK1 has been identified to attenuate chronic β-adrenergic signaling – one of the key symptoms commonly found among the indicated diseases.

One of the early indications for PAK1's anti-adrenergic functions was reported by Zhang et al., demonstrating PAK1 as a potential mediator of RAC/CDC42, and confirming that PAK1 is an upstream mediator in stimulating p38. It is important to note that p38 is a subgroup of the mammalian-stress-activated MAP kinase which plays a key role in regulating inflammatory responses (Zhang et al., 1995). This was later supported by observing PAK1 activation upon extracellular stress factors, such as EGF, angiotensin II, and isopropanol ISO. PAK1 activity significantly increased upon administration of these stress mediators, suggesting PAK1

functions to normalize the induced stress responses (Woolfork et al. 2005; Cheng et al. 2011). Since these findings, various studies have shown that PAK1 activation can reduce chronic β-adrenergic stimulation and normalize an increased heart rate and Ca^{2+} channel activity. Under experimental conditions, constant perfusion of ISO in mice cardiomyocytes normally cause hypertrophy and can increase the heart rate by 40 – 50% (Ke et al. 2009). However, adult cardiac ventricular myocytes expressing constitutively active PAK1 (CA-PAK1) exhibit a significantly reduced ISO-induced heart rate, without affecting the amplitude of the L-type Ca^{2+} currents in the SAN cells (Ke et al. 2012). Moreover, CA-PAK1 demonstrated an enhanced myofilament Ca^{2+}-sensitivity associated with dephosphorylation of cardiac troponin (cTn1) and myosin-binding protein C (MyBP-C) (Ke et al. 2004; 2007). CA-PAK1 expression was also able to repress ISO-induced arrhythmias by restoring both the L-type Ca^{2+} current and the delayed rectifier K^+ current (Ket al., 2007). In addition, CA-PAK1 cardiomyocytes showed an attenuated elevation of the decay constant, reduction in calcium spark amplitudes, and decreased in spatial spreads (Sheehan et al., 2009). The current hypothesis about these anti-adrenergic effects are that they occur through PAK1 activation of protein phosphatase 2A (PP2A), one of the main serine-threonine phosphatases that are active in maintaining cell homeostasis by inhibiting most kinase-drive intracellular signaling pathways. When cardiac myocytes underwent ischemic reperfusion injury (I/R), western blot studies revealed an increased co-localization between PAK1 and PP2A. Furthermore, the suppressive effect of active PAK1 on the response to beta-adrenergic stimulations was partially reversed when the PP2A inhibitor okadaic acid was administered. Taken all together, these evidences provide further support that the anti-adrenergic and ischemic injury is partly relieved through the activation of the PAK1/PP2A pathways (Lei et al., 2015; Liu et al., 2011).

Knocking out the activity of a specific gene can provide useful insight as to the *in vivo* function of the protein in question. To study the PAK1 function in the heart, PAK1 knock-out mice ($PAK1^{cko}$) were bred and characterized. The study revealed that PAK1 deficiency in cardiomyocytes showed an exacerbated pressure-overload-induced hypertrophy, as well as the sensitization of $PAK1^{cko}$ mice to heart failure due to prolonged load stress (Liu et al., 2011). A gross anatomical and histological comparison between ISO-treated WT and $PAK1^{cko}$ hearts

revealed an increase in both the heart sizes and the cross-sectional areas at the mid-papillary level (Taglieri et al. 2011). The exacerbated hypertrophic remodeling in PAK1^{cko} mice is associated with a lack of stress protection from MKK4/MKK7-JNK pathways, downstream signaling cascade of PAK1, and PAK1's inhibitory effect on ERK1/2 (Liu et al., 2011; Taglieri et al. 2011). Consequently, PAK1^{cko} ventricular myocytes showed abnormal Ca^{2+} homeostasis including an increased diastolic $[Ca^{2+}]_i$, decreased sarcoplasmic reticular (SR) Ca^{2+} content, and decreased SERCA function, particularly during β-adrenergic stress (Wang et al., 2014). Additionally, under increased stimulation frequencies, PAK1^{CKO} exhibited more frequent irregular alternating calcium transients and waves (Wang et al., 2014). Prolonged overpressure stress revealed an increased vulnerability of PAK1^{CKO} to undergo the transition into heart failure with blunting of JNK activation (Liu et al., 2011) These accumulating evidence indicate that a lack of PAK1 in cardiomyocytes can lead to a significantly uncoordinated interplay between the kinase and the phosphatases – conclusively increasing vulnerability in developing cardiac diseases.

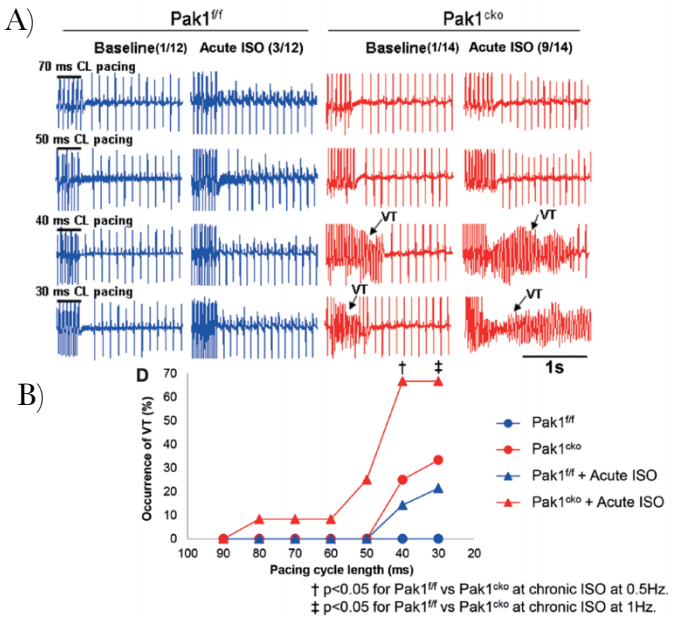

Figure 1.6.1 *Electrophysiological studies between PAK1 and PAK1^{CKO}.* **A)** *in vivo* study examining the electrophysiological traces of PAK1vs PAK1^{CKO} illustrates difference in the vulnerability towards ventricular tachycardia (VT) upon high frequency pacing and β-adrenergic (ISO) stress. **B)** Summary representation of the occurrence of VT. PAK1^{CKO} hearts showed higher occurrences of VT under higher pacing frequencies, particularly under acute β-adrenergic stress. (Figure derived from Wang et al., 2014)

Recent reports on the link between PAK1 and ERK have been crucial in supporting the role of PAK1 in cardiac hypertrophy. The Ras/Raf/MEK/ERK cascade represents a common pathway for alteration of intracellular calcium by Ras and protein kinase C (PKC) in cardiac myocytes (Ho et al. 1998). The MAPK/ERK signaling pathway has typically been associated

with modulation of the hypertrophic response of the heart to neurohumoral stimuli and pressure overload. Clinical studies have demonstrated that patients exhibiting mutations in the Ras/Raf/MEK/ERK signaling pathway often present with symptomatic hypertrophic cardiomyopathy (Rose et al. 2010). The current proposed mechanisms for PAK1's role in attenuating cardiac hypertrophy is via mediation of PP2A conformational changes leading to autophosphorylation and PP2A activations (Lei et al. 2015; Lei et al. 2007; Ke et al. 2007). The activated PP2A is thereby able to induce dephosphorylation of ERK 1/2, reducing its activity and alleviating cardiac hypertrophy. This proposal was strengthened by results from kinase assays and functional characterization of PAK1^{cko} mice. In ERk1 and ERk2 western immunoblotting comparisons between WT and PAK1^{cko}, normalized percentages of ERK1/2 protein expression were shown to increase significantly in PAK1^{cko} compared to that of the WT, while the ISO induction aggravated the protein expression for both samples (Liu et al. 2011). These major findings signify the importance of PAK1 as a natural inhibitor of ERKs - as well as a novel anti-hypertrophic signaling enzyme with a role in modulating beta-adrenergic signaling.

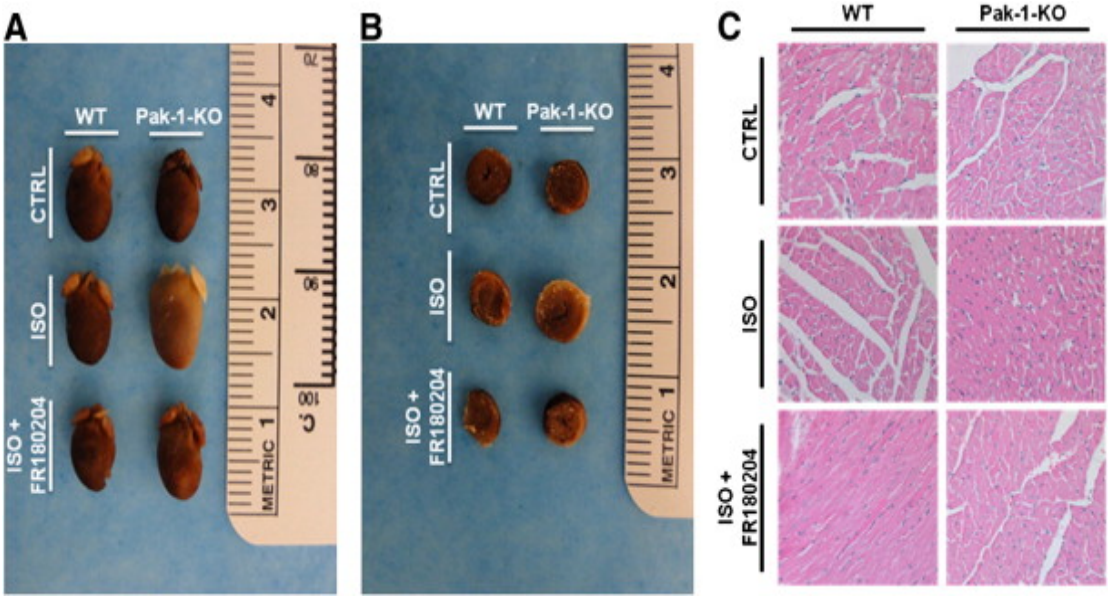

Figure 1.6.2 *PAK1^{cko} gross heart anatomy and histology comparison to WT* **A)** Gross anatomy of heart comparisons between WT and PAK1^{cko} **B)** Cross-sectional area comparisons between WT and PAK1^{cko}. The effect of PAK1^{cko} in heart size A) and area B) were studied upon administration of either ISO or ISO + FR180204, ERK1/2 selective inhibitor. ISO treatment showed a significant increase in the heart mass in PAK1^{cko}, while FR18024 was able to reverse its hypertrophy effect. **C)** Histology comparison showed an increase in cell size for PAK1^{cko} ISO treated when ISO + FR180204 was able to reverse its pathological modification by ISO. Myocardial LV tissue were stained with hematoxylin and eosin. (Figure derived from Talieri et al. 2011).

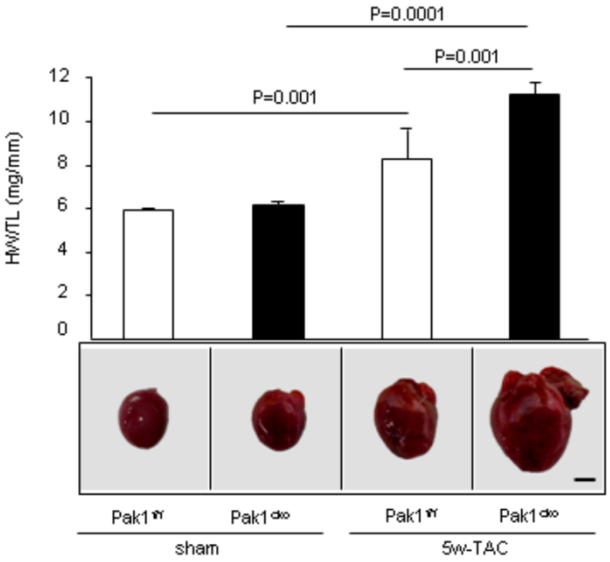

Figure 1.6.3 *Transverse Aortic Constriction (TAC) on Pak1^{cko} mice.* Prolonged TAC on PAK1^{cko} Mice exhibit exaggerated signs of heart failure. HW/TL ratios of Pak1$^{f/f}$ and Pak1^{cko} mice (upper panel). Morphometry demonstrates greater hypertrophy in Pak1^{cko}-TAC mice (lower panel, scale bar: 2mm, n=7 mice per group) (Figure derived from Liu et al., 2011)

1.7 PAK1: Overview Structure

PAK1's essential roles in maintaining homeostasis in cardiac functions and providing cardio-protection show clinical significance and implications for therapeutic purposes. In order to target PAK1 as a therapeutic target however, we would be required to search for a ligand that can stimulate the protein activity. Unfortunately, unlike targeting ion channels or transporters, effort for designing protein activators have been significantly limited and undervalued. In fact, current research in drug designing are heavily limited to inhibiting harmful molecules, rather than activating the beneficial ones. This may be partly due to our lack of understanding of structural detail of beneficial protein as well as limited knowledge in their mechanism of activation. However, with increasing number of protein structures being elucidated and finding similar mechanisms of activation, targeting the beneficial proteins may prove to be the next pharmacological approach in drug discovery. Fortunately for PAK1, much of its structural information and activation mechanism have been well documented and studied over the last two decades. In particular, the crystal structure of PAK1 (PBD 1f3M) has been crucial in providing the necessary structural information in order to perform structure-based drug designing and to develop the PAK1 activators in rational approach (Lei et al., 2000).

PAK1 belongs to the STE Set/Thr protein kinase family (STE20 subfamily) with the molecular mass of 60 kDa (545 amino acids long). It contains the regulatory domain (a.a. 70~140) and the kinase domain (a.a. 270~521). The N-terminus regulatory domain contains the p21 binding domain (PBD, a.a. 70~113), CDC42-RAC1 interaction/binding motif (CRIB, a.a. 75~90), autoinhibitory domain (AID/IS, a.a. 87~136), and the kinase inhibitory domain (KI, a.a. 138~147). Other areas of domain include Nck binding motif (a.a. 13~21), PIX binding motif (a.a. 182~203), CRIPak interacting motif (a.a. 132~270), and $G_{B\gamma}$ binding motif (a.a. ~545). Figure 1.7.1 represents the secondary sequence of PAK1 and its functional domains. Monomeric crystallographic structure of PAK1 (AID + KD) are derived from Lei et al., 2000 (PBD: 1F3M).

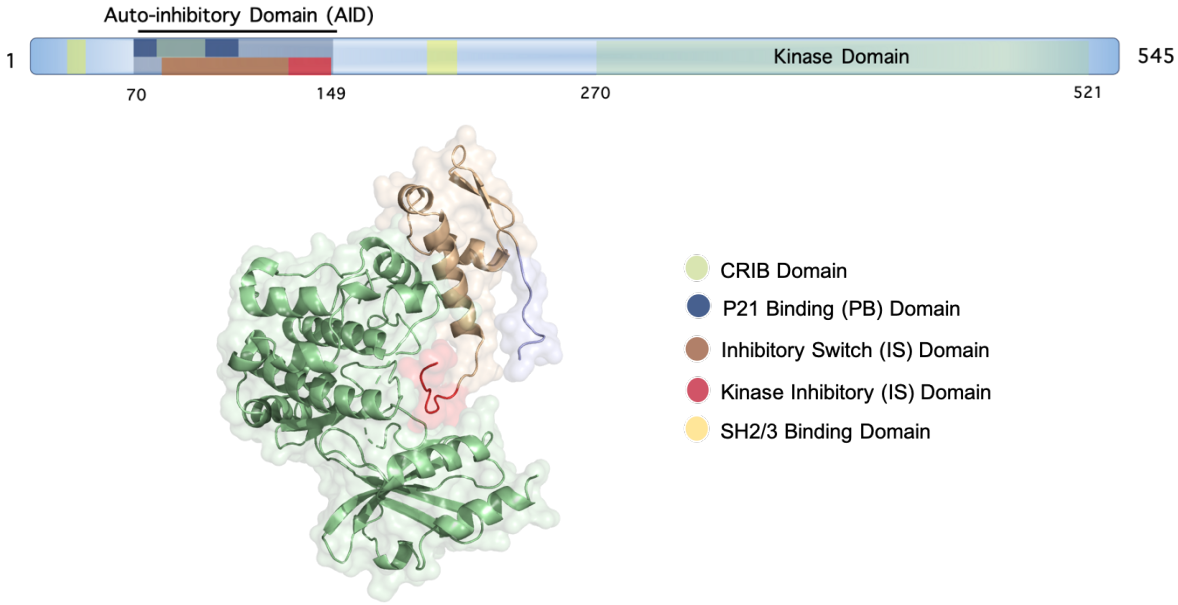

Figure 1.7.1 *Diagram representation of a PAK1 structure.* The primary structure outline of PAK1 and the 3D structural representation of a monomeric PAK1 are shown to highlight the functionality of each regions. The kinase domain is highlighted in green color (■).

1.7.1 PAK1 Auto-Inhibitory Domain (AID)

The auto-inhibitory domain of PAK1 are intercalated antiparallel beta ribbon sheets that allow the PAK1 to form asymmetry dimerization. This regulatory domain can be subdivided into two segments: the inhibitory switch (IS) domain and the kinase inhibitory (KI) domain.

1. The inhibitory switch (IS) domain is the main antiparallel beta ribbon that interacts with the other PAK1 monomer to form a dimer. The core residues are located between residues 80 ~ 87 which form a hydrogen bond between the ribbon structures to stabilize the interaction; two salt bridges from Glu82 and His86 also help in securing the positions (Lei et al., 2000). His86 has also been identified to be an essential residue for PAK1's interaction with CDC42 (Frost et al., 1998). PAK1 H86L mutant has been shown to abolish CDC42 interactions and as a result, significant reduction in the kinase activity occurred (Frost et al., 1998; Zenke et al., 1999). Using mutagenesis, Zhao et al. observed that Glu116, Glutamine117, and Asp126 are also essential for AID's inhibitory functions. Furthermore, Zenke et al. demonstrated that a mutation at the Leu107 do not disrupt the GTPase binding ability, but only affects the inhibitory functions of the AID, leading to a constitutively active conformation of PAK1 (Zenke et al., 1999). Finally, the crystallography studies of PAK1 (PDB:1F4M) also revealed an asymmetric interaction between Phe81–Pro121, Leu125–Ile85, and Pro100–Trp103, all of which are essential in forming the asymmetric packaging between the two beta ribbons of the AID (Lei et al., 2000).
2. In addition to the IS domain, the AID also contains a short segment called the kinase inhibitory (KI) domain which inhibits the catalytic active site of PAK. Crystallography study of PAK1 (PDB:1F3M) illustrates that the Lys141 from the KID form salt bridge bonds with Asp389 of the catalytic loop and Asp407 of the activation loop. The three hydrophobic residues of Tyr142, Met143, and Phe145 also contribute to stabilizing the loop's inhibitory conformations. The orientation of these loop conformations forces the activation loop to be turned (a.a 407–413) and prevents the interaction between the Glu315 of helix C and Lys299, a crucial a.a. in forming the ATP binding site (Lei et al., 2000). Further mutagenesis studies have shown that mutation at Lys299 to arginine disrupts the interaction, and the kinase has been shown to completely lose its catalytic ability (Lei et al., 2000; Johnson et al., 1996). Additional residues (Leu107, Glu116, Asp126) have been reported to be involved in forming a tight junction between KI and the kinase domain. Mutations at these residues have been reported to induce

constitutive activation of the kinase (Brown et al., 1996; Zhao et al., 1998; and Tu and Wigler, 1999).

Overall, both the IS and the KI domains are crucial in preventing the activation of PAK1. The IS domain is specifically involved in forming the dimer between the AID of PAK1 monomers, while the KI domain is responsible for inhibiting the activation loop of the kinase domain. Interestingly, co-expression of designed hetero-dimerization of PAK1 suggests that such auto-inhibitory interaction within PAK1 is in a *trans* conformation. In other words, the kinase domain inhibition requires an association with the AID of the other monomer, not its own regulatory domain (Parrini et al., 2002). These multiple inhibitory mechanisms ensure tight regulations of PAK1 activity and are only relieved upon binding to its corresponding GTPases at the CRIB domain.

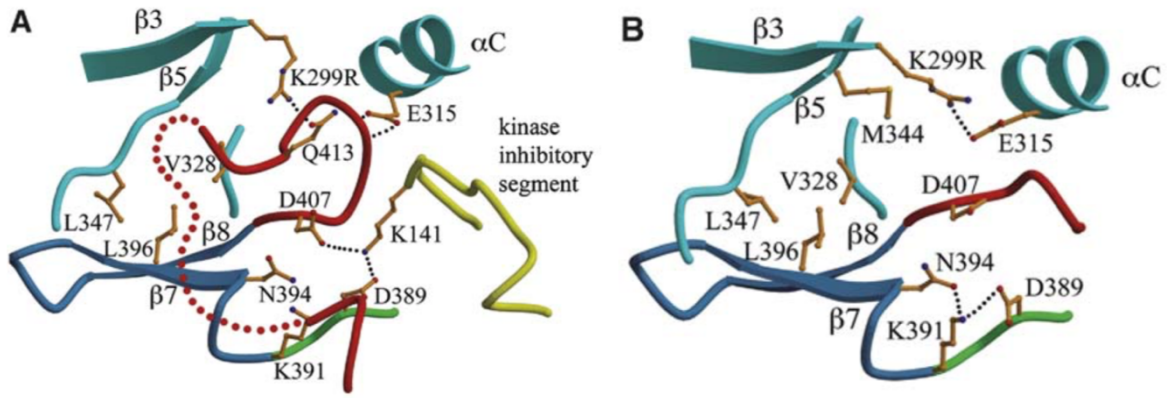

Figure 1.7.2 *Comparison between PAK1 KD (inactive) vs. PAK1 KD (active).* **A)** The kinase inhibitory segment of PAK1 covers the catalytic part of the active site, thereby preventing the conformational changes which allows autophosphorylations **B)** Active PAK1 KD reveals displacement of the KID, thereby exposing the catalytic site and allows the ATP to bind. (Figure derived from Parrini et al., 2002)

1.7.2 PAK1-CDC42 Interactions

PAK1 adopts its active conformation upon biding with its relevant GTPase, GTP bound form of CDC42 and RAC1 (Morreale et al., 2000; Knaus and Bokoch, 1998). These GTPase bind PAK1 at the CRIB site within the regulatory domain of PAK1. Conserved residues in the CRIB motif, especially of the Phe81 and His83 residues, have been confirmed to be essential

for CDC42 interactions (Manser et al., 1997). Mutations at other CRIB motif residues, I75N, S76P and P78A, do not abolish interaction with CDC42, but they reduce PAK1 affinity towards CDC42. Outside of the CRIB motif, few residues have been recognized to stabilize the interaction between PAK1 and CDC42: Met99, Trp103, Leu106 and Leu107 (Zhao et al., 1998). Leu107 mutation to Phe does not disrupt the CDC42 interaction much, but makes PAK1 constitutively active, suggesting its importance in stabilizing the a-helix interactions at the AID (Frost et al., 1998).

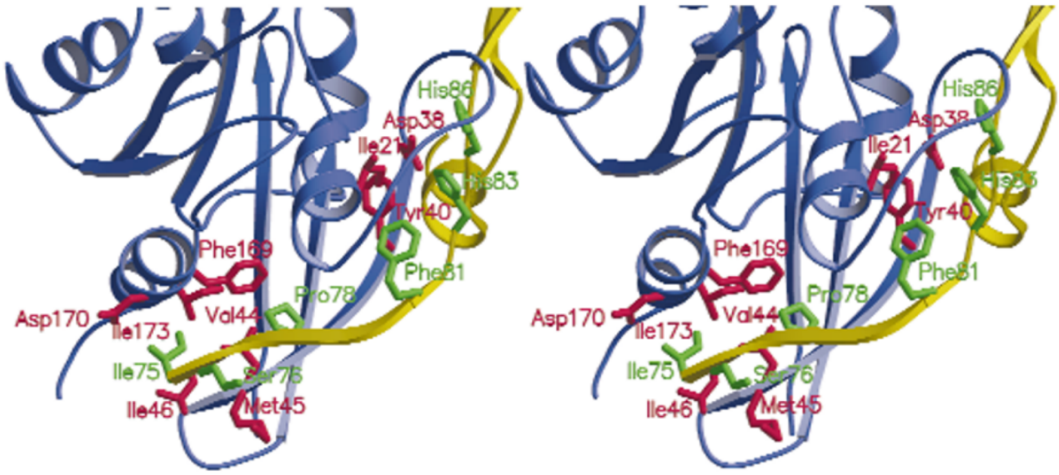

Figure 1.7.3 *Interaction site between CDC42 and PAK1*. This close up view provides key residues essential for the protein-protein interactions. The short segment of PAK1 CRIB (■) contains key residues that interacts with the a1 and a5 of CDC42 (■) (Figure derived from Morreale et al., 2000).

1.7.3 PAK1 Kinase Domain (KD)

In a closed state of the kinase, electrostatic interactions amongst various residues within the kinase domain stabilize the activation loop. Glu423 forms salt bridges with Arg388 and Arg421, helping in positioning the catalytic base, Asp389. The carbonyl of Phe410 and the phenolic oxygen of Tyr411 form an additional hydrogen bond with Arg388 (Lei et al., 2005). Closer examination at the active loop shows salt bridge formation amongst K141 (of the KI domain), Asp407 and Asp389 (of the kinase domain). Upon binding of the GTP-bound GTPase (e.g. CDC42), the regulatory domain of the PAK1 changes its conformation into its active state and relieves its multistage inhibitory mechanisms. This disrupts the Lys141 electrostatic bonding to the kinase domain residues and new stabilization bonds occur amongst K391, N394, and

Asp389. Mutagenesis studies show that such stabilization of the active loop is essential for Thr423 phosphorylation; while mutations at D389N and D393A prevent phosphorylation at the Thr423 and abolish the kinase activity (Wang et al., 2011). Subsequently, the re-orientated active loop causes a shift of the Thr423 by about 10A, making new contact with the Leu470 and Leu473 (Wang et al., 2011). This allows the active loop to be exposed, and for trans phosphorylation to occur at Thr423 by the other monomer. Finally, additional phosphorylation occurs at several serine residues, including S144 and S149, which locks the established active conformation and prevents interaction with the auto-inhibitory domain (Manser et al., 1997; Lei et al., 2004). The irreversible activation state permits the ATP to bind at the catalytic domain, located between the five beta sheets and the two alpha helices. Arg299, Glu315, Met344, Tyr346, Leu347, Val328, Asp389, Leu396, Lys391, Asn394, and Asp407 form hydrophobic pockets surrounding the ATP. Especially the Asn394, Asp389, and Arg299, which form salt bridges with the phosphate groups of ATP, thereby securing the ligand binding (Wang et al., 2011). These multistage mechanisms of activation ensure tight regulation PAK1 activity.

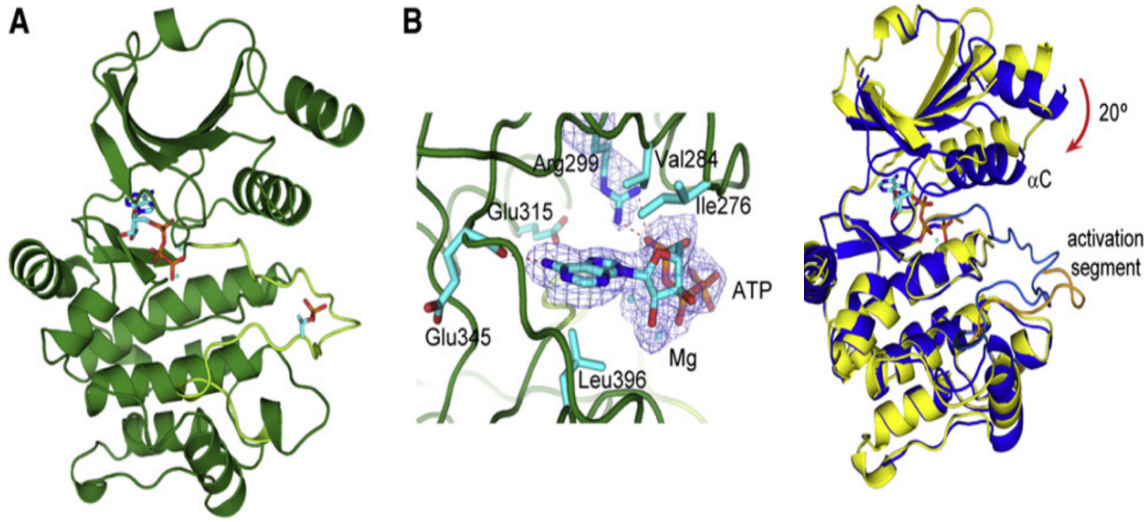

Figure 1.7.4 *Structure of PAK1 Kinase Domain*. A) Unphosphorylated (Inactive) PAK1 kinase domain with Mg-AMP-PNP (ATP analogue, highlighted in different carbon colors). B) ATP binding site of PAK1 kinase domain. The electrostatic surface area and the key residues that are essential for ATP binding are highlighted. C) PAK1 Monomers in phosphorylated (active, ●) vs unphosphorylated (inactive, ●) conformations. Superpositions of these two states of PAK1 exhibits difference in their conformational changes. These changes allow for the ATP binding site to more exposed and alter the position of the catalytic loop, promoting transphosphorylation at T423 (Figure derived from Wang et al., 2011)

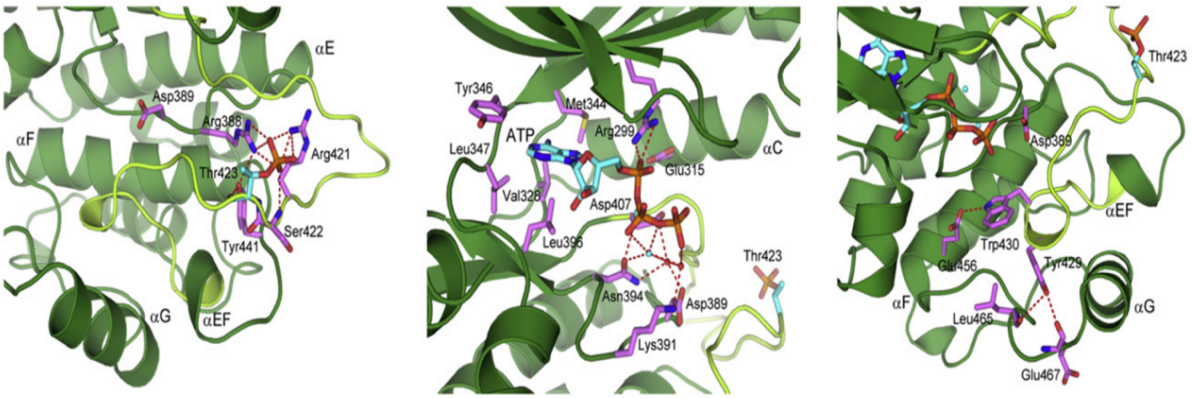

Figure 1.7.5 *ATP Binding of PAK1 Kinase Domain.* The close-up view of the ATP binding site provides further insight into the key residues that are involved in providing the hydrophobic binding pocket, as well as the orientation in which the nucleotide binds. The three figures are derived from the same crystallography figure, PDB: 1YHW, in different orientation (Figure derived from Wang et al., 2011).

1.7.4 PAK1 Protein Binding Motifs

Aside from the regulatory domain and the kinase domain, PAK1 consists of three Pro-rich N-terminal motifs which interact with SH2/SH3-domain-containing adaptor proteins, including GRB2 (a.a. 12~18) and NCK (a.a. 40~45) (Lei et al., 2000). These adapter proteins localize the PAK to membrane bound Tyr-kinase receptors. The residue stretching 148–248 carries the PIX (SH3) binding motif of 18 amino acids (a.a. 186–203). A positively charged basic region adjacent to CRIB domain is critical for PAK1 binding to cell membrane phosphoinositide (Zhao et al., 2012). S21 and T212 that belong to the missing regions in PAK1 crystal structure are phosphorylated by kinases such as AKT/PKB19 and CDC2/CDK5 (Mao et al., 2007; Higuichi et al., 2008).

Within the C-terminus, PAK1 contains somewhat a unique, short alpha helix against the interdomain hinge. Ste20 has been identified as the target for Gby in regulatory signaling (Lei et al. 2000). PAK1-associated guanine nucleotide exchange factors – PIXa, CDC42, and RAC1 have been associated for directional migration of cells. The Gby-PAK1/PIXa/CDC42 pathway has been shown to be essential for the localization of F-actin formation and the exclusion of phosphatase and tensin homolog (PTEN) from the leading ledge, directional sensing, and directional migration of chemotactic leukocytes (Li et al., 2003).

Table 1.7 *Compilation of PAK1 Mutagenesis Studies*

Mutation	Effect	Kinase Activity	Reference
Y3F	Interferes with JAK2 binding, reduces kinase activity; Prevents nucleus translocation	Decrease	Rider et al., 2007; Tao et al., 2011
S21A	Inhibits phosphorylation, leading to decrease in kinase activity.	Decrease	Zhou et al., 2003
I75N	Reduces CDC42 binding affinity	Decrease	Zhou et al., 1998
S76P	Reduces CDC42 binding affinity	Decrease	Zhou et al., 1998
P78A	Reduces CDC42 binding affinity	Decrease	Zhou et al., 1998
H83L	Prevents CDC42 Binding	Decrease	Frost et al., 1998; Zenke et al., 1999
H86L	Prevents CDC42 Binding	Decrease	Frost et al., 1998; Zenke et al., 1999
L107F	Abolishes autoinhibition, leading to constitutive kinase activity.	Increase	Frost et al., 1998
Y131C	Enhances phosphorylation, leading to increase in kinase activity.	Increase	Harms et al., 2018
T153F	Decreases JAK2 phosphorylation, leading to reduced kinase activity.	Decrease	Rider et al., 2007
P191G	Prevents αPIX binding	Decrease	Nie et al., 2012
R192A	Prevents αPIX binding	Decrease	Nie et al., 2012
K299R	Abolishes kinase activity	Decrease	Wang et al., 2011
T359A	Decreases kinase activity	Decrease	Mayhew et al., 2015
R393A	Prevents Thr423 autophosphorylation, leading to abolishment of kinase activity.	Decrease	Wang et al., 2011
S392A	Decreases authophosorylation leading to minimal catalytic activity towards kinase.	Decrease	Wang et al., 2011
D389N	Abolishes kinase activity	Decrease	Wang et al., 2011
D393A	Prevents autophosphorylation at Thr423, leading to abolishment of kinase activity.	Decrease	Wang et al., 2011
V415Gin	Slightly increases the trans-phosphorylation rate, leading to increased kinase activity.	Decrease	Wang et al., 2011
T423A	Decreases autophosphorylation and CDC42-stimulated activity.	Decrease	Zenke et al., 1999
T423E	Constitutive kinase activity	Increase	Zenke et al., 1999

Pro428Ser (of KD^{k299R})	Inhibits trans-phosphorylation of PAK1-$KD^{K299R/D389N}$.	Decrease	Wang et al., 2011
Y429C	Enhances kinase activity and significantly reduces homodimerization.	Increase	Harms et al., 2018
V436Q	Moderately increases the rate of trans-phosphorylation, leading to increased kinase activity.	Increase	Wang et al., 2011
L470D	Decreases the rate of trans-phosphorylation, leading to decreased kinase activity.	Decrease	Wang et al., 2011
A477L	Moderately increases the rate of trans-phosphorylation, leading to increased kinase activity.	Increase	Wang et al., 2011
E456L	Decreases authophosorylation leading to minimal catalytic activity towards kinase.	Decrease	Wang et al., 2011
Pro428Ser (of KD^{k299R})	Inhibits trans-phosphorylation of PAK1-$KD^{K299R/D389N}$.	Decrease	Wang et al., 2011
Pro428Ser (of $KD^{K299R/D389N}$)	Does not affect the trans-phosphorylation of PAK1 KD^{k299R}.	Decrease	Wang et al., 2011
Met431Arg(of KD^{K299R})	Inhibits trans-phosphorylation of PAK1-$KD^{K299R/D389N}$.	Decrease	Wang et al., 2011
Met431Arg (of $KD^{K299R/D389N}$)	Does not affect the trans-phosphorylation of PAK1 KD^{k299R}.	Decrease	Wang et al., 2011

1.8 Development of PAK1 Activators

1.8.1 sphingosine-1-phsophate & FTY720 (Fingolimod)

An early study using membrane lipids showed that PAK1 activation can occur through lipid association with the SH3 domain protein, NCK (Lu et al., 1996). Using sphingosine and several other related long chain spingoid lipids, subsequent studies demonstrated that PAK1 activity can be increased (Bokoch et al., 1998; Chong et al., 2001). Although one study had hypothesized that sphingosine and its analogues can directly bind to PAK1 and regulate its activity, limited evidence supported this statement (Chong et al., 2001). Additionally, we had performed a dose response test using *in vitro* PAK1 kinase assay to verify the above finding; however, sphingosine did not show any significant activation of PAK1 (Bae, Unpublished). These results indicate that the mechanism of PAK1 activation by sphingosine or its related analogue are not through direct binding to PAK1, but rather by indirect activation through activating its own S1P receptors (Egom et al., 2006).

Spingosine-1-phosphate (S1P) is a phosphorylated derivative of sphingosine (a family member of sphingolipids structural backbones). G protein-coupled receptors $S1PR_{(1–5)}$ activation are studied to be essential in playing diverse roles in cytoskeleton organization, survival, growth, and calcium mobilizations (Peters and Alewijnse et al., 2007). In the cardiovascular field, S1PR signaling pathways have been characterized to provide cardio protection against various stressors (Wang et al., 2018; Guo et al., 1999; Nakijima et al., 2000). Although the underlying mechanisms of action for S1P in providing cardio protection remain elusive, the key mechanism of the prophylactic effect of S1P has been suggested through preliminary downstream targets PAK1 and PI3K (Egom et al., 2010, Egom et al., 2011, Ahmed et al., 2011; Wang et al., 2018).

In the P13K activation pathway, for example, S1P binds to its specific receptors, S1PR(1-3), and triggers a G-protein-coupled cascade that activates P13K. The activated P13K is then able to phosphorylate Akt, an upstream regulatory protein involved in activating PAK1 and in increasing NO production through eNOS activation. Exogenous S1P administration in endothelial cells can cause an increase in eNOS activity via intracellular Ca^{2+} mobilization and results in an increased NO protection from apoptosis and cell remodeling (Kwon et al. 2001).

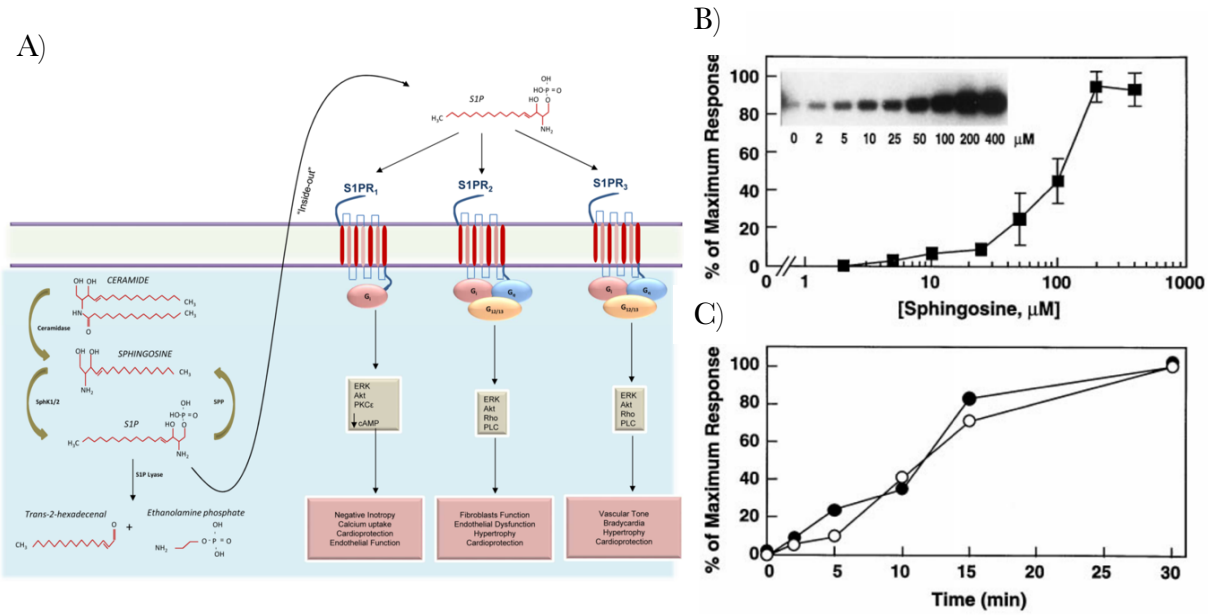

Figure 1.8.1 *Effects of Sphingosine on PAK1.* **A)** S1PR signaling activation in cardiovascular system. Activation of S1PR(1–3) induces negative inotropic effect via G protein (Gi) and decreases cellular cAMP. S1PR activation has been also shown to have downstream activation which causes activation of ERK ½ and AKT, thereby regulating cardiac hypertrophy (Figure derived from Cannavo et al., 2017) **B)** *Pak1 activation by Sphingosine*. Kinase activity was determined by measuring the amount of Pak1 phosphorylation under the treatment of sphingosine using COS–7 cell lysis. **C)** *Time course Pak1 activation of sphingosine* (200uM, ●) *and CDC42* (1 ug, ○). The activity of PAK1 was determined through assessing the amount of autophosphorylation (Figure derived from Morreale et al., 2000).

S1P has also been identified to have a functional alteration effect in regulating intracellular calcium levels and in mediating negative inotropic effects in ventricular myocytes (Egom et al., 1006; 2010; 2018). At an effective concentration, administration of S1P (25 nM) showed significantly reduced isoprenaline (ISO, 5nM)-induced Ca^{2+} waves and diastolic Ca^{2+} release in rat ventricular myocytes (Egom et al., 2016). The improved calcium handling via L-type calcium channel current was hypothesized through S1PR downstream target of PAK1 (Liu et

al., 2011; Jin et al., 2007). Immunoprecipitation results showed increased PAK1 activation and increased co-localization between PAK1 and PP2A, which are suggestive of PAK1-PP2A mediated pathway in regulating intracellular calcium (Egom et al., 2016). These functional interactions suggest potential therapeutic usage of S1P analogues for attenuating beta-adrenergic stimulations in clinical settings. Finally, S1P activation of PAK1 and AKT have been identified to limit cell death and improve functional recovery after ischemic/reperfusion (I/R) injury (Jin et al., 2007). S1P activation, therefore, has been shown to be essential for ischemic preconditioning (IPC) for the prevention of I/R injury (Jin et al., 2007; Egom et al., 2010).

The described mechanisms for S1P's anti-adrenergic effects are further supported through the usage of a sphingolipid analogue. FTY720 (fingolimod, 2-amino-2-[2-(4-octylphenyl)ethyl] propane-1,3-diolhydrochloride) is a sphingolipid drug approved for treating relapsing multiple sclerosis. It has a substantially similar structure to S1P and undergoes similar post-translational modifications as S1P (Brinkmann et al. 2002). When phosphorylated by sphingosine kinase (SphK), phosphorylated FTY720 competes with S1P to bind to the S1P receptor, a G-protein coupled receptor involved in a variety of cellular responses such as cell growth, survival, motility, calcium mobilization, and cytoskeletal remodeling (Spiegel and Milstien, 2003). Most importantly, FTY720 was able to exert antihypertrophic effects through the Gi-coupled GPCR, resulting in the activation of Pak1 (Liu et al., 2013). FTY720 has been shown to significantly increase phospho-Pak1 levels by 56% when treated with 25 nM FTY720 for 15 minutes (Egom et al., 2010). Liu et al. further established that the activation of Pak1 subsequently activates JNK1/2 pathway and inhibits nuclear factor of activated T-cells (NFAT), which are transcription factors that have been highly recognized in mediating cardiac hypertrophy (Molkentin, 2004).

Functional *in vivo* and *in vitro* assays have demonstrated that S1P analogues can effectively manage ischemia-reperfusion (I/R) injuries (Jin et al. 2007; Vessey et al. 2008). Egom *et al.* showed that S1P analogues were able to antagonize both brady- and tachy-arrhythmias induced by ischemia-reperfusion and provide protection against hypoxic and ischemic injuries (Egom et al. 2009). A recent clinical trial that measured the effect of FTY720 on patients with post-cardiac surgery showed a significantly reduced incidence of atrial fibrillation when treated with FTY720 for 24 hours (Ahmed et al., 2017). The same study had performed WB and immunostaining on patients' cardiac tissue, and found an increased expression of PAK1, suggesting that PAK1 activation may provide a potential therapeutic benefit for post-operative AF prophylaxis (Ahmed et al., 2017).

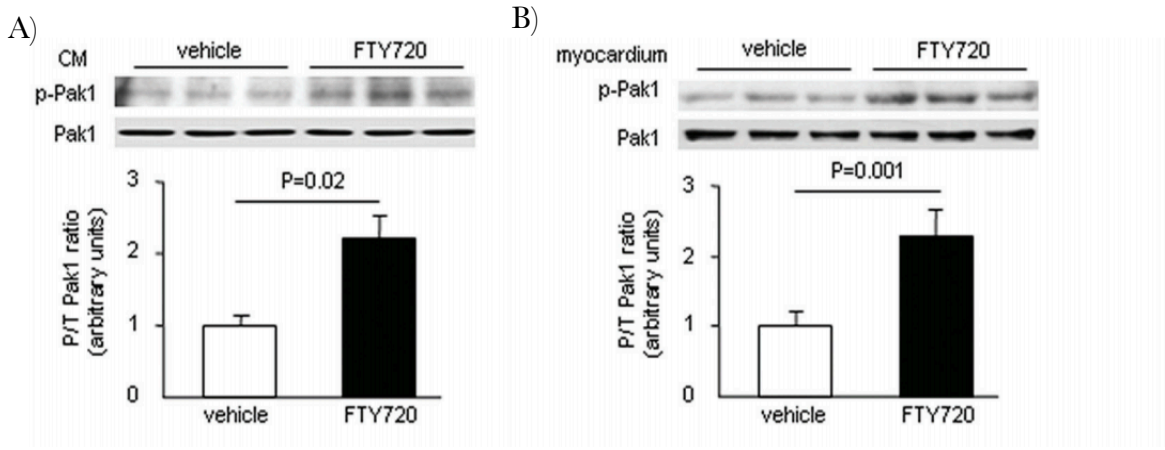

Figure 1.8.2 *Effect of FTY720 on PAK1 activation.* **A)** immunoblot analyses of FTY720- induced Pak1 phosphorylation was examined using NRCMs lysis (100 nmol/L, 1 hour) and in myocardium (10 g/g, 1 hour). **B)** The ratios of P/T Pak1 are represented by the bar graphs n=5. (Figure derived from Liu et al., 2011)

FTY720 was also elicited therapeutic benefit by attenuating Transverse Aortic Constriction (TAC) induced hypertrophy (Liu et al., 2011). Mice that were subjected to two weeks of pressure overload through TAC exhibited a significant increase in their myocardium size – a primary indication of cardiac hypertrophy. Mice that were given a co-treatment of FTY720, on the other hand, showed significantly improved cardiac functions and attenuated pressure overload-induced hypertrophy (Liu et al., 2011). FTY720 treatment was also shown to decrease

fibrosis in TAC induced mice. This was revealed to be through activation of Pak1 in fibroblasts that caused a reduced expression of periostin (Liu et al., 2013). Interestingly, this effect of FTY720 was abolished when using a mice model that had a selective cardiac PAK1 deletion (PAK1 conditional knock out – $PAK1^{CKO}$), suggesting the likely mechanism of FTY720's cardioprotective effect to be primarily through PAK1 activation (Liu et al., 2011; Egom et al., 2011). These abounding evidences support PAK1 as a novel antihypertrophic regulator and suggest that indirect PAK1 activators, such as sphingosine analogue, may be a potential therapeutic intervention for the treatment of cardiac hypertrophy and heart failure.

1.8.2 PAK1 Activating Peptide (PAP)

The cardioprotective significance of PAK1 activators (e.g. S1P and FTY720) suggests its therapeutic usage of developing a direct PAK1 activator – a molecule that can selectively target PAK1 and activate its intracellular activity. One sensible method of activating PAK1 was through targeting the auto-inhibitory domain (AID) of the PAK1 regulatory domain. As the dimer dissociation is required in order for PAK1 to become activated, Lei and his group surmised that disrupting the dimerization through a molecule could directly activate PAK1 by preventing their inhibitory mechanism. Despite later experiments disproving sphingosine's ability to directly bind to PAK1 and causing activation, such concept was also proposed by Bokoch et al. in elucidating the mechanism of PAK1 activation with sphingosine lipid (Bokoch et al., 1998).

Such proof in concept in designing a PAK1-activating molecule was initially attempted through constructing a bioactive peptide called P21-Activating Peptide (PAP). This peptide contained a complimentary sequence of the PAK1 AID domain segment (TSNSQKYMSFTDKSA) along with an attached trans-activator of transcription (TAT) sequence (YGRKKRRQRRRG) which warranted its cell penetrance. The proposing hypothesis of this peptide was to have a complementary binding to PAK1 AID (specifically the ISD), which would thereby interrupt its dimer inactivation. Alternative mechanism of PAP action would be through increasing the

efficacy of its substrate binding. The ligand-based computer-aided drug discovery (LB-CADD) approach was used to analyze the ligand-protein interactions. Docking study of PAP was done in order to predict potential binding sites of PAP on PAK1 (Unpublished data, Figure 4.14).

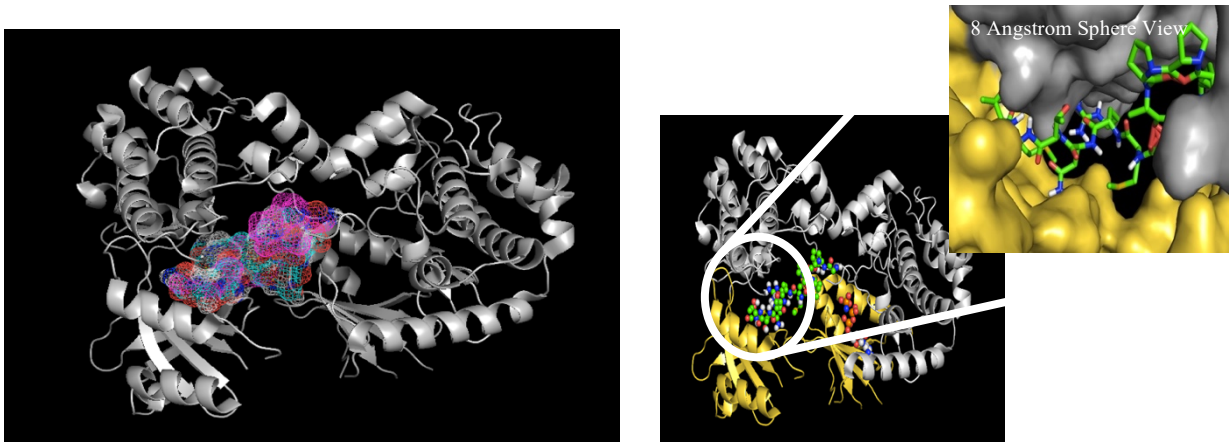

Figure 1.8.3 *In silico prediction of PAK1 activating biopeptides (PAPs) on PAK1*. Ribbon diagram of partial PAK1 crystal structure is indicated in grey color and its ATP bindings regions are indicated in gold. PAP1 (sequence: ■, color: magenta) and PAP2 (Sequence: ■, color: green) exhibited strong affinity near ATP-binding domain (ABD). 8 angstrom sphere display for zoom view. In silico predictions were performed through Autodocking VINA, and Pylmol program was used to illustrate the above figures.

The docking study revealed that PAP binds near the five beta-sheets and two alpha-helix regions, where the kinase inhibitory domain (KID) and the catalytic loop interact. With a relatively high affinity of 6.4 kcal/mol, it was possible to suggest that PAPs may affect the KID, conclusively disrupting the auto-inhibition. An alternative hypothesis to increase PAK1 activity may be through affecting the ATP binding ability in an allosteric manner. Qu et al. previously demonstrated that various drugs can affect P-glycoprotein binding affinity for nucleotides, up to a 4-fold increase, through altering its conformational changes (Qu et al., 2003). Adjustments of the binding affinity to favour association of ATP and dissociation of ADP provide further evidence that modulation of kinase activity may be achieved through targeting the allosteric site.

Through *in vitro* western blot studies, Wang and her collaborators have shown that when cardiomyocytes are incubated with PAP, a two–fold increase in PAK1 phosphorylation could be observed in cardiomyocytes, indicating an increase in PAK1 activation (Wang et al., 2014). Further studies demonstrated that treatment of PAP results in antagonizing stress-induced hypertrophy and ventricular arrhythmias in *in vivo* and *in vitro* models (Wang et al., 2014; Ke et

al., 2015). The PAP treatment also abolished PAP angiotensin II-induced hypertrophy in neonatal rat ventricular myocytes (NRVM). Further comparison studies between PAP treated and non- treated NRVM indicated that PAP is able to protect hearts from ventricular arrhythmia associated with hypertrophy; that is, ventricular arrhythmogenesis frequency was reduced by more than three-fold (see Figure 5.1.A). Furthermore, PAP co-infusion for 48 hours in NRVM showed greater reduction in the areas of fibrosis induced by angiotensin II. PAP-treated cells displayed a decrease in the fibrotic staining around blood vessels and reduced the intensity of interstitial collagen deposition, which are diagnostic markers for fibrogenesis (see Figure 5.1.B). As cardiac hypertrophy and the associated fibrosis are important risk factors for the development of heart failure, and reduction of these symptoms by PAP suggests that activation of PAK1 can provide an effective measurement against the CVD complications.

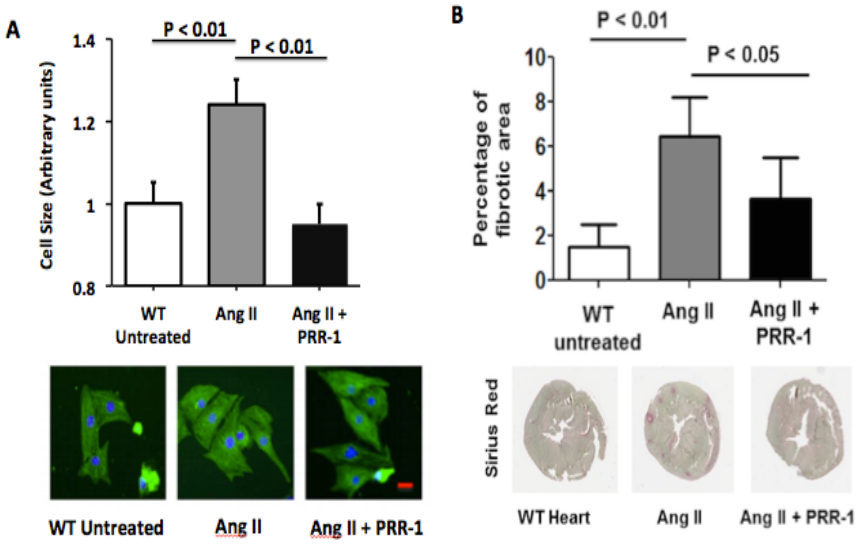

Figure 1.8.4 *PAP attenuates stress-induced hypertrophy and decreases percentage of fibrotic area.* Activation of PAK1 through PAP administration showed decreased in **A)** the cell size and **B)** percentage of fibrotic areas induced by Ang II. Neonatal rat ventricular myocytes (NRVM) were treated with wither Ang II (500nM) with or without co-treatment of PAP (PRR-1) (20u/ml) for 48 hours Images derived from (Figure derived from Wang et al., 2013)

1.9 Aim of Thesis: Small-molecule PAK1 Activator

Therapeutic implications of PAK1 as well as clinical validations of PAK1-activating peptides (PAPs) in providing cardioprotective mechanism showed promising therapeutic implications against cardiovascular diseases. While peptide drugs are ever increasingly recognized as being highly selective and efficacious for therapeutic usage (Vlieghe et al., 2009), their unfavorable intrinsic properties still render them unattractive when compared to the traditional small molecules. Peptide drugs' poor chemical and physical stability account for low plasma half-life and unfavorable as oral drugs. Other downsides include proneness to hydrolysis, oxidation, tendency for aggression, and low plasma permeability (Fosgerau and Hoffman, 2014). Although the peptide drug market is steadily increasing in size and value, small-molecule drugs are still the most favorable drug type today (Vlieghe et al., 2009). For these reasons, we wanted to translate from the current peptide drug (PAP) into a small molecule drug that can activate PAK1 directly.

The aim of this thesis is to explain the rational and the process of developing a small molecular compound that can directly stimulate P21-activated kinase (PAK1) activity. Each chapter entails a short background information, followed by a detailed description of the hypothesis, and concludes with experimental purposes (All the experiments procedures are detailed in the Appendix 1). Results of experiments are analyzed with appropriate statistical methods, and the implications of results are discussed subsequently.

The drug discovery process of small molecule PAK1 activator is outlined as the following: Chapter 2 '*In silico* Drug Discovery: PAK1 Small-molecule Activator' describes how the first PAK1 activators were discovered using modern computational methods. The hit compounds from *in silico* screening were then synthesized and tested for their efficacy in activating PAK1 *in vitro* assays. Chapter 3 'Validation of PAK1 Activators' entails validation of the hit compounds through in vitro kinase assays and immunostaining to confirm their efficacy in activating intracellular PAK1 directly. This chapter also explores other possible PAK1 activating analogues – through limited optimization process – and shows structure activity relationships. In Chapter 4 'Clinical Translation: Small-molecule PAK1 Activators', therapeutic implications

of the selected PAK1 activators were investigated. Various cell lines, cardiac tissues, and ex vivo whole heart were used to measure PAK1 activators' efficacy in providing cardioprotections and improvement in cardiac functions. Chapter 5 'Molecular Insight into PAK1 Activators' provides preliminary studies in understanding the mechanism action of the JB compounds. These results were later found to be crucial in providing foundation for biophysical experiments.

This research has been fortunate enough to have won various awards and support. Amongst all, the LAB282 award, in collaboration with a pharmaceutical biotech company Evotec, has been a crucial support in further developing the compound and understanding the PAK1 activators' mechanism of action. Chapter 6 'Mechanism Action of PAK1 Activators" describes collaborative projects between Evotec and University of Oxford. It explores the lead compound optimization processes, biochemical property improvements, as well as mechanism of action of JB compounds using photoaffinity labelled-mass spectrometry (PAL-MS) and co-crystallography x-ray methods. Finally, the thesis ends with final remarks of the findings and what future applications these small molecule PAK1 activators can provide in today's scientific field and clinical settings (Chapter 7).

CHAPTER 2

IN SILICO DRUG DISCOVERY: PAK1 ACTIVATORS

Summary Points

- Due to its high throughput screening and cost-effectiveness, computational *in silico* method is ever more popular and is becoming a common method of practice for discovering novel therapeutic drugs.
- Structure based virtual ligand screening (SBVLS) approach, utilizing two different software - ICM-VLS and Autodock Vina - were set up, along with virtual ligand screening to screen for ligands with high affinity at the AID of PAK1.
- Compounds with high affinity scores were selected and inspected to filter out any compounds with undesirable physiochemical properties.
- Promising selected compounds were synthesized and tested through ADP-GLO™ kinase assay to assess whether or not the compounds conferred any stimulatory effect on PAK1 activity.
- Of the screened compounds, JB01 exhibited significant stimulatory effect (2.3-fold increase) in the enzymatic activity, proving to be the first validated small molecule PAK1 activator.

2.1 Background Overview

Drug discovery is a process of discovering new candidate medications for a specific therapeutic indication. Creating an effective therapeutic drug is a multi-stage process that involves recognizing clinical symptoms of the disease, finding the molecular defect, and creation of appropriate pharmacological interventions. Accordingly, designing an effective therapeutic drug requires a synergy of various research fields and techniques—including (but not limited to) molecular biology, biochemistry, organic chemistry, and computer science. To illustrate, molecular biology integrates genetic information to be dealt with concrete biochemical and chemical terms, which is essential to explain the mechanism of a defect on the molecular level (e.g., DNA mutation). Furthermore, biochemistry provides a comprehensive understanding of the functioning of therapeutic target functions in a cellular environment and the mechanisms involved in regulation of the target activity (e.g., mechanism of activation). Next, organic chemistry provides insights into the chemical nature of the binding pocket, ligand interactions, and surface structural of information of therapeutic targets. Finally, computational modeling and docking studies are largely reliant on modern software programs that are indispensable for ligand optimizations processes and prediction of the ligand binding sites.

Today's drug design also requires an extensive knowledge of research techniques and available scientific validations. With the advent of genomic sciences, new research techniques—such as rapid DNA sequencing, combinatorial chemistry, cell-based assays, and other *in vitro* assays mimicking the cellular environment—have enabled researchers to explore novel ways to affect therapeutic targets' activity. Applications using recombinant proteins are also essential to validate the target's mechanism of action and selectivity of the molecules. Techniques such as high-throughput screening (HTS), fragment-based screening (FBS), co-crystallography in combination with molecular modeling, as well as combinatorial and parallel chemistry, provide a wide array of chemical lead structures. The results of *in vivo* studies provide a better understanding of the molecule's preclinical therapeutic effect on relevant disease models and can assist in accelerating and de-risking later-stage clinical development (Sim and Kauser, 2015). Finally, *in vitro* cell assays and *in vivo* studies help to validate the safety and toxicity profiles of the compounds. In particular, *in vivo* animal tests make it possible to determine

pharmacokinetics and pharmacodynamics of the drugs' ADMET. In sum, today's rational drug design requires an integration of various applications and a synergy of knowledge accumulated in various research fields.

In the traditional method of finding hit compounds, candidate drugs have been frequently discovered by testing libraries of compounds synthesized in time-consuming multi-step processes, followed by confirming the efficacy of these compounds using both *in vitro* and *in vivo* assays. A common example of this approach is the high throughput screening (HTS) that involves screening large compound libraries against the therapeutic target of interest. However, such synthesizing of compounds and their manual testing is a high-cost and time-consuming process. In view of the growing R&D costs and the decreasing rates of drug approval, an estimated price tag of developing a new drug and introducing it into the market amounts to $2.6 billion (Tuft's Centre, 2014). Due to these high costs and a low hit rate associated with the traditional HTS, in recent years, the computational approach *(in silico)*, which is based on cheaper and faster screening methods, has been encouraged for broader applications (Ripphausen et al., 2010; Cheng et al., 2011).

Accordingly, recent years have witnessed a rapid growth in the popularity of computational methods of therapeutic drug discovery. One of such methods is Virtual ligand screening (VLS)—a hit identification technique based on either ligand similarity (ligand-based virtual ligand screening, LBVS) or target structure docking (structure-based virtual ligand screening, SBVLS). The LBVS method uses statistical approaches to correlate ligand activity to structural information and is frequently applied as an alternative modeling technique when protein structures are not determined (Huang et al., 2010). A commonly used LBVS method involves screening libraries of virtual compounds into the ligand of interest. For both endogenous biologics and FDA proven drugs, the process involves searching the compounds with similar pharmacophore properties and correlating spatial arrangements. As to the SBVS method instead of using a ligand as a model of prediction, it uses the determined protein structure from either X-ray diffraction or NMR to 'dock' virtual ligands onto the active site. Molecular docking is a computational procedure to predict noncovalent binding of receptors and a small-molecule ligand with the aim of predicting the bound conformations and binding affinity.

Computational docking helps to check the stereochemistry, energy profiles, residue environments, and structure similarity to ensure rationality of the model fitting. Both LBVS and SBVLS techniques employ statistics and mathematical modeling to investigate the relationship between structures of ligands and their corresponding effect. For the initial discovery of PAK1 activators, as no PAK1 small-molecule activators were available, the SBVLS method was mainly used. However, during the optimization process of PAK1 small-molecule activators undertaken in the present study, both SBVLS and LBVLS methods were applied to further improve the lead compound (see Chapter 3 and 6 for a detailed discussion).

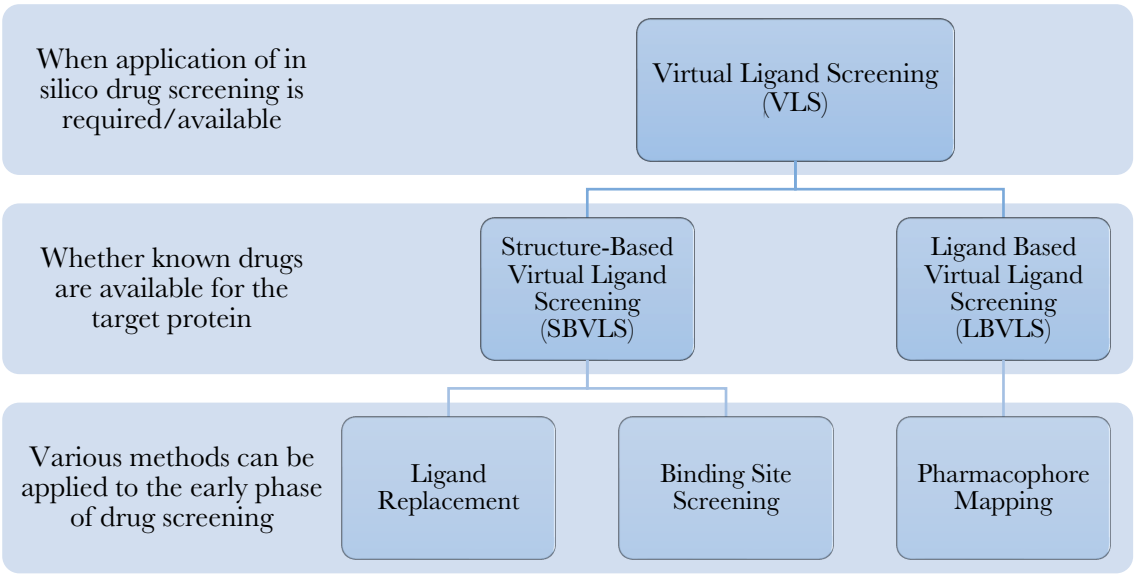

Figure 2.1 *Summary of Virtual Ligand Screening (VLS) Strategies.* Based on whether the structural information is available or not, either the structure-based virtual ligand screening (SBVLS) or the ligand-based virtual ligand screening (LBVLS) is available for the *in silico* drug discovery.

2.2 Structural Based Virtual Ligand Screening (SBVLS)

Structure-based drug design relies on three-dimensional knowledge of the receptor structure and the active sites in order to investigate their interaction, binding energy and steric relationships. The modeling uses an analysis of the complementary chemical features of the predicted binding site and creating an interactive map where the ligands can be screened. Interactive maps include for pharmacophoric features of ligands such as a hydrogen-bond acceptor, a hydrogen-bond donor, hydrophobicity, stereochemistry, energy profile, residue environment, and force fields (Jorgensen et al., 2004). The prediction of small molecule binding to proteins is of particular importance as it is used to screen virtual libraries of drug-like molecules and to predict the bound conformation of the ligands.

Applications of SBVLS continues to play an essential role in various stages of the drug discovery. From hit identifications to drug optimization, SBVLS has become central to developing drug candidates, and the success of the method is evident from the drugs derived from such structure-based approaches (Congreve et al., 2005; see Table 2.2). However, some limitations and assumptions need to be considered when doing the SBVLS approach in drug discovery. The molecular docking approach commits a particular protonation state and a charge distribution of molecules which may not accurately represent the actual biological state. Secondly, the docking set-up assumes that the receptors are rigid and that there are no changes in the conformation of the protein (making the covalent length and the angular torsion constant through the docking process). However, these assumptions are not true of course as proteins have been known to be dynamic and adapting its structures based on its environmental conditions. Molecular docking, therefore, contains some limitation in simulating of ligand binding; it is rather a qualitative assessment with elements of quantitative algorithms to approximate the bound conformation preference and the free energy of binding (Trott and Olson, 2010).

Accurate representation of the binding site through knowing the protein-ligand complex can be derived from either an x-ray co-crystallography or NMR study. These results can significantly increase the chances of success in finding a hit compound through the virtual ligand screening method. In the case where the crystallography or NMR results are not

available, homology modeling is also available as an alternative, when using a comparative 3D protein modeling based on similar homologous proteins. Examples of these protein modelling servers include 'SWISS-MODEL' and 'ProteinModelPortal' which are fully automated online platforms. The homology modeling relies on the 'template' of homologous protein with similar amino acid alignments and requires greater than 30% sequence identity in order to predict its structure with increased preciseness (Marti-renom et al., 2000). Such modeling strategy has been widely applied in many researches and have shown successful usage for SBVLS (Glaab, 2015). However, success in homology docking is highly dependent on the quality of the modeling and the template structure. Large gaps between the conserved sequences and lower than 30% alignment, for example, can lead to inaccurate prediction of the bioactive conformation mapping. Without this rigid reference, the pharmacophore characterization of the active site would not be precise, which may subsequently affect the VLS results.

Fortunately for PAK1, its structural and mechanism of activation have been extensively studied. Solved structures of PAK1 were available at the Uniprot 3D structure database (http://www.uniprot.org/uniprot/Q13153) as well as in the Protein Data Bank (www.rcsb.org/). Amongst the determined structures, however, only two PDB files contained information about the autoinhibitory domain (AI: position 70 ~140) of PAK1 (PDB entry: 1F3M & 2QME), and majority of structures represented only the kinase domain (KD: position 270 ~ 521) (McCoull et al., 2016; Staben et al., 2014; Maksimoska et al., 2008; Ndubaku et al., 2015). Only the PDB:1F3M was suitable for the virtual ligand screening based on the solved structure since the hypothesized mechanism of action of PAK1 activators were thought to bind to the auto-inhibitory (AI) domain. The secondary structure of PAK1 indicated different functional domains are shown below for your reference (see Figure 2.2)

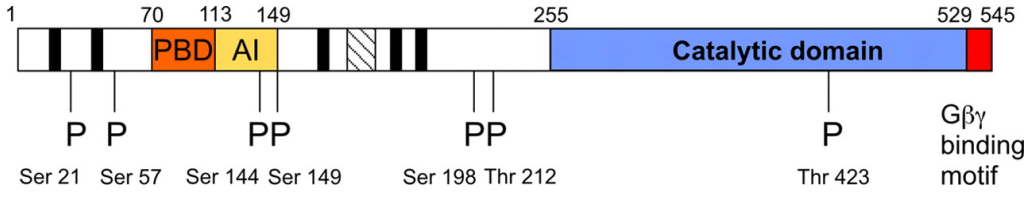

Figure 2.2 *Schematic of PAK1 structure showing functional domains and auto-phosphorylation sites.* The auto-inhibitory (AI) domain conforms PAK1 in an inactivation state in which inhibits the kinase domains. The proposed mechanism of PAK1 activators are through the inhibition of the AI domain – which consequently keeps PAK1 in the active conformation.

Table 2.2 *Drugs Derived from Structure-based Approaches*

Trade name	*Generic name*	*Structures*	*Mechanism*	*Disease area*	*Date*	*Company*	*Reference*
Capoten	Captopril	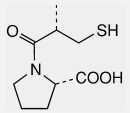	Angiotensin-converting enzyme	Hypertension	1981	Bristol-Myers Squibb	Cushman et al., 1977
Trusopt	Dorzolamide	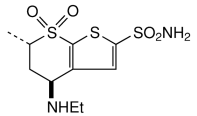	Carbonic anhydrase	Glaucoma	1995	Merck	Baldwin et al., 1989
Viracept	Nelfinavir	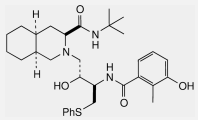	HIV protease	HIV/AIDS	1999	Agouron (Pfizer) and Lilly	Kaldor et al., 1997
Agenerase	Amprenavir	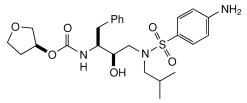	HIV Protease	HIV/AIDS	1999	Vertex and GSK	Kim et al., 1995
Aluviran	Lopinavir	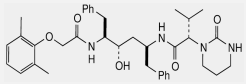	HIV Protease	HIV/AIDS	2000	Abbott	Sham et al., 1998
Relenza	Zanamivir	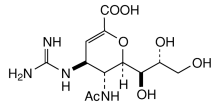	Neuraminidase	Influenza	1999	Monash University and GSK	Von Itztein et al., 1993
Tamiflu	Oseltamivir	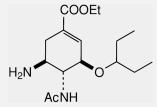	Neuraminidase	Influenza	1999	Gilead and Roche	Kim et al., 1998
Gleevec	Imatinib	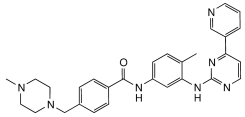	BCR-ABL	Chronic myelogenous leukaemia	2001	Novartis	Zimmerman et al., 1996
Tarceva	Erlotinib	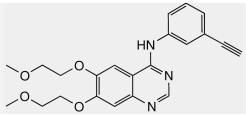	EGFR	Non-small cell lung cancer	2004	OSI and Genentech	Pollack et al., 1999
Exanta	Ximelagatran	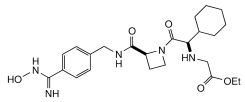	Thrombin	Venous thromboembolic events	2004	AstraZeneca	Gustafsson et al., 2001

Table Derived from Congreve et al., 2005

2.3 Discovery of PAK1 Activator: Virtual Ligand Screening Overview

Studies on PAP illustrated that the peptide drug can relieve the kinase inhibition, disrupting the dimer contract, and allows for rearrangement of the kinase active site into a catalytically competent state (Wang et al. 2011). This has provided supportive evidence that small molecules could also inhibit the AI domain and activate PAK1 – thereby, providing an therapeutic cardioprotective effect. In order to look for a small molecule that can modulate PAK1 activity, through such mechanism of action, we used computational *in silico* approach, specifically using SBVLS, to look for molecules that had high affinity towards the PAK1 AI domain. PDB:1F3M was used to set up SBVLS, as this was this was the only crystal structure which provided structural insight of both the AID and KD of PAK1 (Lei et al., 2000). Other available crystal structures contained only variants of the kinase domains, making it ineffective to screen molecules at the AID.

Althought 1F3M still had missing segments between a.a. 1 – 70 & 149 – 245, this crystallography structure was particularly important for our SBVLS. The study revealed that the PAK1 dimerization is mediated by the AI domain and anchored by the kinase-associated state of the AI domain, demonstrating further level of regulatory complexity in its mechanism of activation. PAK1 required both the residues from 78 to 87 and the intact AI domain to be able to dimerize correctly (Lei et al., 2000). The regulatory domain was folded in association with the large lobe of the kinase domain and allowed the blocking the catalytic kinase cleft and its activity (see Figure 2.3). This preliminary evidence has provided us with a proof of concept that targeting the PAK1 AI domain may be used as an allosteric site of PAK1 regulations.

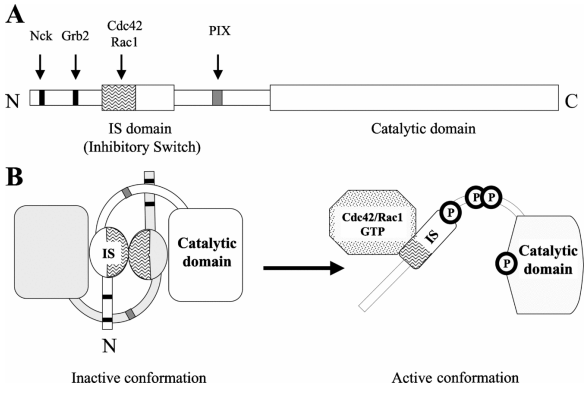

Figure 2.3 *Diagram representation of PAK1 structure.* **A)** secondary structure of PAK1 kinase. The IS domain is the inhibitory switch. CDC42 interaction and RAC1 occurs is highlighted with shades. **B)** *Mechanisms of PAK1 dimer activation*. At inactive state, PAK1 is in a homodimer conformation, where the catalytic domains are covered by IS domains. Upon activation by Cdc42/Rac1 GTP-bound form, the homodimer is dissociated into respective monomers, and the exposed catalytic domain is available for phosphorylating other substrates. Diagram derived from (Figure derived from Parrini et al., 2005)

For PAK1 activator *in silico* methods, a number of protein-ligand docking programs were initially tested to find the suitable SBVLS application. AutoDock (The Scripps Research Institute), AutoDock Vina (The Scripps Research Institute), 1-Click Docking (Mcule), SwissDock (Swiss Institute of Bioinformatics), Glide (Schrodinger) and Molecular Operating Environment (MOE, Chemical Computing Group), and ICM-Pro (Molsoft) were a few names of programs that were initially applied for PAK1 SBVLS (see Table 2.3.1). Programs with high user-friendly mechanics, robust screening sensitivity, and program contact supports were favoured as we had lacked the expertise in computer coding and programing. Amongst the tested protein-ligand docking programs, AutoDock Vina (The Scripps Research Institute) and ICM-VLS Pro (Molsoft) were particularly easy to utilize and contained detailed manual instructions – which made the set up more user friendly compared to other programs. These two programs were then applied to perform initial screening of the PAK1 activators. ICM-VLS Pro (Molsoft) was used firstly used for virtual ligand screening of various compound libraries. Of the few compounds which showed high affinity with energetically favourable scores, these compounds were then re-docked using the AutoDock Vina (The Scripps Research Institute). The purpose of the re-docking using another program is to ensure the scorings of the docking results are consistent between the programs. This is to mitigate any outliers, or incongruent scores found amongst programs which may be using different algorithms to perform the virtual ligand screening.

Program	Organisation	Description	Webservice	License
DOCK (1988)	University of California-San Francisco	Based on Geometric Matching Algorithm	No	Freeware for academy
AutoDock (1990)	The Scripps Research Institute	Automated docking of ligand to macromolecule by Lamarckian Genetic Algorithm and Empirical Free Energy Scoring Function	No	Freeware
ICM-Dock (1997)	Molsoft	Docking program based on pseudo-Brownian sampling and local minimization	No	Commercial
Glide (2004)	Schrödinger	Exhaustive search-based docking program	No	Commercial
Molecular Operating Environment (MOE) (2008)	Chemical Computing Group	Docking application within MOE; choice of placement methods (including alpha sphere methods) and scoring functions)	No	Commercial
AutoDock Vina (2010)	The Scripps Research Institute	New generation of AutoDock	No	Open source
1-Click Docking (2011)	Mcule	predicts the binding orientation and affinity of a ligand to a target	Available	Basic free version
SwissDock (2011)	Swiss Institute of Bioinformatics	Webservice to predict interaction between a protein and a small molecule ligand	Available	Freeware for academy

Table 2.3 *List of protein-ligand docking software used for PAK1 activator in silico studies.* The following list presents an overview of the programs used for development of small molecule PAK1 activator, with indication of the corresponding year of publication, organisation or institute, description, and availability of the website and the license services (See Appendix 2 for a full list of available programs).

2.4 In silico Program: ICM-Pro VLS, Molsoft

ICM-VLS Pro is a virtual ligand screening platform that combines the genuine internal coordinate docking methodology with a sophisticated global optimization scheme. It features fast and accurate flexible-ligand docking and scoring procedures, screen large databases from compound libraries, template docking for pharmacophore-based drug-design, and allow for easy user interface for the screening process (ICM Guide., 2011). ICM docking is considered to be the most accurate predictive tools of binding geometry today as they have ranked consistently in the first place amongst many other competitors (Bursulaya et al., 2003). ICM has therefore been successful in many drug design applications by scientists and academic industries. A number of success in drug discovery work were accomplished using the ICM-VLS Pro software, including INOs inhibitors (Zhong et al., *PLoS One* 2014), Neurophilin inhibitors (Borriello et al., *Cancer Lett.* 2014), Sirtuin 2 inhibitor (Outeiro et al., *Science* 2007), Androgen

receptor antagonists (Bisson et al., *Proc Natl Acad Sci*, 2007) and HIV-1 TAR antagonists (Stelzer et al., *Nat Chem Biol.* 2011).

One of the additional features of the ICM-VLS Pro is its ability to identify potential binding pockets within the targeted structure. Although the PAP study suggested that the binding site is likely to be at the AI domain, the lack of ligand-bound protein crystal-structures and the details of the active site map were not available for efficient and accurate methods of virtual ligand screening. ICM-VLS Pro was able to resolve such issue through using the 'Atomic Property Field (APF)' function – where it can provide a 3D pharmacophoric potential implemented on a continuously distributed grid. This can be used for ligand docking and mapping of 'binding pockets' where the ligand can be screened (Totrov et al., 2008). Using this designed method, we were able to identify potential ligand binding sites within PAK1 and be able to screen libraries of virtual compounds (see Figure 2.4.2). The program was also found to be functional for the ligand optimization processes. The ICM-VLS Pro contained in-house chemical monitor panel which allowed users to understand its physiochemical profiles at a glance. The monitoring chart provides all the relevant chemical properties of the compound with color coding – green indicating drug like property and red indicating lesser drug-like properties (see Figure 2.4.3) These additional features have made the *in silico* processes a lot easier to perform.

2.4.1 ICM-Pro VLS: PAK1 Receptor Preparation

The solved PAK1 structure (PDB: 1F3M) was firstly imported onto the ICM-VLS Pro through the PDM search. The imported PAK1 structure should illustrate a dimer (interlocked monomers) of PAK1 with four different structural domains, under the objects' names 'a', 'b', 'c', 'd'. These four domains represent two auto-inhibitory (AI) and two kinase domains of the PAK1 dimers (see Figure 2.4.1). The protein structures were then converted from the general PDB file to the program specific ICM file. This process allows for optimization of the hydrogen atoms, assign secondary structures, and replace the non-ICM structure with the optimized structure (this conversion is crucial in allowing the program to recognize the protein structural for subsequent molecular docking and VLS studies). In addition to the conversion, the iodine

and surrounding water molecules were also deleted, in order to expose only the protein backbones. The secondary chains were then colored differently for easier recognition of the functional domains (figure 2.4.1).

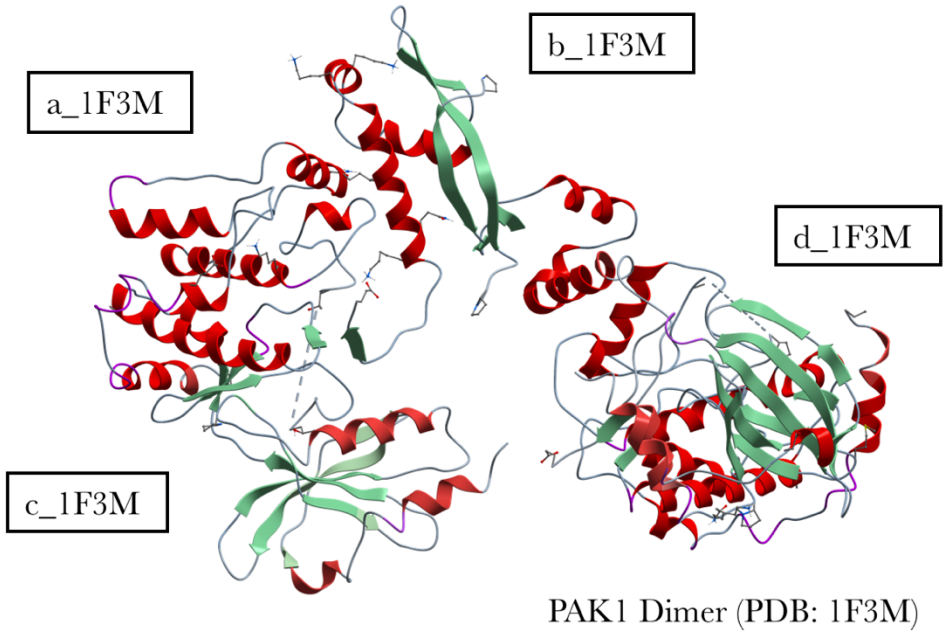

Figure 2.4.1. *PAK1 (PBD:1F3M) Setup for Virtual Ligand Screening (VLS).* ICM-VLS Pro program was used to identify the following potential drug binding pockets in PAK1. a_1F3M & b_1F3M represent AID of PAK1 dimers, while c_1F3M & d_1F3M illustrates the kinase domain. PAK1s are dimerized through the a & b subunits where the two beta sheets are interacting (indicated by the arrow). Secondary structures are colored accordingly for easier understanding of the protein structures: α-helices (●) & β - sheets (●). PDB: 1F3M (Lei et al. 2000).

From the dimer PAK1 structure, only the monomer (domains 'a' and 'c') were used to search for the ligand binding site in order to avoid any duplication in the virtual ligand screenings. It was also important to allow the interlocking AID domain to be fully exposed. Therefore, the other two domain, 'b' and 'd' were deleted when setting up the macromolecule (receptor) for the VLS. Under 'Setup Receptor', receptor object 'a_1f3m.' (the AI domain) was selected and optimized while keeping the tight bound water, optimizing the existing hydrogen and the side chains. When the PAK1 monomer was scanned for potential binding pockets, the ICM-VLS Pro had indicated 4 possible binding pockets within the a_PAK1 & b_PAK1 structures (see Figure 2.4.1.A). Pocket 1 was selected as it was the only pocket within the AI domain, containing a large cavity where the PAK1 monomers were found to interact and to dimerize. Within the pocket, the position of the ligand-probe and size of the screening box were kept the

same as the program had indicated. Ligand libraries obtained from 'ZINC' were subsequently screened using this screening set-up.

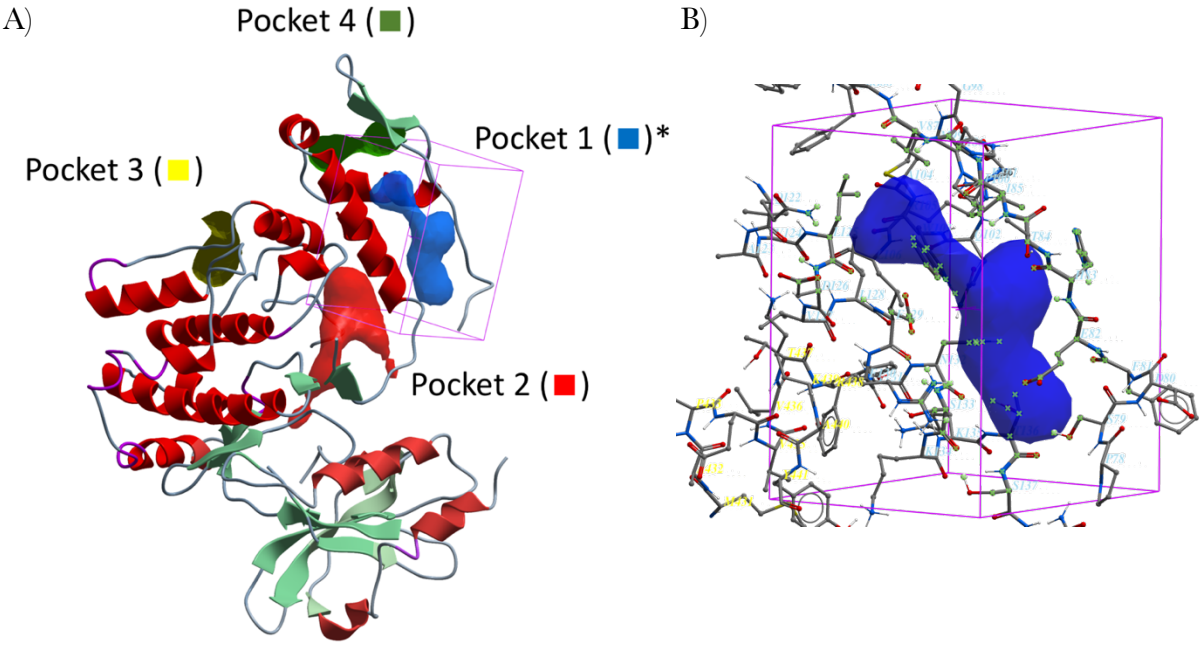

Figure 2.4.2. *Virtual Ligand Screening (VLS) protein pocket setup.* **A)** ICM-PRO VLS program was used to identify the following potential drug binding pockets in PAK1. Among the 4 pockets, pocket 1 was within the regulatory domain were the auto inhibitory resided. Pocket 1 was therefore set up to screen compound libraries. **B)** VLS Pocket with Selected AA in the PAK1 AI domain. The indicated binding pocket at the auto-inhibitory domain (■) was used to screen virtual ligands. Molsoft ICM-Pro was used to generate the screening pocket and to screen compound libraries. The following amino acids (aa) are the key aa in forming the indicated pocket: S79, D80, F81, E82, H83, T84, I85, H86, V87, V103, L125, D126, L128, E129, N131, S133, K134, I136

The ICM-VLS Pro's identifying function was able to detect the amino acids that were essential in creating the VLS pockets (See Figure 2.4.2.B). The AI domain consists of 42 amino acids, amongst in which 19 of these amino acids were form the potential binding pocket: S79, D80, F81, E82, H83, T84, I85, H86, V87, V103, L125, D126, L128, E129, N131, S133, K134, I136. A few of these highlighted amino acids were previously studied through mutagenesis and were found to be important for regulating the enzymatic activity of PAK1. For example, PAK1 mutations at either position 83 (histidine → leucine) or 86 (histidine → leucine) were indicated to abolish the interaction between PAK1 and CDC42 and exhibited a decrease PAK1 activity in comparison to control PAK1/CDC42 activity. Mutagenesis studies at position 107 (leucine → phenylalanine) or at position 131 (tyrosine → cysteine) illustrated an increase in PAK1

activity. This was hypothesized to be due to the mutation having a disruptive effect on the auto-inhibitory function of PAK1 and thereby constitutively activating the kinase (Zenke et al., 1999). Since some of the amino acids (specifically, a.a. 83, 86, and 131) previously studied through mutagenesis were depicted by the ICM-VLS Pro program, we assumed that inhibiting these specific residues through small molecules would be likely to modulate PAK1 activity.

2.4.2 ICM-VLS Pro: Virtual Ligand Screening

ZINC (ZINC Is Not Commercial) is a public access database that has been developed to enable ready access compounds for virtual ligand screening (Irwin and Shoichet, 2005; Sterling and Irwin, 2015). The data base contains libraries of 35 million commercially-available compounds for virtual ligand screening, each compound detailed with 3D structure, biological protonation states, and vendor information. physiochemical properties – such as the molecule weight, calculated LogP, and number of rotatable bonds – are also annotated for each compound, enabling filtration of compounds with unfavorable physiochemical properties (Irwin and Shoichet, 2005). ZINC database offers these compound libraries to be downloaded for free and also offers an analysis tool which contains all the relevant information about the compound's effect on previously studied biological targets. Summary details on these compounds are especially useful for understanding its biological activity and allows for exploring alternative therapeutic indications. ZINC database has been highly utilized and benefited the scientific community, for both the academia and the pharmaceutical companies; as of May 2018, the published ZINC journal paper has been cited by 2696 other literatures. Due to its popularity, the authors had recently launched its new database platform called 'ZINC 15' which contains a better web interface, easier filtration of compounds, improved molecular docking and target-focus libraries, compared to the previous ZINC website (Sterling and Irwin, 2015).

As the ZINC database is widely utilized and for free, we had also used their database to perform the virtual ligand screening. Subset libraries of commercially available lead-like compounds were downloaded and screened against PAK1 AID (Pocket 1). 'Batch docking' is a method of automatically screening compound libraries that contain hundred-thousands of compounds, instead of individually setting up one compound by another. For this screening, the docking

thoroughness was set to 1 as it was considered reasonable value for screening compounds at the buried hydrophobic pocket (personal comm. with Andrew from Molsoft). An estimated total of 780,000 compounds were screened in a period of month, and the docking scores were evaluated based on the total affinity and the energetically favourable. Docking programs generally use a scoring function that can be used to evaluate the approximate standard chemical potential binding. The docking score, VLS-Score, measures the affinity to bind at the active site, whereas the steric measures the hindrance from overlapping electron clouds. The VLS-score also considers the internal force-field energy of the ligand, conformational entropy loss of the ligand, receptor-ligand hydrogen-bond interaction, solvation electrostatic energy change, hydrogen-bond donor/acceptor, desolvation, and hydrophobic energy (Totrov et al., 1999). The score is trained to separate binders and nonbinders and to rank the compounds based on the interaction scores. Therefore, the overall score output measures the cumulative summation of each property scores, and the lower the value indicates that the better docking scores. The scoring function is considered to be the most recognizable method in evaluating the binding affinity and exploring the binding space of a ligand (Cheng et al., 2012).

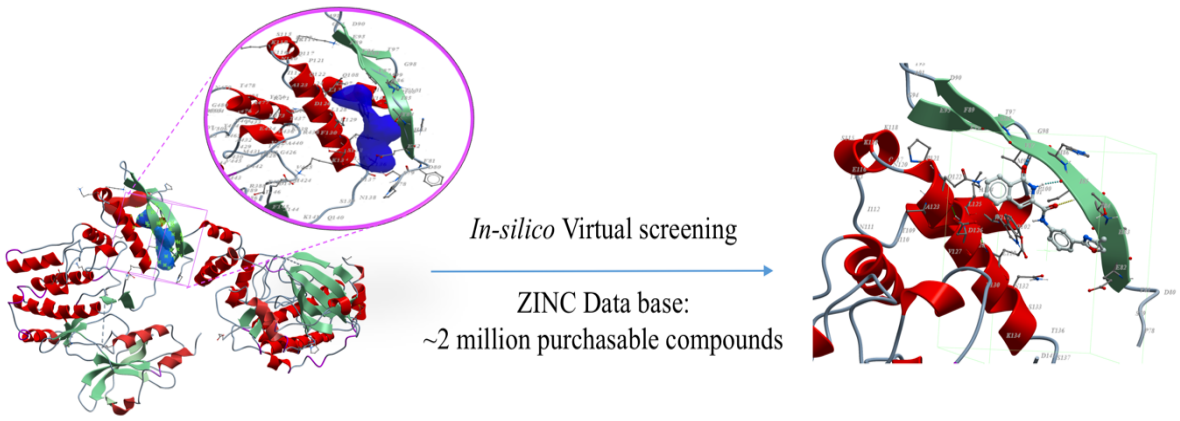

Figure 2.4.3 *In silico ligand screening at the PAK1 auto-inhibitory (AI) domain*. The indicated binding pocket at the auto-inhibitory domain (■) was screened using compound library database. Molsoft ICM-Pro was used to generate the screening pocket and to screen the compounds. The selected compounds were then further subjected to secondary docking studies using Autodock Vina – in order to confirm the compound affinity. Only the acceptable compounds that passed both studies were purchased and tested under *in vitro* kinase assays.

From the results screened compounds, 2,000 compounds ranked by ICM with best scores (representing 0.2% of the total compound database) were selected and further screened for the second time in order to mitigate any false positive readings. The secondary screened

compounds were visually inspected to eliminate any compounds with undesirable physiochemical properties: long carbon chain, metal containing core, radical groups, proton electron transfer, extended pi-system, other known functional groups that were cautious for ADMET and vendor availability. One of the commonly applied methods of filtering trivial analogues is to search for the pharmacophore similar to known actives compounds (seed structures) (Bleicher et al., 2003). In other words, if structure of compounds or drugs with biological effect on the target is already available, comparison can be made between the known effector compound and the screened compounds, and this could lead to design of similar compounds. This is also known as the ligand-based filtering and often utilized for finding alternative analogue of approved drugs. Such method of filtration, however, was not applicable for this PAK1 activator discovery, as no previous PAK1 activators have been ever reported. Therefore, compounds with high scores were manually analyzed individually, and the hit compounds were selected based on their likeliness of binding and favourable 'drug-like' physiochemical properties (e.g. Lipinski's Rule of 5).

In addition to the guidelines for designing compounds with drug-like properties, the ICM-VLS Pro contained in-house chemical monitor panel which allowed users to understand its chemical properties at a glance (see Figure 2.4.2). The chemical monitor provides the following properties: chemical formula, SMILES string, Name/IUPAC, InChI, InChI key, molecular weight, number of hydrogen bonds acceptors (HBA), number of hydrogen bond donators (HBD), number of rotatable bonds (RotB), drug-likeness, molecular area, delta Hf in gas, LogP, LogS, polar surface area, volume, PAINS, and functional groups. The colors of the rows indicate the closeness of the compounds' value to drug-like properties (from green ■, good to red ■, poor). Based on these filtration process, a few of the selected compounds were then further subjected to another docking software called AutoDock Vina to ensure that the binding scores were not bias from one algorithm.

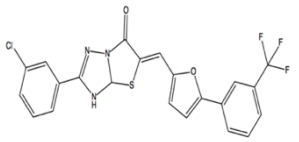

	Name	Value
1	Formula	C22 H13 Cl F3 N3 O2
2	Smiles	C(=CC1OC(=CC=1)C(=
3	Name/IUPAC	3-(3-chloro-phenyl)-7
4	InChI	InChI=1S/C22H13ClF3
5	InChIKey	ZGPNYZAWXDNKIF-WC
6	MolWeight	475.0369
7	HBA	5
8	HBD	1
9	RotB	4
10	DrugLikeness	-0.590838
11	MolArea	423.565
12	MoldHf	-99.2738
13	MolHalfLife	4.7925
14	MolLogP	6.73491
15	MolLogS	-8.55048
16	MolPAINS	0.102
17	MolPSA	48.1299
18	Volume	421.036
19	Chem Alerts	
20	Groups	Phenyl Furan Halo

ICM-VLS Pro Chemical Monitor Properties

1. Chemical Formula
2. SMILES string
3. Name/IUPAC Name
4. InChI
5. InChI Key
6. Molecular Weight (MolWeight)
7. Number of Hydrogen Bond Acceptors (HBA)
8. Number of Hydrogen Bond Donators (HBD)
9. Number of Rotatable Bonds (RotB)
10. DrugLikeness value Druglikeness is not based on other properties, this is separate model built using Bayesian Classifier (See: http://www.molsoft.com/mpropdesc.html). Normaly Bayesian classifier returns either 1 ot 1 (positive ot negative) therefore positive values means drug-like, negative - not.
11. Molecular Area (MolArea)
12. Prediction model build for 'delta Hf in gas' property using public NIST database (description can be found here: http://webbook.nist.gov).A low dHf value means that the compound is more 'stable'.
13. LogP (MolLogP)
14. LogS (MolLogS)
15. Polar Surface Area (PSA)
16. Volume
17. Chem Alert will flag any reactive group, PAINS or Bad ADME-TOX groups.
18. Groups option highlights chemcal groups in the sketch.

Figure 2.4.4 *ICM-VLS Pro Chemical Property Monitor.* The in-built chemical monitor allows for quick analysis of the compounds' physiochemical profiles, allowing us to quickly evaluate the drug likeness of the compounds. Descriptions of all acronyms are described in the chart on the right. The colors of the rows indicate the closeness of the compounds' value to drug-like properties (from green ■, good to red ■, poor)

2.5 Secondary Screening: AutoDock Vina

With the computational drug design methods becoming increasing invaluable in the drug discovery and development process, many different molecular docking programs have emerged to assist in the ligand screening procedure, each with multitude of scoring functions. Current scoring functions can be roughly classified into three categories (Cheng et al., 2012):

(a) Force-field based scoring function: a scoring based on the ligand-target interaction from the computed van der Waals and electrostatic energies. It often considers the GB/SA or PB/SA in order to account for solvation effect (Still et al., 1990; Meng et al., 1992).

(b) Empirical scoring function: calculates the overall binding free energy from several energetic terms, including hydrogen bond interaction and hydrophobic interaction.

(c) Knowledge-based scoring function: computes the ligand–target interactions as a sum of distance-dependent statistical potentials between the ligand and the target. The machine

learning helps to accumulate available structure-ligand complex information which further assists in constructing and optimizing the predictive model (Hechet and Fogel, 2009).

Various comparative studies have investigated the performance of scoring functions, based on the ability to reproduce known ligand-protein interactions from previous co-crystallography studies. As each algorithm and scoring function weights differently and contain both advantages and disadvantages, they had concluded that current scoring functions have levels of accuracy, which makes no single scoring function consistently better than others (Cheng et al., 2009; Warren et al., 2006; Ferrara et al., 2004; Wang et al., 2004). Therefore, depending on the properties of the ligand and the binding site, each algorithm displayed slightly different orientation as well as binding affinities. Based on these literatures, utilization of only one molecular docking software was considered premature and thus, we had decided to apply an additional molecular docking software so that we could confirm the scoring and ranking from the previous ICM-VLS Pro docking study.

Amongst the listed molecular docking software (See Table2.3), AutoDock Vina is one of the open-source programs for performing molecular docking studies, developed by the Scripps Research Institute. AutoDock Vina's molecular docking is a familiar computational procedure that can predict noncovalent binding of receptors and a small-molecule ligand, allowing to predict the bound conformations and the binding affinity. The AutoDock Vina is an upgraded version from the previously developed AutoDock software, in which the Vina version has approximately two times faster and more efficient screening method in comparison to that of AutoDock (Trott and Olsen, 2010). AutoDock Vina has been commonly used and widely applied in the computational drug discovery field; AutoDock is the most cited docking software in the scientific literature (Sousa et al., 2006). Based these approvals, AutoDock Vina was chosen as the secondary docking software to check for the consistency of the binding scores from the ICM-VLS Pro.

Unlike the commercially available ICM-VLS Pro, AutoDock Vina does not contain an application to screen a large batch of compounds with high efficiency and fast screening

methods. Therefore, each screened molecule had to be redocked individually against PAK1 protein using the following protocol:

Monomeric PAK1 crystal structure obtained from ICM-VLS Pro was firstly imported into MGL Tools, a software developed by the Scripps Research Institute for visualization and analysis of molecular structure. MGL Tools does not perform the molecular docking by itself but allows users to set-up the parameters for screening. In addition, it contains Python Molecular Viewer (PMV) – a molecular viewer that can display from molecular surfaces to advanced volume rendering, providing additional information on the interaction between the ligand and the receptor. Using MGL Tools, PAK1 monomer modified from the ICM-VLS Pro was imported to the MGL Tools and saved as 'protein.pdb' under the '\my documents\vina_tutorial' file. The imported protein structures usually do not contain hydrogens, so polar hydrogen was added and optimized. The edited protein was then saved again under the name 'protein.pdbqt' for AutoDock Vina screening. Similarly, the ligand was imported (choose free torsion if desired) and saved as 'ligand.pdbqt'.

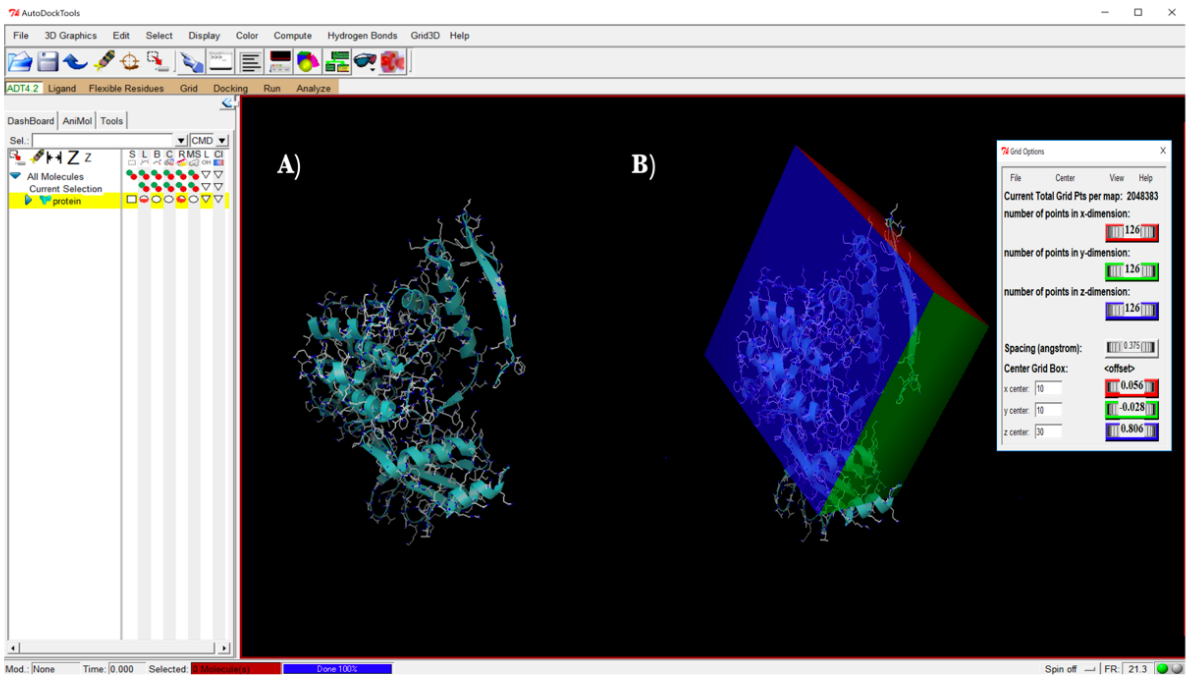

Figure 2.5.1: *PAK1 receptor set-up for AutoDock Vina using MGL-Tools.* A) *imported PDBQT file of PAK1 monomer from ICM-VLS Pro*. Polar hydrogens were added and the water molecules were removed from the structure to expose the carbon backbone. B) *Grid-box size for determining the screening parameters.* the coordination, dimension of the boxes was measured against PAK1 to determine the areas in which the AutoDock screening process will take place.

Under the grid box, autodocking parameters were determined; x- y- z-dimension were 126, 126, and 126, respectively and the center grid box x- y- z-centers were10, 30, and 30, respectively (figure). As we were blindly searching for molecules' highest binding conformation, it was important that the dimensions cover the whole protein to ensure that the molecule doesn't have high affinity towards other areas, except for the AI domain.

Once the set-up is prepared, the following coding were written under the commend prompt: "My Documents\vina_tutorial"; "\Program Files\The Scripps Research Institute\Vina \vina.exe" –help. The addition of '–help' at the end of the cd enlists options available for AutoDock Vina (Figure 2 b)). Once the screening set up is complete, the final commend can be typed "\Program Files\The Scripps Research Institute\Vina\vina.exe" --config config.txt --log log.txt. The commend (cmd) prompt showed successful screening process and enlisted the ligand's conformational positions based on its scoring system under the file name called 'Ligand_out.pdbqt' (figure 2.a))

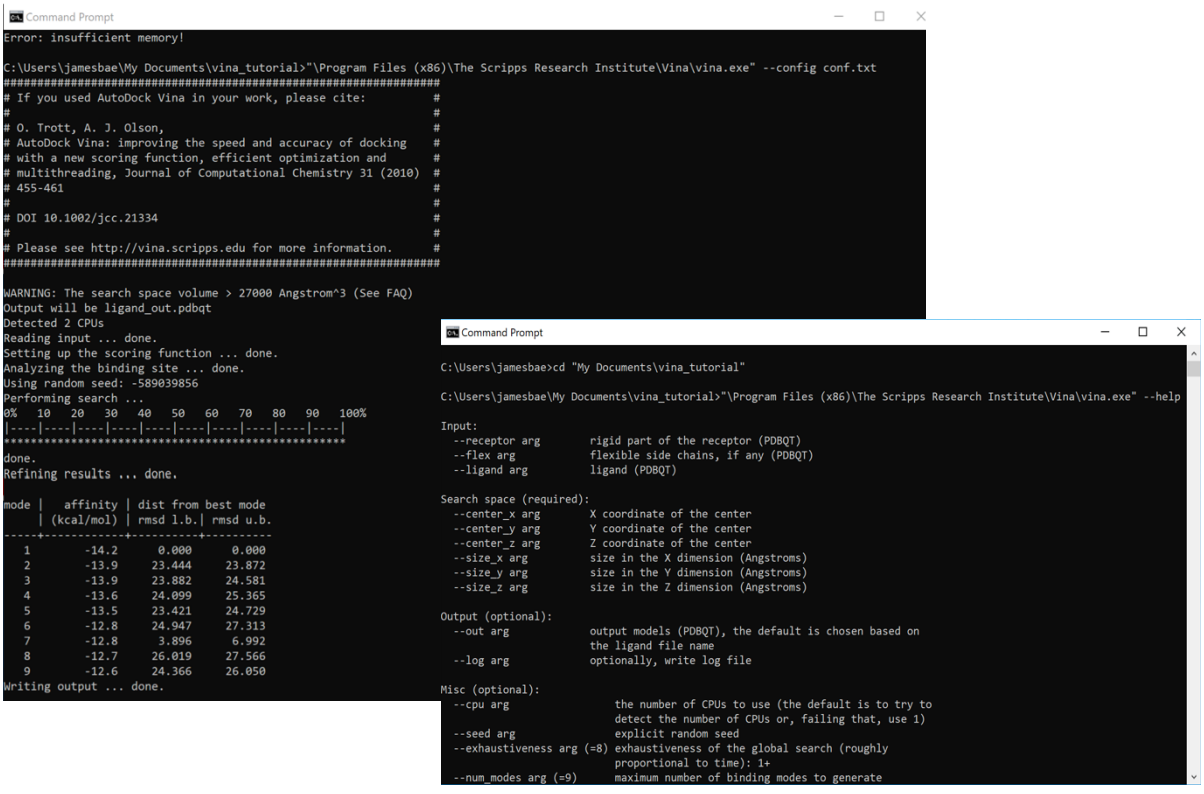

Figure 2.5.2: *Command prompt view of the Autodock Vina program.* Based on the ligand docking scores, top nine different modes of ligand binding sites and affinities are provided as an output for affinity comparisons. Distances from the best modes are also provided as a reference to demonstrate how closeness of each mode predictions are in comparison to the highest affinity mode.

After the screening process had completed, docking study results were saved under the log.txt along with positions of ligands at the thermodynamically favored states. As seen from the above example, AutoDock Vina provides 9 different modes of binding with calculated affinity (kcal/mol); each affinity scores differently due to their variation in conformations and positions within their binding sites. The log text output also provides information about the distance difference between the best mode affinity position and other mode positions. In addition, surface topography allowed for visualization and analysis of surface properties – which helped us to easily portray the conformational position of ligands, analyze the proteins' properties, evaluate compounds' dynamic behaviors and reveal consistence patterns amongst ligand binding sites. This was particularly useful in evaluating the binding positions of the ligands and comparing ligand's potential binding sites. Ligands that showed multiple modes within minimal distances from the highest affinity mode would indicate strong indication for consistency. On the other hand, ligands that showed multiple binding sites indicates inconsistency in their binding site and may lead to false positive reading, despite having a very high affinity score. Careful evaluation of each ligand was therefore required to ensure that all the false positive ligands were filtered before synthesizing the ligand and validating in *in vitro* kinase assays.

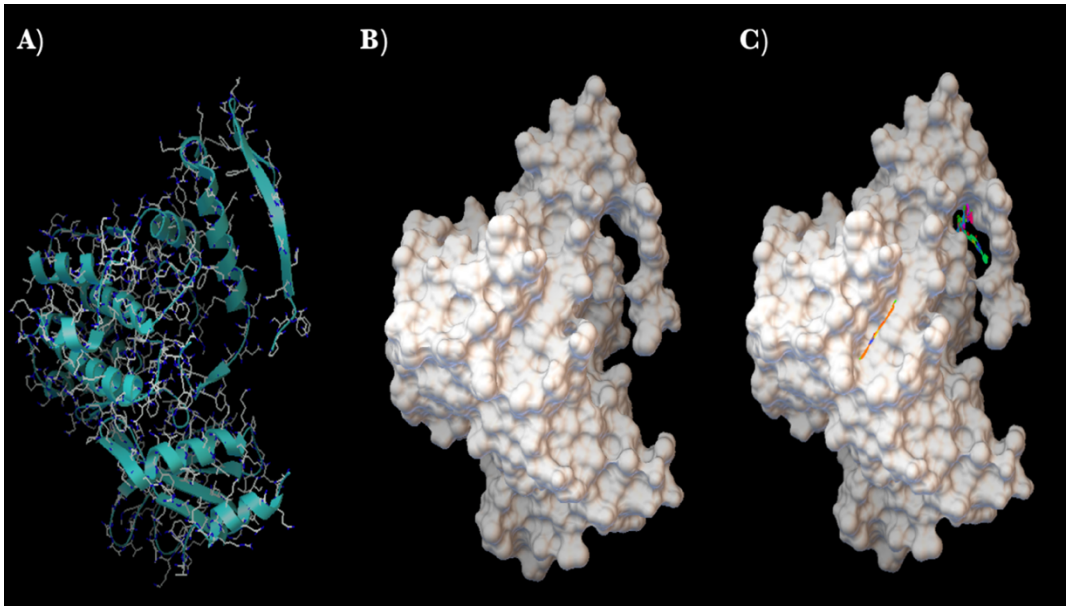

Figure 2.5.3 *The crystal structures of P21-activated kinase (PAK1) using MGL Tools.* **A)** Secondary structure representation of PAK1. The carbon backbones are exposed to allow AutoDock Vina to screen virtual ligands in the grid-box space. **B)** PAK1 surface topography: visual representation of PAK1 surface and surface-distributed properties in 3D. **C)** AutoDock Vina VLS output: The docking result provides 10 potential binding sites of the ligand to PAK1. Each conformation and position provide different affinity scores and allow for evaluation of the compounds' binding ability.

2.6 Hit Validation: Discovery of JB01

Application of the ICM-VLS Pro program enabled a rapid and cost-efficient screening for PAK1 activating ligands. Using the *in silico* approach, over 1,000,000 compounds were screened and evaluated for their binding at the PAK1 AI domain. From the screened compounds, about 2,000 compounds (0.2% of the total compound database) with high scores ranked by ICM were selected. These compounds were then further screened using the secondary screening method, which involved a visual inspection of each compound and eliminating any compounds with undesirable physiochemical properties. Finally, in order to avoid any program bias scoring evaluation, AutoDock Vina, the molecular docking software, was used to confirm the binding affinity of the previously screened compounds. Overall, the application of *in silico* SBVLS using two different molecular docking software packages and personal evaluation of the screened ligands was meant to eliminate as much false reading as possible. This also allowed us to narrow down the choice among thousands of candidate hit compounds.

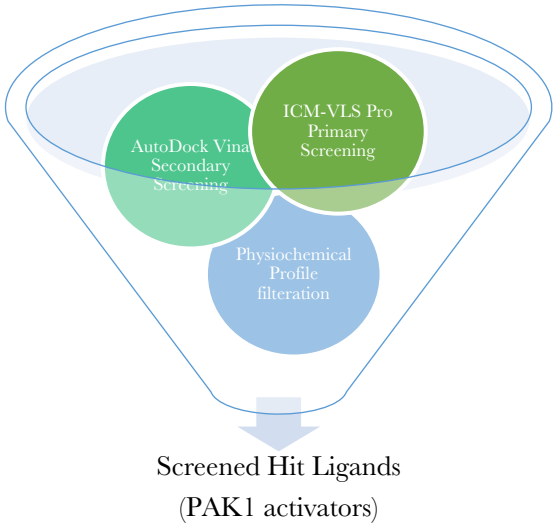

Figure 2.6.1 *Overview of PAK1 activator in silico screening filtration.* ICM-VLS Pro, AutoDock Vina as well as physio- chemical profile filtration was applied in order to screen for potential small molecule PAK1 activators.

Although the filtering and profiling steps were applied to ensure the validity of the screened compounds, and despite the high validating power of these computational algorithms, the *in silico* method of ligand screening should be regarded only as a prediction tool. Therefore, a synthesis of screened compounds and testing in functional assays is necessary to confirm whether or not these compounds contain any biological effect on PAK1 activity.

The method of kinase activity validation was initially done through using the ADP-Glo™ Kinase Assay, a non-radioactive luminescent ADP detection assay that provides a

homogeneous and high-throughput screening method of measuring the kinase activity. More details on the assay method is described in Chapter 3. Amongst the initial ~40 compounds that have been tested, compound Z1231231231 exhibited significant stimulation, two-fold increase in PAK1/CDC42 activity, from the ADP-Glo™ Kinase Assay. The dose response test results and the docking studies are illustrated in the figure below (see Figure 2.6.2)

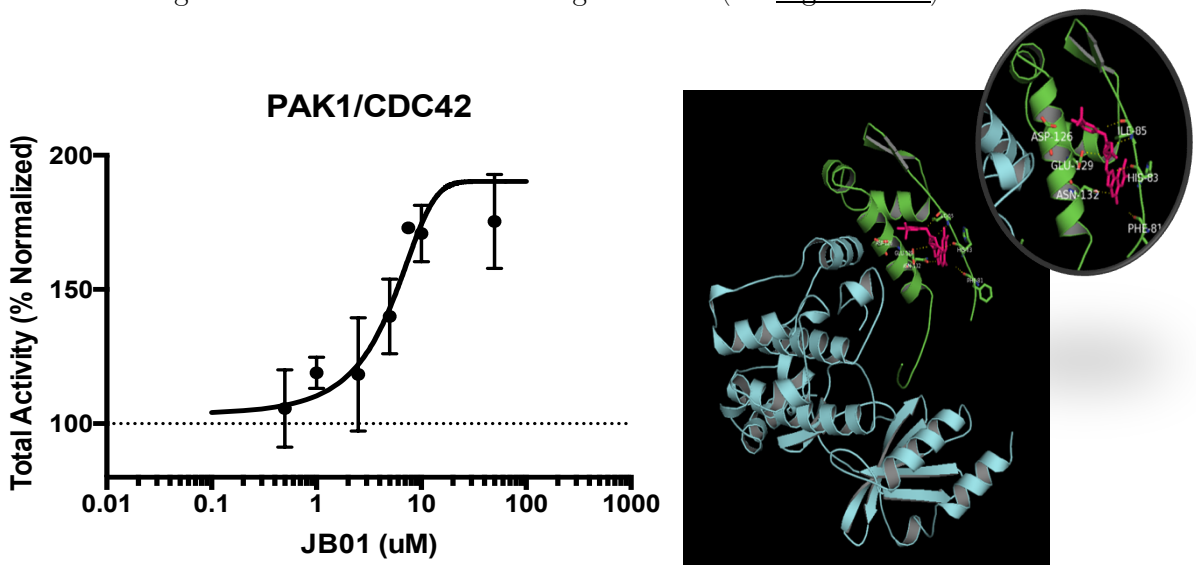

Figure 2.6.2 *Dose-response curve of JB01 on PAK1 activation.* ADP-Glo™ kinase assay was used to correlated the kinase activity and ADP production. All reactions contained 150 ng of PAK1 enzyme (140nM) with 1.5μM of CDC42. Each reaction was incubated for 40 minutes at 30°C. Replicates of three reactions were made at each concentration point. Data are presented as mean ± S.E.M.

Dose response test using JB01 displayed a sigmoid relation between ADP production and JB01 concentrations. As ATP consumption is positively correlated with PAK1 activity, an increase in the ATP usage, therefore, suggests that JB01 was able to modulate and increase the overall activity of PAK1. The effective concentration EC50 was measured to be 3.25uM, with its maximum efficacy being ~200% compared to the DMSO control activity. Based on this ADP-Glo™ Kinase Assay results, we were able to demonstrates that the *in silico* screened hit compound targeting the AI domain of PAK1 can effectively modulate PAK1 activity and stimulate the overall activity of the kinase. Such mechanism of activation was further investigated using the ICM-VLS Pro docking program. The docking score, VLS-Score, measures the affinity to bind at the active site, whereas the steric measures the hindrance from overlapping electron clouds. The overall score output measures the cumulative summation of each property scores, and the lower the value indicates that the better docking scores. For JB01,

VLS-score for the binding was estimated to be -17.61 AU, a relatively negative value suggesting high affinity. However, the exhibited steric properties were measured to be relatively high as well -34.42 AU, making the total scoring for the docking to be slightly lower than the VLS-score, -14.25AU. Although this value of VLS score was not the highest value that we had observed from our *in silico* screening methods, the ten potential binding sites of JB01 from the AutoDock Vina showed consistent binding near the AI domain, illustrating high likelihood of binding to the AI domain. Having confirmed the efficacy of the compound in activating PAK1 and considering both the selectivity and high affinity score at the AI domain, we decided to name this compound as JB01, the first small-molecule compound that has been confirmed to significantly stimulate PAK1 activity.

Despite JB01 compound demonstrating significant stimulation of the kinase activity, the in-built physiochemical profile of the compound raised some concerns about its permeability and solubility properties. Low permeability indicate that the compound may be having difficulty in penetrating through the lipid membrane, therefore exerting lesser effect on PAK1 activation. The low solubility suggests that the compound may not solubilize properly in relevant solutions and may lead to compound aggregates. These highlighted properties indicate that further improvement can be made on the compound to contain properties that are similar to those of the approved drugs – 'druglikeness'. Effort in optimizing PAK1 activating compounds are described in the next chapter 3. Apart from the solubility and the permeability profiles, however, the rest of the chemical properties including molecular weight, size, surface, low PAINS, and volume were illustrated to be drug-like properties for JB01 (see Figure 2.6.3)

	Name	Value
1	Formula	C22 H13 Cl F3 N3 O2
2	Smiles	C(=CC1OC(=CC=1)C(=
3	Name/IUPAC	3-(3-chloro-phenyl)-7
4	InChI	InChI=1S/C22H13ClF3
5	InChIKey	ZGPNYZAWXDNKIF-WC
6	MolWeight	475.0369
7	HBA	5
8	HBD	1
9	RotB	4
10	DrugLikeness	-0.590838
11	MolArea	423.565
12	MolHf	-99.2738
13	MolHalfLife	4.7925
14	MolLogP	6.73491
15	MolLogS	-8.55048
16	MolPAINS	0.102
17	MolPSA	48.1299
18	Volume	421.036
19	Chem Alerts	
20	Groups	Phenyl Furan Halo

Figure 2.6.3 *Physiochemical Properties of JB01.* In-built chemical analysis from Molsoft ICM VLS-Pro was used as a reference to predict the ligand properties. Green color indicates optimal quality, whereas red color signals for caution. In the case with JB01, molecular solubility and permeability were found to be not optimal.

2.7 Summary & Concluding Remarks

In previous research, PAK1 was found to be a dimer, and PAK1 auto-phosphorylation was reported to occur through an inter-molecular activation mechanism where the auto-phosphorylation takes place between two PAK1 monomers (e.g., Lei et al., 2000). Specifically, a segment in the auto-inhibitory (AI) domain was found to displace the activation loop away from key amino acids in the kinase inhibitory segment, leading to exposing the phosphorylating residues essential for its activation. Based on this evidence, we hypothesized that inhibiting the AI domain would lead to an increase in the overall kinase activity. This hypothesis was first tested using a PAK1 bioactive peptide (PAP), which provided us with a proof-of-concept mechanism of regulating PAK1 activity. We assumed that PAP, which was derived from the PAK1 AI domain, would bind PAK1 protein and dislocate the same endogenous sequence as the one involved in forming the kinase dimerization. Previous research on PAPs using functional assays demonstrated that PAPs interact with PAK1 and lead to a more than two-fold increase in its auto-phosphorylation. As a consequence of PAK1 activation, PAP was reported to counteract Ang-II-induced hypertrophy and ventricular arrhythmias, suggesting that modulating of PAK1 activity through AID can increase endogenous PAK1, thus providing cardio-protective mechanisms.

On obtaining evidence confirming that the AI domain is the key region for modulating PAK1 activity and that an increased in the activity of PAK1 can provide cardio-protective effects, we employed the *in silico* computational method to search for the small-molecule PAK1 activator. In order to search for a possible inhibitor at the allosteric site, virtual ligand screening at the PAK1 AI domain was performed. To screen for compounds, we used the ZINC database, along with other ligand libraries, using the ICM-Pro virtual ligand screening software. Based on the scoring outputs (specifically, regarding affinity, binding restraints, torsion, and steric), a number of compounds with a high affinity towards the AID were additionally screened using ADP-GLO™ , an *in vitro* PAK1 kinase assay. One of the compounds which exhibited a significant increase in PAK1/CDC42 activity, according to the results of *in vitro* assays, was JB01. The results of a dose response test showed a sigmoidal curve, suggesting that PAK1 activation is dose-dependent of the compound concentration. As a new step, an additional

kinase method, RapidFire™-Mass Spectrometry (RF-MS) kinase assay, was used to confirm the findings obtained with the ADP-GLO™ kinase assay. The RF-MS kinase assay results confirmed that, in the presence of the JB01 compound, the activators significantly increased the rate of PAK1 substrate conversions, providing further evidence on the molecule's stimulating effect on PAK1 activity (see Chapter 3 for further discussion).

However, although the JB01 compound was found to be able to significantly activate PAK1, the compound's physiochemical profile was still considered unfavourable as a candidate compound. In particular, permeability and solubility of the compound were not found to be within the optimal range of 'drug-likeness' properties. Specifically, low permeability may impede the compound's penetration through the lipid membrane, resulting in its exerting lesser effect on PAK1 activation. Furthermore, low solubility of the compound may prevent its proper solubilizing in certain solutions, leading to compound aggregations. In order to improve these physiochemical properties of JB01(and, accordingly, its efficacy), we explored different ways of its optimization and searched for any structure activity relationship (SAR) within the discovered PAK1 activators. Validation of JB01's efficacy in activating PAK1 and the compound's limited optimization process are further discussed in Chapter 3.

CHAPTER 3

VALIDATION OF PAK1 ACTIVATORS

Summary Points

- Although JB01 confers significant stimulation in PAK1 activity, its physiochemical profiles were observed to be far from being druglike and showed unfavorable solubility and cell permeability.
- JB compounds were optimized using *in silico* computational software to predict for its pharmacophore. The pharmacophore map was utilized to screen for other potential ligands that may have similar chemoinformatic.
- Analogues of the compounds with more favorable physiochemical profiles, while containing strong PAK1 stimulatory effect, were sought and tested *in vitro* kinase assays.
- Two different kinase assays – ADP-GLO™ and RF-MS™ kinase assays – were applied to minimize any potential false results and to increase accuracy of the compound efficacy.
- Confirmed PAK1 activators were also used to provide structure activity relationship (SAR) between ligand-protein interactions to further the ligand optimization process.
- Based from this limited optimization process, lead compound JB79 was discovered and exhibited more favorable physiochemical profile as well as a greater efficacy on PAK1 activity with a higher affinity.

3.1 Background Overview

In recent years, computational *in silico* methods have been widely used to predict potential compounds for therapeutic targets. As illustrated by the increasing number of scientific studies citing a combination of keywords 'in silico' and 'drug discovery' or 'drug design', the discovery of hit compounds has been among key applications of *in silico* computational methods. This suggests a more frequent usage of computational methods for ligand screening (Rognan, 2017). The likely reason for the extensive use of the *in silico* methods is that, unlike traditional methods that require purchasing expensive compound libraries and manually testing each compound through *in vitro* assays (DiMasi, Grabowski, & Hansen, 2016), *in silico* methods are cost-effective and involve a high-throughput screening procedure, allowing to screen many compounds in a short period of time. Therefore, *in silico* methods have been widely recognised as an attractive alternative of drug screening with a significant reduction in developmental costs.

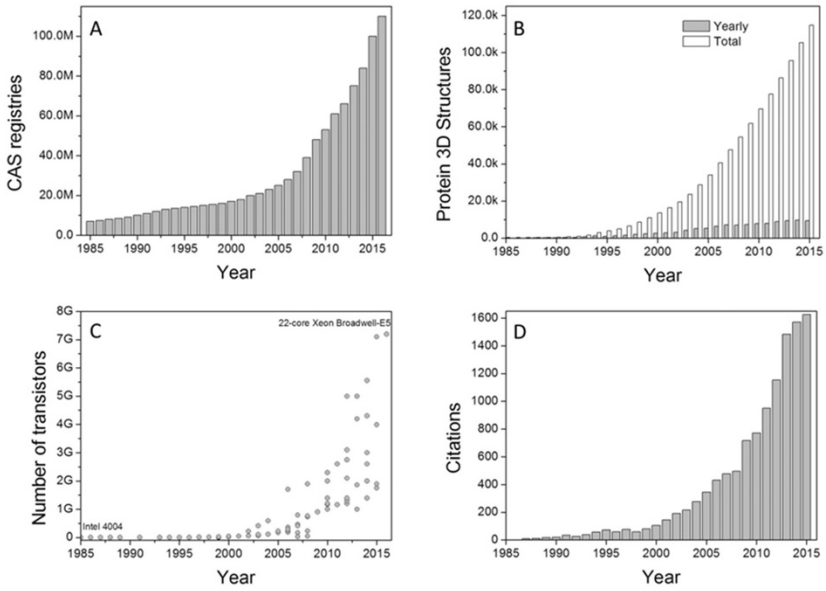

Figure 3.1 Key properties relevant for rational drug discovery over time

A) Registered substances in the Chemical Abstract Service (CAS)
B) Entries in the Protein Data Bank (PBD)
C) Transistor count in micro-processors
D) Citations with the following combination of keywords "in silico" AND ("drug discovery" OR "drug design") in the PubMed resource

(Fig. derived from Rognan, 2017)

Among various methods of *in silico* screening, structure-based methods (SBVLS) are becoming more popular in predicting target druggability. These methods rely on 3D structural descriptors (polarity, hydrophobicity, buriedness, volume, curvature) of ligand-bound cavities to predict its binding site and binding affinity. During our development of PAK1 activators, we also applied *in silico* SBVLS methods to search for the initial hit compounds. Specifically, we screened libraries of compounds in the AID of PAK1. Our working hypothesis was that if a small

molecule could bind to the AID and disrupt the dimer formation of PAK1, it would affect the regulatory mechanism of PAK1 activity, thereby stimulating its enzymatic function. Among the early tested compounds from the screening results, one of the commercial library compound Z254745721 showed a significant stimulation effect on the PAK1 activity. This compound, which was subsequently named JB01, was the first confirmed small-molecule PAK1 activator, exhibiting a significant and direct activation effect on PAK1 enzyme. However, the compound was still at the preliminary phase of its development, and its reportedly poor physiochemical properties (e.g. solubility and permeability) suggested that, before proceeding to the next phase of drug discovery process, i.e. preclinical studies, an efficient optimization process would be necessary.

For a successful optimization of hit compounds, it is necessary to comprehensively understand the nature of the ligand binding site so that to correctly predict the protein ligand interactions. By predicting the correct orientation, position, and interaction with the surrounding pocket residues, *in silico* docking studies help to measure protein-ligand force fields calculated from extensive sampling based on the electrostatic interaction and taking into consideration the internal and external degrees of freedoms. For example, free energy perturbation (FEP) and thermodynamic integration (TI), reportedly useful tools for lead optimizations (Jorgensen, 2009), can also be calculated based on each modification of the ligand. However, a limitation of this application is that it requires that either the crystal structures containing the bound ligand are elucidated or that a high interpretability of pocket properties among homologous structures is available for comparative analysis. This is often used for finding inhibitors for GPCRs and kinases, since the latter often contain several polar hotspots where the chemical properties are found to be conserved across different families; these hotspots have been considered to be favourable locations for drug targeting (e.g., ATP binding site for enzymatic inhibition). Regrettably, in the case of PAK1 activator, no compounds have previously reported to elicit a stimulatory effect on enzymatic activities. Considering the scarcity of previous research on kinase activators, predicting the likely binding site of the ligand was risky and implausible. Therefore, in the present study, we used the *in silico* method of QSAR as the reference for lead optimization.

Although JB01 was originally discovered through screening compounds at the PAK1's AID, none of previous studies confirmed the active site for kinase activators. Assuming that performing lead optimization based on a hypothesized binding site would be too risky, and aiming to get a better understanding of the active site, we applied the structure-activity relationship (SAR) approach. This approach helped us to determine what chemical groups of the compound were responsible for conveying the biological efficacy. The SAR approach is usually applied after the binding site of the ligand is confirmed. In our case, however, due to the lack of co crystallography and biophysical data, the method was used retroactively in order to understand the biochemical environment of the active site. Specifically, this was achieved by testing various compounds with similar pharmacophore cores containing different functional chemical groups. Understanding which functional groups were essential for its functional effect on PAK1 stimulation enabled us to envision chemical properties surrounding the active site. The SAR information can be used for a better optimization lead compound. Moreover, having multiple compounds with a similar mechanistic effect on PAK1 stimulation would provide an array of tools to improve the lead compound. The SAR-based evidence also revealed that the effect of small molecules was through a specific binding, rather than through non-specific bindings, providing us with further confidence in the selective activation of PAK1 activators.

Chapter 3 describes the kinase assays used to validate the efficacy of the PAK1 small-molecule activators. To ensure the consistency of the data results, we used two different kinase assays—the ADP-Glo™ Kinase Assay and the Rapid-Fire™ Mass-Spectrometer Kinase assays. The chapter also discusses the stepwise optimization processes employed to improve lead compounds. *In silico* ligand optimization software and computational methods were applied as supplementary tools to design lead compounds with the required physiochemical properties. The limited optimization also provided us with a better knowledge of the PAK1 activator SAR and indicated potential key interacting chemical groups involved in conveying the stimulation efficacy. Overall, the optimized compounds showed improved physiochemical profiles and efficacy, allowing for subsequent clinical validation studies (see Chapter 4 for further discussion).

3.2 Physiochemical Guideline

Effective development of a candidate compound depends on both innovations in medicinal chemistry and strategies that were predominantly used in the past. For example, conventional physiochemical guidelines, such as Lipinski's rule of five, are commonly used to evaluate the drug-likeness of the compound. These guidelines are essential to predict the likelihood of metabolisms in the human body, including those of absorption, distribution, metabolism, excretion, or toxicity (ADMET). These rules are commonly applied when a pharmacologically active lead structure is being optimized in a stepwise process, in order to increase its efficacy and selectivity. These guidelines in drug development are conceptually simple and easy to follow. Therefore, the original article has been cited over 1,500 times (Leeson and Springthorpe, 2007). Lipinski's rules of five are formulated as follows, with some variants and extensions to improve the prediction of drug likeness (Lipinski, 2004).

Rule of five	Variants/extensions
No more than 5 hydrogen bond donors (the total number of N–H and O–H bonds)	Partition coefficient log P in -0.4 to +5.7 Range
No more than 10 hydrogen bond acceptors (all nitrogen or oxygen atoms)	Molar refractivity from 40 to 130
A molecular mass less than 500 Dalton	Molecular weight from 180 to 500
An octanol-water partition coefficient log P not greater than 5	Number of atoms from 20 to 70 (including H bonds)

Table 3.2 *Lipinski's Rule of Five and its extensions.* Physiochemical guidelines such as the example above are often utilized in the drug discovery field for optimizing and filtering compounds for drug-like properties.

However, these physiochemical guidelines are not absolute in determining the toxicity or bioavailability of the compound. Analysis of recent trends revealed that the chemical properties of current developing drugs are found to be significantly different from those of the previously reported guidelines. For example, compounds that were produced by more recent medicinal chemistry do not occupy the same chemical space as those of the historical drugs (Leeson and Springthorpe, 2007). The mean cLogP values of modern developing drugs were also found to be significantly different from that of the traditional drugs, where the mean cLogP value was 2.5 with the average molecular mass of 338 Da (Wenlock et al., 2003; Vieth et al., 2004, and Proudfoot, 2005). By contrast, 1,117 GlaxoSmithKline compounds and 553 Abbott

compounds that had advanced to pharmacokinetic studies contained a mean cLogP values of 4.3 and 3.9, and molecular mass values of 480 and 434 Da, respectively (Veber et al., 2002;). Furthermore, a group of 1,680 optimized compounds from the recent medicinal chemistry literature had a mean cLogP of 4.0 and molecular mass of 435 Da., exhibiting significantly different values than those of the traditional drugs (Morphy, 2006). It remains to be seen whether or not the changes in trends of drug properties will lead to drugs with better physiochemical profiles (and thus higher drug approval rates).

3.3 Optimization of JB compounds: in silico

JB01 was the first confirmed small-molecule PAK1 activator, exhibiting a significant and direct activation effect on PAK1 enzyme. Through the dose response assay using the ADP-GLO™ Kinase Assay, we were able to observe an 80% greater PAK1 activity at 20uM concentration, compared to the baseline activity. However, according to the ICM-VLS chemical monitor, the physiochemical properties of JB01 was not as promising as those of the candidate compounds (see Figure 3.3.1). The compound showed poor solubility as well as permeability properties. The poor solubility may be due to its large plane surface, as well as its lack of a strong electron donating group, such as hydroxyl, carboxyl or amines. The reduced permeability can be explained by its large polar surface areas, may contributing to a low bioavailability in metabolism (Veber et al., 2002). Finally, the molecular weight of the compound was highlighted to be larger than the current approved oral drugs. The mean molecular weight of approved drugs is found to be lower (<400 da.), and polar surface areas to be less than 140 A (Veber et al., 2002). Therefore, the compound was still at the preliminary phase of its development, and its reportedly poor physiochemical properties (e.g. solubility and permeability) suggested that, an efficient optimization process would be necessary before moving on to measure its therapeutic functional studies.

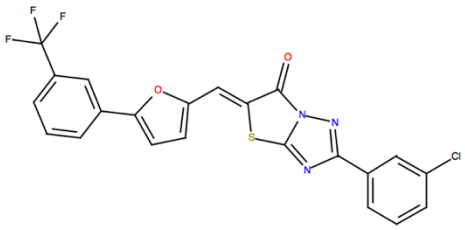

Name	Value
Formula	C22 H11 Cl F3 N3 O2 S
Smiles	C(=CC(=CC1C(=NN(C2
Name/IUPAC	3-(3-chloro-phenyl)-7-((
InChI	InChI=1S/C22H11ClF3
InChIKey	VXGKBNLYXVFMMC-U
MolWeight	473.0213
HBA	6
HBD	0
RotB	4
MolArea	417.308
MolHf	-83.6631
MolHalfLife	9.44556
MolLogP	6.96252
MolLogS	-9.26342
MolPSA	44.7658
Volume	408.064
Chem Alerts	
Groups	Phenyl Furan Halo

Figure 3.3.1 *Physiochemical Properties of JB01.* In-built chemical analysis from Molsoft ICM VLS-Pro was used as a reference to predict the ligand properties. Green color indicates optimal quality, whereas red color signals for caution. In the case with JB01, molecular solubility and HBA were found to be not optimal.

The initial compound optimization was done using ligand-optimizing software, such as Stardust, ICM-VLS Pro, and Mcule to aid in evaluating the modified compounds. In current drug discovery, the chemoinformatic techniques – such as virtual screening, pharmacophore modeling, quantitative structure-activity relationship (QSAR), and data mining – are of great significance, being considerably precise as well as saving time and costs. For the optimization process of JB01, computational software was utilized to predict the JB01 3D pharmacophore. This pharmacophore was used as a map to screen other ligands with similar chemoinformatic but with improved physiochemical properties. Methods of virtual ligand screening for each software consists of their unique algorithm which allows them to compare the pharmacophore with other ligands. Although each software program contains different algorithms, many software packages include similar programs that allow them to predict how well new compounds would fit in to the pharmacophore of the search ligand. This is achieved through compiling relevant data on the ligand's properties (e.g., position, orientation, chemical properties, torsions, rotatable bonds, and 3D flexibility) (Trott et al., 2009).

The mentioned software for optimization was not strictly applied for improving the JB compounds as the resulted optimized compounds from the software were not available commercially and had to be newly synthesized. Synthesis of new compounds were found to be limited within the lab due to a lack of facilities and were too expensive to purchase commercially. At the time of the optimization, the small molecule PAK1 activator project was not financially supported by any funding bodies. Hence, many of the reagents and initial

compounds had to be purchased through personal finance, and this has put major limitations and constraints in my ability to explore different analogues. The alternative option was to search similar analogues through other companies that sold inexpensive compounds from compound libraries. Companies such as Enamine, Mcule, Timtec, Chembridge, and Princeton Biomolecular Research are specialized in providing screening compounds libraries and permits drug discoveries at a low cost. Compounds from the company could be purchased in small quantities with inexpensive costs, but purchasing from these companies had following limitations:

1. Insufficient number of available analogues to explore complete SAR studies.
2. Significant delays in obtaining the compounds that were not in stocked.
3. Small quantity purchases required to pay for the shipping and preparation.

The purpose of this ligand library screening was to find the 'hit' scaffolds, not to perform full SAR studies. Therefore, limited number of each kind of analogues were expected. Furthermore, instead of investigating the SAR of PAK1 activators, the initial JB optimization process was focused solely to find other scaffolds that exhibited better physiochemical profiles while maintaining high efficacy in activating PAK1 activity. It was also to validate whether the compound binding activation of PAK1 is by coincidence or not. Each kinase assays were repeated more than three times to ensure that the activation that was measured were accurate. To demonstrate the specificity of the ligand binding to PAK1, additional analogues that showed activation in PAK1 were required. Therefore, initial optimization of PAK1 activators were done through searching for additional analogues with similar pharmacophores. This required us to search through the commercial vendor databases and computational software for optimization. An exemplary method of *in silico* search for commercially available analogues are shown in below using the Mcule.com website.

3.4 In silico optimization: Mcule.com

Mcule.com is an online drug discovery platform that allows purchase of compound libraries for scientific investigations. Mcule company itself doesn't involve in any synthesis, but it contains libraries of compounds that can be found across different commercial vendors. Similar to the ZINC database, Mcule offers libraries of ligands for both drug discovery and optimization of ligands, however, the Mcule.com constantly updates its information, allowing for allocation of vendors in making the purchases easier for consumers. The ZINC database was often found to be unavailable at times, and its search data information was also found to be outdated. For example, chemical vendors that sell JB01 is found to be only available for Enamine; the rest of the vendors no longer sold the compound or were out of stock at the time of inquiry. Furthermore, recently established chemical vendors such as the Princeton Biomolecular Research was not enlisted as vendors on the ZINC database. This made the purchase of compounds inconvenient as it was difficult to confirm whether or not the vendors had the compounds available. As each small quantity purchase had extra incurring costs from preparation and shipping fees, it was important to keep the purchase limited to as few vendors and purchases as possible. Mcule had updated information on its ligand availability and allows for purchase of compounds through different vendors (see Figure 3.4). It was possible to inquire for a price quote through Mcule, but this was more expensive than purchasing directly from the chemical vendors.

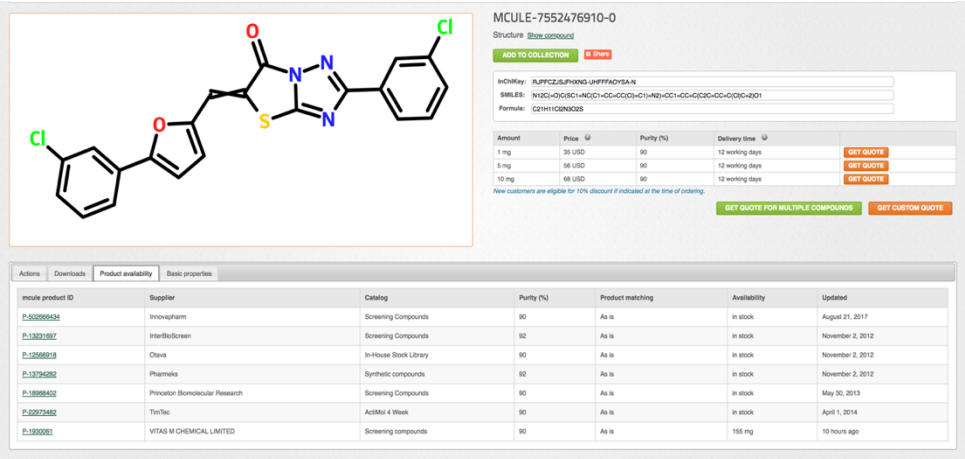

Figure 3.4.1 *Chemical availability using Mcule.com*. An exemplary page to demonstrate how Mcule provides availability of products. The website contains reference information about its properties, functions for dockings studies, and updated product availability from each vendor.

One of other advantages of using Mcule was its ability to search similar analogues based on the search compound. The search engine calculates percentage of similarity between the input compound and its analogues within the database. This was particularly useful for quantitively comparing between the search compound and its similar analogues and allowed for easier recognition of their differences (see Figure 3.3.3). The Mcule platform also has an in-built ligand optimization software, called '1-Click Scaffolds Hop', which searches molecules based on its drawn reference structure and discover a new scaffold for lead optimization. This was also found to be useful in generating new ideas to replace the old scaffolds which may have had unfavorable physiochemical profiles.

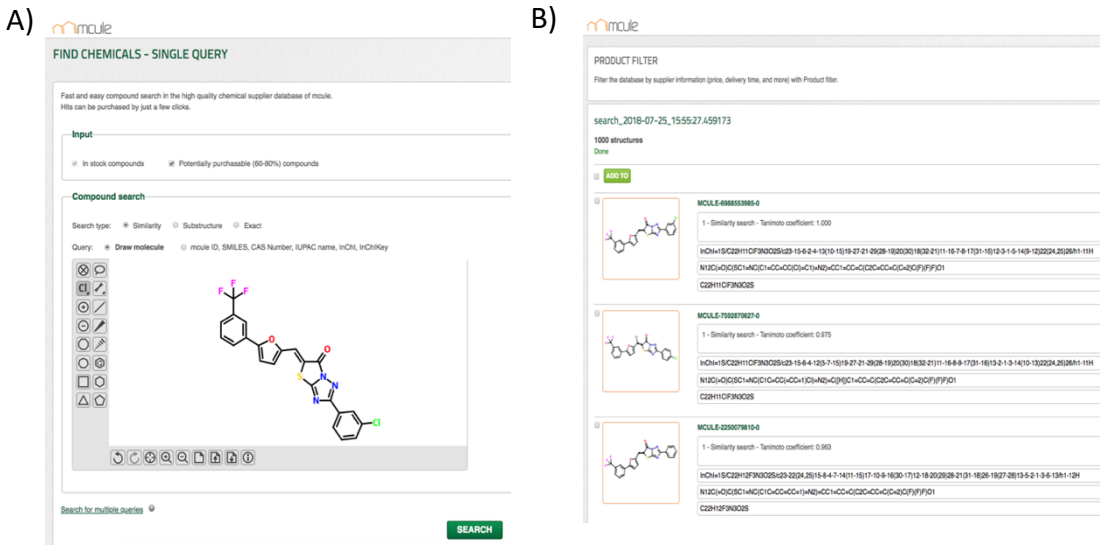

Figure 3.4.2 *Similar compound screening using Mcule.com.* An exemplary page to demonstrate how Mcule provides availability of products. The website contains reference information about its properties, functions for dockings studies, and updated product availability from each vendor.

Despite practical usage of its in-built lead optimization software in Mcule, ICM-VLS Pro was mainly used to aid in evaluating the modified compounds and measuring their affinity at the active site. Much effort had been put in order to improve the current chemical properties of JB01, functional-groups and core-groups were substituted with similar pharmacophore groups to maintain the efficacy yet, improving both its affinity and safety. Optimized compounds were docked using the VLS software. Each compound was docked using the ICM-VLS Pro to checked for the docking scores. Unfortunately, the results of the docking studies did not represent the efficacy of the compounds (as later measured their efficacy using RF-MS kinase assay).

3.5 Optimization of JB compounds: in vitro, ADP-GLO™ Kinase Assay

In today's drug discovery, computational approach provides us with valuable insight in understanding the binding affinity as well as its physiochemical profile of the compound. They are often utilized to improve decision making process in the structural modification of drug candidates, enhancing metabolic stability, and improving their efficacy and binding affinities (Nassar et al., 2004). Although lead optimizations though *in silico* methods may indicate better chemical profile and suggests greater binding affinity through the docking scores, the ultimate validation of improvement can be only confirmed through an actual *in vitro* experiments. A sufficient level of confidence from the *in vitro* assays has to be established first before confirming the validity of the *in silico* results. To investigate whether the optimized compounds contained improved efficacy – while enhancing their pharmacokinetic properties – *in vitro* studies were performed using two functional kinase assays.

The first assay used to validate PAK1 activators was the previously established ADP-GLO™ Kinase Assay which measured the product metabolite from the kinase reaction. The same parameters and conditions as used to search for PAK1 activators were utilized to perform the kinase assay. Ligands from the *in silico* methods were search for commercial availability, and limited number of ligands were obtained for the kinase assay. JB01, JB10, JB11, JB21, JB22, JB23, JB24, JB34, JB35, JB36, JB37, JB38, JB39, JB58, JB79, and JB81 were the first batch of ligands that were tested for their efficacy and to validate whether or not, the computational in silico method was useful in optimizing the ligands. Dose response assay for each molecule's efficacy in stimulating PAK1 activity were shown below:

JB Compounds	Chemical Structure	Dose Response ADP-GLO™ Kinase Assay
JB01	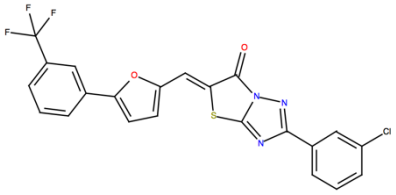	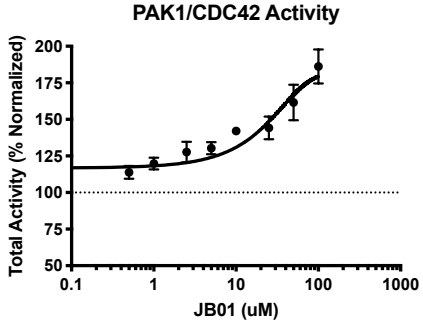

JB10	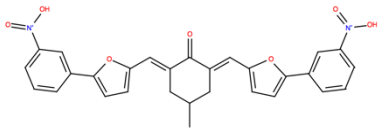	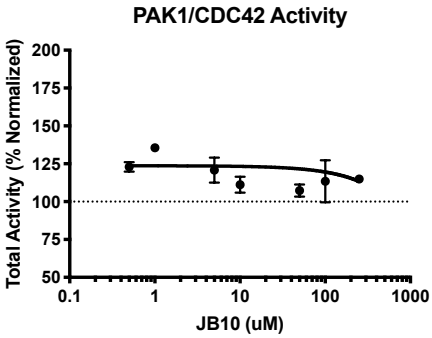
JB11	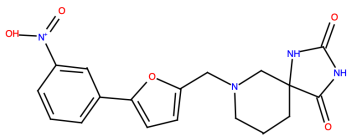	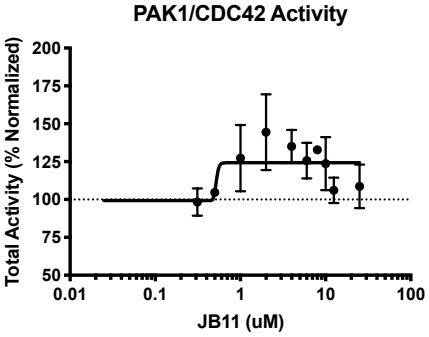
JB21	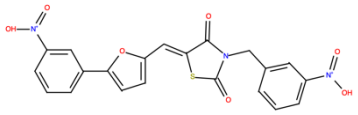	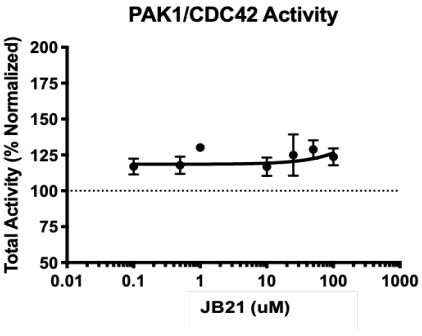
JB22	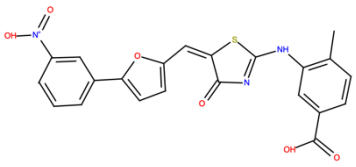	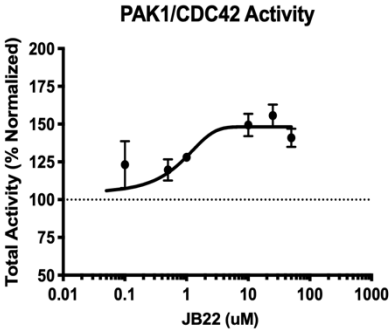
JB23	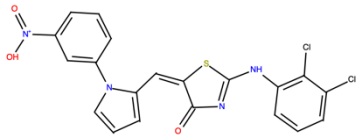	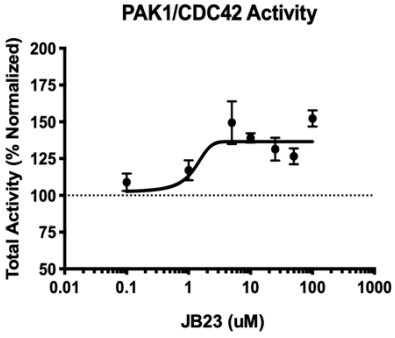

JB24	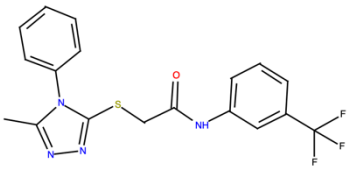	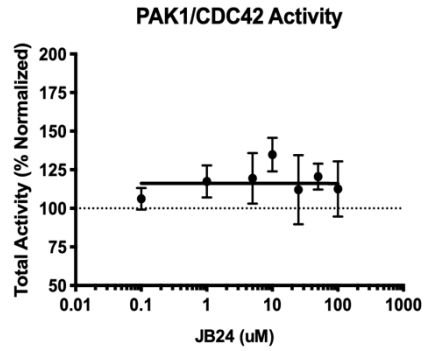
JB34	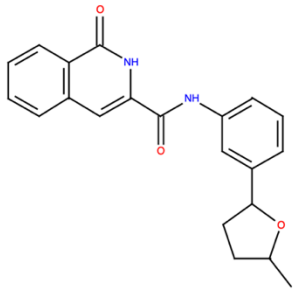	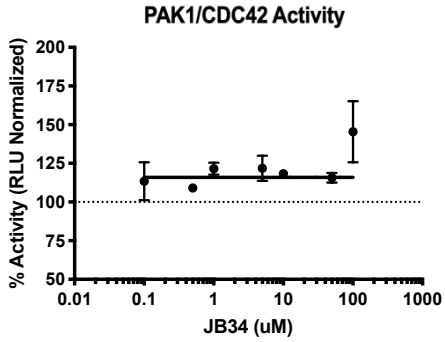
JB35	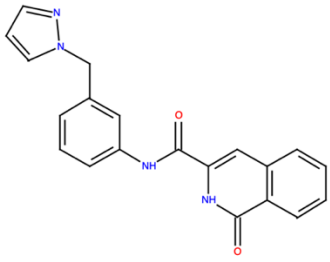	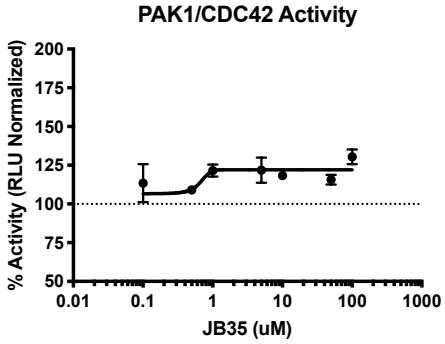
JB36	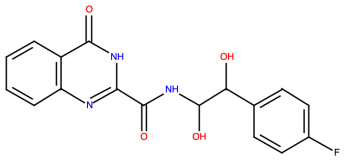	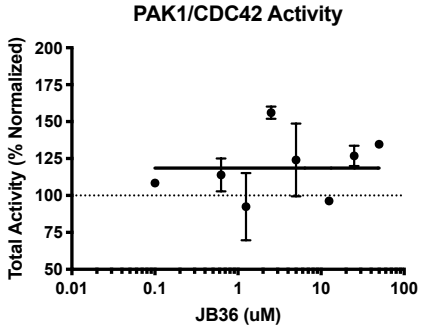
JB37	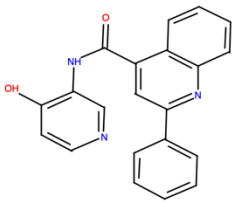	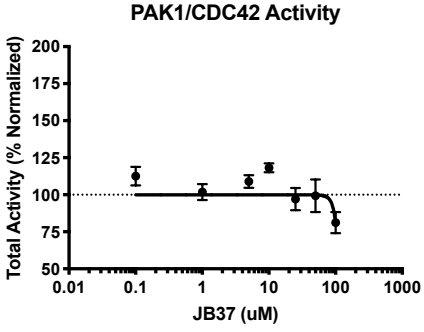

JB38	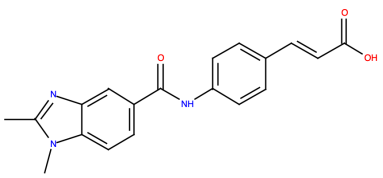	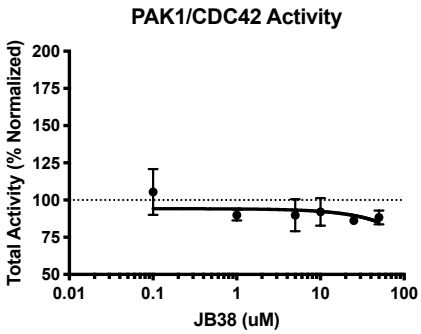
JB39	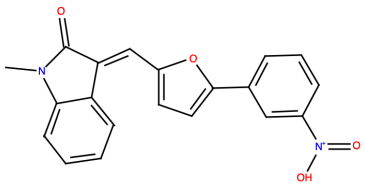	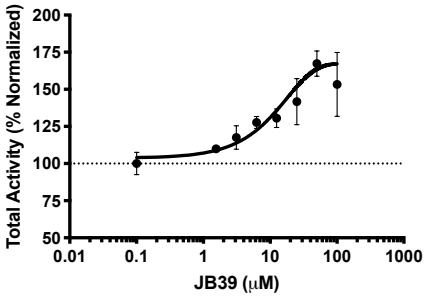
JB58	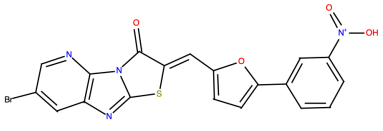	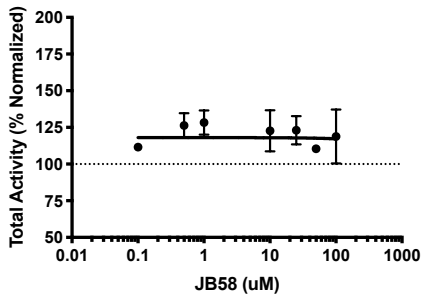
JB79	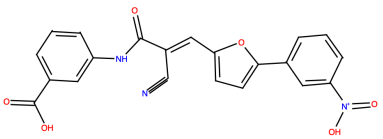	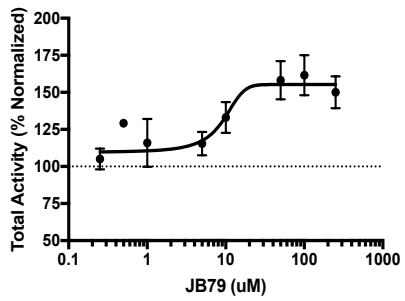
JB81	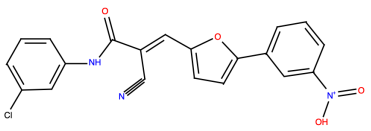	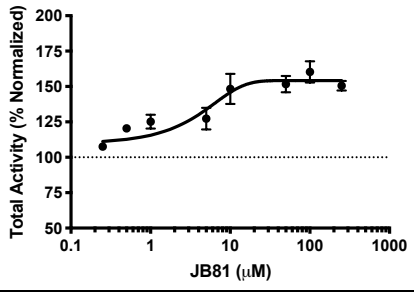

Figure 3.5 *The dose-response curve of JB compounds on the activation of P21-activated kinase (PAK1).* ADP-Glo™ kinase assay was used to measure the effect of JB compounds on the PAK1activity. All reactions contained 100nM of PAK1 and 0.5uM of CDC42 enzymes, and the reactions were incubated for 30 minutes at 30°C. 3 Replicates of reactions were made at each concentration point (mean ± S.E.M.).

Eight different concentrations (ranging from 0.1uM ~ 100uM) were chosen to measure their efficacy in activating the kinase activity. As these molecules were still in the early phase of optimization, it was unlikely that they would have such high affinity at the nanomolar range. Any efficacy at concentration over 100uM was likely to cause inhibitory effect or non-specific binding which makes it hard to determine whether these compounds are actual activators of PAK1 or not. Therefore, a range between 0uM to 100uM was used in order to assess the biological effect of the early JB compounds.

From ADP-Glo™ Kinase assays, JB01, JB22, JB39, JB79, and JB81 exhibited noticeable dose response relationship, showing significant increase in PAK1 kinase activity, while other compounds exhibited either non-significant activation or some inhibitory effect. Maximum activation effect with JB79 was measured to be 155.3%, 1.5 greater activity than the control treatment, with its EC_{50} being 8.92uM. Although the maximum response of JB79 was measured to be lower than that of JB01, the EC_{50} of the JB79 was measured to be lower than that of JB01; higher affinity was achieved with JB79, but the potency of the activator was reduced. JB39 and JB81 dose response assay also demonstrated remarkable increase in PAK1 activity. Dose response relationship between the compound concentration and PAK1 activity was clear, but the concentration in which JB39 and JB81 start to stimulate PAK1 were predicted to be greater than 15uM, which illustrates that the affinity for these compounds in activating PAK1 activation were less than those of JB01 and JB79.

There were other compounds such as JB11 and JB37, which also showed inhibitory effect at higher concentrations. Such mechanism of its inhibition is thought to be non-specific inhibition at the ATP binding domain due to its high concentration. The high concentration of compounds may start to compete with the substrate ATP at the ATP binding site. As seen from 1F3M PDB, the kinase domain – surrounded by the two alpha helixes and give beta-sheets – grooves a large pocket that may allow for non-specific binding of ligand to interfere the substrate binding.

Finally, the rest of the compounds (JB) did not show any clear effect in activating PAK1 enzyme, or their activation was measured to be insignificant. What was particularly interesting was the efficacy comparison between JB79 and JB81. The only difference between the two

molecules was the functional groups, the halide group (JB81) and carboxyl group (JB79). However, the potency for JB79 was measured to be higher (maximum potency difference being 15.5% in comparison to JB81). As halides have lower electronegativity than those of strong electron withdrawing groups like the carboxyl group, this suggested that the functional groups with higher electronegativity at the meta position may provide for a greater potency in activating PAK1. Further investigation was done to compare different functional groups at the meta-position to study their efficacy and to have further understanding of the structure-activity-relationship of the PAK1 activators.

The ADP-Glo™ Kinase assays were proven to be an essential method in validating the efficacy of the compounds and detected the activity of the kinase through measuring the amount of substrate ATP used within the kinase reaction. The ATP metabolite, ADP, were then conjugated with a luminescence tag which allowed us to correlate the kinase activity based on the intensity of the luminescence. Although ATP usage is correlated with the activity of PAK1, there were few limitations to this method, including the fact that the activity is only measured indirectly through measuring the product formation after the kinase reaction has finished. Measuring the product ADP does not confirm whether the transfer of phosphate group by PAK, has been done on the substrate (in this case, PAKtide peptide) or not. The indication of ATP depletion could be due to other factors like the breakdown of ATP (ATP hydrolysis, ATP + H2O → ADP + Phosphate) over a given reaction time or PAK1 being auto-phosphorylated to each other, instead of phosphorylating the substrates. As we are only measuring the product ADP through luminescence, it was difficult to assess whether the final reading of luminescence was directly correlating with the PAK1 activity or not. In addition, the results of the assay could have been affected by the color of compounds as some reactions with higher concentration exhibited stronger color indications. For example, compounds containing a nitro-group within the benzene ring tend to provide yellow/orange colours to the kinase reactions. Control reactions were performed using only wells with increasing concentration of compounds, maintain the same reaction without the addition of the kinases. The results show that the color of reaction had minor affect to the luminescence reading (±5%). However, the luminescence of the reading may be further affected if the compounds

were to bind to the enzymes and thereby producing certain wavelength which may interfere with the actual reading. Therefore, it was important to carefully consider these limitations when assessing the efficacy of the molecules.

Overall, The ADP-Glo™ Kinase assay was a convenient quick method to measure kinase activities and allows us to assess the efficacy of the optimized molecules in modulating PAK1 activity. Compounds such as JB39, JB79, and JB81, exhibited significant increase in the PAK1 activity and suggested them as potent PAK1 activators. With other compounds that showed minor stimulation in PAK1 activity, number of assays had to be repeated to ensure that the reading is accurate and that the indicated limitations were carefully considered when assessing the efficacy of the compounds.

3.6 Optimization of JB compounds: Rapid-Fire™ Mass-Spectrometer Kinase Assay

The ADP-Glo™ Kinase assays were proven to be an essential method in validating the efficacy of the compounds. However, these assays measured PAK1 activity indirectly through detecting the amount of ADP produced from the kinase reaction. Limitations, such as false positive reading from ATP breakdown, had to be considered when assessing the results. To ensure that the reading from the ADP-Glo™ Kinase Assay is accurate, another kinase assay, Rapid-Fire™ Mass-Spectrometer (RF-MS), was performed as a secondary screening to validate the efficacy of the compounds.

Rapid-Fire™ Mass-Spectrometer is a high-throughput liquid chromatography-tandem mass spectrometry (LC-MS) that allows rapid purification and injection of mass-spectrometry samples from quenched enzyme reactions. The mass-spectrometry is an ultimate readout assay since it can directly detect the native substrate, without requiring totag a compatible fluorogenic or antigenic peptides to the readout molecules. The applications of Rapid-Fire™ Mass-Spectrometer is not only limited to *in vitro* kinase assays, but also for measuring ADMET metabolites (Langsdore et al., 2010; Wu et al., 2012). Direct measurement of intracellular compound concentration using the RF-MS have been shown to offer insight into cell permeability of compounds as well its process of metabolism (Gordon et al., 2016). Taken all together, these advantages of RF-MS make the device as one of the most favourable methods of high-throughput screenings of small-molecule ligands.

Unlike the ADP-Glo™ Kinase assay, RF-MS kinase assay can directly measure the kinase activity though detecting the amount of both the substrate peptide and the phosphorylated peptide. In terms of thermodynamics, peptide phosphorylation cannot undergo reaction by itself without the aid from the catalyst (PAK1). Therefore, peptide phosphorylation is directly correlated with the activity of PAK1. The following reaction scheme below illustrates the PAK1 kinase reaction:

PAK1 Kinase Reaction

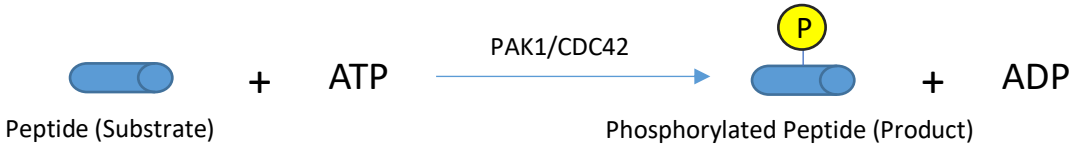

From the assay results, the RapidFire™ integrator software can calculate the percentage conversion from peptide substrate (PAKtide) to phosphorylated product (P-PAKtide), providing accurate measurement of the enzymatic activity. This can be achieved through matching the exact mass/charge ratio of the PAKtide and the phosphorylated PAKtide. As each reaction contains the same amount of substrate peptide initially, the faster activity of PAK1 would produce more P-PAKtide at the end of reaction. Figure 3.6.1 is an exemplary screenshot of the RapidFire™ integrator software, illustrating the peptide detection after the reaction had completed (Quercia et al., 2007).

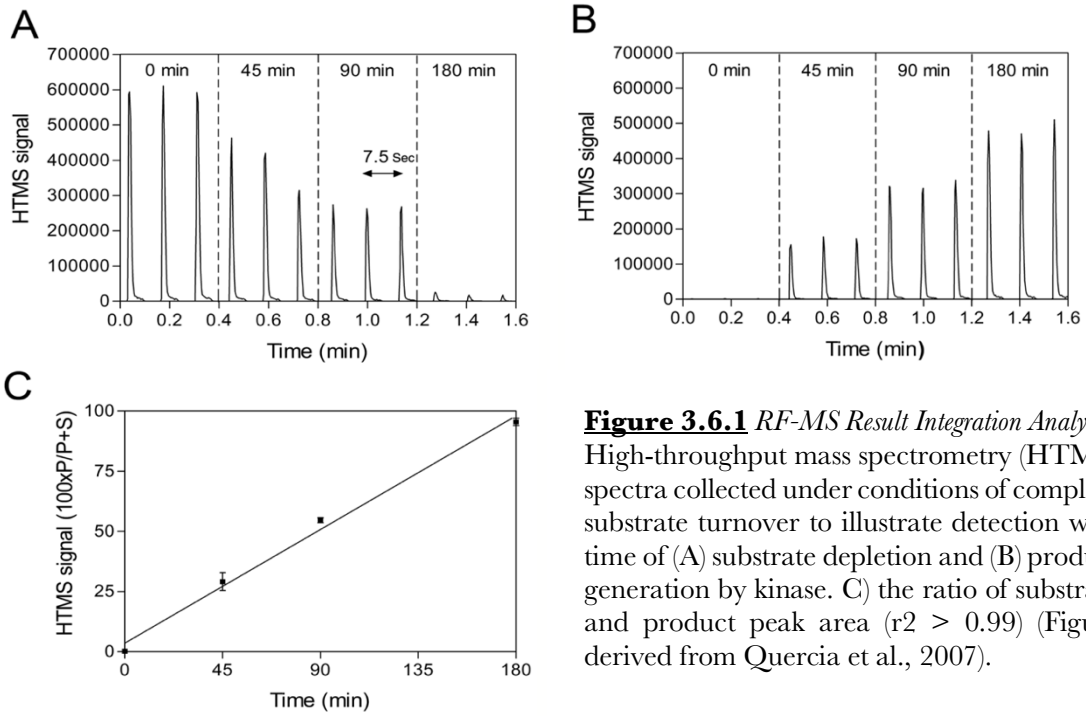

Figure 3.6.1 *RF-MS Result Integration Analysis.* High-throughput mass spectrometry (HTMS) spectra collected under conditions of complete substrate turnover to illustrate detection with time of (A) substrate depletion and (B) product generation by kinase. C) the ratio of substrate and product peak area (r2 > 0.99) (Figure derived from Quercia et al., 2007).

As shown in Figure 3.6.1.A, the initial reaction contains high signal of the substrate peptide while in Figure 3.6.1.B illustrates almost no detection of the phosphorylated peptide. However, as the kinase reaction progresses, the kinase is able to phosphorylate the substrate and thereby depleting the substrate peptide (A) and producing more of the product peptide (B). After 180 minutes since the kinase reaction has started, we can see that there is almost no signal left for the substrate, and the product signal has plateaued, illustrating completion of the kinase reaction. Finally, taking the ratio between the product and the product + substrate, we are able to produce a ratio curve, where the slope of the curve signifies the enzymatic activity. Therefore, if the slope of curve is steeper when the compounds are present, this verifies the compounds ability to elicit stimulatory effect on the kinase activity.

3.6.1 Rapid-Fire™ Mass-Spectrometer Kinase Assay Methods

From the preliminary screening using the ADP-Glo™ Kinase Assay, we have identified a number of potential candidates for PAK1 activators. To exclude the false positive ones from the list, we performed Rapid-Fire™ Mass Spectrometry (RF–MS) kinase assay. Assays were prepared at room temperature using a reaction buffer containing 50 mM HEPES (pH 7.5), 10 mM MgCl2, 2 mM MnCl2, 1 mM DTT, and 0.01% bovine serum albumin (BSA). Compounds dissolved in DMSO were diluted to 100-fold in 700 µL of assay buffer in 1mL deep 96-well plates (final DMSO concentration 0.5%). PAK1 and CDC42 were added to a final concentration of 10 nM and 1μM, respectively. The reaction was initiated by adding substrate solution, containing PAKTide (1 µM final concentration, Sequence: RRRLSFAEPG) and adenosine triphosphate (1 µM final concentration). The total reaction volume was 1000 µL. The peptide substrate and phosphorylated product were co-eluted to the mass spectrometer with 80% acetonitrile, 0.1% TFA. Both peptides were confirmed to yield good electrospray mass spectra for fragment ions (m/z = 1188.36 and 1267.62 for PAKtide and pPAKtide, respectively). Each peak corresponds to a single injection from a different well with the product and substrate peaks detected from the same sample injections. Assays for each format were performed contemporaneously to ensure consistency of testing.

Control assays were initially performed to validate the whether or not PAK1 activity could be measured using the RF–MS kinase assays. PAK1 kinase was performed under the presence of either DMSO (control) and PAK1 inhibitor (Staurosporine 5uM and 10uM). HTMS signal of PAKtide and p-PAKtide were collected over given time period to evaluate the PAK1 activity under the influence of different modulators (see Figure 3.6.5).

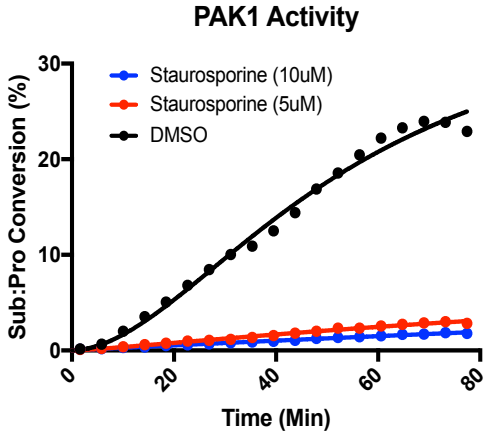

Figure 3.6.2 *Rapid-Fire mass spectrometry PAK1/CDC42 kinase assay: Staurosporine inhibits PAK1 activity*. The rates of substrate to product conversion were compared in PAK1 kinase reaction under the presence of staurosporine (PAK1 non- selective inhibitor, DMSO ■, 5μM ■, 10μM ■). All reactions contained 10nM of PAK1. RAFtide was used as the substrate. Measurements of the substrate weight (1926.1g/mol) and the product weight (2006.1g/mol) were compared throughout the reaction to determine the substrate: product conversion rate. Data are presented at a single point measurement at specific time point.

Under the standardized condition, the control activity (DMSO) was found to reach maximum conversion of 26.70 ± 2.8% and the rate of conversion was measured to be 0.445%/min. This indicates that PAK1 activity in such condition was only able to phosphorylate about ¼ of the substrate peptide into its phosphorylated form. On the other hand, kinase reactions under the influence of its inhibitor, staurosproine, exhibited significant inhibition effect on the PAK1 activity, as indicated by the low conversion (3.51 ± 0.63% at 5uM; 2.38 ± 0.54% at 10uM). The mechanism of staurosporine inhibition was though blocking the active site for ATP binding and thereby interfering with the substrate phosphorylation. We were able to accurately measure the effect of staurosporine inhibition and be able to verify the modulation of PAK1 activity through the RF–MS kinase assay.

To ensure that the RF–MS kinase assay was capable of detecting PAK1 activation modulation as well, another control assay was performed using the active CDC42 protein. CDC42 is one of main modulators of PAK1 and activates PAK1 through dissociating the homodimers of PAK1. This allows the autophosphorylation sites within PAK1 to be exposed and activate the kinase through phosphorylating one another (Parrini et al., 2002). CDC42 (1uM) was added under the same standardized RF– MS kinase assay, and the activity of PAK1 was subsequently detected through the HTMS signal integrations. (see Figure 3.6.3).

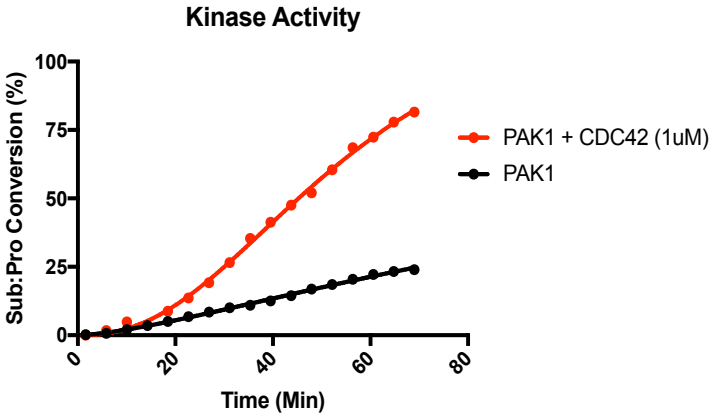

Figure 3.6.3 *Rapid-Fire mass spectrometry PAK1/CDC42 kinase assay: CDC42 stimulates PAK1 activity*. The rates of substrate to product (substrate phosphorylation) conversion were compared in PAK1 kinase. Reactions contained 10nM of PAK1 (■) with 1uM of CDC42 (■). RAFtide was used as the substrate. Measurements of the substrate weight (1188.36g/mol) and the product weight (1257.62g/mol) were compared throughout the reaction to determine the substrate: product conversion rate. Data are presented at a single point measurement at specific reaction time point

The effect of CDC42 on PAK1 activity was observed to be significant. Within 70 minutes of the kinase reaction, more than 80% of the total substrate peptide was converted into the

phosphorylated forms, while less than 25% of the substrate was converted under the DMSO control condition. The rate of conversion for PAK1/CDC42 and PAK1 (alone) were observed to be 1.16 %/min and 0.36 %/min, respectively. The inclusion of CDC42 in the PAK1 kinase reaction therefore had increased the PAK1 activity by 3.6-fold. As both inhibitory and excitatory effect could be observed through the RF-MS kinase assay, we had successfully verified that the RF-MS kinase assay could be used as a method to validate the efficacy of the optimized compound in modulating the PAK1 activity.

3.6.2 Rapid-Fire™ Mass-Spectrometer Kinase Assay: JB01 Validation

The RF-MS Kinase assay is able to directly assess the amount of substrate phosphorylation and thereby measuring the activity of PAK1. By comparing the percentage of substrate conversion between the control (DMSO) group and the compound treated (JB compounds) group, we can evaluate how well the compounds are stimulating the PAK1 activity. Because the first *in vitro* kinase assay (ADP-Glo™ Kinase assays) was only able to indirectly measure the PAK1 activity through measuring the amount of ADP formation, there was a high possibility of false positive reading from the assays. Therefore, the previous confirmed PAK1 activators were measured again using the newly established RF-MS kinase assay.

The efficacy of JB01 was firstly measured in two different conditions – presence of either PAK1 (10nM) or both PAK1 (10nM) and CDC42 (1uM). Based on the ADP-Glo™ Kinase assay results, JB01 PAK1 activator contained EC_{50} of ~5.6uM, and therefore 20uM concentration of JB01 was used to ensure that the PAK1 activation was be measured in RF-MS Kinase assay. Higher concentration was avoided in order to void measuring inhibitory effect on PAK1, potentially due to a non-specific binding at the ATP active site. Standardized RF–MS Kinase assay was performed to compare the rate of substrate phosphorylation at different conditions (See Figure 3.1).

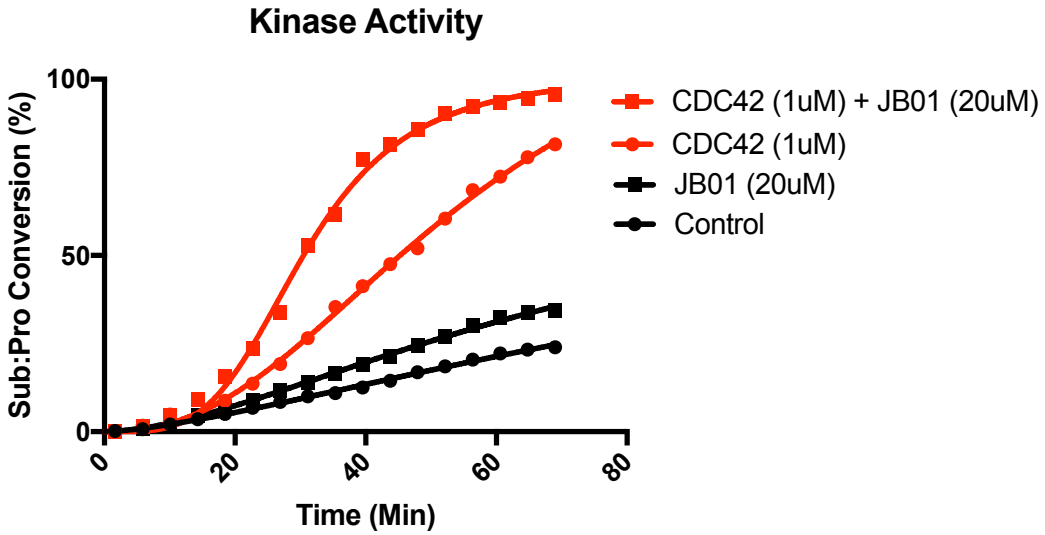

Figure 3.6.4 *Rapid-Fire mass spectrometry PAK1/CDC42 kinase assay*. JB compound is able to activate PAK1 directly, even without the presence of CDC42. This efficacy of PAK1 activation by JB compounds becomes augmented under the presence of CDC42. The rates of substrate to product (substrate phosphorylation) conversion were compared in PAK1/CDC42 kinase reaction under the presence of JB compounds (10um ■, 20uM ■, and DMSO ■). All reactions contained 10nM of PAK1 with 1uM of CDC42. Data are presented at a single point measurement at specific reaction time point.

Presence of JB01 (20uM) under the kinase assay exhibited higher conversion of substrate phosphorylation. The standard PAK1 activity was measured to be 1.2 ~ 1.7%/sec, and the activity was further increased to 1.5 ~ 1.9%/sec, under the presence of JB01 (20uM). The effect of the PAK1 activator was found to be not as high as the effect from the PAK1 biological modulator CDC42, which increased PAK1 activity to 2.0 ~ 2.6%/sec. When both JB01 and CDC42 were present in the kinase assay, however, the activity of PAK1 was further augmented by the PAK1 activator and started to exhibit sigmoid curve in its rate of substrate conversion (3.3 ~ 4.3%/sec); Within 50 minutes of the start of the kinase reaction, most substrate (> 90%) were already converted to its phosphorylated form in CDC42 + JB01 condition, while the control DMSO condition only exhibited a quarter (~ 25%) of substrate being able to be phosphorylation. The increase in the kinase activity by JB01 was found to be greater when the CDC42 was present than without it.

Such augmented increase in the kinase activity was intriguing as it provided further support in validating our proposing mechanism action of PAK1 activators. The PAK1 activators are thought to further activate PAK1 through preventing the dimerization of the monomers and thereby, keeping the PAK1 in its active form and allowing for more substrate to be

phosphorylated. Without the catalyst, such as CDC42, the frequency of PAK1 dissociation becomes low, and the number of exposed AI domain (ligand binding site) become limited for JB compound to bind. This may explain the lower efficacy in JB compounds ability to active PAK1, compared to that of when CDC42 is present in the system.

The rate of PAK1 dimers dissociating into monomers have a constant equilibrium rate, where PAK1 dimers can dissociate into monomers and the monomers can associate back as dimers. The equilibrium equation of PAK1 dissociation is as shown below:

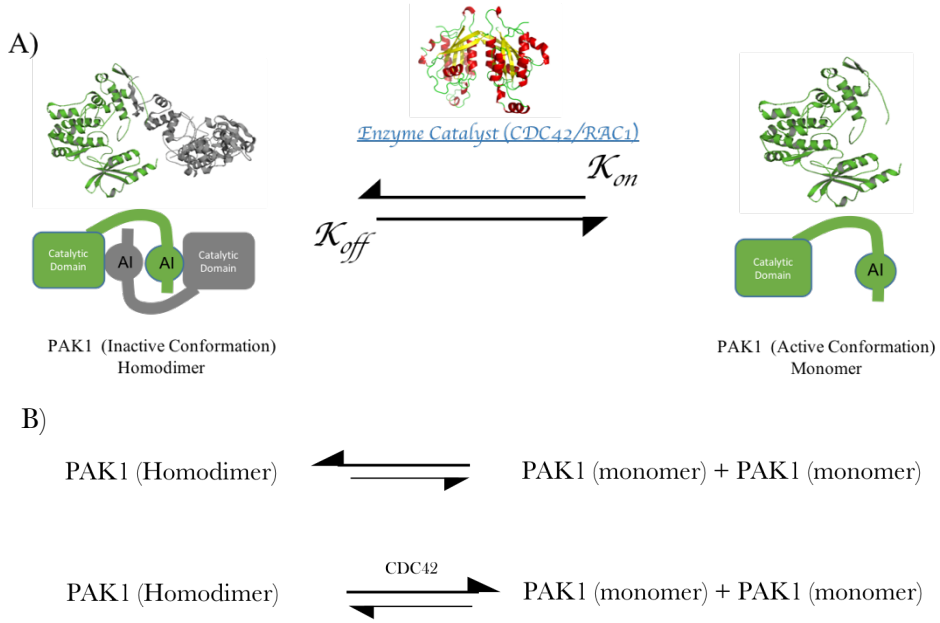

GTPases, such as CDC42 and RAC1, function as catalyst in dissociating PAK1 into monomers through binding at the PBD (protein binding domain). The equilibrium of dissociation therefore shifts more towards the monomer formation when CDC42 is present. As the PAK1 activators are thought to bind at the auto-inhibitory (AI) domain, the PAK1 needs to be dissociated at first to be able to expose the ligand binding site. The shift in the equilibrium by the presence of CDC42 allows more monomers to be present, more ligands to bind to their active site and make further prevention in dimer formations. Without the CDC42 protein, the rate of PAK1 dissociation into monomers is slower and therefore, only provides a few biding sites available for JB01. This may explain why the efficacy for JB01 was augmented when CDC42 was present, compared to without.

3.6.3 Rapid-Fire™ Mass-Spectrometer Kinase Assay: JB Compounds

The confirmation of PAK1 activation by JB01recognizes that the RF–MS Kinase assay is a valid method in measuring PAK1 activity. Furthermore, the effect of activation by JB01 was observed to be amplified when CDC42 was present in the kinase system. This had provided further support in our hypothesis of the compound's mode of action – where the increased PAK1 dissociation rate by CDC42 allows for more ligands to bind to PAK1-AID and thereby maintaining more active monomers for substrate phosphorylation. In order to amplify the effect of the PAK1activators, CDC42 was included for the subsequent kinase assays in order to signify for the activation effect. The CDC42 was synthesize with GppCP (non-hydrolysable analogue of GTP) complex, hence no additional GTP was needed and interfered with the kinase reaction.

The standardized condition as previously established in the control assays was applied when testing for the optimized JB compounds. Two concentrations – specifically, 10μM and 20μM – were chosen to test the efficacy of the compound in modulating PAK1 activity. Limited number of concentrations had to be used as the availability of the machine was limited due to its high occupancy. There was only one RF-MS machine available within the University, and its wide applicable usage of the machine limited its usage for only a short period of time. 10uM and 20uM concentrations were chosen based on its predicted affinity of the compounds. The molecules had been optimized limitedly, and it was highly likely that the EC_{50} of the compounds would not have change much. As the main purpose of the initial optimization process was to find compounds with better physiochemical profile, we were only concerned whether or not the compounds had any mechanism of modulating the activity of PAK1. Hence, 10μM and 20μM were chosen as these concentrations were thought to be sufficient in modulating PAK1 activity and requiring higher concentration would signify that the molecules are likely to be acting as non-specific binders.

JB01

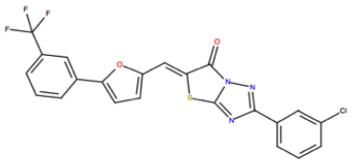

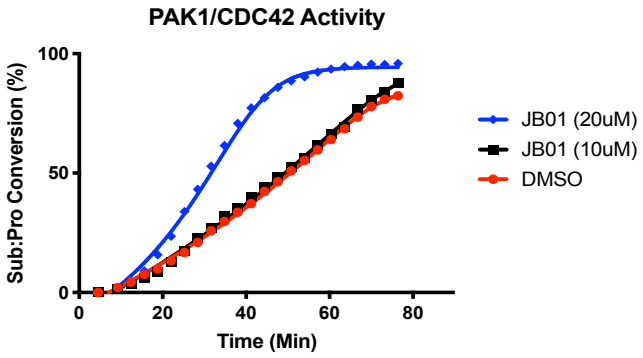

JB09

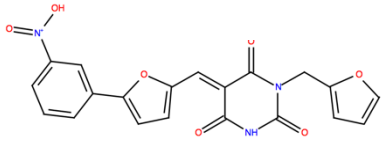

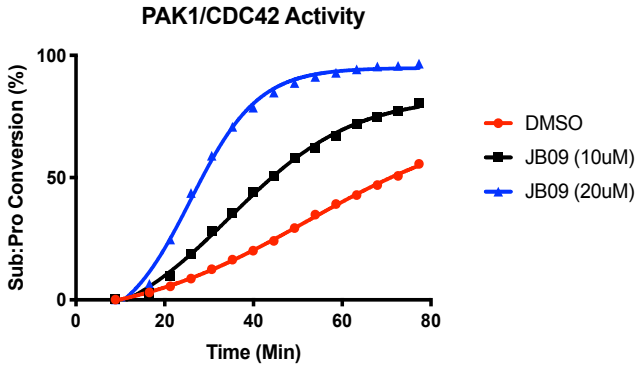

JB10

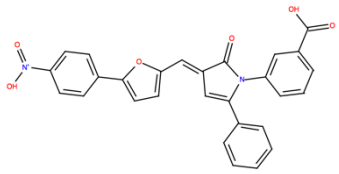

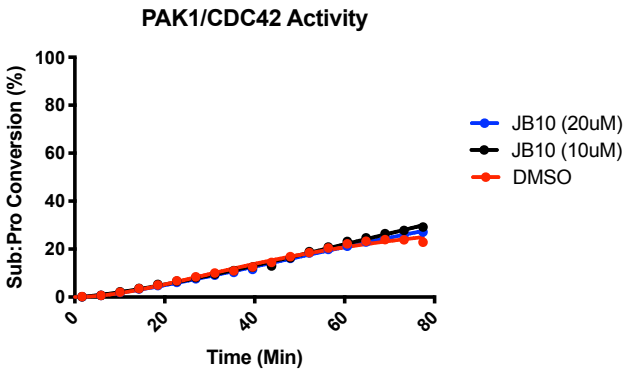

JB11

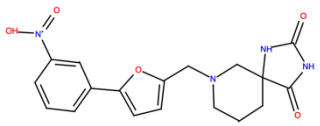

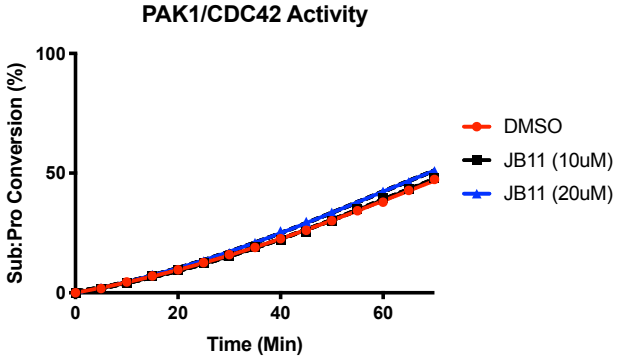

JB21

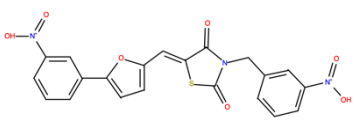

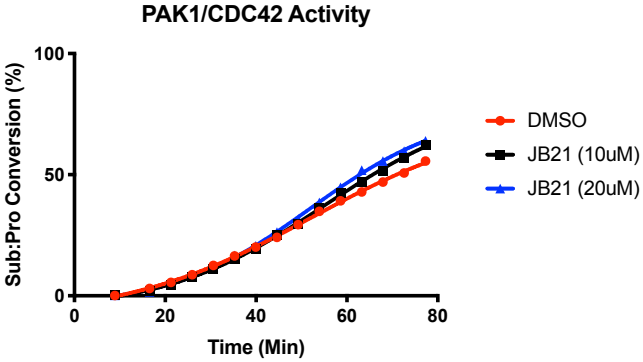

JB22

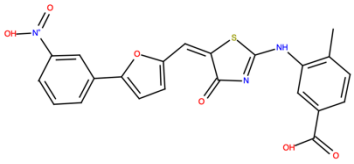

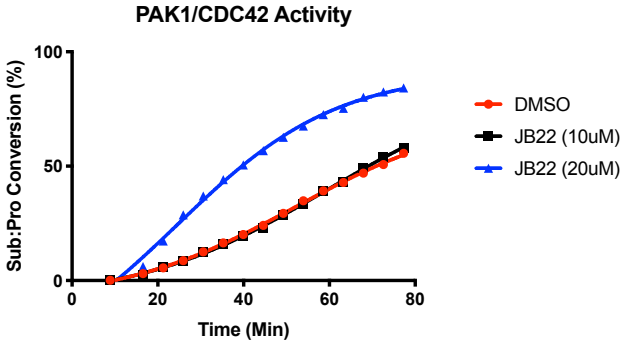

JB23

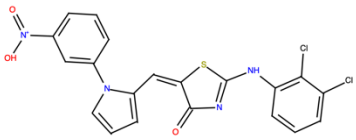

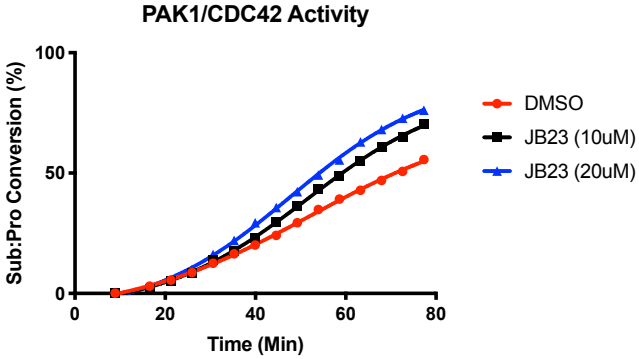

JB24

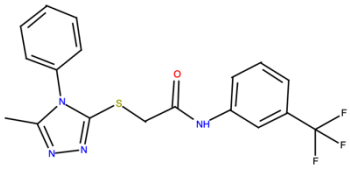

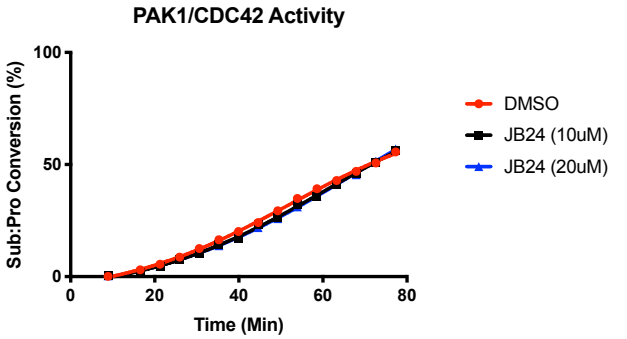

JB31

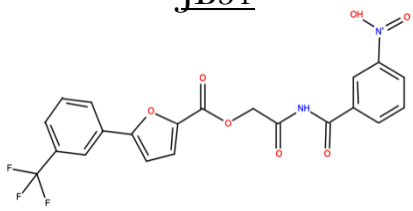

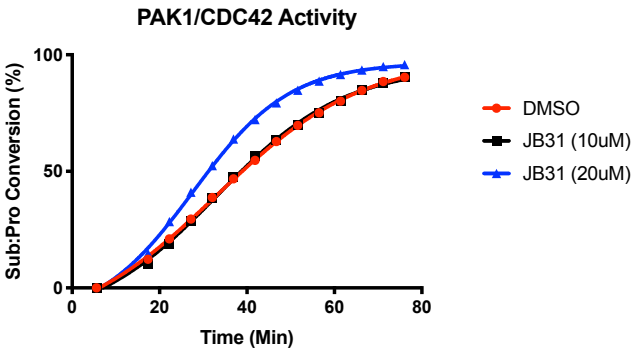

JB34

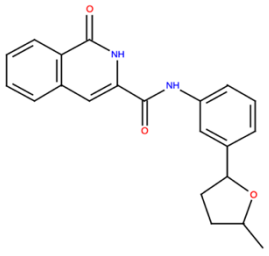

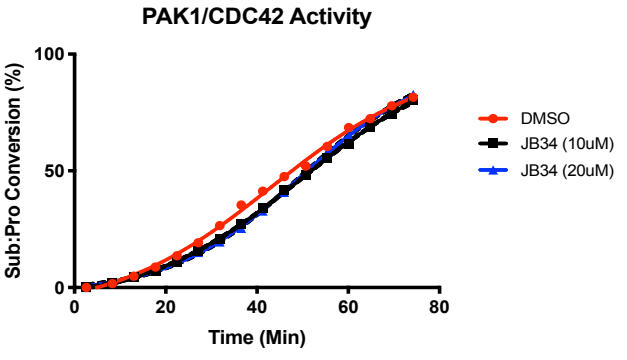

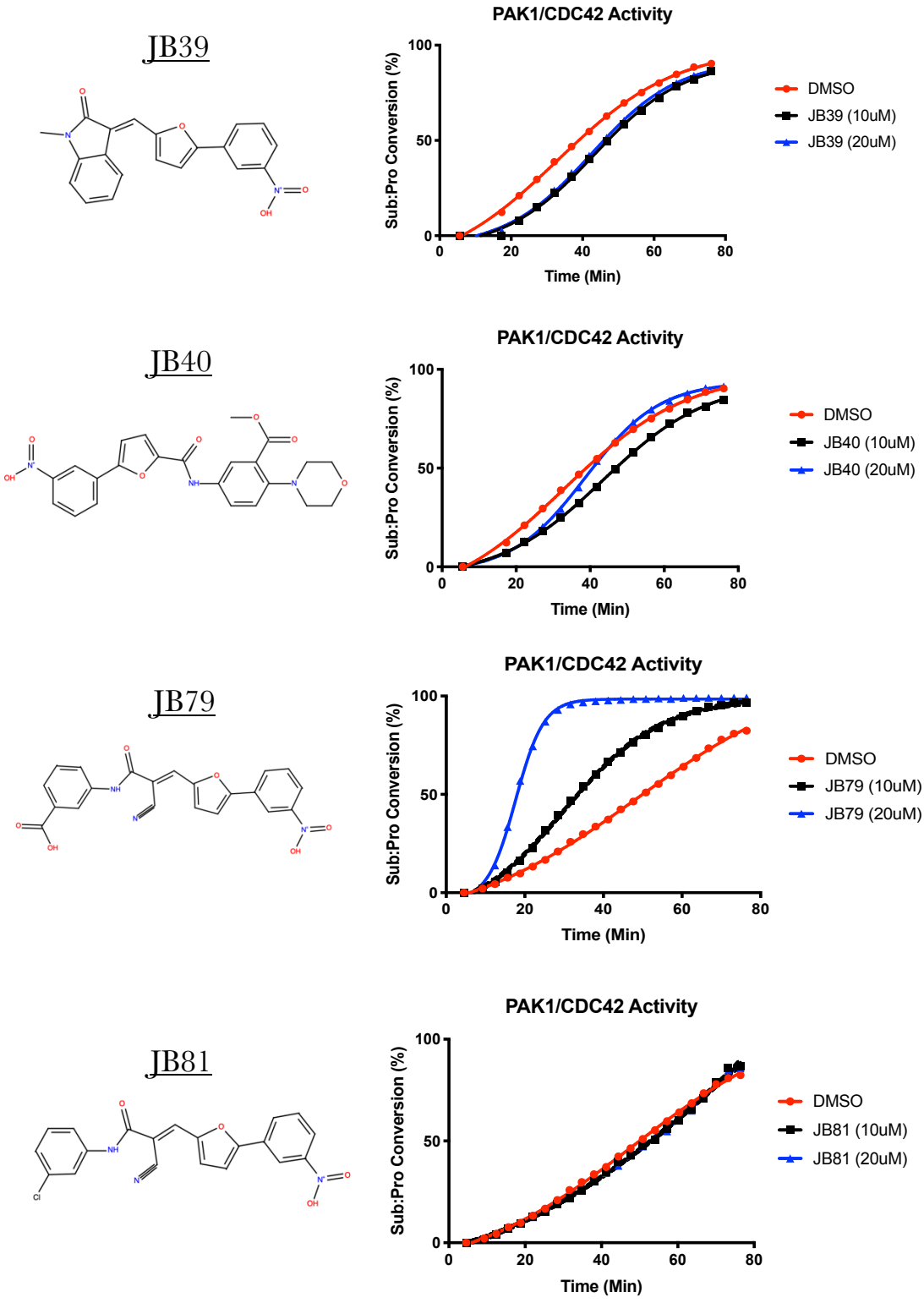

Figure 3.6.5 *RF-MS Kinase assay: Effect of JB compound activation on PAK1/CDC42.* The rates of substrate to product (substrate phosphorylation) conversion were compared in PAK1/CDC42 kinase reaction under the presence of JB compounds (10um ■, 20uM ■, and DMSO ■). All reactions contained 10nM of PAK1 with 1uM of CDC42. RAFtide was used as the substrate. Measurements of the substrate weight (1188.36 g/mol) and the product weight (1257.62 g/mol) were compared throughout the reaction to determine the substrate: product conversion rate. Data are presented at a single point measurement at specific reaction time point.

The optimized compounds that were previously tested using the ADP-GLO kinase assay were verified using the RF–MS Kinase assay. CDC42 was added in all subsequent kinase assays in order to amplify the difference in the kinase activity, in case there were any activation effect by the compounds. PAK1 activity was measured over time and it was compared with the previous results from the ADP–Glo Kinase assay as shown in Figure 3.5.

The RF–MS kinase assays show that compounds JB01, JB09, JB22, JB23 and JB79 at the observed concentrations exhibited significant activation effect on the PAK1 activity. Some compounds had less efficacy and required higher concentration (20uM) than others in order to raise the PAK1 activity. For compounds like JB01 and JB22, as examples, 10uM concentration was not sufficient in having any activation effect on the kinase activity; their slope of the enzymatic curve (1.13% substrate conversion/min) was similar as the DMSO control curves (1.08%/min). However, as the drug concentration exceeded the threshold concentration, the enzymatic activity slop became much steeper, estimating their highest rate to be at 3.35%/min for JB01 and 3.87%/min for JB22. Both compounds had increased the rate of substrate conversion by about 3.5-fold in average.

Although their substrate conversion rate was measured to similar between JB01 and JB22, the best fit curves of their data were set out to be different. JB01 exhibited a sigmoid curve, in which the curve followed the predicted phase of lag phase, exponential growth phase (highest rate of conversion), transitional phase and plateau phase – due to substrate limitation. JB22, on the other hand, illustrated more of a logarithmic curve, in which the rate of conversion was found to be highest initially and quickly plateaued as the substrate became limited. The reason for the difference in dose response curve shape could not be explained without firstly defining the exact mechanism of drug's activation. One could predict that JB01 may have had some cooperative activation effect, in which binding of the molecule not only kept the PAK1 in the activated state but may have also facilitated in the interaction between PAK1 and CDC42. However, such hypothesis could not be verified yet as the result for the co-crystallography was not available to confirm the mechanism of compound's action.

Compounds like JB09 and JB79 had already exhibited significant activation effect on PAK1 activity even at 10uM. Their slope of enzymatic curves were 2.1%/min and 3%/min, respectively, which were 2.8-fold and 2.1-fold higher than their control enzymatic activity. By

20uM, their slope of the enzymic curves had dramatically increased. Kinase reactions that contained 20uM JB79 exhibited substrate conversion rate of 7.66 %/min, which was 7.23 times greater than that of the control activity; within 20 minutes start of the kinase reaction, > 90% substrate had been already phosphorylated to its product form, illustrating a significant activation effect. Similarly, JB09 also showed a significant action, 4.83 %/min, which translated to be around 4.76 times greater than the control rate of substrate conversion. According to the ADP-GLO kinase assay, the dose response curve show that JB79 has lower EC50 than that of JB09. This may explain for the difference in the affinity and thereby its potency as well; greater concentration for JB09 would have required in order to reach similar activation as JB79.

RF–MS kinase assay results for JB11, JB39, and JB81 were unexpected as these compounds were previously confirmed to have activation effect on PAK1. According to the ADP-GLO kinase assay result, JB39 portrayed a dose dependent activation on PAK1 activity, reaching over 150% activation within 20uM concentration. JB81 also showed a distinct dose response relationship between the compound concentration and the kinase activity despite low maximum activation effect. These kinase assay results revealed that some of the results from the ADP–GLO were uncertain and require further attention when verifying the compound's effect. ADP-Glo kinase assay uses an indirect method of measuring the kinase activity and uses luminesce as a way to detect the labelling probes. Although the assay had successfully showed that JB01, JB09, JB22, and JB79 were significant PAK1 activators and validated others to be non-PAK1 activators, it was proven to have lower sensitivity and more vulnerable towards false positive reading in comparison to the RF–MS Kinase assay. Therefore, unless the modulation of activity was significant (<2-fold increase), using the ADP–GLO kinase assay was demonstrated to be inefficient in accurately measuring the compound's efficacy.

In conclusion, RF–MS kinase assay had directly confirmed that JB01, JB09, JB22, and JB79 have stimulatory effect on PAK1. JB09 and JB79 were especially more significant activators amongst the confirmed ones. The rest of the first batch of compounds, however, were proven to be non-significant PAK1 activators. The RF–MS kinase assay also proved that the ADP–Glo assay requires attention when assessing the compound's efficacy. Hence for all subsequently studies, RF-MS kinase assay was only utilized for confirming the efficacy of the compound on PAK1 activity.

3.7 Summary & Concluding Remarks

As discussed above, the wide use of *in silico* computational methods has been underpinned by their higher cost-effectiveness as compared to that of the traditional methods of ligand-library screening. However, when applied in the optimization of novel ligand molecules or in the improvement of compounds' physiochemical properties, all *in silico* tools require verification through *in vitro* experiments. This chapter reports the results of our validating the efficacy of the screened *in silico* compounds and provides further insight on the structure activity relationship (SAR) of protein-ligand interactions. The screened hit compounds were examined in two different types of *in vitro* kinase assays: the ADP-Glo™ and Rapid-Fire™ Mass-Spectrometer (RF-MS). The ADP-Glo™ Kinase Assay was used as a preliminary method to establish whether or not the compounds contained any stimulatory effect on PAK1. Next, those compounds that showed a significant stimulation on PAK1 activity were subsequently confirmed using the RF-MS kinase assays. The secondary kinase assay was used to ensure that the assay results between the two assays were consistent, as well as to minimize the risk of any false reading.

The results of RF-MS Kinase assay results provided several interesting insights about the mechanism of action of PAK1 activator. Specifically, these ligands were found to confer their activity through binding at an allosteric site that was different from that of the regulatory proteins (e.g., CDC42 and RAC1). Furthermore, when CDC42 was presented in the *in vitro* setting, JB compounds were shown to induce PAK1 activity in an amplified manner. Competitive observation between CDC42 and the PAK1 activators could not be measured, which was illustrated by observing an increased dose- dependent activation in all concentration ranges. This finding demonstrates that the mechanism of the compound's activation on PAK1 is most likely to be at a different allosteric site than the one which the regulatory protein binds to. We hypothesized that the compound binds to the AID, while the CDC42 binds to the PBD, eliciting an augmented stimulatory effect in the presence of both the ligand and CDC42. However, further biophysical research to confirm the mechanism action of the PAK1 activators outlined above would be necessary.

Finally, observing the direct stimulatory effect of JB compounds on PAK1 led us to the next phase of the drug discovery process—that of optimization of hit compounds. To this end, in

order to optimize the compounds with enhanced physiological chemical profiles, as well as to improve their selectivity and efficacy towards PAK1 activation, we used *in silico* QSAR. Due to limited funding availability at the time of this experiment, ligand optimization was based on the libraries of compounds available from commercial companies. Novel compounds were evaluated through a comparison of their docking scores with their efficacy in PAK1 activation through *in vitro* kinase assays. Possible correlations between compounds' efficacy and the docking scores were examined. Regrettably, no such correlations were found. Possible explanations of this result include insufficient representativeness of the software in terms of recreating the protein-ligand active site (e.g. due to imprecise algorithm), or the fact that the ligand binding site used for the docking study was not the actual ligand binding site. Uncertain correlation of the docking studies led us to design subsequent compounds through exploring other chemical series. Accordingly, early optimization of the ligands was designed through comparing similar pharmacophores and using SAR results from the RF-MS kinase assays. Through the optimization process, we were able to discover other JB compounds with a significant stimulatory effect on PAK1 activity. JB79, one of the early optimized compounds, showed a significantly higher affinity towards PAK1 and improved physiochemical properties as compared to those of JB01. These characteristics determined our decision to use JB79 as the lead compound to be tested in functional studies and to examine its clinical applications for alleviating CVDs complications.

CHAPTER 4

CLINICAL TRANSLATION: SMALL-MOLECULE PAK1 ACTIVATORS

Summary Points

- Lead PAK1 activator compound JB79 was used to evaluate the clinical translatability of PAK1 activators for CVD therapeutics.
- Cardioprotective effect of JB79 on human cardiomyocytes derived from induced pluripotent stem cells (ISPC) showed significant anti-arrhythmic effect and reduced β-adrenergic stress.
- Ex vivo heart pretreated with JB79 displayed a significantly higher threshold voltage required to stimulate ventricular fibrillation than the vehicle treated groups.
- PAK1 activators also exhibited significant benefit in alleviating TAC-induced cardiac myopathy caused by pressure overload.
- Potential side effects of cancer development by kinase activation was evaluated through using cancer cell models – examining effects of JB79 on proliferation, migration, and invasion characteristics.
- Overall functional improvement by PAK1 activators was observed, while exhibiting promising therapeutic application for prospective drug discovery in the cardiovascular field.

4.1 Background Overview

Recent research on the therapeutic validation of PAK1 has demonstrated the anti-hypertrophic effect of PAK1 in cardiac cells. PAK1 has been reported to maintain ventricular Ca^{2+} homeostasis and electrophysiological stability through the regulation of SERCA2a expression (Ke at al., 2012; Liu et al., 2011, 2012). Mouse hearts with a cardiomyocyte-specific PAK1 deletion ($Pak1^{cko}$) have displayed arrhythmic instabilities, particularly after either acute or chronic β-adrenergic stress (Desantiago et al., 2013). The cause of arrhythmias are likely due to aberrant cellular Ca^{2+} homeostasis from the downregulation of SERCA2a expression modulated by the lack of PAK1 during cardiogenesis (Niu et al., 2007; Miano et al., 2007). In addition, evidence is available showing that PAK1 activation rescued by FTY720 – indirect activators of PAK1 – leads to a significant improvement in mice models, thereby providing a proof of concept that Pak1 activation contributes to restoring the mechanism of improving the control and contractile function of a failing arrhythmic heart (Egom et al., 2010). Unfortunately, due to the activation of the cardiac G protein-gated potassium channel (I_{KACh}) through a S1P receptor (mostly S1P3), FTY720 treatments are known to lead to infrequent delays in the AV conduction and asymptomatic bradycardia in clinical trials. Taken together, the results of previous studies suggest that there is a need to find a way to directly activate PAK1 so that to provide cardio-protection, but without affecting the S1P pathway and inducing adverse effects.

In the present study, using the *in silico* drug discovery method (see Chapters X-Y), we found small-molecule PAK1 activators that can directly stimulate the kinase activity. Two different *in vitro* kinase assays were used to verify the results of each other's assay results. The results confirmed that the discovered PAK1 activators have a significant stimulatory effect in PAK1. For example, PAK1 treated with JB01 (20uM) exhibited a 2-fold increase in its activity as compared to the control group. In order to improve the efficacy and physiochemical profiles of X, we sought to optimize the small-molecule PAK1 activator. Among the compounds derived from this limited optimization procedure, JB79 was found to have the highest activation effect on PAK1 activity with the lowest EC_{50}. Compared to JB01 compound, JB79 showed improvements in both its physiochemical properties and the activation effect. In addition, since JB79 has a lower molecular weight, it has a greater ability to permeate through the lipid bilayers and greater ability to dissolute into water, resulting in improved water solubility. In addition, JB79 is predicted to have a lower first-pass metabolism, exhibiting lower half-life and reducing likelihood of causing toxicity in liver. Its relative efficacy enhanced 2.3-fold as compared to

JB01, and 4-fold as compared to its vehicle DMSO treatments. Based on this evidence about the overall improvement in small-molecule PAK1 activators, we chose JB79 as the lead compound for subsequent functional studies. As PAK1 activators have not been reported in previous research, we deemed it necessary to examine whether the PAK1 activators would provide any therapeutic benefits or have any adverse effect.

In this chapter, we aimed to characterize the physiological effect of small-molecule PAK1 activators on various cellular models, including *ex vivo* whole heart, isolated cardiomyocytes, and induced pluripotent stem cells (IPSCs). To this end, the lead compound JB79 was used to evaluate the clinical translatability of PAK1 activators, particularly for symptomatic diseases involved in the progression of heart failure (e.g., arrhythmia and hypertrophy). In previous research, activation of kinase has been reported to be involved in the development of cancers (Kumar et al., 2006). To ensure that the activation of PAK1 through the JB compounds would not produce any unintended cancer-promoting consequences, potential side effects of JB79 were tested using two cancer cell lines: HOP92, a cell line from human non-small lung carcinoma, and MDA-MB-231, a cell line from human breast adenocarcinoma. Using functional studies, we characterized potential therapeutic applications of using small-molecule PAK1 activators. Although our results did not provide a comprehensive physiological characterization of Pak1 activation in cellular models, early indications for therapeutic benefits of PAK1 activators suggest its potential druggability for future novel therapies against cardiovascular complications.

4.2 Anti-arrhythmic effect of JB79 on ISO-induced adult cardiomyocytes

Cardiac arrhythmia is defined as a deviation from the normal heart rate and rhythm, which is attributed by various underlying causes. As there are several schemes used to classify the mechanism of cardiac arrhythmias, the term cardiac arrhythmias incorporate a wide spectrum of abnormal cardiac contractions, including atrial fibrillation (AF), ventricular tachycardia (VT), polymorphic and singular VT, premature ventricular tachycardia (PVT). Individual cardiac arrhythmias are often result from dysregulation between cardiac action potential and electrical cell coupling, affected by both genetic heterogeneity of ion channels and environmental factors (Barth and Tomaselli; 2009). Sustained cardiac arrhythmias has been reported to lead to sudden arrhythmic deaths, accounting for more than 75% – 80% of sudden cardiac deaths (Adabag et al., 2010). This have been a major concern for public health, and much effort has been put in the last years in order to reduce the prevalence of the disease. However, with each cardiac arrhythmic symptom found to be unique for individual patients, both the prognosis and the treatment becomes elusive and may lead to an ineffective development anti-arrhythmic therapy.

Current medical therapies for cardiac arrhythmias possess significant cardiac and extracardiac side effects, the most concerning of which are their pro-arrhythmic properties. Amongst the patients with heart failure, who has high risks of cardiac arrhythmias, both angiotensinogen-converting-enzyme (ACE) inhibitors and β-blockers have been shown to reduce mortality and the incidence of sudden death (Van der Horst et al., 2007). However, prolong usage of these drugs have been labeled with deterioration in their quality of life, and patients become more vulnerable towards overdosing. Other classes of anti-arrhythmic drugs such as flecainide and propafenone, have been contraindicated and reported to have high pro-arrhythmic risks (Andrikopoulus et al., 2015). These findings have highlighted a need for a better anti-arrhythmic drug through exploring other therapeutic signaling pathways.

As described in Chapter 1, PAK1 has been extensively studied to provide essential roles in providing anti-arrhythmic effect. Therefore, we wanted to evaluate whether or not the newly developed PAK1 activator JB79 had any therapeutic benefits in providing cardioprotective

mechanisms, specifically in alleviating cardiac arrhythmias. Amongst various models of mimicking arrhythmias, isoprenaline (ISO) induced β-stimulations on cardiomyocytes was one of common methods of mimicking the disease symptoms. Using the Fluo-4 AM dye, we were able to record irregular calcium transients induced by ISO and look for any therapeutic effect of JB79. Detailed established protocol is described in the Appendix 1.

To measure the effect of JB79 on calcium regulation in cardiomyocytes, Krebs solutions containing the following reagents were prepared and perfused over the cells: Solvent 1 (Krebs solution), Solvent 2 (isoprenaline, 5nM), Solvent 3 (JB79, 20uM), and Solvent 4 (ISO 5nM + JB79 20uM). All protocols involved 5 minutes of buffer perfusion at first, followed by perfusion of other solvents. All recordings were made after 5 minutes of perfusion.

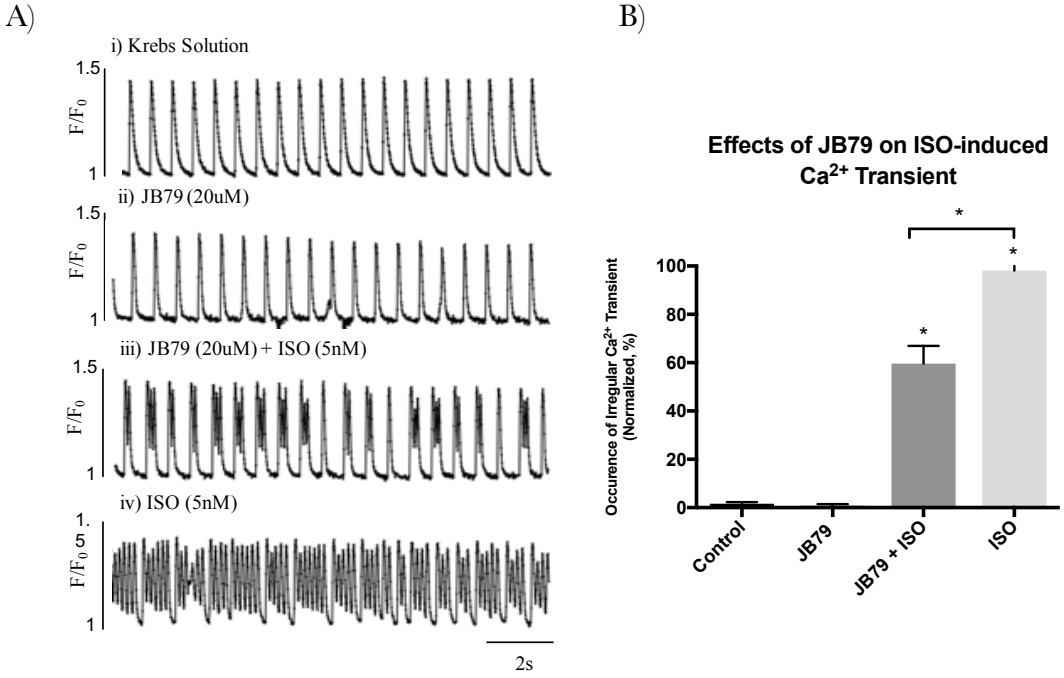

Figure 4.2 *Calcium transient recording of cardiomyocyte* **A)**Time course and representative effects of transient perfusion with i) Kreb's solution ii) JB79 (20uM) iii) JB79 (20uM) + ISO (5nM) iv) ISO (5nM). **B)** Normalized occurrence of irregular calcium transients. Quantification based on the total number of irregular calcium transients divided by the total number of calcium transients measured. Presence of JB79 exhibited a decrease in the number of irregular calcium transients induced by isoprenaline, while showing no abnormalities when administered alone. Calcium-dependent fluorescence dye Fluo 4-AM was used to measure the transients and the fluorescence was recorded at 490nm. Measurements were recorded for 60 seconds after five-minutes of solvent perfusion.

Phenotypic observations of irregular calcium transients were compared between ISO (5nM) and JB79 (20uM) + ISO(5nM). After 5 minutes of perfusion, ISO-induced cardiac myocytes

exhibited irregular calcium transients – including double transients, triple transients, and no transients (see Figure 4.2, iv). The number of ISO-induced irregular peaks, however, was significantly decreased when the cells were co-administered with JB79 + ISO (see Figure 4.2, iii). Anti-arrhythmic effect seen with JB79 was hypothesized to be due to the activation of PAK1, leading to protein phosphatase 2A (PP2A) activation normalizing the calcium handling disruption caused by isoprenaline. Finally, JB79 pre-treatment alone in the system did not exhibit any significant abnormalities in cell calcium handling, indicating no pro-arrhythmic effect on the cardiomyocytes. (see Figure 4.2, ii).

Further investigation was made in order to see whether or not, the arrhythmia induced by ISO could be reversible by the JB79 administrations. After 5 minutes of ISO perfusion, isolated cardiomyocytes were switched to JB79 (10uM) + ISO (5nM) perfusions and the rate of calcium transients were measured. Regrettably, the reversible effect of JB79 could not be measured. Even after perfusing with JB79 (10uM) alone solution for more than 5 minutes, no significant improvement could be observed in the cardiomyocytes' ability to handle calcium levels. These results illustrate that an extensive β-stimulation shock may lead to an irreversible damage to cardiomyocytes in which above a certain threshold, the cellular damage may become too difficult to repair.

When comparing phenotypic irregular transients between ISO treatment and JB79/ISO treatments, co-perfusion of JB79 cardiomyocytes had exhibited higher tolerance for ISO. Quantification was based on the total number of irregular calcium transients divided by the total number of calcium transients measured in 60 seconds. The results were normalized to the value obtained from ISO, which showed the highest ratio between irregular to normal calcium transients (see Figure 4.2 B.). In comparison to the control, JB79 at 20uM did not show a significant effect on calcium transients in cardiomyocytes; both control and JB79 alone exhibited normal transient values, with only a few irregular transients. JB79 + ISO exhibited about 53 ± 16% irregular transients, while ISO induced irregular transients in almost all calcium transients. The statistical P-value between JB79/ISO and ISO was calculated to be 0.0003 using the unpaired T-test, indicating a significant difference between the two groups.

From the *in vitro* assays above, we were able to demonstrate that the JB79 treatment can provide cardio-protection against beta-adrenergic stressors. Administration of JB79 along with isoprenaline resulted in a significant reduction in the number of irregular calcium transients, compare to that of the isoprenaline treated group. Our control data also confirms that the administration of JB79 alone does not cause any significant disruption of calcium transients, indicating no toxicity to the cells. The likely mechanism of JB79 providing greater calcium handling is through its PP2A interactions and NO productions (Kwon et al., 2001, Ke et al., 2013). These results provide preliminary evidence for JB79 as an effective prophylactic measure in relieving adrenergic stress responses and possibly in preventing arrhythmia.

4.3 Anti-arrhythmic effect of JB79 on Induced Pluripotent Stem Cells (IPSC)

Calcium transient assay have demonstrated that PAK1 activation by JB79 was able to repress ISO-induced arrhythmias, through providing prophylactic measurement against disturbance in calcium handling. The current hypothesis about these anti-adrenergic effects of PAK1 is though the activation of protein phosphatase 2A (PP2A), one of the main serine-threonine phosphatases active in maintaining cell homeostasis by inhibiting most kinase-driven intracellular signaling pathways. However, PAK1 activation characterization have been only proven through using animal models, not in human samples. Therefore, in order to mitigate concern for transability, our lab has recently developed a method to mature the human iPSC-derived cardiomyocytes (iPSC-CMs). These iPSC-CMs have been widely recognized to be an invaluable *in vitro* model for human translational research and for drug discovery (Malepu et al., 2017; Li, 2016; Alamo et al., 2016). IPSC-CMs may offer significant advances in the study of cardiac disease and treatments as these cells have been confirmed to contract rhythmically (Snir et al., 2003) and respond appropriately to numerous cardioactive drugs (Denning and Anderson, 2008; Dick et al., 2010). Therefore, IPSC-CMs are useful for measuring therapeutic translatability from animal models to human tissue, providing early evidence on effectiveness of the drugs on human patient models.

In order to measure the translational therapeutic application of JB79 for humans, the effect of PAK1 activators were examined using IPSC-CMs. Specifically, the β-adrenergic stimulation,

induced by isoprenaline (ISO), were compared between JB79 treated group vs. non-treated group.

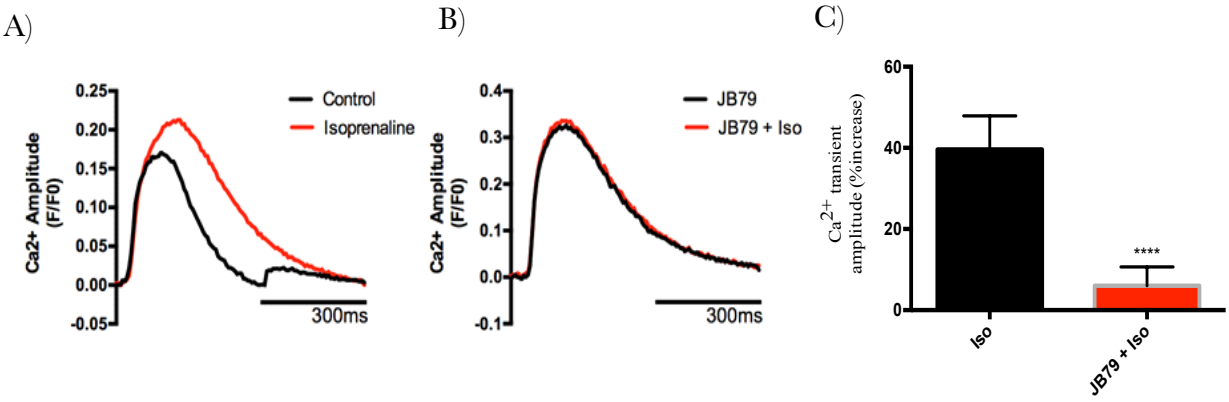

Figure 4.3 *Representative Ca^{2+} transients recorded from human iPSCs showing the effects of 100nM isoprenaline and 20μM JB79.* Cells were loaded with fluo-4 at 37°C. **A)** Isoprenaline evoked an increase Ca^{2+} transient amplitude within the control experiments. **B)** Pre-treatment with 20μM JB79 with and without application of 100nM isoprenaline evoked significantly smaller increases with pre-treatment with JB79**. C)** Quantitative analysis comparison between the ISO alone and ISO + JB79 (20uM) pre-treatments. $P < 0.05$, n = 5.

Cardiomyocytes from Days 25-30 post initiation of differentiating human iPSC derived cardiomyocytes were used to assess the effect of isoprenaline on Ca^{2+} transient amplitude (see Figure 4.3). These cells were differentiated and obtained from Faizaan and Meng, who were working on IPSC-CMs in Ming's Lab at the time. When IPSC-CMs were perfused with 100nM isoprenaline, there was a significantly higher fluorescence intensity observed during the calcium transients (39 ± 10 %, $P < 0.05$, n = 5), mainly due to β-adrenergic stimulation which increased the calcium flow within the SR during contractions. The observed increased in calcium transient amplitude, however, was significantly attenuated when the cardiomyocytes were pretreated with 20uM JB79. The pretreated JB79 cells had abolished the ISO induced alteration of Ca^{2+} transients ($P < 0.05$, n = 5), while having minimal affect in its baseline activity. These findings were similar to the previous characteristics of PAK1 (CA-PAK1) – genetically modified mice which had constitutively active – PAK1 (CA-PAK1). CA-PAK1 overexpressed cardiomyocytes had exhibited an altered Ca^{2+} transient decay constants (τCa) and reduced adrenergic signalling – attenuating the activity of LTCCs and other Ca^{2+} regulating proteins (Sheehan et al., 2009). Observation of cardioprotective mechanisms by JB79 PAK1 suggests evidence of therapeutic applications in human tissue for the first time.

4.4 Ex vivo Heart: Anti-arrhythmic effect of JB79 on PES-induced arrhythmia

Abnormal intracellular Ca^{2+} handling has been attributed as a major cellular mechanism underlying ventricular arrhythmias associated with cardiac hypertrophy (CH) and heart failure (HF). Cardiac hypertrophy is often associated to elicit arrhythmic substrates in ventricle – creating transient factors that can lead to initiate ventricular tachyarrhythmia (Wang et al., 2014). Therefore, any agents limiting hypertrophic remodeling could potentially be used as an anti-arrhythmic drug. As JB79 PAK1 activator has been previously shown to reduce cardiac hypertrophy, we wanted to investigate whether or not, the PAK1 activators had prophylactic measurement against ventricular arrhythmogenesis.

To firstly assess propensity to exhibit ventricular arrhythmias, Langendorff-perfused hearts from 3 to 4-month old mice were subjected to programmed electrical stimulation (PES). PES method utilizes miniature catheter which inserts through the diaphragm directly, arriving at the epicardial surface of the heart and stimulating at the programed pace. Surface ECG is then used to measure the electrogram of the heart activity using a digital electrophysiology lab to determine the arrhythmia inducibility. Ventricular arrhythmia was defined as six or more consecutive premature ventricular waveforms (tachycardia with regular waveforms defined as VT, while VF was characterized by irregular fibrillating waveforms). PES was performed using a standardized protocol that included trains of eight basal stimuli (S1) delivering at 8Hz, followed by up to 3 extra stimuli (S2–S4), delivered with a coupling interval decreasing in steps of 1 ms until ventricular or atrial refractoriness was reached. The ventricular electrogram under the standard PES settings are as illustrated in Figure 4.4 A) Through high pace stimulation, underlying primary electrical disorders, including ventricular fibrillation, ventricular tachycardia, and premature ventricular contractions (PVCs), were evaluated for measuring the severity of heart disease and for arrhythmia risk predictions. PAK1 activator JB79 (5mg/kg and 10mg/kg) was pre-treated for 2-week periods, before the excision of the heart in order to measure the prophylactic effect of PAK1 activators against stimulation-induced arrhythmia. Occurrence and duration of inducible arrhythmias (PVC) were firstly documented in Figure 4.4.1 B)

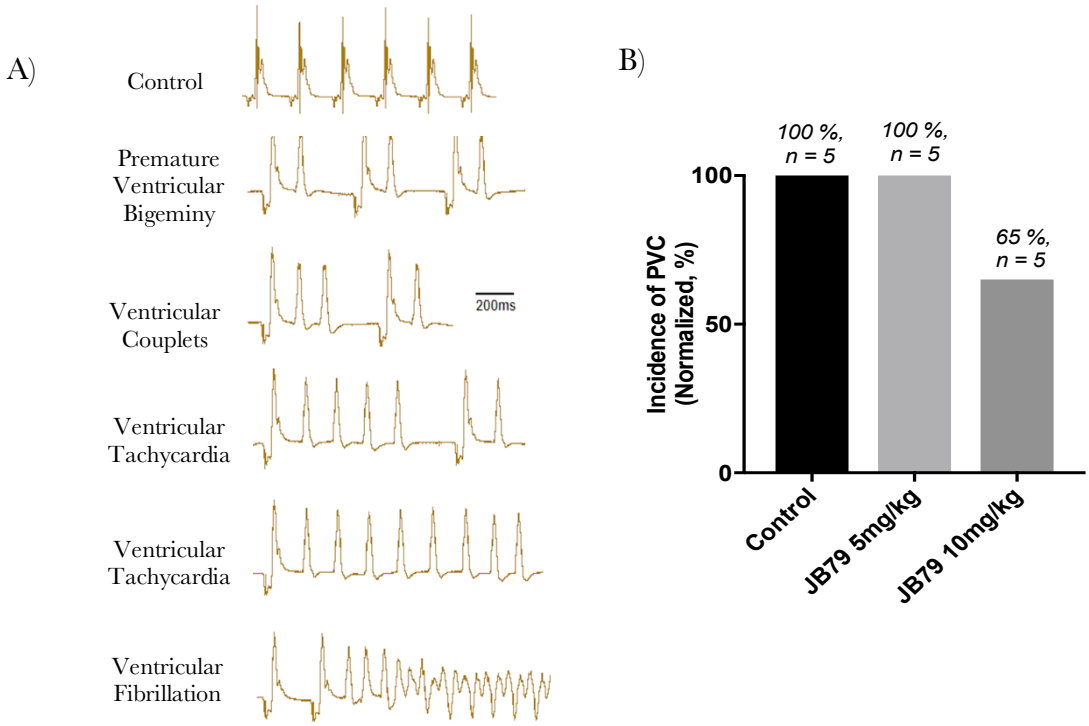

Figure 4.4.1 *Electrocardiography under PES with different indications of arrhythmia.* **A)** PES was performed using a standardized protocol that included trains of eight basal stimuli (S1) delivering at 8Hz, followed by up to 3 extra stimuli (S2–S4), delivered with a coupling interval decreasing in steps of 1 ms until ventricular or atrial refractoriness was reached. **B)** *incidence of PVC under standardized PES conditions with JB79 treatments.* JB79 10mg/kg exhibited significant reduction in the incidence of PVC in comparison to the vehicle treated groups. $P < 0.05$, n = 5.

PES setting was established in such condition that it would always promote premature ventricular contraction (as illustrated as 100% in the control group). Two different conditions of JB79 were administrated to compare their anti-arrhythmic effects: 5mg/kg and 10kg/kg. JB79 concentration at 5mg/kg was measured to have the same PVC incidence rate as that of the control group (all mice showed PVC at the control PES setting). JB79 at 10mg/kg however were found to have lower incidence of PVC; 60% of the mice exhibited symptoms of PVC. While this was only a preliminary study before conducting a larger scale experiments and therefore, the number of samples was too low to provide any statistical significance, these results along with previous study conducted using indirect PAK1 activators provide further support PAK1 activators as having anti-arrhythmic effect. Larger scale experiment will be conducted in due course to confirm the above study.

Another underlying symptom of a failing heart is ventricular fibrillations, which is a significant cause of sudden cardiac death (SVDs) (Baher and Valderrabano, 2013). The triggering mechanism of ventricular fibrillation (VF) are poorly understood as of today. However,

previous report has indicated that spontaneous VF in the form of arrhythmic storm are often initiated by PCV (Munoz et al., 2010). As a lower incidence rate of PVC was observed when the hearts were pre-treated with PAK1 activators, we wanted to further investigate whether or not the pre-treatment of PAK1 activator JB79 had any cardioprotective effect in reducing the incidence of VF as well.

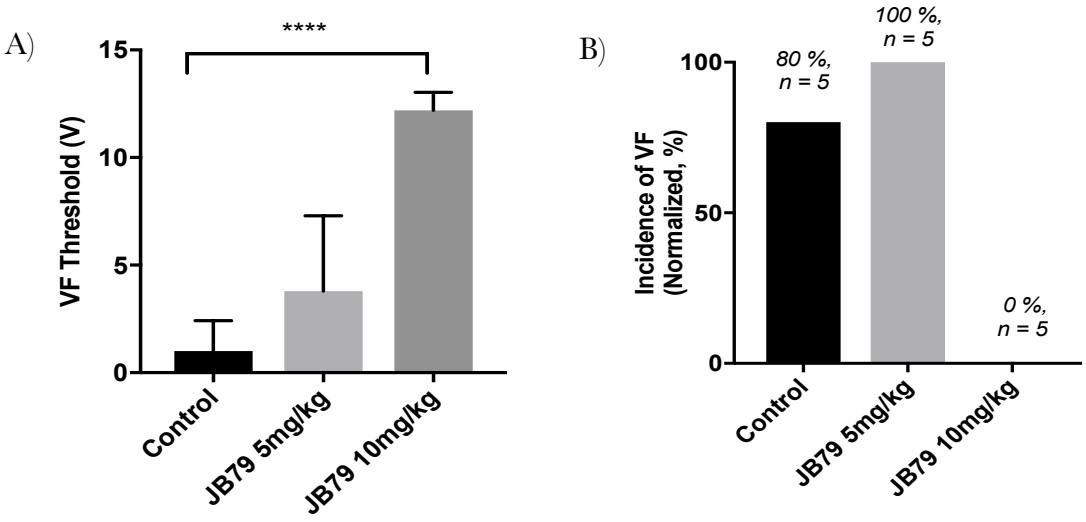

Figure 4.4.2 *Effect of JB79 on the VF Voltage threshold* **A)** Pre-treatment of PAK1 activator showed significant increase in the voltage required to trigger VF in comparison to the vehicle group ($P < 0.05$, n = 5). **B)** *incidence of VF under standardized PES conditions with JB79 treatments.* JB79 10mg/kg exhibited significant reduction in the incidence of VF, while the PES setting caused VF in most of the control group and JB79 5mg/kg group. $P < 0.05$, n = 5. VF was defined as six or more consecutive premature ventricular waveforms.

Incidence of VF was measured under the same setting as that of PVC (See Figure 4.4.2 **B**). Similar to the previous results, both the control and the JB79 (5mg/kg) pre-treated groups exhibited high occurrence of VF (defined as six or more consecutive premature ventricular waveforms); 80% of the control group had shown a form of VF, while all of the pre-treated JB79 (5mg/kg) mice showed VF. Interesting, when the treatment concentration of JB79 had doubled to 10mg/kg, none of the mice had displayed any signs of VF. Therefore, higher concentration of JB79 was observed to be sufficient in abolishing the trigger for VF. Upon further measuring the voltage that was required to initiate VF, we measured a dose dependent relationship between the JB79 concentration and the VF threshold; progressively higher voltage threshold was observed as the treatment concentration increased (See Figure 4.4.2 **A**). The

mean voltage threshold required to trigger VF were 1 ± 0.63, 3.8 ± 1.58 and 12.2 ± 0.37, for vehicle, JB79 (5mg/kg) and JB79 (10mg/kg), respectively. Although no statistical difference was observed between the control group and JB79 (5mg/kg) pretreated group, JB79 (10mg/kg) pre-treated mice group exhibited significantly higher threshold voltage required to stimulate VF (P-value < 0.0001). This may explain the higher resistance against PES-induced VF and lower incidence of VF for the JB79 (10mg/kg) pre-treated groups, compared to the control group.

One of the early studies of PAK1 have indicated that PAK1 deficiency in myocardium can increase the heart's susceptibility to ventricular tachyarrhythmia (Wang et al., 2014). Mice with a cardiomyocyte-specific Pak1 deletion ($Pak1^{cko}$) showed high incidences of ventricular arrhythmias and electrophysiological instability during either acute β-adrenergic or chronic β-adrenergic stress, leading to hypertrophy (Wang et al., 2014). Unfortunately, VF susceptibility on CA-PAK1 (constitutively activated PAK1) cardiomyocytes have yet been characterized. Using JB79 PAK1 activator, however, we were able to demonstrate for the first time that activation of intracellular PAK1 is able to significantly reduce the vulnerability of ventricular arrythmia. The mechanism may be related to the previous findings of PAK1 signaling activation, in which JB79 pretreated cardiomyocytes had exhibited a significantly improved ability to handle calcium. However, subsequent molecular studies will be required in order to further verify it mechanism.

4.5 Ex vivo Heart: Anti-hypertrophic effect of JB79 on TAC-induced Cardiac Hypertrophy

Earlier reports (Liu et al., 2011) had identified PAK1 as a novel regulator of hypertrophic remodeling whose cardiomyocyte specific deletion showed exacerbated cardiac hypertrophy, leading to heart failure, following a transverse aortic constriction (TAC) procedure. Administration of the indirect PAK1 activator FTY720 in wild-type showed improved TAC induced heart failure symptoms, but not in the PAK1^{CKO} mice (Liu et al., 2013). In addition, over expression of CA-PAK1 mice exhibited improved cardiac function and decreased myocytic apoptosis compared to WT under TAC stress conditions. These evidences illustrate potential cardioprotective roles of PAK1 involved in alleviating the TAC-induced cardiac hypertrophy and suggest potential therapeutic applications for the PAK1 activator. In order to evaluate PAK1 activator's therapeutics in providing anti-hypertrophy, cardiac hypertrophic heart model was recreated through performing TAC procedure either with or without two-weeks of PAK1 activator JB79 treatments.

A)

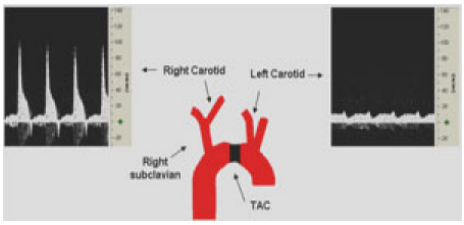

B)

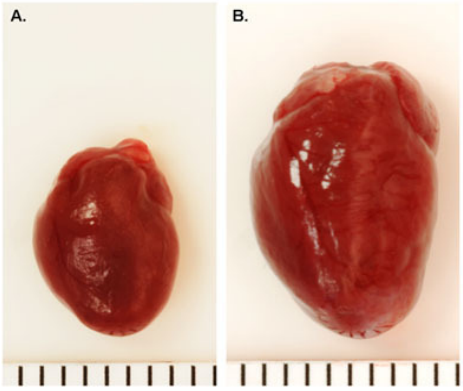

Figure 4.5.1 *Transverse Aortic Constriction (TAC) on mice heart.* **A)** Confirmation of Transverse Aorta Ligation using Doppler Velocity Measurement. Representative Doppler velocity signals of the right (RC) and left carotid (LC) arteries 6 days post-TAC. These recordings demonstrate a successful ligation with a RC/LC flow ratio of ~6.8.

B) *Representative Whole Heart Images Following TAC.* A. Sham-operated wild type mouse heart. B. Wild type mouse heart 16 weeks post-TAC. Each line = 1mm. (Figure derived from DeAlmeida et al., 2010).

Transverse aortic constriction (TAC) is a commonly used animal model used to recreate the symptomatic of cardiac hypertrophy and heart failure. The procedure involves tying surgical knots on the transverse aorta, which yields a constriction of 0.4mm in diameter (Rockman et al., 1991) (see Figure 4.5.1 A). The aortic constriction initially leads to pressure overload and

causes mechanical stress against the cardiac chambers. Constant stress will lead to inflammation signalling of hypertrophy, often associated with a temporary enhancement of cardiac contractility (see Figure 4.5.1 B). long term sustained pressure, however, causes a cellular response to the chronic hemodynamic overload to become maladaptive, resulting in cardiac dilatation and heart failure (Heinke and Molkenin., 2006). For these reasons, the TAC model has been extensively used as a valuable assay to develop heart failure symptoms and used for elucidating fundamental signaling processes involved in the cardiac hypertrophic response.

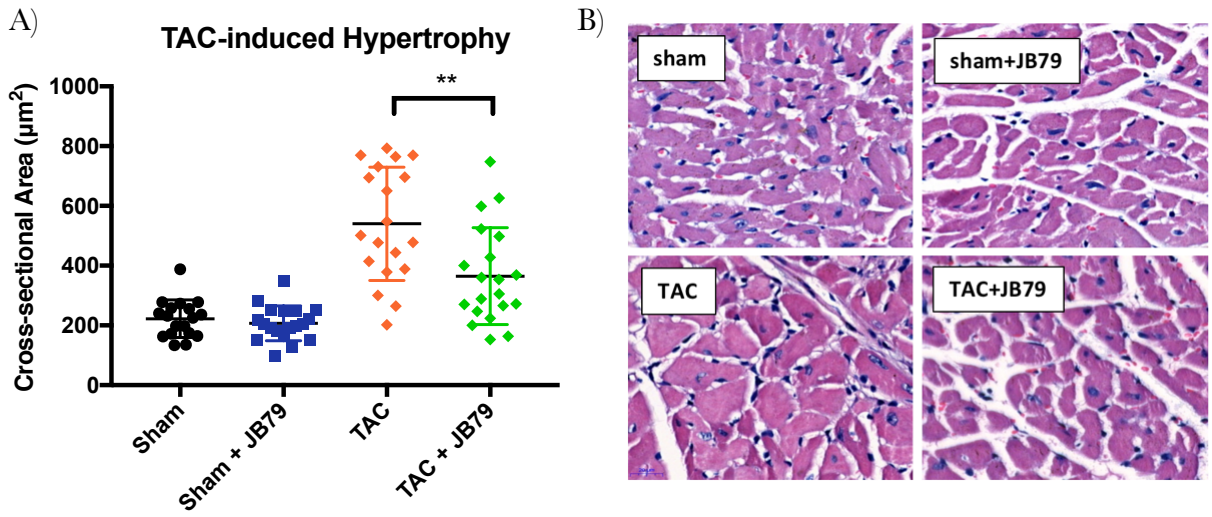

Figure 4.5.2 *Effect of JB79 on TAC-induced hypertrophy* **A)** Quantitative analysis results of cross-sectional areas of myofibrils. Co-perfused heart with JB79 PAK1 activator (10mg/kg) demonstrated significantly attenuated TAC-induced cardiac hypertrophy, illustrated by reduction in cross-sectional areas (uM^2) **B)** Representative images of H&E staining comparing cross sectional areas. JB79 10mg/kg exhibited significant reduction in cross sectional areas of myofibril and showed vascular remodeling. $P < 0.05$, n = 20.

Therapeutic efficacy of PAK1 activator JB79 was examined on cardiac hypertrophy model induced by pressure overload through TAC (See Figure 4.5.2). 2 weeks' TAC was sufficient to induce steady hypertrophy and early stage of heart failure in mice model, evidenced by the significant increase in heart weight/tibia length ratio and a substantial increase in cross-sectional areas by 245%; the mean cross-sectional-area difference between the Sham and the TAC-induced mice groups were 317.8 ± 47 uM^2, (P-Value < 0.0001). Under the similar pressure gradients (30 mm Hg), TAC-mice receiving JB79 manifested lesser cardiac hypertrophy compared to the mice receiving vehicle. The mean cross-sectional areas for TAC-mice receiving JB79 was measured to be 364.9 ± 36.3 uM^2, while the TAC-mice receiving

vehicle was 540.3 ± 43.5 uM^2; the difference was found to be statistically significant (P = 0.0036). The mechanism is thought to be through activating PAK1 pathway and thereby improving the calcium modulation in cardiac tissue and reducing the cardiac hypertrophic effect from the pressure overload. However, from the TAC model assay, co-perfusion of JB79 was found to be not sufficient to completely block the effect of TAC–induced hypertrophy (P-value = 0.0013), suggesting that cardiac hypertrophy is modulated by complex signal pathways, including the PAK1 signaling. Nevertheless, co-perfusion of PAK1 activator JB79 on TAC mice group exhibited significant alleviation on TAC-induced cardiac hypertrophy, providing preliminary indications for PAK1 activator's potential therapeutic usage as an anti-hypertrophic agent.

In summary, the pre-treatments of JB79 PAK1 activator have indicated significant improvement in TAC induced cardiac pathologies, including those of fibrosis, cardiac hypertrophy and cardiac dysfunctions. The results suggest that stimulation of PAK1 was shown to improve regulatory mechanism involved in modulating hypertrophy responses, and the data seems to be consistent with their previous findings by Liu et al. 2011. These authors have demonstrated that $PAK1^{cko}$–TAC myocardium contains higher expression levels of P53, BAX, and BAD – apoptotic molecules involved in cardiomyocyte cell death signaling. These may explain for the observation of exacerbated cardiac hypertrophy in $PAK1^{cko}$ in comparison to that of the wild type (Liu et al., 2011). Western blot analysis between WT and $PAK1^{cko}$ revealed an increased expression levels of MKK4/MKK7-JNK in TAC induced WT heart, while this effect was not observed in PAK1 (Liu et al., 2011). These data suggest that PAK1 is an upstream activator of the MKK4/MKK7-JNK pathway, and activation of the JNK pathway is essential for modulating cardiac hypertrophy signaling. From our own *ex vivo* TAC experiments, we were able to demonstrate for the first time that an activation of PAK1 through JB79 can significantly alleviate TAC induced cardiac hypertrophy. Although further molecular study (e.g. measuring level of proteins activation involved in the JNK pathway) maybe required to support the above findings, these preliminary benefits of PAK1 activators in heart provides another therapeutic indication for CVDs treatments.

4.6 Potential Roles of PAK1 in Cancer

Protein kinases are involved in a number of key intracellular signaling pathways, including in cytoskeleton dynamics, cell adhesion, migration, proliferation, apoptosis, mitosis, and vesicle-mediated transport processes. Despite essential roles of these functions, kinase signaling have been often identified as drivers of the growth, survival, and therefore spread of human cancers (Gross et al., 2015; Giamas et al., 2007). Extensive research has successfully identified several important signaling pathways and allowed for the discovery of pharmacological intervention through development of small molecule kinase inhibitors. Few exemplary oncogenic small molecules include Cetuximab, approved in 2006 to inhibit EGFR (epidermal growth factor receptor), and Cobimetinib, recently approved to inhibit MEK (mitogen-activated protein kinase). These target-based drug discoveries have benefited significantly in understanding how the oncogenic pathway can be modulated and to what extent these molecules have effect on the progression of the disease.

Amongst the number of kinases that have been studied to contain oncogenic effect in promoting the progression of the disease, PAK1 also has been labeled to play a central role in cancer development and been associated with a positive correlation with advanced tumour grade and decreased patient survival (Radu et al., 2014). PAK1 has been reported to function in growth factor signaling networks, morphogenic process that control proliferation, cell polarity, and actin cytoskeleton organizations (Ong et al., 2011). When PAK1 is over-expressed in most cell types, increased in cell cycle progression and promotion have been previously observed (Balasenthil et al., 2004; Arias-Romero et al., 2008). PAK1 mechanism of growth signal regulation is mainly thought to be associated with activating the components of ERK, AKT, and WNT signaling, all of which are closely tied to cell cycle progression (Radu et al., 2018). Further studies have also demonstrated that PAK1 promotes cell survival through inhibiting apoptosis; PAK-mediated phosphorylation of CRAF at Ser338 results in its translocation to the mitochondria and subsequent binding to and phosphorylation of BAD, which prevents BAD from binding to BCL2 and inhibiting apoptotic signaling (Schumann et al., 2000). These observations, together with the fact that PAK genes are frequently amplified (PAK1 and PAK4) or mutated (PAK5) in human cancers, are consistent with a role for these enzymes in promoting

oncogenesis by stimulating cell proliferation in the absence of growth signals (Lundgren at al., 2008). This has raised the possibility that inhibiting the PAK1 activity may hinder the tumor growth and provide a potential therapeutic treatment for various types of cancer.

Regrettably, despite these abundant evidences of PAK1 in association with cancer, PAK1 as therapeutic of cancer were shown to be ineffective. Developing PAK1 inhibitors are proving to be too challenging and shown minimal therapeutic value during clinical trials (personal communication with marketing consultant, Thomas Hanks, Evotec ltd.). Previously developed PAK inhibitors, for example PF-3758309, have been shown to be a potent inhibitor for PAK1 (Chow et al., 2012; Murray et al., 2010). However, the compound was found not to be selective, and the tumours were quickly able to adopt to obtain resistance against PF-3758309 (Murray et al., 2010). In addition, the compound contained pharmacokinetic issues and side-effects, which led the drug to be ultimately removed from the clinical trials (Bradshaw et al., 2013). PF-3758309 was not the only PAK inhibitor which was not successful in getting into the market. In terms of the PAK1 inhibitors alone, pharmaceutical companies have been trying to make PAK1 inhibitors as a method to manage different types of cancer, but the results have been unfruitful (See Table 4.6).

As shown in the table, six out of seven companies have tried to design PAK1 inhibitors, but all of them have either ceased or stalled in their drug development projects. According to their investigation report, inhibiting PAK1 has been shown to cause either major side-effects or insignificant therapeutic value in many cancer patients (Personal Communication with marketing consultant, Thomas Hanks, Evotec ltd.). The exact reason for ineffectiveness of PAK1 inhibitors in cancer patients is still being investigated, nonetheless, these discouraging results have reduced attractiveness of PAK1 as a therapeutic target to treat cancer.

Drug Name	Overview	Activity	Originator
CRT-0276621 CRT0276621 PAK inhibitors, Cancer Research Technology	CRT-0276621 is an oral PAK1/4 inhibitor, under development by Cancer Research Technology for the treatment of cancer (Company Web Page, CRT, 3 Jun 2013, http://www.cancertechnology.com/licensing/pak/; Company Web Page, CRT, 28 Jun 2016, http://www.cancertechnology.co.uk/novel-pak-inbititors-cancer-therapy).	Stalled	Cancer Research Technology
PF-3758309 PF-03758309 PF-03758609 PF-309 PF309	Pfizer has discontinued development of PF-3758309, an orally-active ATP-competitive pyrrolopyrazole PAK inhibitor, for the treatment of cancer (ClinicalTrials.gov 13 Jul 2009, http://clinicaltrial.gov/ct2/show/NCT00932126; Company pipeline, Pfizer, 27 Jan 2010, http://media.pfizer.com/files/research/pipeline/2010_0127/pipeline_2010_0127.pdf & 11 Aug 2011, Page 12, http://www.pfizer.com/files/research/pipeline/2011_0811/pipeline_2011_0811.pdf).	Ceased	Pfizer
PKN1 inhibitor, CRT	Cancer Research Technology (CRT) was developing protein kinase N1 (PKN1) inhibitors to treat prostate cancer.	Ceased	Cancer Research Technology
PAK1 inhibitors, Astex Pharmaceuticals	Astex Pharmaceuticals (now Otsuka) was developing 2-arylamino-4-aryl-pyrimidines as potent p21-activated kinase (PAK1) inhibitors, for the treatment of colon cancer (Bioorg Med Chem Lett, 2013, 23, 4072, PMID:23756368, http://www.ncbi.nlm.nih.gov/pubmed/23756368).	Ceased	Astex Pharmaceuticals
PAK-1 inhibitors, Priaxon	Priaxon was developing small-molecule PAK-1 inhibitors, for the treatment of cancer (Company pipeline, Priaxon, http://www.priaxon.com/content/technology/integrated/index.php).	Ceased	Priaxon
PAK-1 inhibitors, Novartis	Novartis was developing novel and highly selective allosteric inhibitors of PAK1, for the treatment of cancer (246th ACS (Indianapolis), 2013, MEDI 35).	Ceased	Novartis
CGX-0682 PAK1 inhibitors, CompleGen	CGX-0682 is the lead in a series of p21-activated kinase (PAK1) inhibitors, which was under development by CompleGen for the treatment of breast cancer (BIO 2009 (Atlanta)).	Ceased	CompleGen

Table 4.6 Development of PAK1 inhibitors by various pharmaceutical companies. Majority of PAK1 inhibitors were shown to be ineffective and therefore, they were either stalled or ceased for development.

In addition to these failed drug developments, the emerging evidences of PAK1 role in cancer, are proving to be complex and unresolved. there are a number of puzzling aspects which remains to be studied. For example, in the Erk pathway, PAK1 have been shown to phosphorylate c-RAF at S338 and MEK1 at S298 (Slack-Davis et al., 2003). While it has been proposed that these phosphorylation events are required for efficient Erk activation and subsequent expression of Cyclin D1, a key driver of cell cycle (G1) progression, over-expression of kinase-dead forms of PAK1 can still activate Erk in the absence of phosphorylation of c-RAF on S338. This questions whether Pak1 has a significant role in activating the Erk pathway or

constitutes only a minor role, while the Erk pathway is modulated by other signaling cascades. Recent review literature of cancer genome landscapes has provided comprehensive insight into intrageneric mutations on various types of cancers (Vogelstein et al., 2013). The authors have highlighted that progression of cancer requires mutations at the 'driver genes', which are essentially the 'drivers' of tumorigenesis. These driver genes are often classified into 12 signaling pathways that regulate three hall marks of cellular process: cell survival, cell fate, and cell cycle.



Figure 4.6 *Regulation of cancer cells: main cell signaling pathways.* 12 main singling pathways highlighted to be essential for promoting selective growth advantages. These signaling pathways have been further organized to three hallmarks of cancer: cell survival, cell fate, and genome maintenance. Dysfunctions in any of these main signaling targets have been indicated to drive cancer progression (Figure derived from Vogelstein et al., 2017).

The remaining mutations are considered as 'passengers' that provide no selective growth advantage but are often associated in the cancer development. Mutation in driver genes are required in order for selective growth advantage to occur, while passenger mutations would not provide significant contribution in neoplastic processes. Based on observing minimal therapeutic benefits of PAK1 inhibitors, the results suggest that PAK1 may be one of the contributing 'passenger' genes that is associated in various cancer types but confers minor role in the hallmark signaling pathway. Therefore, PAK1's involvement in the cancer development still requires further research as the current gap in knowledge makes it difficult to assess whether or not PAK1 plays any essential role in aggravating cancer. Nevertheless, the association between PAK1 and cancer has raised concerns for small molecule PAK1 activators' potential side effect of promoting cancer. In order to determine whether the PAK1 activators have had any effect in developing cancer or involved in aggravating the oncogenic symptoms, we used several different cancer cell lines to evaluate the lead compound's potential toxicity and side effects in cell proliferation, motility and growth – key hallmark characteristics of cancer.

4.7 Effects of JB79 on human umbilical vein endothelial cells (HUVECs)

PAK1 in growth signaling regulation is mainly thought to be associated with activating the components of ERK, AKT, and WNT signaling – all of which are closely tied to cell cycle progression, tumour growth and proliferation (Radu et al., 2014). These signalling pathways have been also indicated to be crucial in endothelial cells' survival and growth. In order to evaluated whether the JB compounds provide any alternation in endothelial growth or accelerates in cell proliferation, we used human umbilical vein endothelial cells (HUVECs) to measure PAK1 activators' effect. HUVEC cell proliferation was monitored through counting the number of cells that have been dyed with CellMask Green Plasma membrane stain. Cell were count after 48 hours of incubation at various dosage of JB79 small molecule PAK1 activators (see Figure 4.7.1).

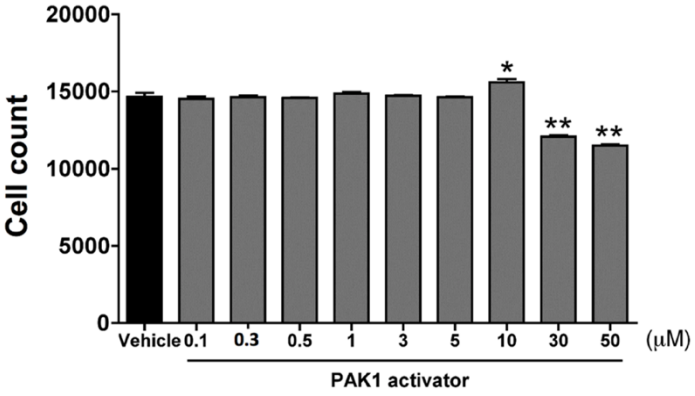

Figure 4.7.1 *Dose response test of JB79 on HUVEC proliferation effect.* The total number of cell counts were based on the DAPI positive cells were normalized to the Vehicle control, which was set at 100%. Data from four wells for each concentration, and nine fields per well were analyzed, and are expressed as mean ± SEM. Statistical analysis was compared with vehicle (DMSO).

The overall cell proliferation effect by PAK1 activator was found to be minimal at the observed concentrations. The total cell count was measured to be constant until the concentration had reached 10uM, by which the cell count had only increased by 6%. Although such increase in the cell count was statistically significant, the relative increase in the cell count was considered to be minimal in comparison to other oncogenic promoters, such as VEGF. Cell growth essay using HUVECs exhibited ~ 300% increase in the cell count after 48-hour treatment of VEGF (50ng/mL) (Zhao et al., 2016). At higher concentrations 30uM and 50uM, the cell count was significantly reduced, indicating that prolong treatment at such high concentrations impedes cell proliferation. These results indicate that the direct activator of PAK1 does not have malign

cell proliferation effect in HUVECs and that concentrations higher than 30uM may cause hinderance in HUVECs proliferation.

Following the confirmation that the PAK1 activators do not promote cell proliferation in HUVECs, we wanted to evaluate if the compound had any effect in cell motility and possibly involved in exacerbate in metastasis. As PAKs are well-known regulators of cytoskeletal remodeling and cell motility, it was plausible that PAK activators may be involved in assisting metastatic promotions. Cell migration assays, specifically barrier migration assays, were performed using HUVECs in order to measure the rate of gap closure and to correlate endothelial transmigrations. A ring barrier-based migration assay consists of an insert in the culture chamber, which prevents cells from entering the defined area. Cells are then seeded around this barrier, and after the formation of a peripheral monolayer, the barrier is removed and migration into the cell-free area is monitored (Asha et al., 2015). This assay is efficient in determining several parameters of migration, including total and effective migration, velocity and cell polarization. This assay was chosen over the traditional scratch assay as it does not harm the surrounding cells, and the assay is performed over an undamaged and even surface area (Asha et al., 2015).

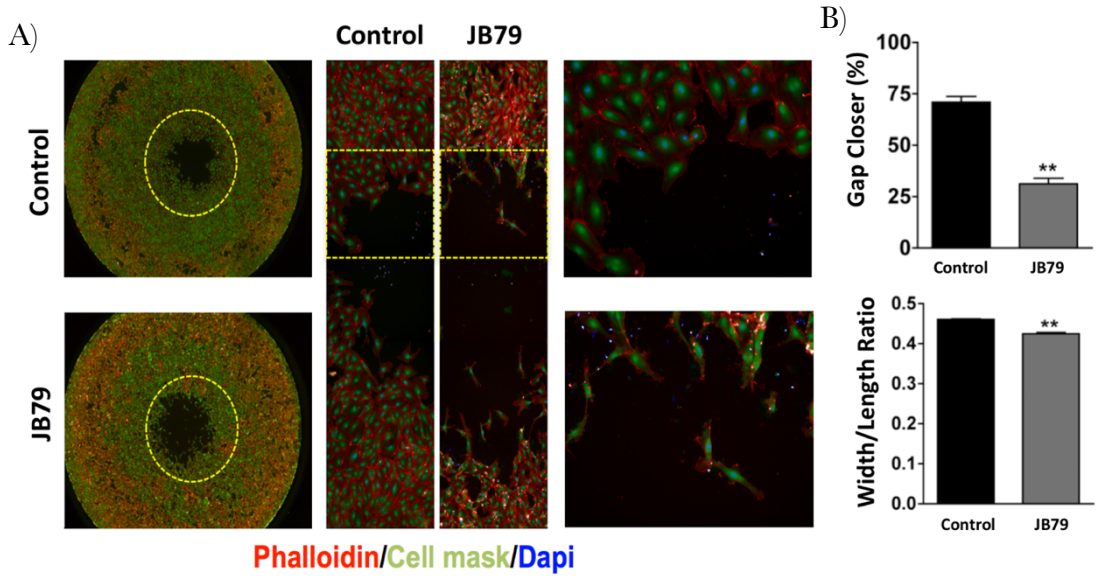

Figure 4.7.2 *Effect of JB79 20uM on the motility of HUVECs.* The ring barrier-based migration assay revealed that treatment of JB79 (20uM) for 48 hours impedes HUVECs' motility and causes lower percentage in gap closer. The morphology of JB79 treated cells also exhibited slightly lower LWR ratio on the cell morphology. Cells were labeled with phalloidin (, intracellular cytoplasm (CellMask), and nucleus (Dapi,) in order to outline the cell morphology. Data represents replications of 5 assays, presented as mean ± S.E.M.

The cell motility between vehicle (DMSO) and PAK1 activators (JB79) were compared after 48-hours of treatment (See Figure 4.7.2). The gap closure for the control group under the vehicle treatment was 73 ± 1.73% of the barriered area, while the JB79 20uM treated cells exhibited significantly lower percentage in the gap closure, displaying 31 ± 1.89%. The difference in the behavior between the control and the compound treated cells was therefore measured to be statistically significant, confirming that the JB79 (20uM) had decreased the motility of HUVECs.

Effort had been put to identify the cellular basis of this movement defect. Upon closer examinations of cell morphology, we observed that the expression of actin cytoskeleton had been significantly reorganized. The HUVECs had shaped longer in length and narrower in width compared to those of the control cells (See Figure 4.7.2 B). We analyzed the shapes length to width ratio (LWR), where the length and width represent the largest measurable distances along each cellular axis. The vehicle treated HUVECs exhibited LWR of 0.46 ± 0.0052, while JB79 displayed LWR of 0.42 ± 0.009. Lower LWR results suggest that JB79 may have potential effect in activating signaling pathway that mediates in cell elongation, which may hinder cell movements. Studies have reported several proteins (e.g. PAK1) are involved in cell stretch and elongations, including actin-depolarizing factor/cofilin, tropomyosin, alpha actin, and phalloidin. In order to determine whether these cell elongating factors had been changed upon treatment of PAK1 activator, we measured the expression of phalloidin within the cell's intracellular environment (See Figure 4.7.3).

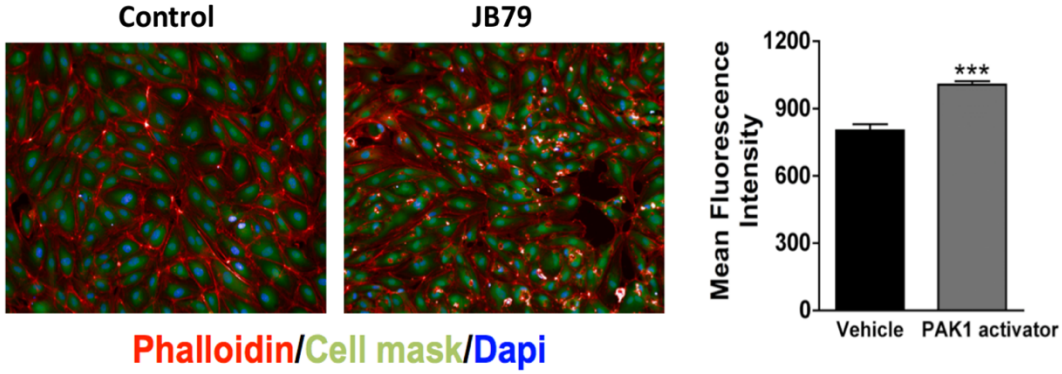

Figure 4.7.3 *Effect of JB79 20uM on the actin organization on HUVECs.* Higher magnification observation on HUVEC cells revealed difference in the actin organization between the vehicle and JB79 (20uM) treated cells. PAK1 activation by JB79 was confirmed to produce more actin reorganization and exhibited higher mean fluorescence intensity (MFI). Cells were labeled with phalloidin (●), intracellular cytoplasm (CellMask, ●), and nucleus (DAPI, ●) in order to outline the cell morphology. Data represents replications of 5 assays, presented as mean ± S.E.M.

The HUVECs that had been pretreated with JB79 (20uM) for 48-hours displayed significantly higher expression of phalloidin as illustrated by higher fluorescence intensity of Fluor 568 (Red). MFI for the control cells was measured to be 821 ± 42 AU, while the cells treated with JB79 showed MFI of 1046 ± 16 AU, displaying 27.3% increase in its expression of phalloidin (P-value < 0.001). Studies of various cultured cells have indicated that the actin-organizing activity of phalloidin plays a central role in providing mechanical support (Goicoechea et al., 2008; Najm et al., 2014). Amongst these signaling pathways, PAK1 has been highly cited to be associated in actin phosphorylation and cytoskeletal organizations (Sells et al., 1997; Edwards et al., 1999; Papakonstani and Stournaras, 2002). The prolonged overexpression of Pak1 amino-terminal mutants that are unable to bind CDC42 or RAC1 results in the accumulation of filamentous actin in large, polarized membrane ruffles and the formation of vinculin-containing focal complexes within these structures (Sells et al., 1997). Subsequent studies identified that the PAK1 can affect the actin organizations through activating LIM-Kinase pathways and inhibiting the PAK1 has been shown to comprise such cytoskeleton dynamics (Edwards et al., 1999). Since JB79 is a direct potent activator of PAK1, the actin reorganization observed in HUVECs provides further support in the compound's permeability and direct activation of the intracellular kinase. The HUVECs' morphological changes upon PAK1 activation by JB79 confirms previous results on PAK1 being an important regulators of actin organizations.

4.8 Effects of JB79 on Malignant Cancer Cells: HOP-92 & MDA-MB-231

HUVECs behavior upon PAK1 activator treatment provided supporting evidence that JB79 at therapeutic concentrations do not produce malign effect in cell proliferation and cell motility. Although the conducted assays do not cover all parameters involving carcinogenesis, these results provide early evidence that JB79 contains minimal aggravating effect in developing cancer. Having said that, HUVECs are normal cells and tend to be more resilient towards stress factors, in comparison to actual cancer cells. Cancer cells contain various damages in their genome and disruption of cellular metabolic processes, which makes them more vulnerable towards external stress. Although we have observed minimal carcinogenic effect of JB79 on HUVECs, this does not verify that the effect will still be the same for cancer cells as well. Therefore, further experiments were needed in order to confirm the safety of PAK1 activator in development and progression of cancer.

In order to ensure that activation of PAK1 by JB79 do not constitute in advancing the oncogenesis, two different types of human cancer cells (HOP92 and MDA-MB-231) were treated with JB79 at therapeutic concentrations. HOP92 is a cell line from human non-small lung carcinoma, and MDA-MB-231 is a cell line from human breast adenocarcinoma. Both malignant cell lines have been characterized to have highly aggressive and invasive properties and they are commonly used in medical research laboratories to study carcinogen factors or to evaluate different treatments. Using both cell lines obtained from our collaborators, Dr. Daniela Pankova and Prof. Eric O'Neil, we decided to perform four different cell transformation assays 1. spheroids invasion in 3D collagen matrix assay, 2. Boyden chamber invasion assay 3. Wound healing scratch assay, and 4. Resazurin proliferation assays in order to measure the potential side effects of JB79 at its therapeutic concentrations.

4.8.1 Effects of JB79 on Cancer Cells: Resazurin Proliferation Assay

Resazurin dye has been broadly used as indicator of cell viability and serves as an effective tool for assessing cell proliferation and as a screening technique. It is based on enzymatic reduction of indicator dye by viable cells. Mitochondrial enzymes, as carriers

of diaphorase activities, are responsible for the transference of electrons from NADPH + H^+ to resazurin, which is reduced to resorufin. The level of reduction can be quantified by spectrophotometers; resazurin exhibits an absorption peak at 600 ηm, and resorufin at 570 ηm wavelengths (Ricardo et al., 2009). Using the resazurin proliferation assay, the cell proliferation effect of JB79 on carcinoma cells, HOP-92 and MDA-MB-231, were quantified (see Figure 4.8.1).

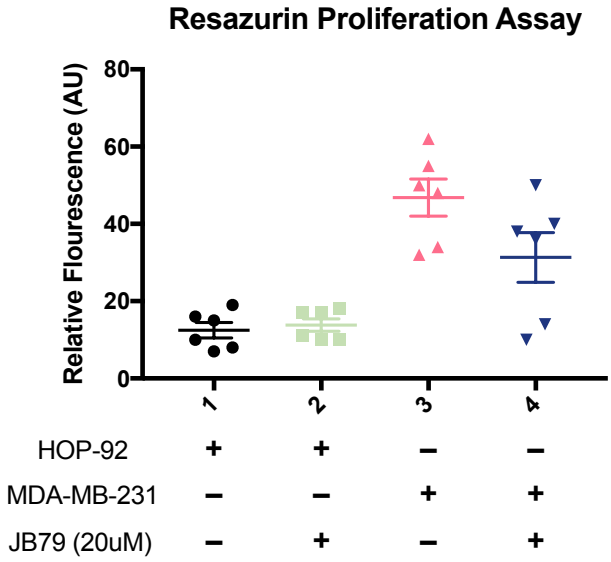

Figure 4.8.1 *Resazurin assay results of HOP-92 & MDA-MB-231after prolonged JB79 treatment.* Cell viability of malignant cancer cell lines were evaluated under the effect of JB79 PAK1 stimulation. No statistical significance was measured between control (DMSO) and JB79 treated cells. Data represents replications of six assays, presented as mean ± S.E.M.

Resazurin proliferation assay revealed that JB79 at 20uM does not provide any significant proliferation effect in both types of adenocarcinoma cells. After 6 days of JB79 treatment, HOP-92 cells were observed to have slightly higher fluorescence, 1.333 AU (~ 10%), indicating that cell number were higher on the JB79 treated cells. However, such increase in the cell count was measured to be non-significant (P - value = 0.61). Furthermore, the effect of JB79 on MDA-MB-231 cells were shown to reduce the number of cells, in comparison to the vehicle-treated cells (P - value = 0.0857). Such difference in the cell proliferation effect indicate that cell intracellular signaling pathways between HOP-92 and MDA-MB-231 may be significantly different and therefore, activation of PAK1 signaling pathways may have different consequences. Nevertheless, observation of nonsignificant effect in cell proliferation in both strains of cancer cells provide preliminary safety profile of JB79.

4.8.2 Effects of JB79 on Cancer Cells: Spheroids invasion assay in 3D collagen matrix

Both cancer cell lines HOP-92 and MDA-MB-231 did not express significant increase in cell proliferation after prolonging treatments of the PAK1 activator JB79. Despite these results suggesting that PAK1 activator may not be substantiating in cell proliferation, potential concerns for having oncogenic growth still applies as solid tumours naturally grow in 3D environment, not in a monolayer (2D). Cells grown in 2D culture has been shown to incorrectly imitate the architecture and microenvironments of in vivo, which has been shown to affect their morphology, proliferation, cell-cell interconnections, signal transduction, and differentiation (1,2). Therefore, in order to improve these simulations of cancer cells' microenvironments, spheroid invasion assays in 3D collagen matrix was performed. In a brief summary, the method generates multicellular tumor spheroids using the hanging-drop method – incubating them as droplets and allowing them to perform multicellular aggregation for 48 hours (Foty et al., 2011). After in which, the spheroids were implanted onto a drop-matrix and treated with medium containing either JB79 or vehicle for 15 hours. The cells were then monitored for their cell-cell cohesion and cell-ECM adhesion, which are cornerstone studies of evaluating cell interaction in malignant invasion, through counting the number of invasive spikes per spheroids.

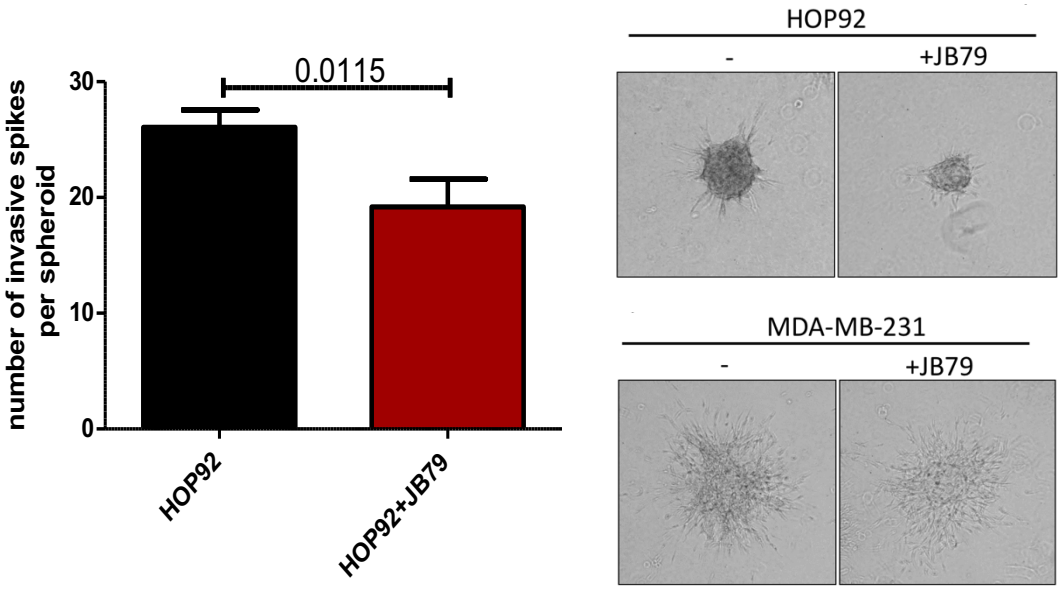

Figure 4.8.2 *Three-Dimensional (3D) Tumor Spheroid Invasion Assay results of HOP-92 & MDA-MB-231after prolonged JB79 treatment.* Cell viability of malignant cancer cell lines were evaluated under the effect of JB79 PAK1 stimulation. No statistical significance was measured between control (DMSO) and JB79 treated cells. Data represents replications of six assays, presented as mean ± S.E.M.

Through the spheroid invasion assays, we observed difference in their invasive properties between the two malignant tumour types. HOP-92 exhibited thicker spheroid shape in cell coagulating properties than that of MDA-MB-231 and contained a limited number of spikes (25 ± 2). Meanwhile MDA-MB-231 cell coagulation revealed flatter and greater cell adhesion towards the matrix plate, sprouting more invasive spikes (55 ± 5) than those of HOP92. Interestingly, upon treatment of PAK1 activator JB79 (20uM), both cancer cell types exhibited difference in their morphology and cell adhesion properties. The coagulating properties amongst the cells seem to reduce and the cells became flatter, as illustrated by Figure 4.8.2. In addition, the number of invasive spikes also measured to decrease. HOP-92 control had an average mean spike number of 25, while the JB79 treated spheroids only had 19. MDA-MB-231 also displayed significantly lower number of invasive spikes, decreasing from to when treated with JB79. These assay results demonstrate that activation of PAK1 signaling by JB79 does not provide significant attribution in promoting cells to become more cancerous.

4.8.3 Effects of JB79 on Cancer Cells: Wound Healing Scratch Essay

Cell migration is another key hallmark of cancer characterization. Cell migration contributes for the progression of cancers from a primary, localized mass to an invasive and/or metastatic phenotype. Previous study involving the usage of HUVECs have confirmed that PAK1 activator JB79 do not stimulate cell motility in normal cells. However, as cancer cells and normal cells have notable differences in many different aspects, the consequence of PAK1 activation in malignant cancer cells may have altered signaling mechanism that may diffes those from those of the non-cancerous cell. In order to determine whether JB79 contains any side effect of promoting cell motility in malignant cancer cells, HOP-92 and MDA-MB-231 cells were examined in a wound healing scratch essay under the influence of JB79 (20uM) and compared with that of the control (DMSO). The cell motility was based on the ability for the cells to cover the scratched assay. The area gap made by scratch was measured at time 0 hr and was compared after 24 hr of incubation with appropriate treatments (see Figure 4.8.3)

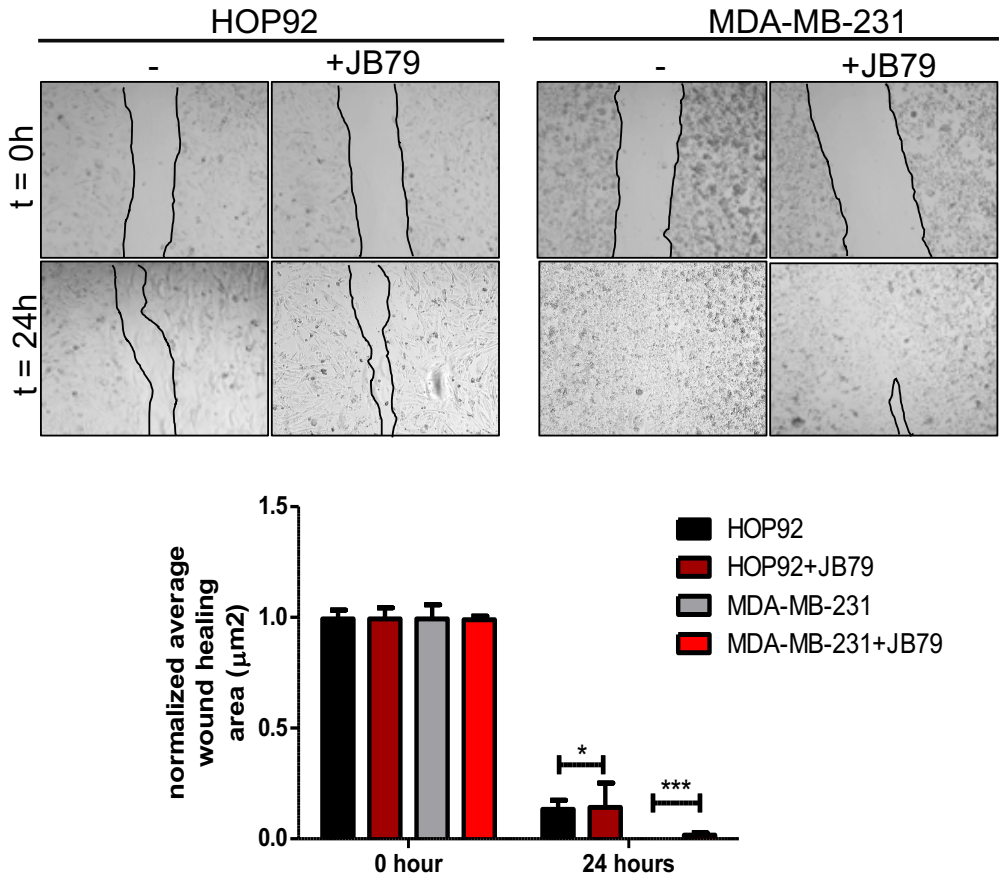

Figure 4.8.3 *Effect of JB79 on cell migration: HOP-92 & MDA-MB-231.* Treatment of JB79 exhibited minor significant differences in cell migration after 24 hours of JB79 treatments, in comparison to vehicle (DMSO) treatment. The rate of migration was measured through average area coverage of cells at the centre of the scratch. Data represents replications of 6 assays, presented as mean ± S.E.M.

The scratch assay was monitored for 24 hours and covered areas were analyzed between the vehicle and JB79 treated plates. In comparison to HOP-92, MDA-MB-231 wound healing ability was observed to be faster; the MDA-MB-231 scratched gap was completely covered again after 24 hours, while HOP-92 plate still had ~10% gap left. The greater healing ability of MDA-MB-231 was expected from the previous results, as higher invasive properties and faster cell proliferation rate were observed through the cell proliferation assay and the 3D spheroids invasive assay, respectively. Upon activation of PAK1 signaling by JB79, significant difference of only 0.02uM^2 was measured for HOP-92 strain, demonstrating that PAK1 activator did not have significant effect in cells' motility. Similarly, treatment of JB79 on MDA-MB-231 cell had a minor significant effect in altering their cell motility, illustrating a slower cell motility phenotype than those of the vehicle treated ones. From these scratch-wound healing assays, it was concluded that JB79 did not augment in cell motility phenotype in cancerous cells.

4.8.4 Effects of JB79 on Cancer Cells: Boyden Chamber Invasion Essay

The Boyden chamber assay is one of the widely used *in vitro* assay, quantifying both the invasive property and motility of cells. The method is based on using a chamber of two medium-filled compartments separated by a microporous membrane and calculating the number of cells that had migrated through the membrane (Chen et al., 2005). Cells with high invasive and cell migration properties tend to be more embedded within the membrane and allow us to compare their oncogenic characteristics. Although the effect of JB79 on both HOP92 and MDA-MB-231 exhibited minimal motility and invasive properties – based on the previous 3D spheroids invasive assay and the scratch assays – the Boyden chamber assay was still performed as an added measurement to verify the previous findings.

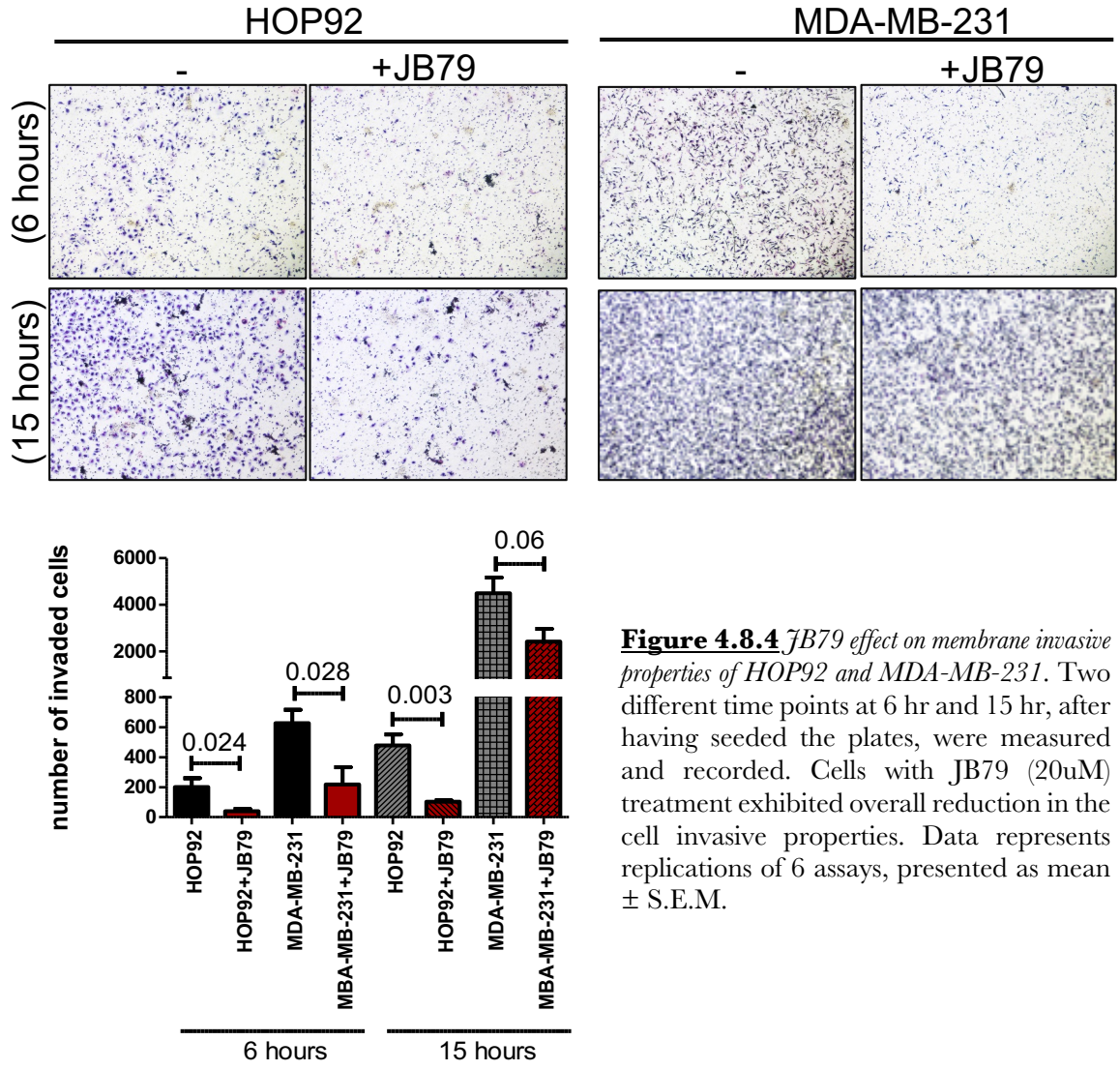

Figure 4.8.4 *JB79 effect on membrane invasive properties of HOP92 and MDA-MB-231.* Two different time points at 6 hr and 15 hr, after having seeded the plates, were measured and recorded. Cells with JB79 (20uM) treatment exhibited overall reduction in the cell invasive properties. Data represents replications of 6 assays, presented as mean ± S.E.M.

The Boyden chamber assays was able to assess the aggressive properties of the cancer cells (See Figure 4.3.4). The number of invading cells were compared between 6 hours and 15 hours from the time of their seeding. HOP-92 cells displayed significant invasive properties; the number of invading cells had increased from 200.7 ± 59.07 to 479.73 ± 73.04 (247%) during the 9 hours of incubation. MDA-MB-231 also demonstrated significant increase in the cell count after the 15 hour-period, increasing from 627.7 ± 89.24 to 4495 ± 679.8 (717%). These significant higher number of invading cells suggested that MDA-MB-231 had much higher invasive property than that of HOP-92. This provide further supports to previous results of cell proliferation, cell motility, and 3D invasive spheroids assays.

To measure whether or not the PAK1 activator had any effect in amplifying the invasive properties, the cells were treated with JB79 under the same conditions and their motility was measured. The results showed that the cancer cells had exhibited a significant reduction in their ability to penetrate through the membrane when they are treated with JB79, in comparison to the DMSO treated group. After 6 hours of co-incubation with the PAK1 activator, HOP-92 exhibited 90% reduction in the number of invading cells; the control cell count was 200.7 ± 59.07, while the JB79 treated group was only 39.67 ± 13.78. After 15-hours of incubation, JB79 treated count was only increased to 103.3 ± 8.74 cells, observing 80% reduction. Similarly, MDA-MB-231 exhibited reduction in their motility when the cells were treated with JB79; the number of invading cells had significantly decreased by 66% (after 6 hour from seeding, control cell count: 627.7 ± 89.24 and JB79 treated cell count: 218.7 ± 115.1) and 38% (after15 hours from seeding, control cell count: 4494 ± 679.8 and JB79 treated cell count: 2412 ± 549) in comparison to their respective control groups. Despite such impediment in their motility, activation of PAK1 did not impair the cancer cells motility as the number of invading cells had continuously increased throughout the course of the experiment. These results provide additional support of the previous results substantiating that JB79 does not amplify in either cell proliferation, motility, or cancer invasiveness, providing safe profile against concerns for its potential oncogenic effects.

4.9 Summary & Concluding Remarks

Target identification and clinical validations are essential for designing good drugs. A recurring problem in the drug industry has been that, without capturing the appropriate clinical spectrum of therapeutic applications, many drugs fail to meet their therapeutic purposes (Jones, 2016). Furthermore, costs of candidate compound optimization, particularly when the compound's desired therapeutic effect is not perceivable, are also quite high. Therefore, before performing full optimization process of the JB compounds, a limited modification of JB01 was performed to improve its physiochemical properties required for clinical validation. This process led to the development of JB79, the current lead compound characterized by an improved efficacy and chemical profiles, allowing it to be tested for its indicative therapeutic purposes. In Chapter 4, we examined the functional effect of JB79 on various functional assays and cellular models in order to evaluate clinical transability of JB79 for therapeutics.

First, in order to assess the functional effect of JB79 in myocardium, JB79 was tested in *in vitro* and *ex vivo* assays. As demonstrated by the results of these tests, perfusion/co-incubation of optimal concentration of PAK1 activators successfully promoted the cardio-protective mechanism against stress-induced cardiomyopathy and arrhythmias. Furthermore, therapeutic validations were performed using various cellular models, ranging from single cardiomyocytes to whole heart organs, in order to explore different mechanisms of PAK1 activation on different levels of organism complexity. Furthermore, early proof of anti-arrhythmic effect of JB79 was observed when we measured the reduction of irregular calcium transients induced by ISO. This result was further verified using a human iPSC model, which showed that the JB79 treatment reduced the adrenergic stimulation of calcium transient amplitudes, thereby effectively improving the cell's ability to handle intracellular calcium movement. In the next step, an *ex vivo* whole heart model was used to examine the cardioprotective effect of JB79 against programmed electrical stimulation (PES)-induced arrhythmia, with the specific focus on PVC and VF. The results of these tests showed that a sufficient activation of PAK1 signaling, at the concentration of 10mg/kg, yielded a significant benefit in terms of increasing the voltage tolerance for PES-induced VF and PVC, thus lowering the incidence of cardiac arrhythmia. Finally, in a TAC-induced cardiac hypertrophy model, we observed a significant alleviation of cardiac hypertrophic upon a prolonged treatment of PAK1 activator. Taken together, these preliminary results suggest potential therapeutic applications of JB79 in providing both the treatment for and the prophylactic measurement against cardiovascular complications.

Among various functional roles of PAK1, many previous studies have emphasized its biological role in providing a strong cardio-protective mechanism (Liu et al., 2004; Wang et al., 2007); in addition, PAK1 has also been suggested to be involved in the development of cancer. Due to the overall difference in their physiological mechanisms, cancer and cardiovascular treatments are intrinsically connected. Specifically, while the purpose of cancer treatment is to prevent further proliferation of cancer cells through promoting cells death, in cardio, many drugs promote cell survivability so that to keep the cells from dying and to prevent cardiac fibrosis. Therefore, many cancer treatments (e.g., chemotherapy and radiation) lead to cardiac cell deaths, also known as cardiotoxicity, while the opposite is true for cardiovascular drugs. Therefore, developing a safe therapeutic drug to prevent the progression of HF would require finding the safest treatment while monitoring for potential side effects. In the present study, potential side effects of cancer development by PAK1 activation were also evaluated using several cell lines—namely, HUVEC, HOP92, and MDA-MB-231.

HUVEC was mainly used to examine the effect of kinase activation in endothelial cells. While the results of cell count through immunostaining suggested no significant cell proliferation, a closer examination of the cell morphology revealed clear changes in cytoskeleton remodeling. However, further research in needed to determine whether or not such changes in the cell shape were an indication of functional changes. PAK1 has been previously reported to be involved in modulating extracellular matrix (ECM). Therefore, observations of changes in cell morphology provide some certainty that JB79 PAK1 activator molecules can permeate through the cell membrane, thereby stimulating intracellular PAK1 signaling.

Finally, we investigated a potential oncogenic side effect of PAK1 activation using aggressive cancer cell lines. HOP92 is a cell line from human non-small lung carcinoma, while MDA-MB-231 is a cell line from human breast adenocarcinoma. In order to examine different oncogenic phenotypic effects, the following four types of assays were used: resazurin assay (to assess proliferation), spheroid invasion assay (to evaluate 3D tumor spheroid growth), scratch assay (to assess migration/cell motility), and Boyden chamber assay (to evaluate penetrance/invasiveness). Preliminary results suggested that JB79 did not exaggerate the oncogenic effect on malignant cancer cells. Both proliferation and cell motility assays revealed minimal differences as compared to those of the control (DMSO) treated cells. The measurements of the effect of PAK1 stimulation on its invasive properties revealed a reduction in the invasive properties of both cancerous cells. These findings deviated from what was previously indicated for PAK1 stimulation in cancer. Specifically, several previous studies

reported PAK1 over activation in many cancer types; accordingly, there were several attempts to design PAK1 inhibitor for cancer therapeutics (Kumar et al., 2006, Dummler et al., 2009; Singhal et al., 2012). However, our results demonstrate that JB79 does provide a significant attribution in cancer qualities. This could be due to a subthreshold level of PAK1 activation by JB79; a 3-fold increase in PAK1 activation by 20uM of JB79 may not be sufficiently high to aggravate the overall RAS signaling (e.g. PAK1 mediated signaling pathway in cancer). Thus, while the therapeutic concentration may have promoted cardio-protective mechanisms, it remained sufficiently safe not to induce any potential side effects. Although these preliminary results do not conclusively confirm that activation of PAK1 does not aggravate the progression or development of cancer characteristics, an exploratory insight into the effect of JB79 on cancer promotion suggests the overall safety of PAK1 small-molecule activators.

CHAPTER 5

MOLECULAR INSIGHT INTO PAK1 ACTIVATORS

Summary Points

- Mechanism action of JB compounds were explored in order to gain a greater insight into how the small molecules are able to confer stimulatory effect in PAK1 enzymatic activity.
- Three constructs of PAK1 proteins (full length (FL-PAK1), a.a. 70 deletion (-70 PAK1), and kinase domain(KD)) were purified and characterized using the kinase assays. Effects of the compounds were also measured to observe any difference in the compound efficacy on the enzymatic activity.
- Characterization and comparative fragment-based QSAR was studied using JB79 as the lead compound, allowing for a greater understanding of the active site.
- JB compounds were observed to cause an inhibitory effect at significantly higher concentrations.
- Such mechanism of inhibition was explored through applying various *in vitro* biophysical assays to test for plausible explanations, whether they are non-specific binding, ligand co-angulations, or covalent modifications to the protein.
- In collaboration with Proteros ltd., x-ray co-crystallography was performed between PAK1 and JB compounds in an effort to identify the protein-ligand interaction site and to confirm the mechanism action of the PAK1 activators.

5.1 Background Overview

Enzymatic phosphorylation is a key method of cellular communications. Enzymatic phosphorylation is involved in various biological processes, ranging from regulating enzyme activity to determining gene expressions. Dysregulations in enzymatic phosphorylation with an inappropriate amount of frequently result in pathological conditions. In order to overcome these disease drivers, current kinase inhibitors are designed to predominantly interfere with the substrate binding of proteins. Owing to the modulation of this substrate binding, inhibitor drugs can reduce overactivation of diverse biological processes, such as those involved in the immune system, degenerative diseases, and cancers. Kinase inhibitors, such as dasatinib, are ATP competitive inhibitors and are extensively used to treat non-selective cancer types (Gross et al., 2015). Cetuximab and erlotinibs, other small-molecule drugs that inhibit epidermal growth factor receptors (EGFRs), modulate their signaling pathways and are effectively used in the treatment for colorectal and lung cancers (Messersmith and Ahnen, 2009; Kobayashi and Hagiwara, 2013). However, until now, very few kinase inhibitors have been characterised for therapeutic indications other than for cancer treatments. One of such kinase inhibitors is KDU691 that targets PfPI(4) kinase. KDU69 has been reported to affect a number of plasmodium strains and to effectively prevent malarial transmission (McNamara et al., 2013). Furthermore, in several recent chemical genome studies, other potential kinases have also been screened for therapeutic indications, expanding available strategies to deliver novel remedies for various diseases. However, a limitation of this body of work has been that most relevant studies have predominantly focused on the development of kinase inhibitors. As a result, available research on designing kinase activators that can stimulate beneficial proteins has remained scarce.

From the pharmacological perspective, the predominant focus of previous studies on the development of kinase inhibitors (and the lack of research that would seek to design kinase activators) contradicts the traditional approach to drug discovery—specifically, the one where both activators and inhibitors would be designed to explore their mode of action and their functional implications for therapeutics. For instance, in the case of catecholamine receptors, both receptor agonists and antagonists have been extensively explored and developed (see

Table 5.1). In this case, accumulated data have eventually led to the design of therapeutic drugs for pharmacological interventions, thereby contributing to the alleviation of various pathological symptoms.

Receptor	Agonist	Antagonists
α (non-selective)	NA > A > ISO	Phenoxybenzamine
α_1	phenylephrine	Prazosin
α_2	Clonidine	Yohimbine
β (non-selective)	ISO > A > NA	Propranolol
β_1	Dobutamine	Atenolol
β_2	Salbutamol	Butaxamine

Table 5.1: Examples of catecholamine receptor agonists and antagonists.

The scarcity of previous research on the development of kinase activators is underpinned by the following two factors: (1) impact of the pharmaceutical industry and (2) challenges associated with developing kinase activators. With regard to the first factor, from the early days, the pharmaceutical industry has been strongly interested in designing small-molecule kinase inhibitors. As cancer is a leading cause of death in many developed countries, the potential for making a block-buster drug has been enormous; therefore, kinase inhibitors have been a priority in terms of research funding and collaborations. This bias in funding has limited the opportunities to fund other initiatives, such as those aiming to investigate therapeutic applications for kinase activators. In addition, extant research on kinases has mostly addressed cancer progression and developments. While the human genome encodes 518 different kinases involved in multiple regulations in biological processes, the initial impression of kinase activator tends to distress researchers, thereby impeding relevant research.

Secondly, the development of kinase activators has been limited due to the lack of understanding on the enzymatic mechanism of activation. While most kinase inhibitors may require a simple blocking of the active site, which prevents their access to the substrates (e.g. ATP or GTP), kinase activators can only modulate the enzyme activity through an allosteric mechanism. However, the development of an allosteric modulator is complicated by the fact that it requires in-depth knowledge of the kinases' mechanism of activation and their 3D

structural information. Other aspects essential for the development of kinase activators include kinase dynamics and conformational changes. Regrettably, the current lack of structural and mechanistic knowledge in many kinases impedes the pursuit of drug discovery in these therapeutic targets.

Fortunately, however, structural information and the mechanism of activation of PAK1 have been thoroughly characterized (Lei et al., 2000). Specifically, the analysis of the crystal structure of PAK1 revealed that PAK1 adopts a trans-inhibited conformation, where the N-terminal inhibitory portion of PAK1 dimers interlocks and auto-inhibits the catalytic domain, also called the auto-inhibitory domain (AID), of other monomers (Lei at al., 2000). Previous research has also revealed that mutations occurring in the AID can lead to a significant reduction in affinity between the dimers, leading to a constitutive activation of the kinase (Jha et al., 2011). Another mechanism of the PAK1 kinase activity regulation is the GTPase-independent mechanism, which includes phosphorylation by other kinases such as ERK, PDK1, and CDC2 (Bagheri-Yarmad et al., 2001; He et al., 2004; Banerjee et al., 2002). Along with contributing to phosphorylating downstream targets, PAK1 has also been reported to have kinase-independent functions, also referred to as the scaffold capacity, whereby PAK1 can confer its activity through facilitating the assembly of multiprotein signaling modules (Brown et al., 2002). The extensive structural information about PAK1 outlined above provides an in-depth understanding of its primary structure and 3D conformation dynamics, thereby laying down the foundations necessary for an efficient designing of small-molecule drugs that may stimulate PAK1 activity.

In the present study, we hypothesized that the mechanism of action our small-molecule PAK1 activator (i.e. JB79) would be through binding in the AID of PAK1, thus preventing the trans-inhibited dimerization. As the PAK1 cannot revert to its dimerization formation, PAK1 would be preserved in the monomeric form (active conformation) and continue to phosphorylate its downstream targets. The increase in the PAK1 activity by JB79 was confirmed by performing two independent *in vitro* assays: ADP-GLO™ Kinase assay and Rapidfire™-Kinase assay. The results of these assays confirmed a significant activation of PAK1 activity upon co-incubating with JB79, amounting to a ca. 3-fold increase in PAK1 activity. Furthermore, as demonstrated

by the immunohistochemistry results, the compound was also found to have a good permeability and to directly activate intracellular PAK1. Finally, our results on the therapeutic benefits of PAK1 activators in cardio-protection also confirmed previous reports on PAK1's homeostasis functions. These preliminary findings provide a proof of concept that kinase activators can be designed through allosterically targeting the auto-inhibitory mechanisms, which could be a novel approach in drug discovery.

While our previous findings on JB79 confirmed its stimulatory effect on PAK1 activity and therapeutic effect for CVDs, the mechanism of PAK1 activation still had to be elucidated biophysically. To this end, in this chapter, we used experimental approaches to understand the molecular mechanism of JB79. Specifically, in order to gain a better understanding of the ligand binding site, we performed SAR studies based on fragment compounds and co-crystallography. In addition to conferring a stimulatory effect on PAK1, JB compounds also demonstrated to have an inhibitory effect on PAK1 activity at high concentrations (<50uM). The causes of this inhibitory effect were investigated using chemical analysis and mass spectrometry. Overall, the chapter provides an insight into PAK1 activators' mode of action and contributes to current understanding of ligand interactions on a molecular level.

5.2 PAK1 activators: binding at the Auto-inhibitory domain

Initial *in silico* design of PAK1 activator was achieved through performing comprehensive virtual ligand screening (VLS) at the auto-inhibitory domain (AID) of PAK1. The computational screening method allowed for cost-efficient method of discovering small molecules which showed high affinity at the AID. These molecules were then validated through *in vitro* kinase assays, confirmed to stimulate PAK1's activity significantly. Similarly, PAK-activating Peptide (PAP) – a small peptide which contained complimentary sequence to the AID – exhibited significant activation on the PAK1 activity, providing further evidence that the disruption of dimerization can affect the total activity of the kinase (Wang et al., 2014). Through both small molecule and peptide activators, proof of concept in which PAK1 activity can be modulated through targeting the AI domain had been confirmed. The next effort was to determine the mechanism in which how these JB compounds were able to activate PAK1. In order to identify their mechanism of action, we had synthesized and purified a truncated version of PAK1 – which had the auto-inhibitory (AI) domain removed from the full-length structure. The truncated PAK1 protein only contained the kinase domain (PAK1-KD), expressing only the half of FL–PAK1 (a.a. 249~545) and missing the AID (a.a. 70~149). Having removed the AID on PAK1, we hypothesized that JB compounds will no longer have its effect as the proposing binding site for molecules (e.g. AID) was no longer present. In order to confirm this, we measured the activity of PAK1-KD alone and compared its activity with PAK1–FL. If the PAK1–KD were to show greater activity than PAK1–FL, this would confirm the auto-inhibitory mechanism in PAK1. Using Rapid-fire™ kinase assay, the activity of two versions of PAK1 were measured and compared in the following figures (see Figure 5.2.1).

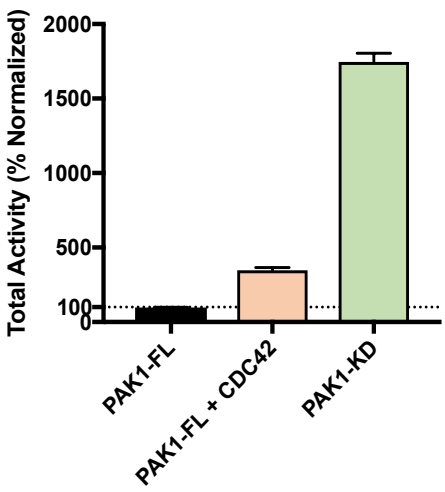

Figure 5.2.1 *Comparative kinase activity between PAK1-FL, PAK1-FL + CDC42, and PAK1-KD.* Rapid-Fire™ mass spectrometry PAK1/CDC42 kinase assay was used to measure the activity of the enzymatic activities. The measurement was examined through detecting the amount of substrate (1926.1g/mol) to product (2006.1g/mol) conversation after 30 minutes of kinase reaction. The signal from HTMS is given by [P/(P + S)] × 100, where P and S are the product and substrate mass spectrum peak areas, respectively. This was normalized and represented as '% normalized' in the Y-axis for easier interpretation.

The relative total activity difference between those of PAK1-FL and PAK1-KD was measured to be significantly greater for PAK1-KD, observing 17 times greater in its activity in comparison to that of PAK1-FL (P-value < 0.0001). For comparison, CDC42 was introduced to PAK1-FL and its effect on increasing PAK1 activity was shown to be relatively smaller in comparison to the PAK1-KD activity alone – illustrating about 3.5-fold increase in PAK1 activity when CDC42 was present. PAK1-KD had lacked the AID which allowed for the ATP substrate to freely access the catalytic domain and to allow for the peptide phosphorylation to occur. Assuming that the observed PAK1-KD was the maximum potential catalytic activity of PAK1, this confirmed that AID dimerization exhibits ~95% reduction in PAK1's activity and implicates for potential capacity to increase PAK1 activity when the AID is disrupted.

Following the confirmation that AID modulation can affect PAK1 activity, we wanted to investigate whether or not JB79's method of PAK1 activation was also through obstructing the AID dimerization. If JB79 binds to the AID and AID is removed from PAK1 structure, we would expect to see no change in the activity for PAK1-KD, Meanwhile, we would observe an increase in the PAK1-FL activity by JB79 as the AID is still intact for the full-length proteins. Using the RF-MS kinase assay, the activity of both PAK1-FL and PAK1-KD were quantified under the influence of either vehicle or JB79 (20uM) (see Figure 5.2.2).

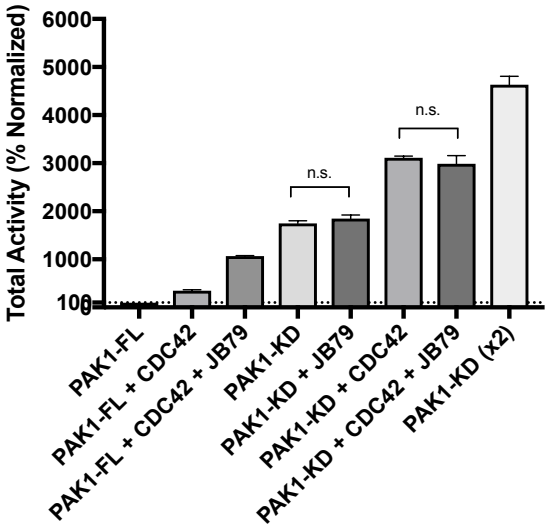

Figure 5.2.2 *Comparative kinase activity between PAK1-FL and PAK1-KD, under the presence of different modulators.* Rapid-Fire™ mass spectrometry PAK1/CDC42 kinase assay was used to measure the activity of the enzymatic activities. The measurement was examined through detecting the amount of substrate (1926.1g/mol) to product (2006.1g/mol) conversation after 30 minutes of kinase reaction. The signal from HTMS is given by [P/(P + S)] × 100, where P and S are the product and substrate mass spectrum peak areas, respectively. This was normalized and represented as '% normalized' in the Y-axis for easier interpretation.

The results showed that JB79 in conjunction with the activity of CDC42 had significant effect in modulating PAK-FL activity, increasing its total activity by 10 times greater in comparison to the PAK1-FL activity. Amplification of PAK1 activation by JB79, in addition to CDC42, was very intriguing as this had suggested that the mechanism of JB79 is likely though binding at an allosteric site that is different from that of the CDC42 binding site. Indeed, there is also the possibility that JB79 may facilitate in protein-protein interaction between CDC42 and PAK1 and thereby, stimulating the kinase activity. However, this would require very strong binding to the surface of PAK1; the likeliness of such mechanism was low since compounds usually need a deep hydrophobic pocket in order to stay stabilized. Lack of such pocket at the CDC42 binding site on PAK1, as well as, small molecular size of compound implies that the mechanism of JB79 was likely through the former, binding at an allosteric site of PAK1.

Another supporting evidence for the JB79 mechanism of action was found through comparing the effect of JB79 on PAK1-FL and PAK-KD. When PAK1-FL was treated with JB79, we had observed significant activation on PAK1 activity. However, such effect was lost when PAK1-KD was treated with the same concentration of JB79. This demonstrated that PAK1-KD does not contain the binding site for JB79, and therefore, the likely mechanism of JB79 is not through modulating the conformation of the kinase domain. This had provided further evidence in which the JB79's allosteric binding site is likely be within the deleted domains of PAK1-KD.

5.3 Characterization and comparative analysis of fragment-based binding

Previous *in vitro* results, along with the *in silico* studies, have given us with a reasonable degree of confidence that the likely binding site of PAK1 activators is at the large hydrophobic pocket within the AI domain. However, we still had lacked the structural studies to support the binding site of PAK1 activators. Thus, we applied fragment-based drug discovery (FBDD) approach in order to perform the hit expansion (ligand-designing) and to further explore the interaction between the PAK1 activators and the AI domain pockets. FBDD is a ligand optimization method, based on the obtained structural activity relationship (SAR) data, to explore the chemical space within the ligand binding site. FBDD method is considered as a cost-efficient and robust method in improving the hit ligands. Since its application from the 1990s, FBDD method has been successfully applied in discovering two novel drugs and 30 other compounds – which are now in their clinical trials (Davis et al., 2017). Using the FBDD method, therefore, we also sought to understand the molecular recognition site of where the ligand binds to, as well as to facilitate in the ligand optimization process.

From the limited optimization process and *in vitro* kinase assays, we observed an unique chemical structural pattern of the PAK1 activators. Current PAK1 activators that showed stimulatory effect on PAK1 had an average molecular weight of ~400 and contained polarizing aromatic ring moieties. Exemplary compounds such as JB01, JB09, JB22, and JB79 all contain functional groups with strong electron withdrawing groups at the ends, exerting significant activation effect on PAK1. On the other hand, the compounds which failed to stimulate PAK1 activity contained either a hydrophobic or neutral pharmacophore (e.g. JB34 and JB58). Specific relative locations of substituents were also found to be crucial in providing efficacy in PAK1 activity. Comparing the chemical structures of JB79 and JB81, these compounds contain almost identical pharmacophore properties (see Figure 5.3.1). The length core group and its functional groups are all the same except for the halogen group (chloride, JB81) and the carboxylic group (JB79). Halogen groups and carboxylic groups are both considered to be electron withdrawing groups, with the latter being stronger. Despite such similarities, we observed significant difference in its ability to stimulate PAK1 activity (see Figure 5.3.1). RF-MS kinase assay results showed that JB81 contains almost no efficacy in stimulating PAK1, yet

JB79 even at lower concentration 10uM showed significant effect in increasing PAK1 activity. These comparative SAR study revealed that the meta-position of the aromatic ring is essential for conferring the compounds' efficacy.

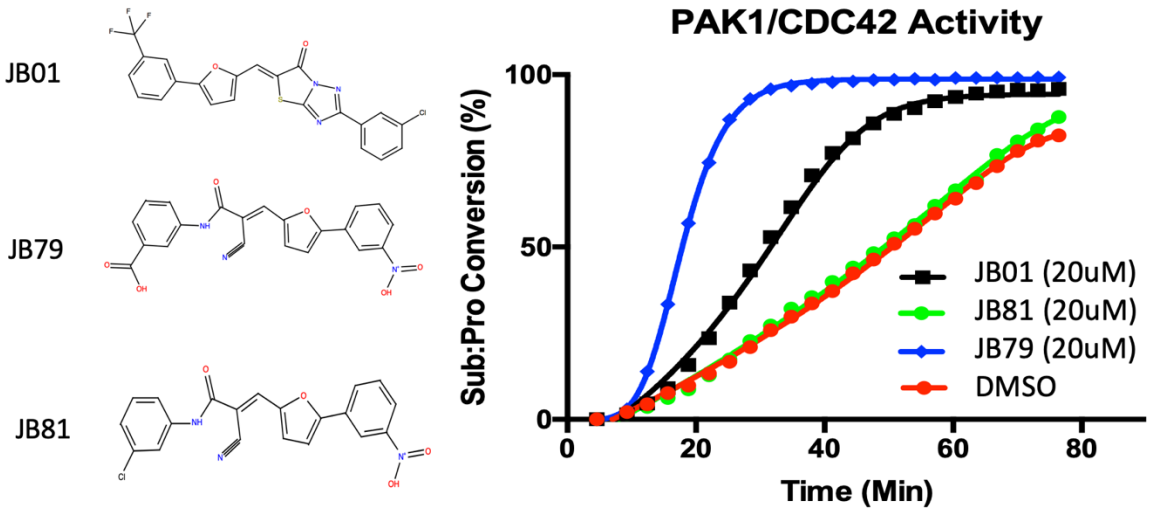

Figure 5.3.1 *Time Dependent Kinase assay on JB01, JB79 and JB81.* Rapid-Fire™ mass spectrometry PAK1/CDC42 kinase assay was used to measure the activity of the enzymatic activities. Notice how the JB81 compounds has no efficacy in activating PAK1 activity, while a very similar compound JB79 confers significant activity in PAK1. The measurement was examined through detecting the amount of substrate (1926.1g/mol) to product (2006.1g/mol). The signal from HTMS is given by [P/(P + S)] × 100, where P and S are the product and substrate mass spectrum peak areas, respectively. This was normalized and represented as '% normalized' in the Y-axis for easier interpretation.

The core group of each compound, however, was found to be non-essential for conferring its efficacy in increasing the PAK1 activity. From the limited optimization process, we had identified several different compounds which had different core groups, yet these compounds were still able to stimulate PAK1 activity. Compounds such as JB01, JB09, JB22, and JB79 and JB88 all have different core groups (A, position below), yet maintain similar pharmacophore branches – indicating that the branching groups are more important in conferring the PAK1 stimulatory effect than those of the core groups. The degree of electronegativity of the functional groups was also found to be correlated with its ability to confer stimulatory effect. Compounds that contained moderate to strong electron withdrawing groups (EWG), e.g. NO_2, COOH and CF_3) exhibited significant stimulatory effect, meanwhile compounds with weak or neutral electronegativity groups (e.g. halogens) showed minimal stimulatory effect on PAK1, as

demonstrated by the difference in the efficacies between JB79 and JB81. These results suggest that the group A linker (as shown in Figure 5.3.2) may be acting as a linker between the two fragment groups and does not confer much to the stimulatory effect, making it a flexible for modifications. That being said, the two outer side rings/fragments must have moderate to strong EWG at para- or meta- positions in order to confer its activating effect.

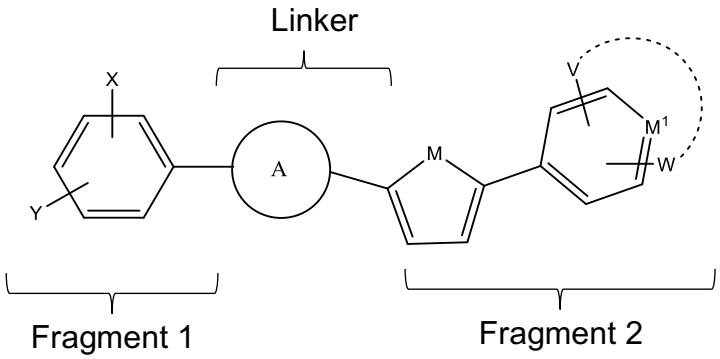

Figure 5.3.2 *General compound formula for PAK1 activators.* M1, M2, V, W, X, Y, are the functional groups with high electron withdrawing (EW) moieties. The strength of the electrophilic groups and the position of these functional groups are found to be essential in conferring its efficacy. Z is the linker moiety where it connects the two fragment groups together.

To achieve further understanding of the chemical nature of the binding pocket, JB79 compound was used as the exemplary compound and was broken down into its two smaller component compounds (JB96 & JB97). We hypothesized that the individual fragments would have low efficacy in activating PAK1, while simultaneous binding of both fragments would induce similar stimulatory effect as that of JB79. Therefore, JB79 was broken down into two separate fragment compounds, as illustrated by Figure 5.3.3, and each compounds were measured for their activity. If simultaneous binding of fragment 1 and fragment 2 were to induce similar activity as that of JB79, this would support that the linker groups is not essential for conferring PAK1 activation, but rather the fingering moieties are the essential component in the kinase activation.

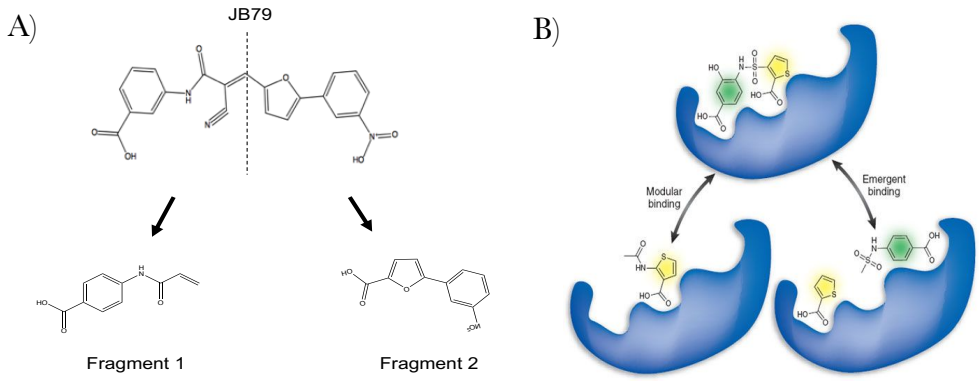

Figure 5.3.3 *Fragment Drug Discovery*. **A)** Chemical structures of JB79 fragments. The PAK1 activator JB79's fragments were designed in order to mimic the pharmacophores of JB79. **B)** predicted mechanism of fragment activation. individual molecular docking should be insufficient to confer its activity. But simultaneous binding of two fragments would allow for its activation effect.

Kinase assays were used to validate whether or not fragment binding studies could be achieved or not. Both ADP-Glo™ and RF-MS kinase assays were performed to measure the effect of the fragment compounds on the PAK1 activity. The kinase assays were set at three different conditions: fragment 1, fragment 2, and fragment 1 + 2 together. The result of the ADP-Glo kinase assay were shown as below:

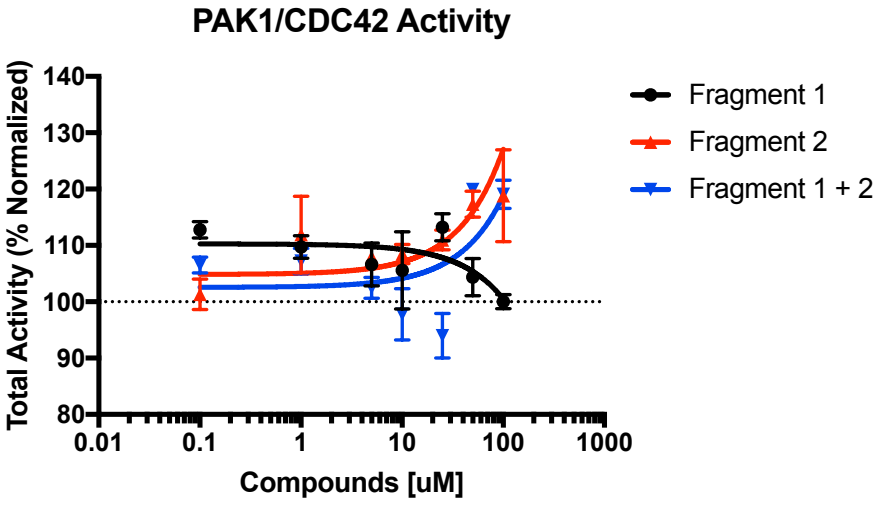

Figure 5.3.4 *The dose-response curve of JB79 fragment compounds (JB96 & JB97) on the activation of P21-activated kinase 1 (PAK1).* ADP-Glo™ kinase assay was used to correlate the kinase activity and ADP production. All reactions contained 150 ng of PAK1 enzyme, and the reactions were incubated for 60 minutes at 30°C. Replicates of three reactions were made at each concentration point. Data are presented as mean ± S.E.M

The kinase assay result revealed no significant differences of PAK1 activation, amongst different concentration of each fragment compound. Individual fragment by themselves did

not show significant activation in PAK1 activity; fragment 1 (JB96) showed inhibitory effect at higher concentration, while fragment 2 (JB97) exhibited only a minor increase (118 ± 2.3 %) at high concentration of 100uM. When these compounds were simultaneously tested in the kinase assay, co treatments of fragment 1 and 2 exhibited similar dose response curve as that of the fragment 2, illustrating only a minor increase in its activity (119.1 ± 2.5 %). Overall, ADP-Glo kinase assays using the fragments of JB79 did not show any significant increase in PAK1 activity, concluding that these fragments of JB79 was not successful in activating PAK1 activity.

As the ADP-Glo kinase assay lacks the sensitivity in detecting minor changes in the kinase activity, RF-MS Kinase assay was also performed as an additional assay to confirm the above findings. The results of the following RF-MS time dependent kinase reaction results are shown as below (see Figure 5.3.5):

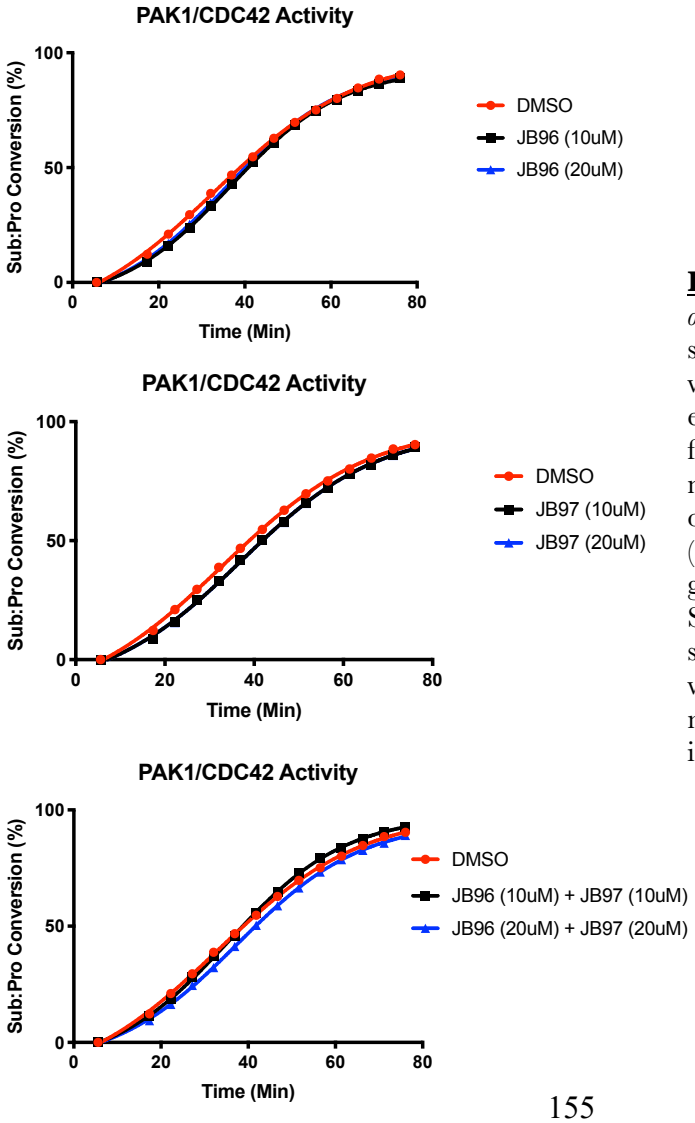

Figure 5.3.5 *Time Dependent Kinase assay on JB79 Fragments.* Rapid-Fire™ mass spectrometry PAK1/CDC42 kinase assay was used to measure the activity of the enzymatic activities. The effects of fragment binding were observed and measured through detecting the amount of substrate (1926.1g/mol) to product (2006.1g/mol). The signal from HTMS is given by [P/(P + S)] × 100, where P and S are the product and substrate mass spectrum peak areas, respectively. This was normalized and represented as '% normalized' in the Y-axis for easier interpretation.

The rate of substrate conversion for PAK1 under the presence of the fragment compounds exhibited similar rate as seen with the vehicle treated ones. The hillslope for individual curves were found to be non-statistically different (hillslope for DMSO: 0.026, Fragments 10uM: 0.033 and Fragments 20uM: 0.032), indicating that the fragment compound did not confer any functional effect in PAK1. In addition, higher concentration up to 20uM for each fragment compound exhibited only minor changes, confirming the previous results from ADP-GLO kinase assay that these fragments do not confer any increased activity in PAK1. Despite the pharmacophore nature of these fragments being almost identical to those of JB79, the compounds still did not contain any efficacy, demonstrating that the binding pocket requires specific orientation of ligand binding. The core moiety of the compound may be acting as a stabilizer that orientates the two important moieties together and thereby allowing it to confer its stimulatory effect. Within these limited number of compounds available, it was hard to make any conclusive findings on the SAR. However, this experiment has provided additional insight into the essential roles of the core moieties, length of compound, as well as specific orientations that are important for conferring specific activity on PAK1.

5.4 Mechanism of inhibitory effect of PAK1 Activators at high concentrations

One of the interesting remarks of PAK1 activators was the observation of stimulatory effect at the therapeutic concentrations, followed by inhibitory effect at higher concentrations. With exemplary compounds like JB08, JB53, JB79, and JB120, dose response test for these compounds showed that the kinase activity becomes significantly increased at their therapeutic concentrations ~ 10uM (increases by 10- and 8- folds), but the activity becomes dramatically decreased as the compound concentration gets higher (<50uM) (see Figure 5.4.1)

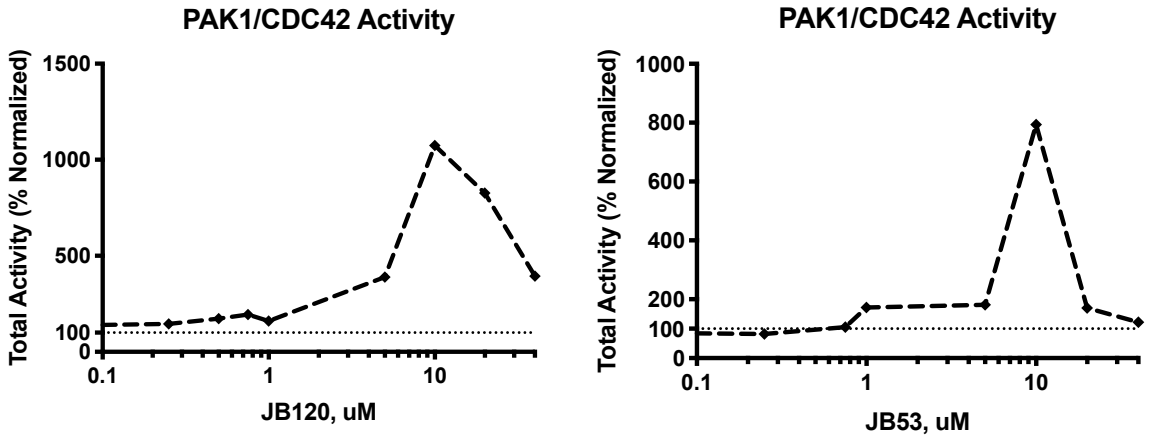

Figure 5.4.1 *PAK1 inhibition at high concentrations, using JB53 and JB120 as exemplary.* Rapid-Fire™ mass spectrometry PAK1/CDC42 kinase assay was used to measure the activity of the enzymatic activities. After the stimulation of PAK1 activity, the compounds were observed to cause inhibitory effect at higher concentrations.

Due to the novelty of this research, current literature on small-molecule kinase activators are significantly lacking, making it difficult for us to predict the mechanism of inhibition. Understanding such mode of inhibition was crucial for perspective ligand optimization as it allow us to avoid adding chemical moieties that may confer the inhibition effect. PAK1 inhibition was also a concern for a potential adverse effect, contradicting with our initial therapeutic intentions of activating the enzyme in providing cardioprotective mechanism. In effort to reduce such potential side-effect, we wanted to understand how the small molecules are causing inhibition and whether or not we could find alternative ways to prevent inhibitions from occurring at higher concentrations. With the help from our collaborators from TDI, several mechanisms have been considered for the mechanism of inhibition:

A) Non-specific binding at the kinase domain
B) Covalent modification to PAK1, causing irreversible inhibition.
C) Compound coagulations and precipitation, thereby causing non-specific binding.

First hypothesis was the non-specific binding inference to PAK1, in which high concentration of PAK1 activators leads to a higher chance of interfering with the kinase activity. Presence of surplus compounds can increase the entropy and the probability of random binding at the kinase domain, may interfering with the substrate binding. Another mechanism of its inhibitory effect could be due to the covalently modification (Michaels adducts) between PAK1 and the ligands, leading to an irreversible inhibition of PAK1. Compounds with an activated double bond such as, α,β-unsaturated aldehydes/ketones, vinyl esters, vinyl sulfones, imidazole, and maleimides have been previously reported to undergo a Michael addition with a nucleophile, leading to a covalent modification onto the protein. Unfortunately, a few of the confirmed PAK1 activators contained the α,β-unsaturated aldehydes/ketones within the core group, which may lead to a covalent binding to PAK1. Such covalent modification at stabilized carbanion, such as thiole or amine, may obstruct the substrate binding at the kinase domain and consequently, causing an inhibitory effect on PAK1 activity. Finally, the inhibitory effect could have been due to compounds coagulations, causing precipitations at high concentrations. Because the compounds in solution contain both nucleophile groups and electrophiles groups, these groups can interact within themselves and lead to intermolecular coagulations. The intermolecular bonding amongst the ligands can cause series of chain reactions, forming a new molecule entity and possibly conferring unintended consequences, such as the kinase inhibition. In order to investigate this matter, each plausible explanations were tested using biophysical *in vitro* assays.

5.4.1 Mechanism of inhibition: Non-specific binding at the kinase domain

One method of inhibition at high concentrations is thought to be through a a non-specific binding at the substrate binding site. The binding of the compound, instead of other substrates (ATP, peptide, etc..), may decrease the likelihood of substrate binding and thereby, affect the kinase activity. Methods for validating the ligand binding require in-

dept understanding of the PAK1 equilibrium kinetics. As the concentration of ligand increases, more ligands will start to bind to the active site until eventually reaching the saturation point where all ligands have pre-occupied the active site. This is likely to be the concentration range where the maximum activity of PAK1 is observed from the dose response tests. Any concentration that is higher than this threshold level would lead to a biding of surplus ligands to non-specific hydrophobic regions of PAK1. The kinase domain may be one of the possible non-specific binding sites that leads to an inhibitory effect. Currently, additional biophysical assays (e.g. ITC and SPR) in order to investigate whether or not, higher concentration of the ligand would cause any interference with the substrate binding. These assays should provide additional insight into the kinetics of the ligand bindings and allow us to comprehend the protein-ligand interaction at the molecular level.

5.4.2 Mechanism of inhibition: Covalent modifications

Another possible mechanism of inhibition of PAK1 at higher concentration could be due to its unintended covalent modifications of the ligand to PAK1. Covalent binding are usually found in monomers with an activated double bond, such as, α,β-unsaturated aldehydes/ketones, vinyl esters, vinyl sulfones, imidazole, and maleimides. These activated groups can undergo a Michael addition with a nucleophile, forming a covalent irreversible bonding to PAK1. Current PAK1 activators contain, α,β-unsaturated ketones groups, which may lead to forming covalent adducts through Michael additions.

Modification by covalent bonding is one of common drug mechanisms of action. Covalent inhibitors, for example, contain specific functional groups, designed to react with a corresponding target, typically an amino acid side-chain and permanently affecting the protein target through an irreversible binding. In recent years, a significant number of covalent inhibitors have been increasingly used to design cancer drugs that bind to the ATP binding pocket and form covalent modifications. For instance, Ibrutinib is a potent BTK inhibitor that has been confirm forms irreversible covalent bond with Cys481 of the BTK's ATP binding pocket (Barf et al., 2012). Although such mechanism of action has been studied to be practical for designing many pharmacological tools, off-target

modification is a potential concern for its side effects and toxicity. Cancer drugs have been previously reported to have high rate of having off-target effects (e.g. CYP450) and thereby leading to production of highly reactive metabolites (Lonsdale and Ward, 2018). In order to ensure that our small-molecule PAK1 activators do not constitute any off-target side effects, we wanted to check whether or not there was any evidence for covalent adducts being formed on PAK1.

Amongst different methods of validating covalent adducts, direct mass spectrometry (MS)-based identification provides the most experimentally accessible opportunity to define the potential off-target adductome of a given drug. MS provides valuable information about the exact mass of metabolites and corresponding abundance of each metabolite. Therefore, if any covalent modifications were to occur on PAK1 enzyme, we should be able to detect the shift in the mass of PAK1 and confirm the covalent modifications. Two different compounds of PAK1 activators (JB79 and JB08) were incubated in an *in vitro* kinase assay to observe for any formation of covalent adducts on PAK1. The results of the MS assays are shown below after 12 hours of incubation (Figure 5.2).

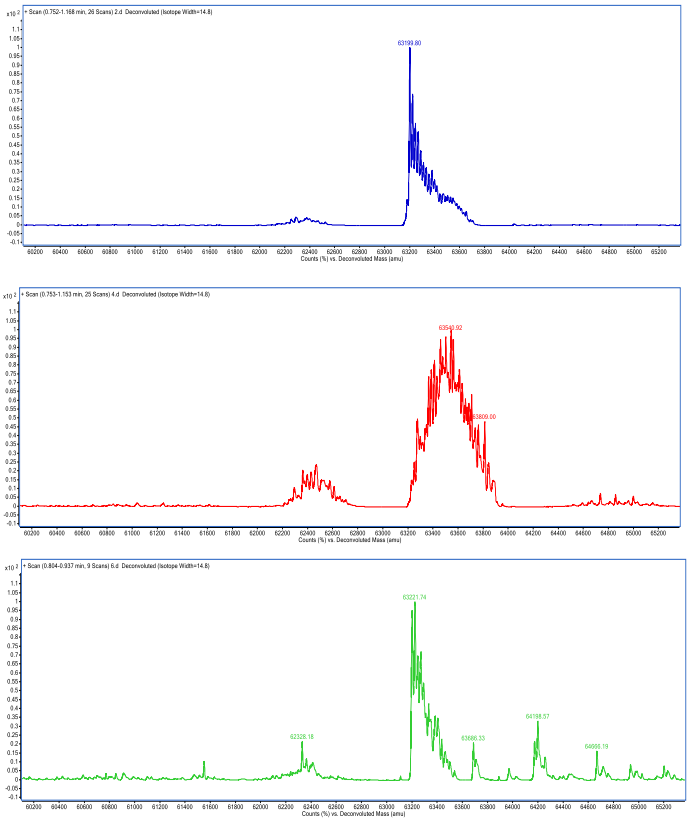

Figure 5.4.2 *Mass-spectrometry results of PAK1 kinase assay with compounds DMSO, JB08 & JB79, respectively.* PAK1 kinase reaction was incubated in room temperature for 12 hours under the presence of either DMSO, JB79 (100uM) and JB08 (100uM). Shift in the mass/charge ratio of PAK1 were examined in order to detect any presence of covalent adducts on PAK1.

With DMSO, the mass charge (*m/z*) ratio peaks for PAK1 were found to be distinctive at 63200.03 *m/z*. However, under the presence of the PAK1 activators, JB79 and JB08, the MS results showed lower resolution of peaks with multiple peaks at different m/z ratios. For example, PAK1 co-incubation with JB79 showed higher concentration of multiple peaks at around 63200.03 *m/z*, different from the *m/z* value of DMSO treated PAK1. These observations may suggest some modifications of PAK1 by the compound; however, it was not clear as to what modifications were being made. Furthermore, indications of *m/z* shift which corresponded to the molecular mass of JB79, 404.1 g/mol could not be detected based on the mas-spectrometry. Taken all together, the overall modification by JB79 at high concentration was found to be inconclusive.

On the other hand, the MS results on JB08 showed distinctive *m/z* peaks at 63221.74 (PAK1), 63686.33, 64198.57, and 64666.19. Apart from the 63221.74 m/z which corresponded to PAK1, these new peaks contained a difference in the molecular weight of 487.23 – which was equivalent to the MW of JB08 (487.23 g/mol), suggesting that the m/z shifts may be due to the JB08 covalent adducts being formed on PAK1. In order to further investigate whether or not these modifications can occur at lower concentrations, the assays were repeated at lower concentrations of JB08 (DMSO, 10, 25, 50, 100uM). CDC42 was also introduced to the reaction in order to see whether the presence of CDC42 had made any difference to compound effect. It had any effect to the compound binding and resulted in a difference in MS results (Figure 5.9):

A) PAK1-FL with JB79

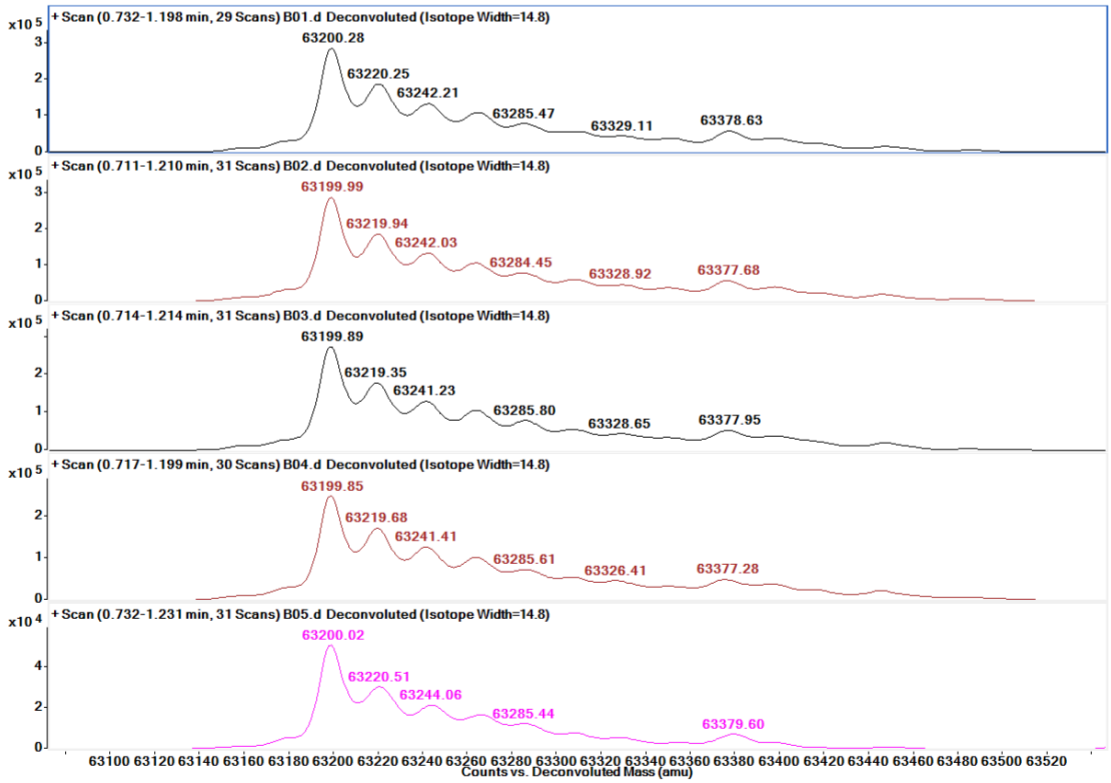

B) PAK1-FL + CDC42 with JB79

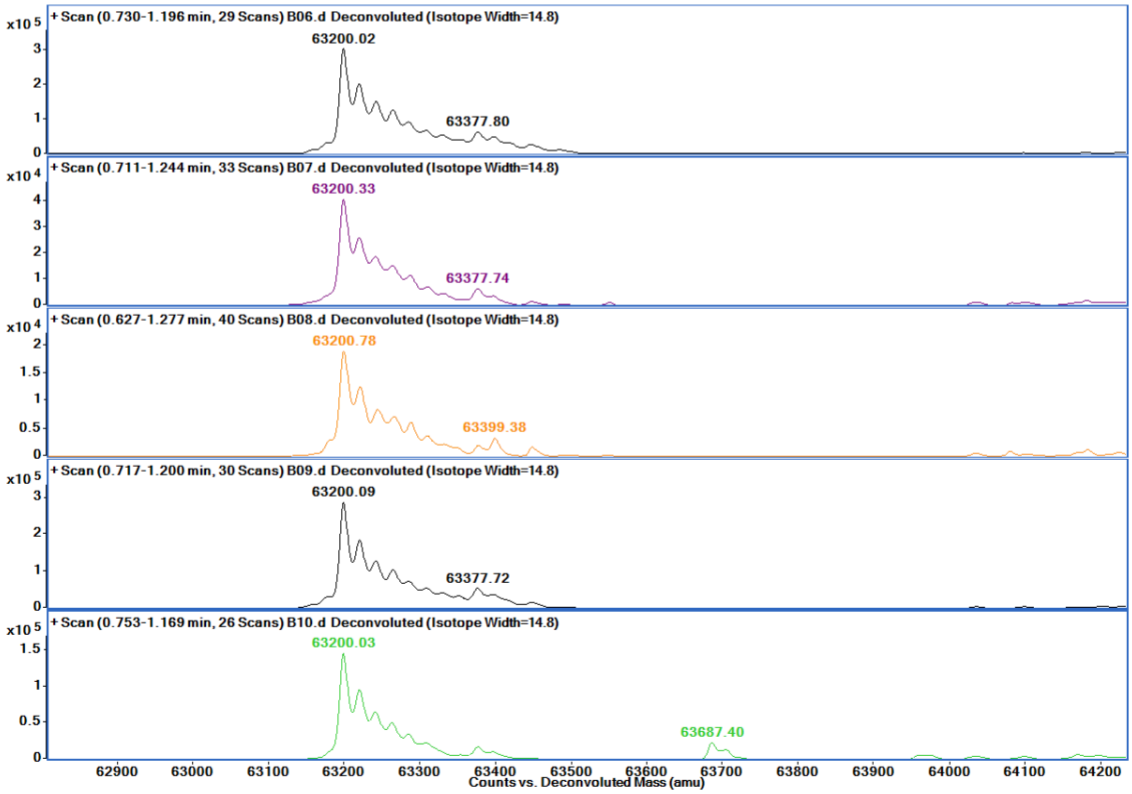

C) PAK1-FL with JB08

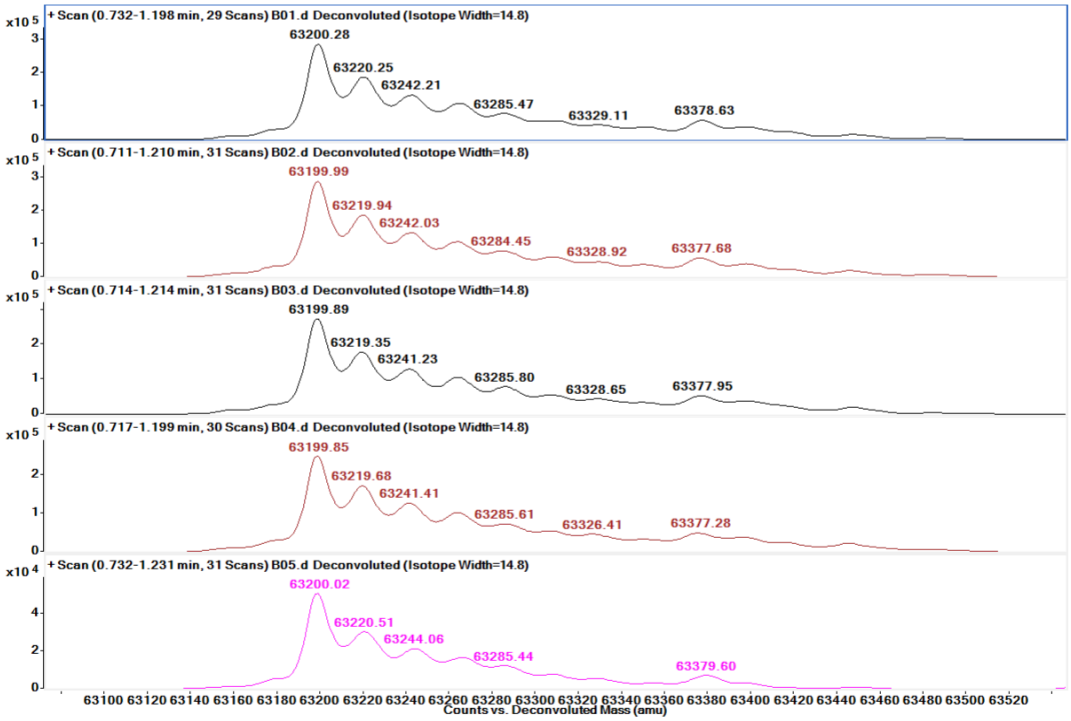

D) PAK1-FL+ CDC42 with JB08

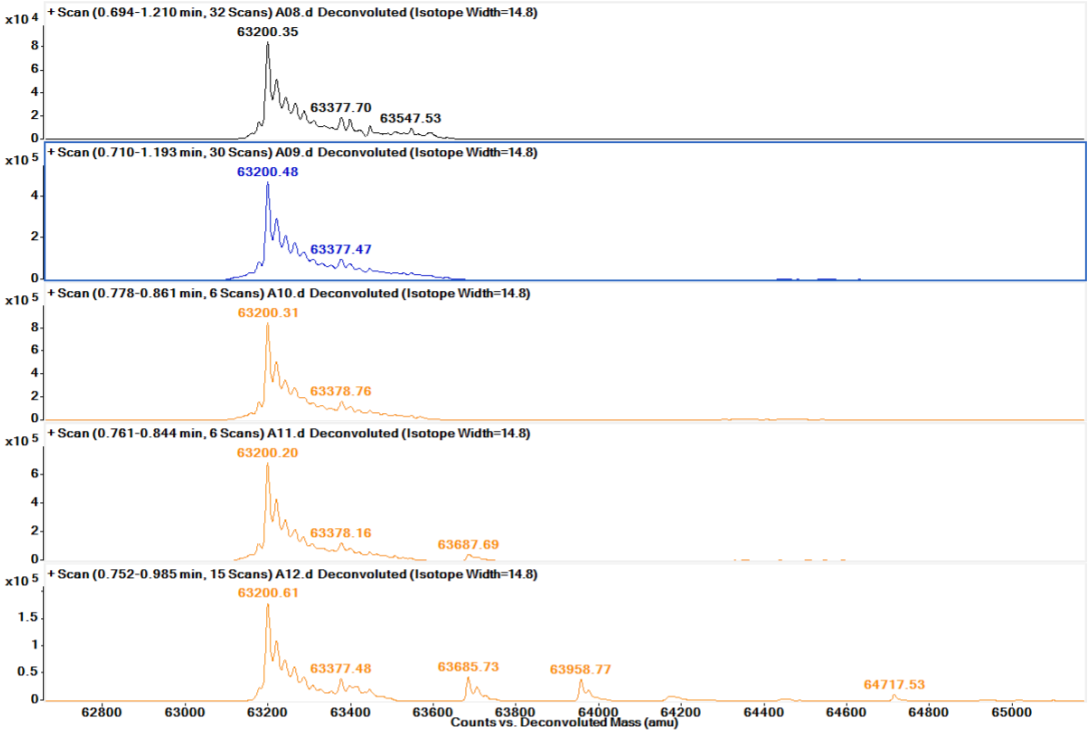

Figure 5.4.3 *Mass-spectrometry results of PAK1 with compounds JB08 & JB79, respectively.* PAK1 kinase reaction was incubated in room temperature for 12 hours under the presence of either DMSO, JB79 and JB08 (0, 10, 25, 50, 100uM). **A)** PAK1 FL + JB79, **B)** PAK1 FL + CDC42 + JB79 **C)** PAK1 FL + JB08 **D)** PAK1 FL + CDC42 + JB08. Presence of CDC42 were found to stabilize PAK1 protein. Shift in the mass/charge ratio of PAK1 were examined in order to detect any presence of covalent adducts on PAK1.

Unlike the previous results, PAK1's *m/z* peaks were found to be significantly blunted and blurred. The difference in resolution could been due to the dilution in buffer solutions and/or presence of DMSO dissolved compounds. Presence of other compounds bound to proteins may affect its ion acceleration and magnetic field deflections, resulting in an overall effect on its ion detection. Interestingly, this interfered detection of PAK1's *m/z* peaks were significantly improved upon presence of CDC42 protein; the stabilization effect of CDC42 on PAK1 may contribute to this improvement. Overall, the presence of CDC42 had greatly stabilized PAK1 proteins and made the covalent adducts to be more visible under the mass-spectrometry.

The MS results show that JB79 compound contained negligible modifications to PAK1 protein, as seen from Figure 5.4.3 A) and B). Small *m/z* peaks shifts are found to be too small to be JB79 nor its breakdown components. Despite the presence of CDC42, no noticeable covalent modifications on PAK1could have been observed, suggesting that the JB79 act through a transient binding mechanism. On the other hand, JB08 exhibited visible covalent modifications at higher concentrations. Under co-incubation with CDC42, JB08 treated PAK exhibited a dose dependent *m/z* peaks shifts for PAK1. Interestingly, as the concentration of JB08 increased, more *m/z* shift peaks were observed from the MS. These peaks were later confirmed to correspond to the exact molecular mass of JB08, 487.23 g/mol. To our interest, these mass shift peaks were only present at higher concentrations, not at the therapeutic concentrations. These results may explain for the cause of the inhibitory mechanism of JB compounds at high concentrations. At the maximal activity concentrations (~ 20uM), no observational covalent adducts were formed on PAK1. However, at the higher concentrations (<100uM) where we start to observe the inhibitory activity of PAK1, we also start to detect the covalent adduct peaks. Thus, there seems to be a threshold concentration in which, only after certain saturation point, the probability of collision becomes sufficient to form covalent bonds. Possible covalent modifications at the kinase domain may explain for the inhibitory observations. Although possible digestion and sequencing study may be required in order to confirm this mechanism, these preliminary studies provide one plausible explanation for the inhibitory effect of JB compounds at higher concentrations.

5.4.3 Mechanism of Inhibition: Compound Coagulations

In recent years, there has been a growing awareness of solubility-related limitations on many aspects of drug discovery. At supersaturated concentrations, compounds have been confirmed to form polymers and aggregates, in which these aggregates have inhibitory effect on their targeted enzymes. Effects of polymer formations have been detailly studied in Xu and Dai, 2013, illustrating how the thermodynamically unstable compounds may form coagulates and consequently exerting inhibitory effects (Xu and Dai, 2013). These compounds have been reported to be responsible for the false-positive hits in diverse bioassays, especially when compounds are screened at concentrations >10 mM, (McGovern et al., 2002; McGovern et al., 2003). Compounds like our PAK1 activators also have α,β-unsaturated carbons that may form intramolecular bonds, and such coagulations may explain for the inhibitory effect at high concentrations. In an effort to investigate whether or not the PAK1 activators form coagulates, we used JB08 as an exemplary compound to examine for any intermolecular coagulations. Mass spectrometry was used to detect the mass of the metabolites and to quantify the abundance of each metabolites (Figure 5.4.3)

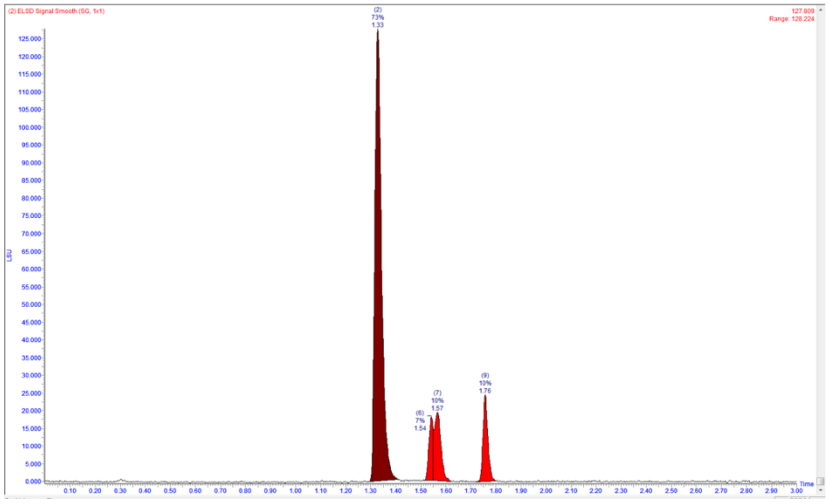

Figure 5.4.4 *Mass-spectrometry results of JB08 overnight incubation.* Compound breakdown was examined under the buffer solution to observe any coagulation/breakdown of the metabolites. 4 different peaks corresponding to different molecules were detected under the buffer solution, indicating possible dissociation or coagulations of compounds.

MS results shown above illustrates the abundance of each metabolites at specific retention times – after overnight incubation in kinase assay buffer. Interestingly, in addition to the

parent compound, three other different metabolites were observed in our MS analysis. Upon further analysis, we were able observe 4 different metabolites in total present in the buffer solution:

Compounds	Retention time	Mass
A)	1.266	758.23 (73%)
B)	1.270	271.03 (8%)
C)	1.508	486.23 (8%)
D)	1.695	232.23 (10%)

The highest abundant compound A) was measured to have a mass of 758.23 g/mol, consisting relative abundance of 73%. Other compounds had masses containing 271.03 g/mol, 486.23 g/mol and 232.23 g/mol. The molecular mass of JB08 was 486.23 g/mol, consistent with the compound C), however this was found to contribute only a portion (8%) of the total abundance. Compounds B) and D) were predicted to be the broken components of JB08, where the linker between prazole and the furan group were oxidized and broken into their components (see Figure 5.4.5)

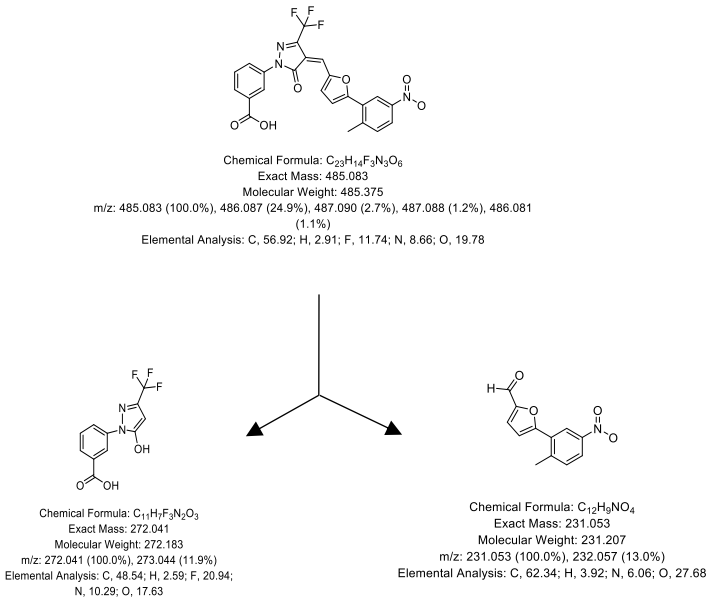

Figure 5.4.5 *Chemical breakdown of JB08 compound.* Predicted chemical structures of JB08 metabolites observed after overnight incubation in buffer solutions. The compounds B) and D) have corresponding similar molecular weight as predicted metabolite structures as shown above.

Interestingly, compound A which consisted of MW of 758.23g/mol was something that was not added previously in the kinase assay buffer. Upon further chemical analysis, it was predicted that the compound A is a polymer form of JB08 – formed through intermolecular bonding between the JB08 and its metabolite compound B). After the breakdown of JB08 into its corresponding metabolites, compound B) may have had an intermolecular reaction through Michael's addition with JB08 and formed a bigger metabolite (Compound A: 486.23 g/mol + 271.03g/mol = 758.23 g/mol). The chemical reaction of formation is as shown below:

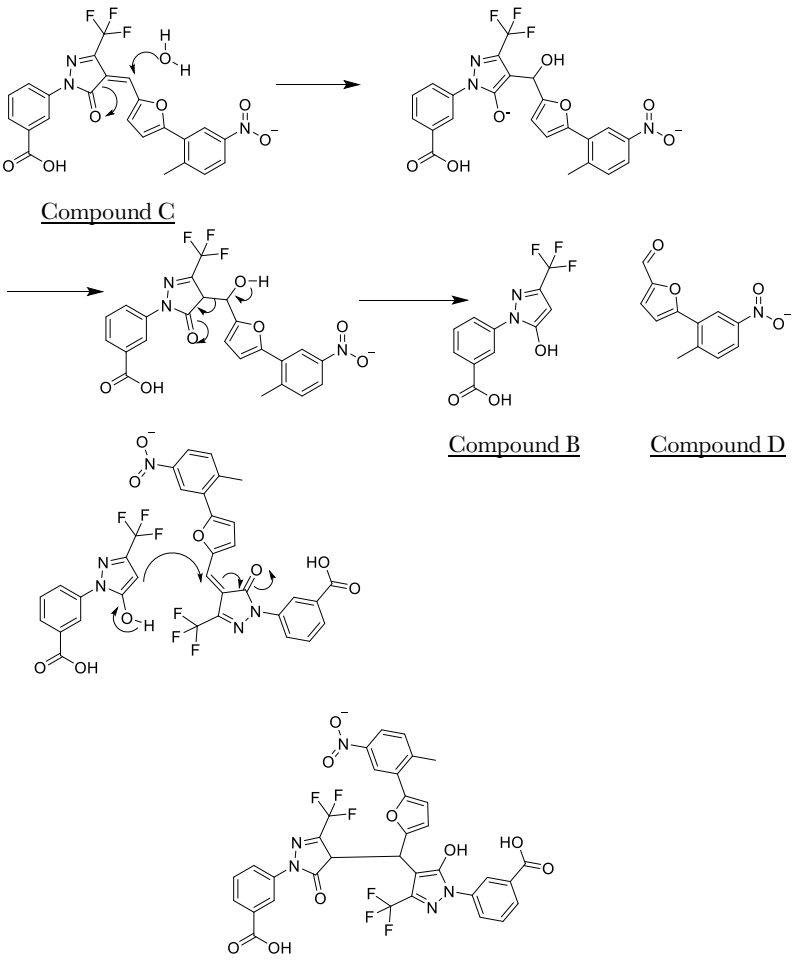

Figure 5.4.6 *Mechanism of intramolecular coagulation.* Predicted chemical structures of JB08 metabolites observed after overnight incubation in buffer solutions. The compound A which showed the most abundance was found to be formed from the breakdown metabolite of the JB08 compound.

One possible mechanism was through the water hydroxyl group, a nucleophile, undertaking a beta addition to the carbonyl electron withdrawing group and reducing the double bond. Upon reduction, the lone pair electron from the hydroxyl group broke the compound into JB08 components, compound B and D. Because compound B contained greater nucleophilicity than that of compound D, compound B was more favorable to undergo Michael addition to JB08 and to form a coagulate compound (Compound A). Amongst these metabolites, compound A was measured to be most abundant after prolong hydrolysis and coagulations, indicating that the PAK1 activators are able to form coagulates and may explain for the inhibitory effect. Further MS-analysis have shown that these coagulates are formed only at high concentrations and that the rate of coagulation kinetics is measured to be significantly slower at lower concentrations (results not shown). The next phase of work is to differentiate these metabolites through a HPLC and to extract each of the purified compounds. These metabolites would be then further examined in our established kinase assays to validate which of these metabolites are responsible for conferring the inhibitory effect.

Overall, the inhibitory effect of PAK1 activators at higher concentrations (<50uM) may be contributed by combinations of different mechanisms – non-specific binding, covalent modifications, and compound coagulation. These mechanisms may all be working in conjunction to confer the inhibitory effect on PAK1 activity. Further experiments are still required in order to determine the extent of each inhibition mechanisms. However, the mass spectrometry results above provide early insight to the reasoning behind the inhibitory effect of JB compounds at high concentrations.

5.5 Co-crystallography: Understanding the activate site of PAK1 activators

Detailed crystallography structure of PAK1 has been already described by Lei et al. in 2000. The group was able to form a 2.3 Å resolution crystal structure of a PAK1 complex, consisting the N-terminal autoregulatory fragment (a.a. 70 – 149) and the C-terminal kinase domain of PAK1 (a.a. 249 – 545). The structure showed the GTPase binding site where the regulatory proteins such as CDC42 and RAC1 bind, as well as the AID where the PAK1s interlock and dimerize in a homomeric manner (Lei et al. 2000). The study further validated that the binding of a GTPase trigger a series of conformational changes in which disrupts the PAK1 dimers and rearrange themselves into a catalytically competent state. Mutagenesis studies have also highlighted some of the residues that were responsible for the auto-phosphorylation and thereby activating the kinase domain (Parrini et al., 2002). Understanding these overview structures of PAK1 and its mechanism of activation has been the key for the development of PAK1 activators.

As described in previous chapters, we have discovered a number of evidences suggesting that the mechanism of activation of PAK1 activators is through binding at the auto-inhibitory domain and consequently, preventing the dimerization of PAK1. The proof of concept (PoC) of blocking the AID was firstly confirmed through the usage of PAK1-activating peptide (PAP), in which Ming et al. showed that a peptide that had a complementary sequence to the AID contained high affinity towards PAK1 AID and disrupted PAK1 dimerization. Testing these PAP in PAK1 kinase assay have revealed a significant stimulation on the PAK1 activity, validating our PoC of kinase activators (Wang et al., 2014).

Using this PoC, this peptide drug was further translated into small molecules through in silico ligand screening. The screened ligands were validated using *in vitro* kinase assays and confirmed to significantly increase PAK1 activity. In addition, PAK1 structure without the AID (PAK1-KD) structure showed no significant activation effect of the PAK1 activators, suggesting that the binding site is likely to be outside of the kinase domain. Finally, presence of GTPase (CDC42) was shown to augment the effect of PAK1 activators significantly, validating that the pre-activation of PAK1 by CDC42 is crucial in exposing the binding sites (AID) for the PAK1 activators. Taken all together, these evidences provide supporting indications for the PAK1

activator's mechanism of activation. However, direct evidence for confirming the binding site have still yet been confirmed through the co-crystallography.

In drug discovery, co-crystallography is the golden standard of validating the ligand binding site. Not only does it provide the atomic level insights to the complex formations, but the understanding complex also allows for structure-guided drug discovery and ligand optimizations. The detailed analysis of crystal structures of protein–ligand complexes allows us to the study of the specific interactions of a particular drug with its protein target at the atomic level. Therefore, this has been the most ideal method of validating ligand-protein interactions. In effort to verify the binding site of PAK1 activators, as well as to further investigate the mechanism of these activators, we had collaborated with Proteros ltd., a structural biotech company based in Germany, and performed co-crystallography between PAK1 and the Pak1 activators.

For this crystallization of PAK1-ligand complex, we firstly attempted to deduce the full length PAK1 structure (a.a. 70 – 545), conserving as many sequences as possible, without the ligand. The sequence had to be started off from the -70 as the N-terminus was considered to be too unstable to be able to obtain a good resolution. The following protocol from Lei et al. 2000 paper was used to model the new PAK1 crystallography, however, the new structure was slightly different from the previous crystallography of PAK1, which contained two linked constructs of PAK1 AID (a.a. 70 –145) and KD (a.a. 249 – 545) (Lei et al., 2000). The purpose of recrystallizing PAK1 structure was to intact the endogenous structure of PAK1 as much as possible in order to not to miss any binding site for the ligand. Although the predicted binding site for the Pak1 activators is at the AID, it was well possible that the ligand may be binding at another areas, including the region between a.a. 145 – 249 which the PAK1 crystallography (PDB:1F3M) did not have during the *in silico* screening. Hence, in addition to crystallizing the established PAK1 structure (a.a. 70– 145; 249 – 545), another single construct of PAK1 (a.a. 70 – 545) containing previously lacking domain was also expressed and purified for the x ray crystallography.

The process of x-ray crystallography involves several different steps with various check points in between. Several protocols have been reported since the discovery of the method, but the main steps in determining the x-ray co-crystallography still remains similar in most. The target protein is firstly expressed and purified, followed by formation of crystals. Soaking and co-crystallization are the two most common methods used to prepare crystals of protein–ligand complexes (Carvalho et al., 2010). The soaking method involves incubation of crystals with the ligand of interest, while the co-crystallography consists of preparing crystals of the protein-ligand complex. The success of both methods is related to the properties of protein crystal lattice, crystal stabilizations, and experimental conditions. The standard procedure often requires trying thousands of different conditions to pre-equilibrate the crystals in the most stable manner, including optimizing with different temperature, pH, salts, buffers, and additives. Once the crystals are successfully formed, diffraction data, either in-house or using a synchrotron X-ray source, is collected and analyzed. The analysis includes series of computational calculations to solve the phase problem (deducing the 3D structure) and the electron density map. These electron density map can be useful in predicting the individual atoms – allowing protein sequence fitting – and in refining the structural model. The summary of the crystallography procedure is shown as beside.

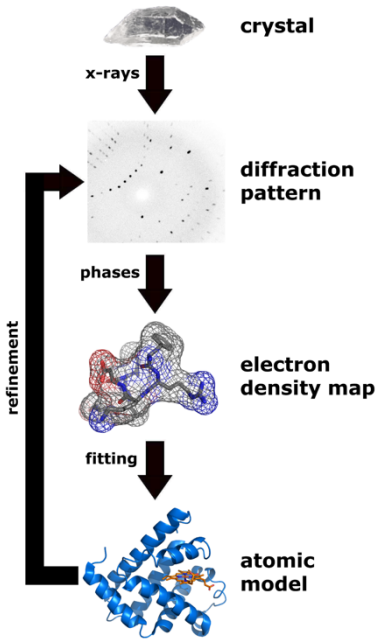

In order to create the crystals, protein production for individual constructs were established:

- PAK1 (Hs a.a.70-149) + PAK1 (Hs a.a. 249-545)
- PAK1 (Hs a.a.70-545)

The first production of PAK1 (His-tag a.a.70-149 + His-tag a.a. 249-545) were expressed in E.coli and collected from purification. From the pooled fractions, the purification yielded ~ 2.5 mg of pure protein per batch (concentration: > 16 mg/mL), making it an optimal protein concentration for the co-crystallography (Figure 5.1.A). PAK1 (Hs a.a. 70 – 545), on the other

hand, yielded in a much higher amount: 30mg pure protein per batch, concentration >16mg/mL (see Figure 5.1.B).

A) PAK1 (Hs a.a. 70 – 545)

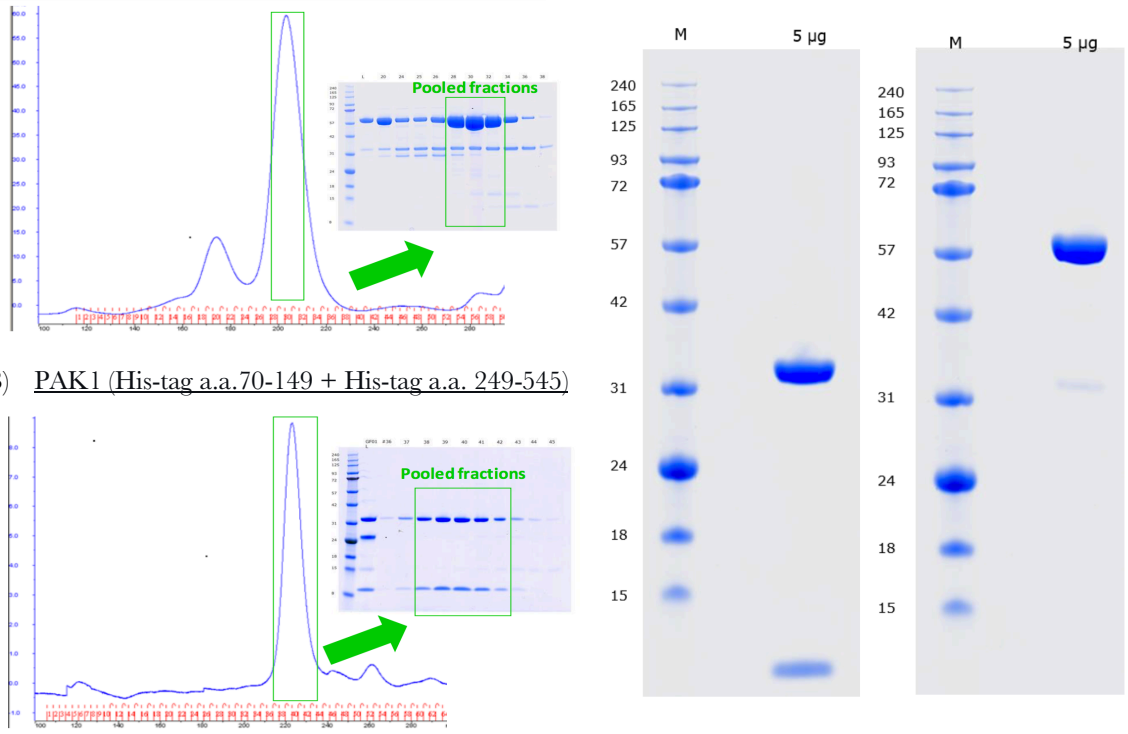

Figure 5.5.1 *Western blot results of purified PAK1.* The results shows successful expression and purification of PAK1 FL (Hs a.a. 70 – 545) & PAK1 (Hs a.a.70-149) + PAK1 (Hs a.a. 249-545)

After successful protein production and purifications, PAK1 (Hs a.a. 70 – 545) was screened at 1,600 different conditions set by Proteros protocol in order to determine the most optimal condition required for crystallization. These conditions were tested at various parameters, examining in different solvents, temperature, acidity, vessels and methods of crystallography. Given by this grid screening, PAK1 (Hs a.a. 70 – 545) crystals in all these conditions were tried and repeated three times. Unfortunately, no favorable crystals could have been observed from the solutions and therefore it was decided that PAK1 (Hs a.a. 70 – 545)could not be crystallized under such conditions that were set by Proteros Ltd. These results were quite a disappointment; however, this was somewhat anticipated as the previous group, Lei et al., would have done the PAK1 (Hs a.a. 70 – 545) from the beginning – if the crystallography had been worked out – rather than dissecting the construct into two different domains. In addition to trying different crystallography conditions, ligands that can form hydrogen bonding with the proteins have

been reported to assist in co-crystallography, so attempts were made to crystalize the protein under the presence of JB79 and JB08 (Manor and Carroll, 2016). Nonetheless, no good crystals could still be formed for the PAK1 (Hs a.a. 70 – 545).

This led us to revert back to using the previous crystallography construct of PAK1 (Hs a.a.70-149) + PAK1 (Hs a.a. 249-545). Fortunately, the grid screening for PAK1 (Hs a.a.70-149) + PAK1 (Hs a.a. 249-545) were observed to be successful. Four novel hit conditions had been confirmed to have optimal conditioned crystals, diffracting beyond 3 A. The data collection and processing were achieved through a cryo-protocol established by Proteros Standard Protocols. X-ray diffraction data have been collected from crystals of PAK1 at the SWISS LIGHT SOURCE (SLS, Villigen, Switzerland) using cryogenic conditions. The final results were processed using the programmes XDS and XScale. The details of the data collection and processing statistics for the crystals are shown in the Appendix 5. Structure modeling and refinements for new PAK1 structure was modeled after the previous PAK1 structure 1F3M. Statics of the final structure and the refinement process are listed in the Appendix 6. The final x-ray crystallography model of PAK1 (Hs a.a.70-149) + PAK1 (Hs a.a. 249-545) structure is shown below (Figure 5.1.A). Each domain of PAK1 are indicate in different colors for easier comparison. The auto-inhibitory domains are colored green (●) and cyan (●), whereas the kinase domains are yellow (●) and magenta (●). the AID domains are inter-locked through their long beta sheets; specifically, the alpha helixes from one AID and the beta sheet of another AID holds strong complimentary binding. Seven main chain hydrogen bonds link the two segments, and there are salt bridges between Glu82 on one strand and His86 on the other. The PAK1 kinase domain contains two alpha-helixes and five beta-sheets, which can be observed distinctly from our x-ray crystallography. In comparison with the previous low-resolution PAK1 crystallography structure 1F3M (grey, ●), the newly determined crystal structure had near identical superimposition (95% alignment), exhibiting consistent structure. PyMol program was used as a method to align the structures together in order to make direct comparison at the amino acid level (Figure 5.1.B).

A) PAK1 (Hs a.a.70-149) + PAK1 (Hs a.a. 249-545)

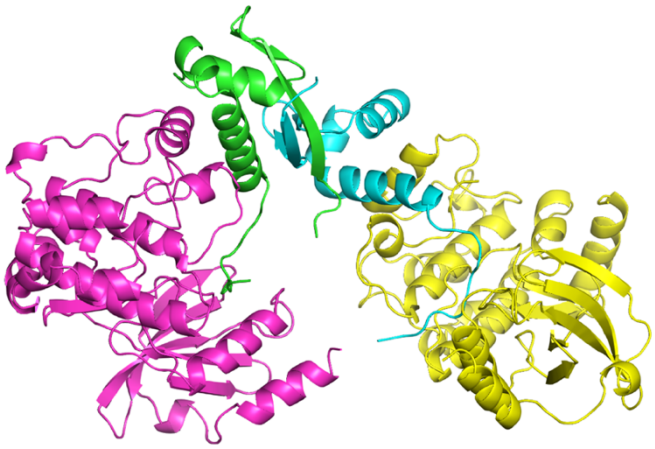

B) PAK1 (Hs a.a.70-149) + PAK1 (Hs a.a. 249-545), Superimposed with 1F3M (●)

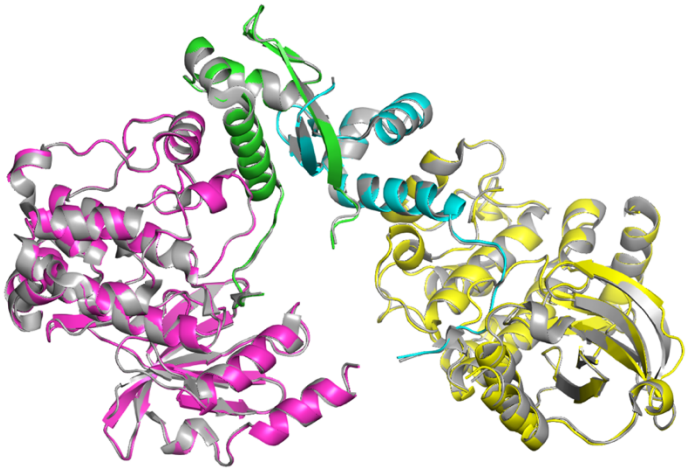

Figure 5.5.2 *Crystallography structure of PAK1.* PAK1 (Hs a.a.70-149) + PAK1 (Hs a.a. 249-545) crystallography was successfully crystallized and its structure was superimposed with 1F3M (●). Close similarity of the structure was observed with the newly crystallized PAK1.

Through the newly optimized condition, we were able to successfully crystallize the PAK1 (Hs a.a.70-149) + PAK1 (Hs a.a. 249-545) structure with higher resolution than previously reported. After successful structure determination, PAK1 activators were soaked in crystals in order to look for potential binding sites. JB79 compounds and JB08 compounds were initially tested for the crystallography. However, the additional soaking with more than 2mM PAK1 activators were found to be difficult due to the high sensitivity of crystals against DMSO. Further attempts in stabilizing the crystals, through cross-linking with glutaraldehyde, exhibited severe reduction in diffractions (~7 Å), making it not feasible for getting a good resolution. To make the matter

worse, high concentrations of JB79 and JB08 had exhibited signs of precipitation, which hindered the formation of crystals. Overall, JB79 and JB08 compounds were determined to be not to be feasible for the crystallography and additional attempts were made with the newly optimized compounds with Evotec (details of the optimization process is discussed in the next chapter).

JB120, JB124, and JB131 were concluded to be the mostly optimized PAK1 activators we have created so far. Their high stability in solvents, optimal solubility, along with high potency, made them better candidate compounds for the crystallography than the previous lead compounds – JB79 and JB08. Using the new lead compounds, then, co-crystallography was re-attempted to determine the ligand binding site. From the preliminary co-crystallography steps, the newly lead compounds were observed to have better solubility and soaking availability than the previous JB79 and JB08 compounds (results not shown). Six grid screens around previous hit conditions were found to be optimal, with each condition providing dataset with resolution < 3A; JB124 and JB131 contained the same grid condition required for the co-crystals, but crystals with ligand JB120 required different condition for their co-crystals. In all cases, higher resolution of PAK1 protein backbone structures could be observed under presence of each ligand and allowed for better screening of potential ligand binding site.

Although the resolution of crystals was better and the solubility issue for the ligands were not observed, we could not find any potential difference in the electron density that could belong to compounds JB131 and JB124. Crystals formed in different conditions were all examined, but no difference in the ligand density could be observed for these compounds. Interestingly for ligand JB120, we observed a novel crystal form at the space group $P222_1$ (at the auto-inhibitory domain); a small difference in the electron density could be observed at the site. Unfortunately, upon further scrutiny, the difference in the electron density did not align with the chemical structure of compound JB120. Therefore, it was concluded that the observed difference in the density was most likely the segments/residue from the auto-inhibitory domain (see Figure 5.5.3).

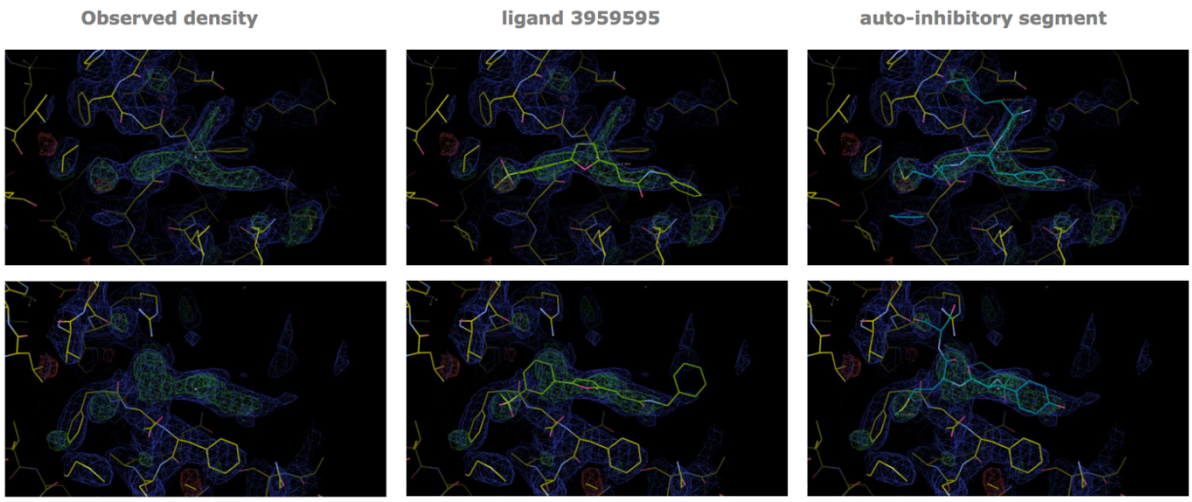

Figure 5.5.3 *Observed difference in density in PAK1 Co-Crystallography.* JB120 compound was thought to bind to PAK1, however this was turned out to be a segment of the AID.

The exact cause for the negative result is known at the moment, but suggestion for creating a better construct of PAK1 was raised. Current method of co-crystallography requires interaction of three different molecules (AID, Kinase domain and the PAK1 activators) and capturing the exact moment when the three molecules coincide together may have been too difficult. In addition, there is a chain discontinuity between the residues 149 and 249 which could have affected the overall structure of PAK1 and thereby, affecting the ligand binding as well. High concentration of proteins may also affect the binding ability of the ligands through shifting the equilibrium towards dimer formation and potentially blocking the ligand binding site, AID. Introducing CDC42 was also considered to see whether adding the GTPase will help to dissociate PAK1 in its monomeric conformations. However, this was found to be extremely difficult as we would require a large amount of CDC42, and too much proteins and ligands presence may also reduce the crystal formation abilities, reducing the overall resolution. As co-crystallography provide most comprehensive information about the ligand-protein interactions, another attempt at x-ray co-crystallography is currently being discussed. The next co-crystallography is being planned with Evotec using functional FL-PAK1 proteins.

5.6 Summary & Concluding Remarks

In Chapter 5, we explored the molecular mechanism of PAK1 activators in eliciting its PAK1 stimulation and its inhibitory effect at extreme concentrations. Although our results confirmed that JB compounds can effectively stimulate PAK1 activity and thus have potential therapeutic applications in counteracting CVDs complications, the definite mechanism action of JB compounds was not fully verified yet. Seeking to understand the method of activation of PAK1 on the molecular level, we designed the following three different PAK1constructs with specific segmental deletions: FL-PAK1 (a.a. 1~545), Δ-70 PAK1 (a.a. 70~545) and KD-PAK1 (a.a. 245~545). These three constructs were expressed in bacterial cells and successfully purified. The KD-PAK1 construct was designed to lack the auto-inhibitory domain (AID) of PAK1 (a.a. 70~149), which allowed us to selectively examine whether or not the loss of AID affected the compound's efficacy. The results of PAK1 kinase assay using RF-MS™ confirmed that the loss of PAK-AID leads to an overall increase in PAK1 activity, confirming that the AI domain contains an internal inhibitory mechanism preventing the kinase from being constitutively active. Interestingly, the results of dose response tests using JB compounds on KD-PAK1, which lacked the AID, did not show any stimulatory effect by PAK1 activators. This dose-dependent activation on FL-PAK1, but not on KD-PAK1, suggested that the likely binding site for the ligand is in the regulatory domains (e.g., AID), rather than in the kinase domain. Considering that the screening was based on the pocket model from the PAK-AID, the aforementioned finding proves the accuracy of the *in silico* method of compound screening. Finally, FL-PAK1 and Δ-70 PAK1 did not show any difference in their kinase activity or in their response to JB compounds, suggesting that the deletion of the first 70 amino acids resulted in neither a regulatory effect on the kinase activity, nor in its response to PAK1 activators.

Upon validation of the likely binding domain of JB compounds, in collaboration with Proteros Ltd., we performed co-crystallography between PAK1 and JB compounds. This was meant to verify the mechanism action of the compounds through locating the exact binding site of the ligand. Yet, due to protein coagulations, the first attempt at crystallizing FL-PAK1 was unsuccessful. Therefore, we redesigned the FL-PAK1 construct into (Hs a.a.82-149) & PAK1

(Hs a.a. 249-545), which exhibited a better crystal formation and a higher resolution of the protein backbone. Regrettably, as the proteins were soaked with JB compounds during crystallization, the electron density highlighting the compounds was found to be unavailable. In further research, it would be necessary to verify whether this was due to the low affinity of the compound (EC_{50} in micromolar) or the lack of binding site for JB compounds due to truncation.

Finally, we investigated possible mechanisms of inhibition of PAK1 activators. At a significantly high concentration (>50uM), several JB compounds were observed to elicit an inhibitory effect on PAK1; this was usually followed by a significant stimulatory effect on PAK1 at therapeutic concentrations (<20uM). This inhibitory effect can have the following three explanations. The first explanation is the ligand's non-specific binding at high concentrations. At concentrations above a certain threshold, the active site may become fully saturated with ligands and, therefore, any surplus ligands would likely bind to other regulatory sites. For instance, any surplus ligand binding at the ATP biding site or another allosteric site near the kinase domain may interfere with the substrate binding and, consequently, inhibit the enzymatic activity. The second explanation of the inhibitory effect is the potential covalent modification by JB compounds. Current PAK1 activators contain an α,β-unsaturated ketones group, which may allow for the Michael addition to occur and form covalent adducts. In support of this explanation, mass spectrometry results showed covalent adducts that occur only at high concentrations. Finally, the third explanation is that compound degradation and coagulations could have contributed to the inhibition mechanism. Repeated processes of thawing and freezing were found to have a fragmentation effect on the compounds, causing intermolecular bindings among different fragments. The results of mass spectrometry showed that new compounds were formed through fragment intermolecular binding, which could have been the cause of the inhibition effect. In summary, although further biophysical experiments would be necessary to confirm the above findings, our preliminary results provide a first insight into the potential mechanism of inhibition of small-molecule kinase activators.

CHAPTER 6

MECHANISM ACTION OF PAK1 ACTIVATORS

Summary Points

- Structure activity relationship (SAR) at the active site was explored through optimizing the lead PAK1 activator JB79.
- The SAR studies allowed for the design of better compounds with improved efficacy as well as its physiochemical profiles, exhibiting 'drug-likeness' properties with improved selectivity, permeability, and solubility.
- Photo-affinity labelling (PAL-MS) study provided novel insight into the binding site of PAK1 activator. The compound was identified to bind at the interface between the kinase inhibitory segment of PAK1-AID and the kinase domain (KD).
- Newly optimized JB131 compound was used in *ex vivo* heart perfusion assay to assess its cardioprotective mechanism on catecholaminergic polymorphic ventricular tachycardia (CPVT) mice hearts.
- Short term perfusion with JB131 was sufficient to reverse the ISO induced arrhythmia in CPVT mice heart and to provide alleviation in β-adrenergic stimulation, demonstrating to be a potential novel treatment for CPVT conditions.

6.1 Background Overview

Preliminary supporting evidence on small-molecule PAK1 activators was obtained through validating their stimulation of PAK1 activity and examining their therapeutic applications for CVDs. Along with being the first small-molecule PAK1 activators reported thus far, these compounds also provided a proof of concept for their novel mechanism of action – namely, that of targeting the auto-inhibition and thereby eliciting an enzymatic stimulation. Such mode of action has not been previously demonstrated in the drug discovery field; therefore, if validated, small-molecule PAK1 activators could be meaningfully used for various applications in the drug discovery field. In this relation, stimulating beneficial proteins is a novel method of delivering a therapeutic approach that is drastically different from conventional approaches used in drug design. In fact, most current drugs that target kinases aim to inhibit kinases' enzymatic activity and to prevent their harmful effect. Therefore, validating the mechanism of PAK1 activators may be used as a blueprint to design other beneficial kinase activators, providing thus a novel approach to deliver therapeutic treatments and offer new treatment options. For that reason, elucidating the mechanism of JB compounds has long been among the top priorities in the drug discovery field. Fortunately, important implications of elucidating the mechanism of JB compounds have also been recognized by Oxford University Innovations (OUI). In cooperation with the industry company Evotec Ltd., the OUI granted our project the LAB282 award, which enabled us to further pursue the drug development of PAK1 activators. This collaboration was essential for the success of both the development and understanding of the studied drug mechanisms.

Since its introduction to Oxford University in 2016, LAB282, a funding program on drug discovery acceleration aiming to translate basic research into clinic therapeutics, has supported a series of drug discovery projects, including, among others, "Screening for hit compounds for the therapeutic purpose of treating cardiac fibrosis" with Prof. Svetlana Reilly, "Developing novel-mode anti-infectives" with Prof. Ben Davis, "Inhibiting tissue damage in rheumatoid arthritis through a first in class therapeutic antibody" with Prof. Mark Coles, and "Therapeutic targeting of a novel cytokine in inflammatory bowel disease" with Prof. Alison Simmons. Many of these projects have tested candidate compounds using *in vitro* and *in vivo* models, thereby

facilitating a speedy translation of the findings in therapeutic applications. For instance, owing to cooperation with Evotec Ltd., Dr. Shoumo Bhattarcharja's research group was able to develop Evasin candidate molecules for myocarditis treatment. The pharmacokinetic (PK) and pharmacodynamics (PD) properties of the compounds were successfully characterized, and the results obtained from *in vitro* and *in vivo* models showed clinically useful applications for myocarditis. Overall, Evotec's expertise in accelerated drug discovery has been extremely useful for the funded projects, and we are sincerely grateful for the valuable opportunity to collaborate with the Evotec team.

Chapter 6 of the present study reports the results we obtained in collaboration with Evotec. The first aim of our project was to optimize the lead JB79 compound and to create a ligand characterized by favorable physiochemical properties for subsequent *in vitro* and *in vivo* research. As discussed in detail in Chapter 3, due to insufficient funding of the project, only a limited optimization process could be performed. Nevertheless, in the support of the LAB282 award, we were able to perform a detailed optimization of PAK1 activators, improving their efficacy, affinity, and physiochemical profiles. The optimization process also enabled us to acquire a thorough understanding of the structure activity relationship (SAR) and to gain a deeper insight into the binding site of PAK1. Through these SAR studies, the newly optimized and chemically improved compounds were synthesized and then tested in a cellular assay to measure their efficacy. For the preliminary testing of potential therapeutic benefits of the newly optimized PAK1 activators, the catecholaminergic polymorphic ventricular tachycardia (CPVT) mice model was used. *ex vivo* studies are currently being conducted to further validate clinical applications of PAK1 activators for CPVTs. Finally, we also investigated the mechanism action of lead compounds using photoaffinity labeling combined with mass spectrometry (PAL-MS). Using the PAL-MS analysis, we obtained structural data about ligand-protein interactions, which allowed us to determine the residues that the probe interacted with. These PAL-MS results were essential for the prediction of the required PAK1 structure constructs in the prospective co-crystallography study.

6.2 Optimization of JB compounds

At early stages of drug discovery, lead generation frequently entails a discovery of a hit small molecule from a high throughput screening (HTS); optimization to identify promising lead compounds is also needed. Chapter 2 discussed the structure activity relationship (SAR) of confirmed PAK1 activators and the performed optimization. However, the optimization was based on a limited number of compounds available from commercial providers. Synthesis of novel compounds was too costly. We used the limited optimization process to validate the specificity of the compounds in activating PAK1 activity, rather than to find novel candidate compounds. Overall, validations of a small amount of confirmed compounds can be useful when conducting QSAR or ligand-based optimization. The obtained lead compound from the JB79 optimization process has a more favourable physiochemical profile as compared to those of the previous hit compounds, such as JB01. This enabled us to perform preliminary clinical studies examining the therapeutic applications of PAK1. Focusing on the interactions between PAK1 and JB compounds, we biophysically investigated the mechanism of activation and its inhibition at higher concentrations. Finally, considering the concern about a potential developmental role of PAK1 activation in cancer, the potential side effects of PAK1 activation were analyzed in various cancer cell models. These preliminary results were a crucial stepping-stone for the validation of therapeutic applications of small-molecule PAK1 activators, as they enabled us to gain further support from the LAB282 program to accelerate in the PAK1 drug development.

With the assistance from the medicinal chemists from Evotec, we first made several analyses of the initial JB compound lists, comparing their molecular weight, solubility, chemical groups, surface permeability, and other related physiochemical properties. Amongst 127 JB compounds in total, 92 carboxylic acids, 82 aromatic nitro groups, 30 michaels acceptors and 27 different PAIN (10 different types) were found on the compounds – only 10 compounds were found to contain more drug like properties that may contain favorable ADMET properties. Chemical moieties of each compounds were further broken down for their analysis as well and examined for functional groups that may cause potential problem during drug development (see Figure 6.2.1)

A) Analysis MW vs cLogD

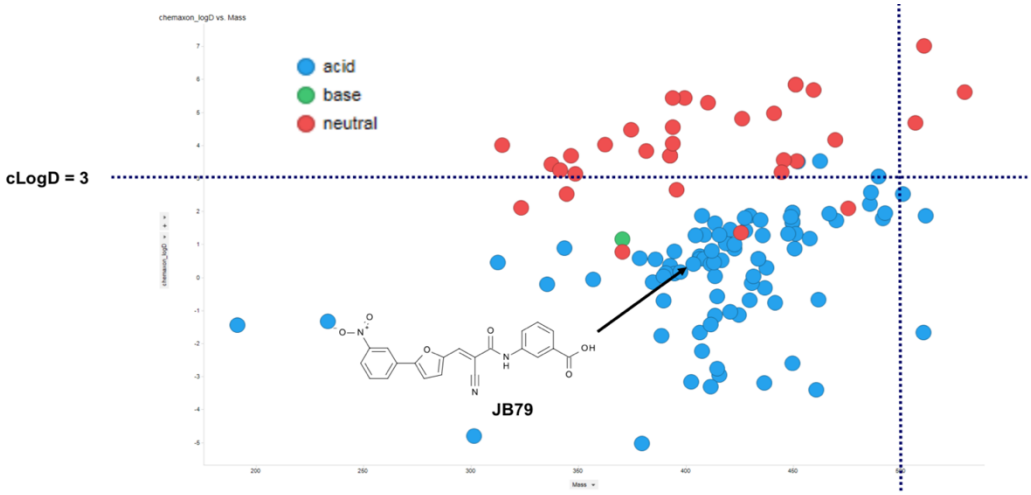

B) Analysis MW vs PSA

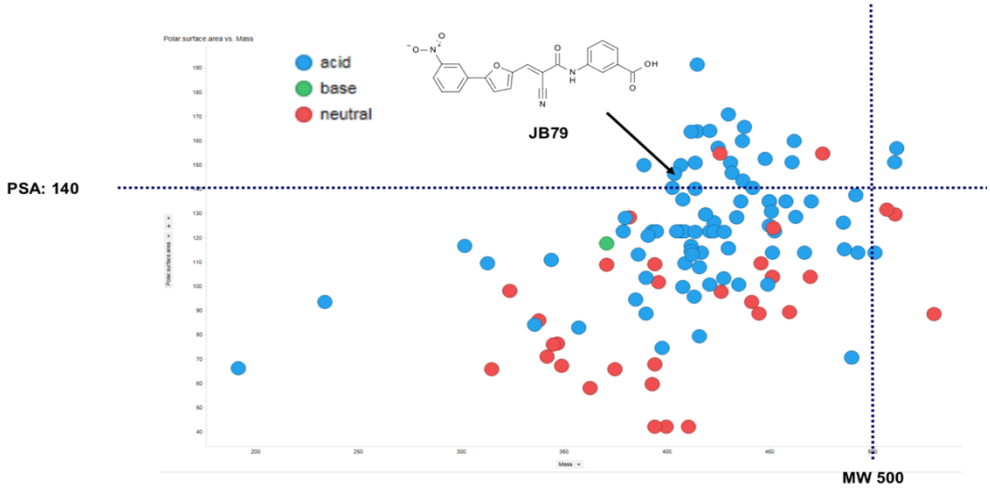

C) Analysis of PAINS

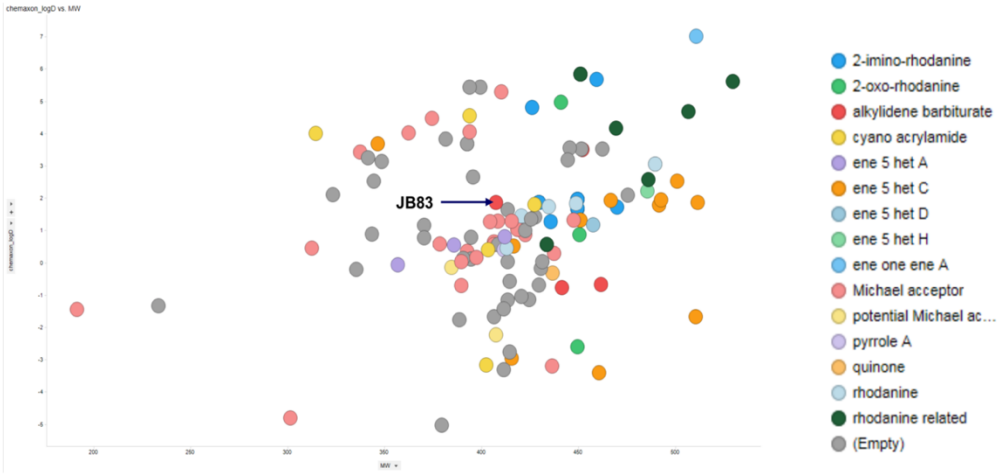

Figure 6.2.1 *Comparative analysis of MW vs cLogD, PSA, and PAINS.* ChemAxon program and Evotec internal compound profile filtration were applied in order to compare the physiochemical profiles of *in silico* designed JB compounds. Many of compounds that have been confirmed to stimulate intrinsic PAK1 activity was found to contain high PSA and low lipophilicity, indicative of poor 'druglike' properties.

Based on the cLogD of many of these chemicals, 68% of JB compounds were shown to contain benzoic acids (e.g. calculated pKa for JB79:3.92). Therefore, one possible mechanism of PAK1 activator was through forming a salt bond with basic residues adjacent to the AID of PAK1 and thereby interrupting the dimer formation. PSA analysis of the current compounds also displayed high polar surface area which may interfere with the cell membrane permeability. Finally compounds with Michael acceptors and cyano acrylamide were concerned for their chemical moieties for PAINS. These moieties have been indicated to cause irreversible binding to their cysteine residue and potential to cause toxicity in cell. That being said, some drugs that contain cyano acrylamide moiety have been approved for therapeutic usage. For example, AG490 (Tyrphostin) is the first small molecular JAK2 inhibitor that is clinically used as an anticancer agent and is also effective in various models of inflammatory and autoimmune diseases. AG490 works through forming covalent modifications at the kinase domain, thereby permanently interfering with the protein activity. Compounds containing the acrylamide, therefore, does not determine their potentiality to become candidate drug, but plausible side-effect on ADMET should be considered with caution.

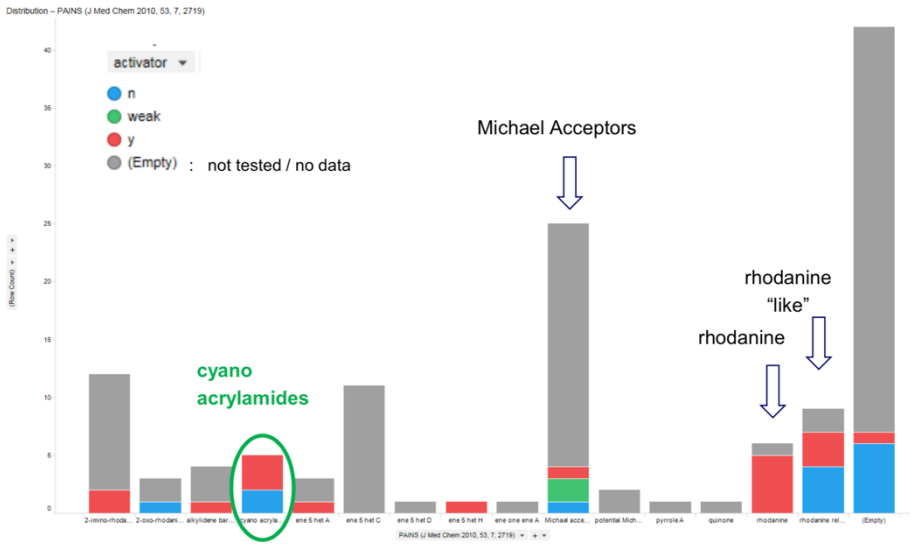

Figure 6.2.2 *PAINS and Micheal acceptors in JB compounds.* Majority of compounds that were shown to activate PAK1 contained either cyano acrylamide or rhodamine groups which were potential concerns for DMPK properties and PAINS. A large portion of the any of the designed compounds from the library were shown to contain micheal acceptors which could potentially cause covalent modifications. Each color represents the state of compounds: strong activators (●), weak activators (●), no activators (●) or no available data (●).

In addition to having poor indications of JB compounds' physiochemical profiles, many of the compounds still had not been physically tested *in vitro* settings, as most compounds were intially designed for *in silico* optimization. Of the number of PAK1 activators that we were able to synthesize and test *in vitro* assays, most compounds have been confirmed to have significant activation effect on PAK1 (Chapter 3). The number of confirmed PAK1 activators were sufficient to validate in potential selectivity of the compounds to PAK1 as well as to minimally explore SAR. However, this was not enough analogues to fully understand the chemical properties of the ligand binding site. Therefore, in collaboration with Evotec, we have optimized several different analogues of PAK1 small molecules in effort to improve the overall physiochemical properties, as well as its affinity towards the active site. Total of 89 new compounds were synthesized from Evotec and were incorporated to the newly organized JB compound lists (see Appendix 3).

The main purpose of the optimization was to improve its affinity and physiochemical properties (specifically, its solubility and permeability). A subset batch of compounds were tested, and results of these compounds were directly presented to the medicinal chemists' team. Bi-weekly meetings were made to ensure that they were able to work with the most updated information available and able to make subsequent modification to next analogues. As RF-MS Kinase assay were determined to be the most accurate and fast screening methods of detecting the stimulatory effect of JB compounds, this was used as a main validation assay to confirm PAK1 activity. The results of the dose response test assays are shown in Appendix 4.

Previous results of JB compounds were integrated with the newly develop JB compounds. Majority of other analogues surrounding the functional groups of the compounds were specifically modified in order to understand the SAR. Taking JB79 lead compound as an example (see Figure 6.2.4), JB60 and JB81 were developed, however, found not to have any stimulatory effect in activating PAK1. While substituting the nitro group with ortho positioned carboxylic group were found to reduce the stimulatory effect. JB93 does not contain the nitro group but having a halogen group were found to still maintain the stimulatory effect of JB compounds, indicating that the having a nucleophilic groups at the meta position of the left-side aromatic ring may be advantage for stimulating PAK1. From the collaborative work with Evotec, compounds such as JB60, JB81, JB80, JB93 analogues of JB79 compounds were synthesized to expand our current interpretation of the SAR.

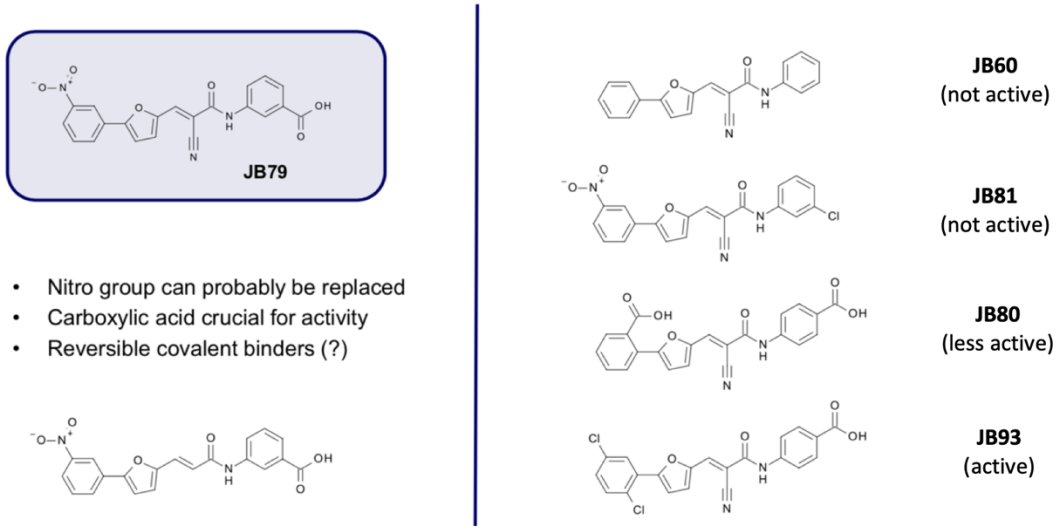

Figure 6.2.3 *Structure activity relationship (SAR) of JB79 compound and its analogs.* Phenyl, furan, linker (core), and aniline groups were substituted with listed functional moieties. By comparing their efficacy in PAK1 activation, effects of each substitution were measured, and overall SAR were examined. These SAR studies were found to be

On the left-hand side group (R1), having a strong electron withdrawing group at the para position were found to provide the highest stimulatory effect on PAK1. Carboxylic acid groups were found to be more activating in comparison to relatively weaker groups, such as the ester COOR. The relative length of the compound was also found to be essential for maintaining stimulatory effect in PAK1. For example, JB86 (EOAI3950723) contains one carbene shortage in comparison to JB113 (EOAI3952635), however, JB86 was shown to cause inhibition of

PAK1 activity, even though JB113 was causing significant increase in PAK1 activity. Observing the activation effect of JB114 (EOAI3951313) also demonstrates that extending the compound by a methylene increases the stimulatory effect of the activators.

EOAI No	R	Total activity @ 20 uM (% normalised)
3952635	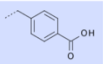	1537
3951313	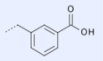	433
3950720	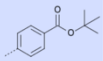	388
3950717	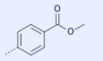	185
3951310	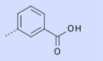	172
3950723	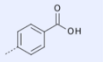	inhibition

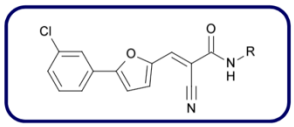

- extending the linker (methylene) increases activity
- esters are tolerated!

matched molecular pairs on next slide

On the right-hand side of the compound, the nitro group was found to be not too crucial in conferring the stimulatory effect of PAK1. Using similar pharmacophore groups, compounds such as JB102 (EOAI3950716) were shown to still be able to significantly activation PAK1. Halogen substitutions also illustrated that ortho- and para- positions more favorable in producing its efficacy than the meta-positioned groups. As nitro groups were often reported to cause hepatoxicity, replacing the nitro group with another lesser deactivating group were found to be more favorable towards improving the physiochemical profiles of the activators.

EOAI No	R	Total activity @ 20 uM (% normalised)	curve
3952639		1132	not complete
3952640		549	not complete
3951311	 JB79	281	"sigmoidal"
3950716		263	"sigmoidal"
3953455		180	no
3951310		164	"sigmoidal"
3951309		140	no

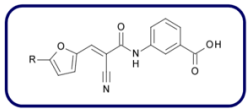

- replacement of nitro group is possible

SAR information obtained from the optimization and *in vitro* testing allowed us to further understand the interaction between the small molecule activators and PAK1. Through mapping the overall structure of the ligand and listing which functional groups were still able to tolerate the substitution, we can explore other possibility of ligand optimization and improve the overall compound efficacy and profiles (see Figure 6.2.6). By understanding which functional groups can be replaced and which position of the group it confers the most activity, we can selective choose which functional groups to incorporate that may confer optimal activity, while ameliorating the physiochemical profiles.

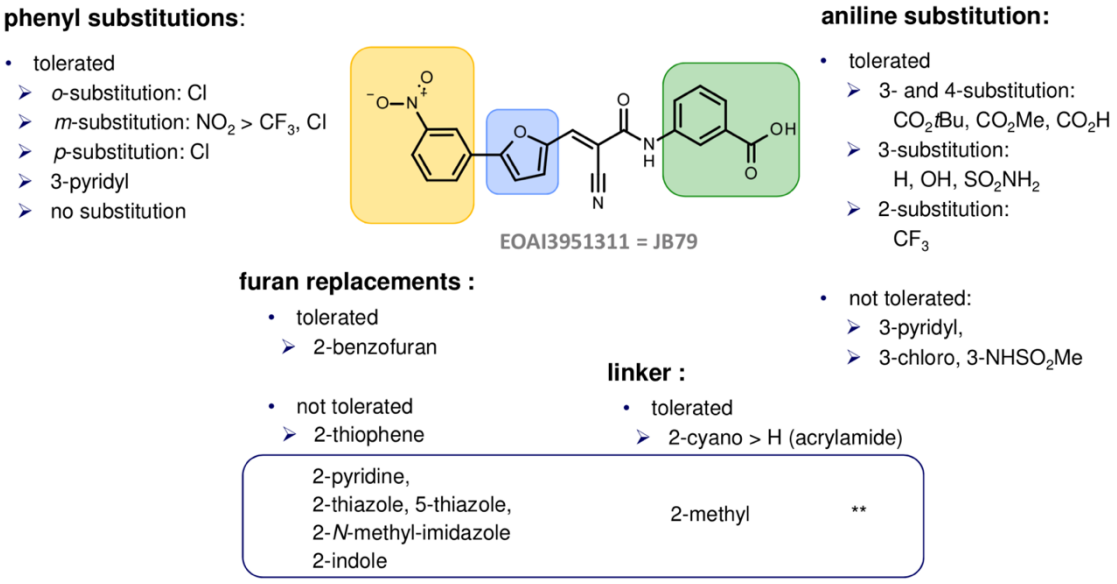

Figure 6.2.4 *Structure activity relationship (SAR) of JB79 compound Overview.* Phenyl, furan, linker (core), and aniline groups were substituted with listed functional moieties. By comparing their efficacy in PAK1 activation, effects of each substitution were measured, and overall SAR were examined. These SAR studies were found to be crucial in optimizing for current lead compounds and improving the physiochemical profiles of the PAK1 activators.

In addition to changing the surrounding functional groups of compounds, replacement of the core group was also considered in order to substitute for the acrylonitrile core. In animals and fetus, these compounds were shown to have carcinogen, embryotoxicity and teratogenic properties. Acrylonitrile exposure in humans, some reports of slight excess of deaths from lung cancers and other malignant tumors were found, however, many epidemiological studies in were shown to be inconclusive (Butcher and Peter, 1984). To ensure to minimize any potential toxicity of the compound effect, the replacement for the core groups were also consider during

the optimization process (see Figure 6.2.7). As demonstrated by the example compounds below, five different core groups were tested while containing similar pharmacophore properties. Based on the RF-MS Kinase assays, some compounds activity was still retained even after the 'Knoevenagel core' groups were replaced. Amongst these different core groups, the amide core group were shown to confer the highest stimulatory effect in PAK1 activation, while significantly reducing with the MW and TPSA. Removing the nitrile and the carboxylic acid moiety were also shown to lower the melting point and improve its aqueous solubility. The priority idea of this optimization was to create a compound that contains better chemical properties.

ID	Structure	MW	cLogP	cLogD	TPSA
EOAI3953458	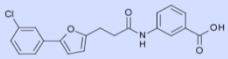	370	4.2	1.0	80
EOAI3957213	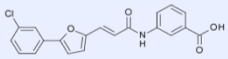	368	4.5	1.3	80
EOAI3957210	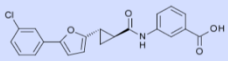	381	4.2	1.0	80
EOAI3953453	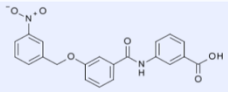	392	4.2	1.0	119
20,444	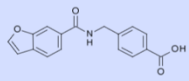	295	2.6	- 0.5	80

EOAI No	Structure	Total activity @ 20 uM (% normalised)	Total activity @ 40 uM (% normalised)	MW	cLogP	TPSA
3951310	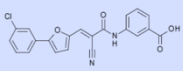	172	164	393	4.3	103
3957213	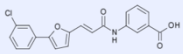	598	345	368	4.5	80
3957210*	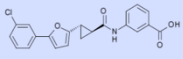	154	339	381	4.2	80
3953458	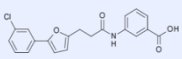	154	218	370	4.2	80

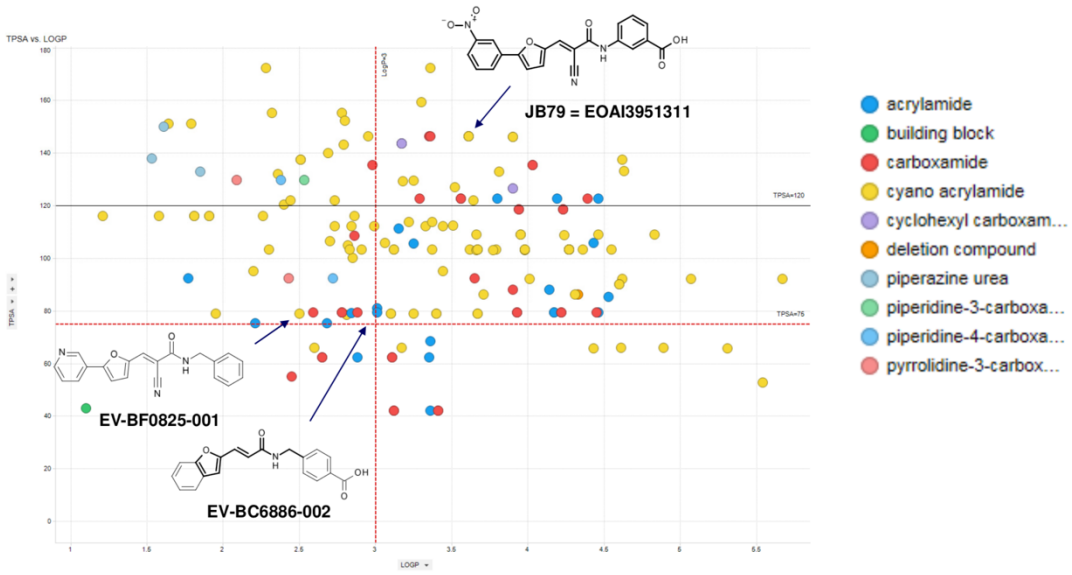

Figure 6.2.5 *Effects of core group changes on physiochemical and efficacy of PAK1 activators.* Previous acrylamide core group of JB79 were substituted to test for their efficacy in PAK1 stimulation. These core substitutions were exhibited to contain higher efficacy as well as improved physiochemical profiles, in comparison to those of JB79 properties. MW, molecular weight; cLogP, partition coefficient; cLogD, distribution coefficient; TPSA, total polar surface area.

Majority of the compounds which have been tested for *in vitro* kinase assay were sent for DMPK studies (results can be provided upon request). Unfortunately, not all compounds were profiled due to either calibration issues or technical errors. However, of the ones with promising efficacy and improved properties were successfully examined. After a careful analysis, comparing both their efficacies and DMPK results, the final chosen lead compounds from the optimization process were JB124, JB120 and JB131. All three compounds showed significant improvement in their ability to stimulate PAK1 activity; at 5uM concentration, their percentage activations were 848, 389, 353%, respectively. The lipophilicity (cLogD) were measured to have notably increased in comparison to the value from the previous lead compound (JB79), 0.40. TPSA was also significantly decreased, illustrating potential capability of the compound's permeability to membrane. Finally, both the melting point and the MW of the compounds became substantiality reduced, overall demonstrating characteristics that are more druglike. Comparison summary table is illustrated below (Figure). Although we weren't successful in reducing the affinity of the compounds (EC_{50}) towards the nanomolar concentration, we were able to make substantial improvement in the compound physiochemical profiles, enabling us to carry the therapeutic functional examinations and the next phase of biophysical studies.

	Previous Lead Compound	Optimized Compounds (LAB282)		
	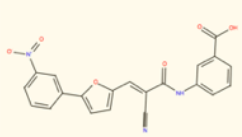	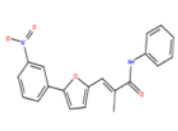	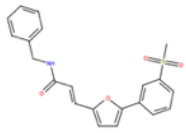	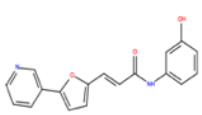
EOAI No	3951311 (JB79)	3958378 (JB124)	3959595 (JB120)	3959587 (JB131)
cLogD /MW/TPSA	0.40/403/146	4.53/348/85	2.75/381/76	2.67/306/75
PAK1 EC50 (uM)	7~10	5	5	11
%PAK1 activation 5uM	185	848 (4.6-Fold)	389 (2.2-fold)	353 (1.9-fold)
%PAK1 activation 10uM	256	1133	1074	433
%PAK1 activation 20uM	281	1411	827	1063
%PAK1 activation 40uM	289	934	394	2070
Aqueous Solubility (uM)	Poor Calibration curve	240.6	19.8	71.3
eLogD	1.04	4.50	3.02	3.28
h Mic $t_{1/2}$	Solubility Issues	25	32	17
Melting Point (°C)	> 300	200	Glass/foam	220

Figure 6.2.6 *Optimization results of JB79.* Three new lead compounds were generated through the optimization process: JB124, JB120, and JB131. These compounds expressed higher fold increase in PAK1 activity, higher solubility, lipophilicity, and better stabilization in plasma in comparison to those properties of JB79 compound.

6.3 Ligand Binding Study: Photoaffinity Labeling (PAL) – MS

Identifying the binding site of biologically active small-molecules is often the rate-determining step in drug developments. Through understanding where the ligand interacts on the targeted protein, we can optimize the lead compound to improve its affinity and to develop favorable physiochemical properties. The ligand-protein interaction can also help us to comprehend the mechanism of action, allowing us to use the SAR to help us find other potential analogues or novel kinase activators. Other studies such as quantitative structure-activity relationship (QSAR) can be done without having identified the binding site, however, this was suggested to be difficult for PAK1 small molecule activators based on the previous ligand optimization process. Other biochemical technique such as isothermal titration calorimetry (ITC), and surface plasmon resonance (SPR) are available to confirm the ligand protein binding interactions, however, these assays do not provide sufficient information about the ligand-protein interaction site. Other biochemical assays were, therefore, so that the binding site for JB compound could be determined and use this information to make candidate compounds with high affinity.

X-ray co-crystallography is considered as the gold standard for identifying the binding site of ligand-protein interaction. Not only does it provide the active site of the compound, but it also reveals the orientation in which the ligand is bound. This allows us to see which of the amino acids that are essential for interreacting with the ligand and obtain the whole 3D structure of the ligand-protein complex. Despite the advantages of using co-crystallography, the application of x-ray crystallography involves high resources and costs. There is also no necessary guarantee that the proteins will be crystallized in which the crystal structures will be examinable. Therefore, before committing to doing the co-crystallography, we needed a preliminary assay to ensure that the ligand is binding specifically to PAK1 and that we have an approximate estimate of where the ligand-binding site is. To study this molecular interaction, we used a photo-affinity labeling (PAL) coupled to mass spectrometry (PAL-MS).

In photo-affinity labeling, the technique involves using an analog of a biologically active small-molecule, known as a photo-affinity probe, that bears photo-reactive and functional reporter groups. The photo-affinity probe is usually designed and synthesized based on the SAR (structure-activity relationships) of a parent small-molecule, having obtained its biological response to PAK1 activation. When a ligand possessing a UV-photoactivating group is incubated with its targeted protein, ligand will initially form a noncovalently-bound-ligand-receptor complex. The initial binding to the protein is based solely on the specificity and affinity to the binding pocket. However, upon UV irradiation, the high energy triggers activation of the nucleophile (of the photoactivating group of the ligand) and leads to the conversion of the noncovalent binding into a covalent link between the ligand and its receptor at the binding site. The covalent ligand-protein makes the study of the ligand interaction easier as it prevents dissociation between the ligand and the protein. This tolerates the usage of aggressive identification methods, e.g. protein digestion or SDS-PAGE, which can be used to breakdown the proteins into segmental peptides and use a mass-spectrometry to determine the covalently modified MW. The application of PAL-MS has been highly successful and been recognized now as a common approach for understanding 3D ligand-protein complex allowing us to investigate the ligand binding region. Ultimately, this structural proteomics can provide valuable information about the molecular modeling and structure-based drug designing.

For the development of PAK1 small molecule activators, we used two of the lead compounds JB120 in order to redesign the ligand with PAL. Three types of photoactivating probes are commonly used for photoaffinity labeling: azido groups, benzophenone groups and diazirenes (Robinette et al., 2006). For JB compounds, it was recommended by the medicinal chemistry group that diazirenes were considered to be the suitable photoaffinity label. Hence, using JB120 compound as the parent compound, three new PAL probes were designed and synthesized: JB119, JB121, and JB122 (Figure 6.3). The position of the PAL groups was focused based on the preliminary SAR studies discussed in Chapter 5. The SAR study revealed that high polar groups at the meta- and para-positions were shown to improve PAK1 stimulations. Hence, these two different ligands were based on this design and were added to para and meta accordingly.

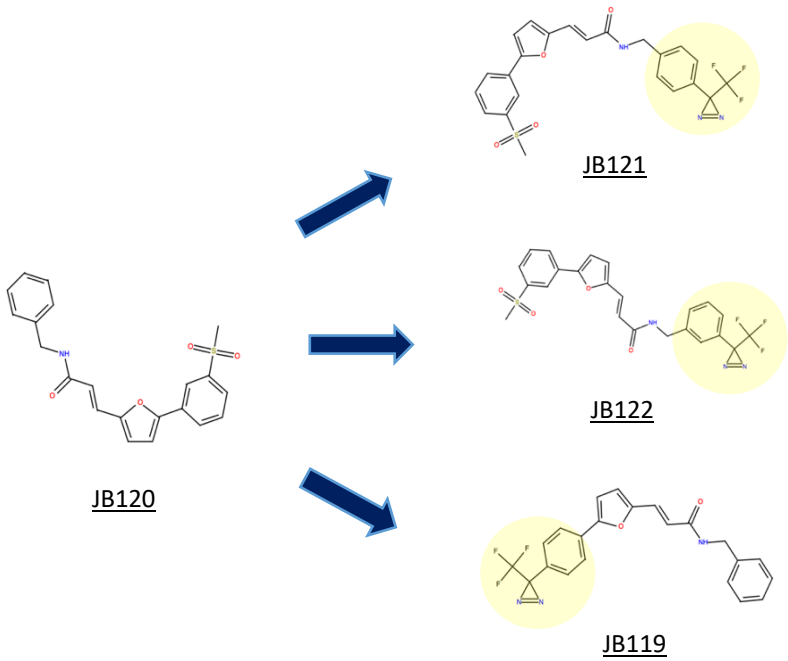

Figure 6.3.1 *Photoaffinity labelling ligands of JB120.* Diazine photoaffinity labels were incorporated to the JB120 in effort to understand the ligand-protein interaction site. UV radiation causes the photoaffinity label group to become activated and form covalent modification to the nearby residues, allowing us to identify where the interacting binding sites are. Three ligands (JB119, JB122, and JB121) with PAL were created for the PAL-MS coupled assays.

It is important to establish that the incorporated photoactivating groups does not significantly alter the binding affinity of the ligand and its functionality, compared with the nonderivatized ligand. In order to ensure this, we used the RF-MS kinase assay to reconfirm the efficacy of the ligand in stimulating PAK1 before performing the PAL-MS studies. The results of the kinase assays are shown as below:

A) JB120

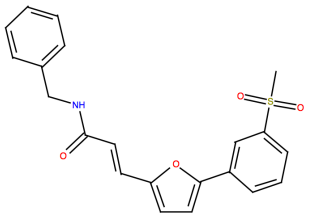

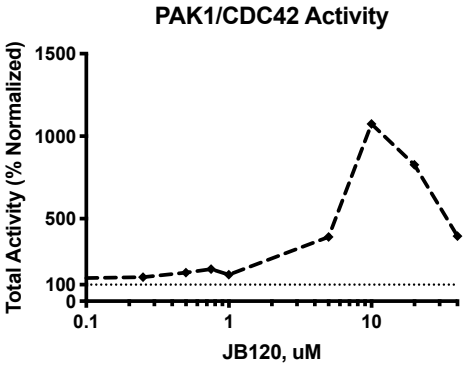

B) JB119

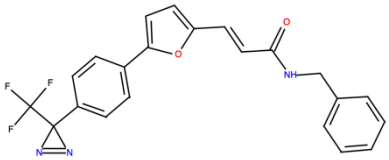

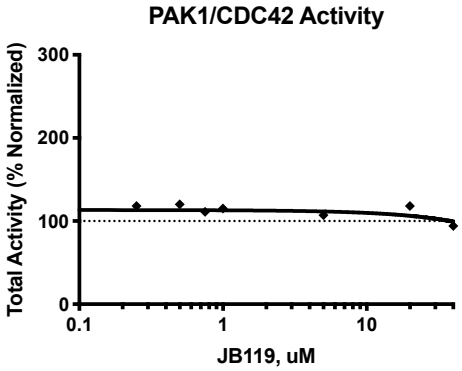

C) JB121

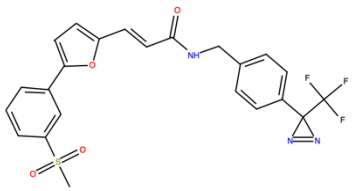

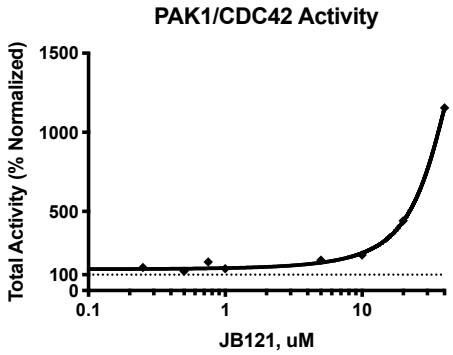

D) JB122

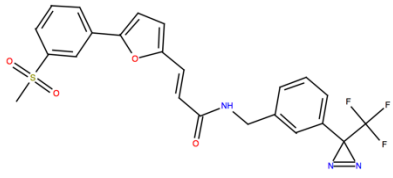

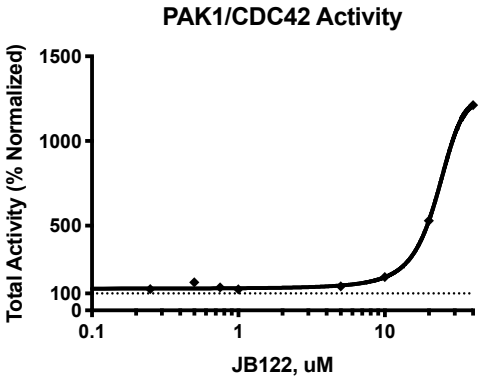

Figure 6.3.2 *Dose response test on PAK1 activity by PAL probes.* Diazine photoaffinity labels were incorporated to the JB120 and RF-MS Kinase assay was used to measure the stimulatory effect of PAK1 activation. JB121 and JB122 shows significant activation effect on PAK1, while JB199 failed to show any stimulatory effect the kinase.

The RF-MS kinase assay results showed that by adding the diazine photo affinity group to JB120, it did not cause significant effect on the compounds' ability to stimulate PAK1. For both labelled JB121 and JB122 compounds, they showed significant stimulation on PAK1 activation (showing highest measured PAK1 activity of 1120% and 1080%, respectively). Unfortunately, JB199 did not show any activation effect on PAK1, indicating that modifying the methylsulfonylmethane group may affect the affinity of the ligand binding. The high efficacies of JB121 and JB122 compounds, on the other hand, were similar to what was observed with JB120, except its maximum activity was measured to be at a lower concentration than those of JB121 and JB122; for JB120, maximum activation was observed at 10uM. This suggests that the addition of the photo affinity may have reduced the affinity of the ligands to PAK1 and therefore shifting the dose response curve more towards right. Testing at higher concentration is required to confirm whether the maximum efficacy of the labelled compounds have changed or not. Nevertheless, having confirmed that the PAL probes still maintained its efficacy validated that the molecules are binding to PAK1 and this can be used to label the ligand interacting residues.

Having confirmed that the added photo affinity label does not interfere with the compound ability to activate PAK1 activity, the compounds were sent for PAL-MS studies. The general workflow for PAL-MS are described in Figure 6.3.3. Due to the importance of CDC42 in potentially increasing the affinity of the compound binding, another condition was added to introduce CDC42 in addition to the PAK1 FL alone. A competitor compound was also tested to assess the specificity of the PAL probe and to ensure that there was no false positive reading from the PAL (negative control). After three hours of the incubation with the compounds, diazine photolabeling group were activated through irradiation and digested for peptide analysis.

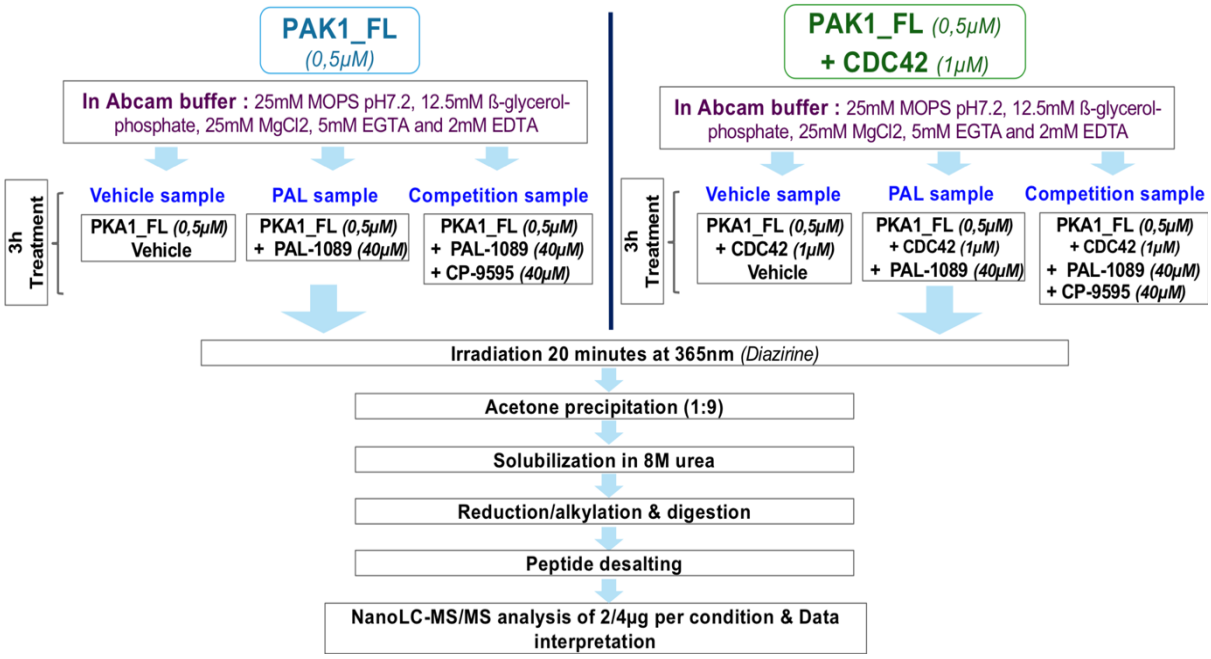

Figure 6.3.3 *PAL-MS Workflow using JB122.* Diazine photoaffinity labels were incorporated to the JB120 to allow the covalent modification to occur once the UV radiation treatments were gvein. The figure above provides the working plans for the PAL-MS study on PAK1. PAL-1089 is JB122, and CP-9595 is the parent compounds, JB120, in order to measure the competition between the two ligands.

The automatic peptide sequencing was achieved using the MaxQuant Software. MaxQuant is a quantitative proteomics software package designed for analyzing large mass-spectrometric data sets. The criteria that was used for the detection of peptides with an unknown modification was with a DP Score >60 and mass error tolerance < 6ppm. For PAK1 treated with JB122, there were four modified peptides with ΔM mass shift corresponding to JB122 (461.09086 Da) (see Figure 6.3.3). From the MS results, we can see that there was much higher abundance of the five specific peptides which exhibited mass shift corresponding to PAL-1089-N_2. The dynamic programming (DP) score directly count the number of peptides occurring at each score in the distribution. Hence, the higher the DP score, the higher the abundance of the specific peptides. In comparison to the compound treated PAK1, the five peptides were not detectable in control samples. Furthermore, the five peptides were less abundant under the presence of the competitor JB120, indicating competitive antagonism to the PAL. These results confirm that the peptide mass shift by the covalent modification is evident by the PAL probe compound.

Peptide sequence	Δm mass shift	DP Score
ECLQALEFLHSNQVIHR	461.09134 Da (1ppm)	182
ECLQALEFLHSNQVIHR	461.09263 Da (3.8ppm)	182
KELIINEILVMR	461.08820 Da (5.7ppm)	146
KNPQAVLDVLEFYNSK	461.09191 Da (2.3ppm)	163
YMSFTDK	461.08884 Da (4.3ppm)	69

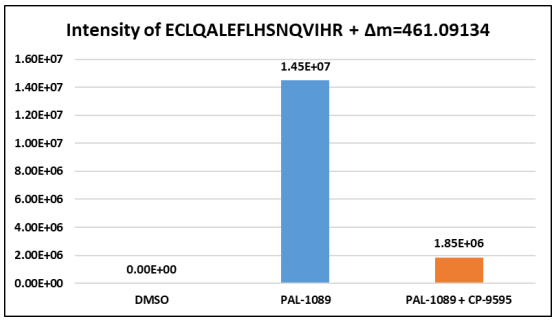

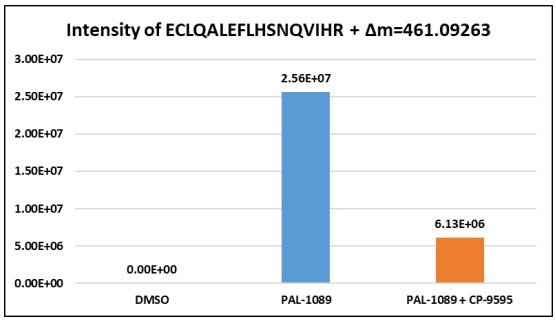

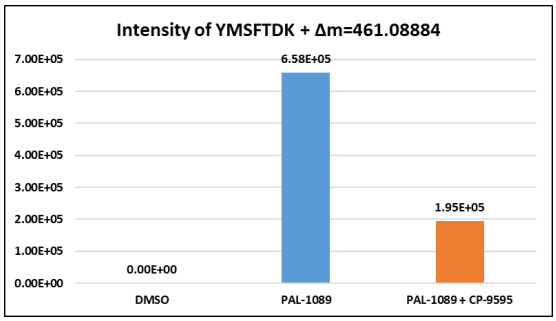

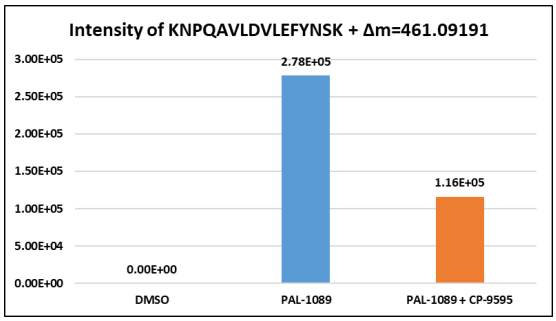

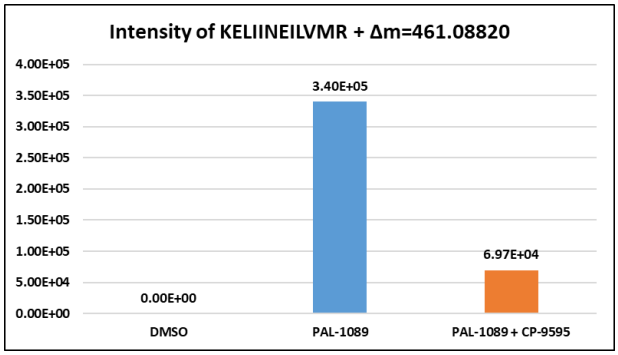

Figure 6.3.4 *Analysis of PAL-MS peptide with JB122.* A) Peptides following digestion were subjected to liquid chromatography-mass spectrometry, and sequence was obtained. Peptide sequences with following mass shifts according to the MW of the photoaffinity label probes (MW: 461.088 g/mol) were detected and modified residues were identified. DP score correlates the abundance of peptide amount in corresponding to a specific sequence. B) Competitive assay between the probe and the parent compound. Reduction of peptide intensity confirms competitive antagonism, which shows the specificity of the compound binding site.

When PAK1 was co-incubated with CDC42, on the other hand, the mass spectrometry results only showed three modified peptides which corresponded to the MW of PAL-1089-N_2 (461.09086 Da):

Peptide sequence	Δm mass shift	DP Score
ECLQALEFLHSNQVIHR	461.09003 Da (2ppm)	192
KELIINEILVMR	461.09256 Da (3.8ppm)	166
KELIINEILVMR	461.08948 Da (2.2ppm)	130

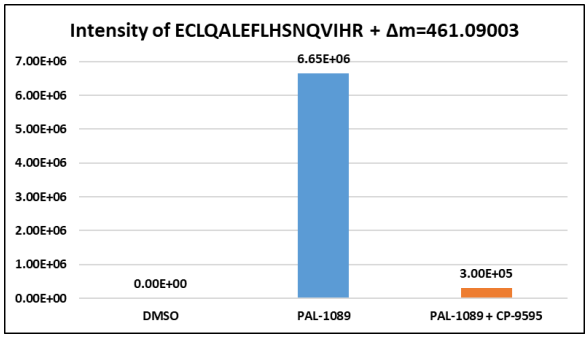

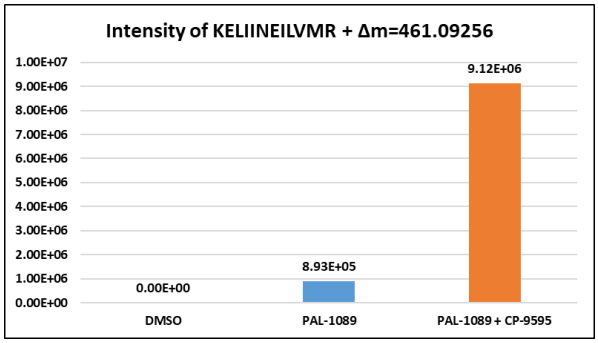

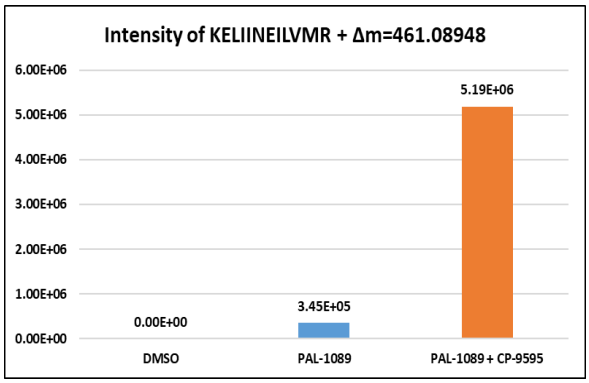

Figure 6.3.5 *Analysis of PAL-MS peptide with JB122, under the presence of CDC42.* A) Peptides following digestion were subjected to liquid chromatography-mass spectrometry, and sequence was obtained. Peptide sequences with following mass shifts according to the MW of the photoaffinity label probes (MW: 461.088 g/mol) were detected and modified residues were identified. DP score correlates the abundance of peptide amount in corresponding to a specific sequence. B) Competitive assay between the probe and the parent compound. Reduction of peptide intensity confirms competitive antagonism, which proves the same binding site between the two compounds.

Three interesting remarks could be observed from the PAK1 + CDC42 mass spectrometry results. Firstly, only three peptides (ECLQALEFLHSNQVIHR and KELIINEILVMR) were indicated to have the MW shifts, instead of four peptides that was previously observed with PAK1 MS results. Such difference in the peptide modifications could suggest different conformation of PAK1 due to the interaction with CDC42, which may alter PAL's binding affinity. Having differences in the amount of modified peptides (based on the results of the DP scores) indicate that there has been a change in the selectivity of the ligand due to the PAK1 conformational changes induced by CDC42. As we have previously seen from *in vitro* kinase assays that CDC42 promotes significant increase in PAK1 stimulation, ligand-binding site at these two peptide regions could be the key for the mechanism of the compound in regulating the PAK1 activity. Finally, another curious observation was measured when the PAL probe was in a competitive assay with its parent compound. The competing ligand is the parent

compound of the PAL probe; thus, it contained the same chemical structure as that of the PAL probe but lacked the diazine photoaffinity group. Through kinase assays, we had confirmed that both the parent and the probe compounds were able to stimulate PAK1 significantly, suggesting that these compounds were likely to bind to the similar binding site. Therefore, when the parent compounds were present, it would compete with the same binding site as the PAL probe and interfere with the photo affinity labeling. This is illustrated in Figure 6.3.3, where significantly reduced mass shift of peptides was observed when the competitive compound was co-incubated with the PAL probe. Such confirmation is crucial as it demonstrates that the PAL and the parent compounds are binding at the same site and that the mass shift of the detected peptides are the likely regions where the compound efficacy is produced. When PAK1 and CDC42 are co incubated, the labeled peptide ECLQALEFLHSNQVIHR was less abundant in the presence of the competitor JB120 indicating that the incorporation of PAL-1089 into the peptides was prevented by JB120. For peptide KELIINEILVMR, on the other hand, higher number of peptide modifications were observed when the reaction was co-incubated with the parent compound. This was quite a contrasting result as we had expected that the peptide modifications are less likely to occur due to the competitive antagonism. Instead, higher abundance of the peptide mass shifts was occurred when the parent compounds are present. One possible explanation for such results could be that the CDC42 promote conformational changes that uniquely shows a novel allosteric site where the parent compound may have higher affinity towards. Upon binding of the parent compound, it further allows conformational changes to PAK1 which in turn allows for the KELIINEILVMR peptide region to be more exposed for PAL probe binding and cause covalent modifications. Further kinetic studies may be interesting to see whether or not, the binding affinity changes for the PAL probe when CDC42 is present. However, these PAL-MS results demonstrate difference in the PAL prob mechanism when CDC42 is present, which may explain for the difference in the efficacy of the compounds in PAK1 activation. Upon further analysis, we were able to locate the list of modified peptides on PAK1-FL sequence and look for any plausible indication of its mechanism of action (See Figure 6.3.5).

PAK1

ECLQALEFLHSNQVIHR
ECLQALEFLHSNQVIHR
KELIINEILVMR
KNPQAVLDVLEFYNSK
YMSFTDK

PAK1/CDC42

ECLQALEFLHSNQVIHR
KELIINEILVMR
KELIINEILVMR

MSPILGYWKI KGLVQPTRLL LEYLEEKYEE HLYERDEGDK
WRNKKFELGL EFPNLPYYID GDVKLTQSMA IIRYIADKHN
MLGGCPKERA EISMLEGAVL DIRYGVSRIA YSKDFETLKV
DFLSKLPEML KMFEDRLCHK TYLNGDHVTH PDFMLYDALD
VVLYMDPMCL DAFPKLVCFK KRIEAIPQID KYLKSSKYIA
WPLQGWQATF GGGDHPPKSD LVPRGSMSNN GLDIQDKPPA
PPMRNTSTMI GAGSKDAGTL NHGSKPLPPN PEEKKKKDRF
YRSILPGDKT NKKKEKERPE ISLPSDFEHT IHVGFDAVTG
EFTGMPEQWA RLLQTSNITK SEQKKNPQAV LDVLEFYNSK
KTSNSQKYMS FTDKSAEDYN SSNALNVKAV SETPAVPPVS
EDEDDDDDDA TPPPVIAPRP EHTKSVYTRS VIEPLPVTPT
RDVATSPISP TENNTTPPDA LTRNTEKQKK KPKMSDEEIL
EKLRSIVSVG DPKKKYTRFE KIGQGASGTV YTAMDVATGQ
EVAIKQMNLQ QQPKKELIIN EILVMRENKN PNIVNYLDSY
LVGDELWVVM EYLAGGSLTD VVTETCMDEG QIAAVCRECL
QALEFLHSNQ VIHRDIKSDN ILLGMDGSVK LTDFGFCAQI
TPEQSKRSTM VGTPYWMAPE VVTRKAYGPK VDIWSLGIMA
IEMIEGEPPY LNENPLRALY LIATNGTPEL QNPEKLSAIF
RDFLNRCLEM DVEKRGSAKE LLQHQFLKIA KPLSSLTPLI
AAAKEATKNN H

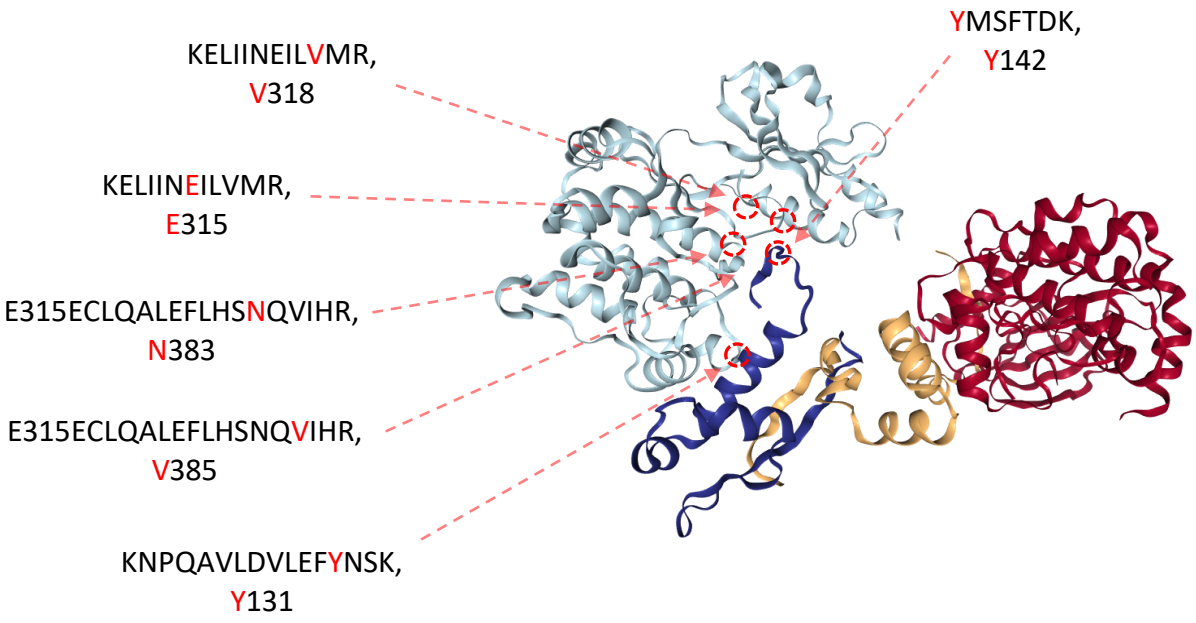

Figure 6.3.6 *Overview map of PAL bound peptides, under the presence or absence of CDC42.* **A)** Representation of the full-length sequence of PAK1 (), highlighted peptides covalently modified with PAL probe (), and GST tag (). The highlighted peptides were located to be at both the autoinhibitory domain (AID) and kinase domain (KD). **B)** 3D crystal structure of PAK1 and locations of PAL modified residues. Most of peptide modifications were found to be at the KI domain of PAK1 and thought to interfere with the kinase domain inhibition, consequently causing activation effect in PAK1. The crystal structure figure was derived from PDB: 1F3M (Lei et al., 2000).

The modified peptides were shown to be located at both the regulatory domain and near the kinase domain. Within the 3D structure of the PAK1 FL, these peptides were shown to form at the interface between the kinase domain and the autoregulatory domain, where the auto-inhibition of the kinase mechanism is regulated (See Figure 6.3.5). Covalent modifications made by the probes were shown to highlight only at this interface between the autoregulatory and the kinase domain. Such region has been previously indicated to be the kinase inhibitory (KI) segment of the AID where the short fragment inhibits the kinase domain and thereby providing an additional mechanism of activity regulations. The KI segment of the autoregulatory fragment has been shown to occupy the cleft between the N-lobe and the C-lobe of the kinase domain (Lei et al., 2000). As indicated by the figure below, Lys141 makes hydrogen bonds with Asp389 of the catalytic loop and Asp407 of the activation loop. Asp389 is the catalytic base in an active kinase. The KI segment (residues 138 to 147) interacts with the activation loop between residues 407 and 413, stabilizing the loop's inhibitory conformation. Lysine 141 projects directly toward the catalytic residues, forming salt bridges with both key aspartates (Asp389 and Asp407). The activation loop is forced to make a turn (407–413), which blocks the contact between Glu315 and K299R and prevents binding of ATP. The arrow indicates the shift in helix C that would be required for it to move to its expected position in an active enzyme. More detailed structural information about the activated conformation of PAK1 can be found in Chapter 1. Finally, Mayhew et al, have previously indicated that the conserved Y131 and Y142 are within the autoinhibitory domain that partially overlaps the CRIB/PBD domain. Y131 is a SRC phosphorylation site in the autoinhibitory domain that regulates the kinase activity of PAK1 (Renkema et al., 2002). Y142 phosphorylation has been also shown to implicate in PDGF receptor binding and may also be involved in regulating kinase activity via modulation of the inhibitory domain (Mayhew et al., 2007). These previous mutagenesis study all indicate that the highlighted amino acids by the PAL prob are essential for regulating the kinase activity. Physical interference through small molecule binding are therefore expected to affect the kinase activity, and this may suggest how the JB compounds were able to significantly stimulate the kinase activity.

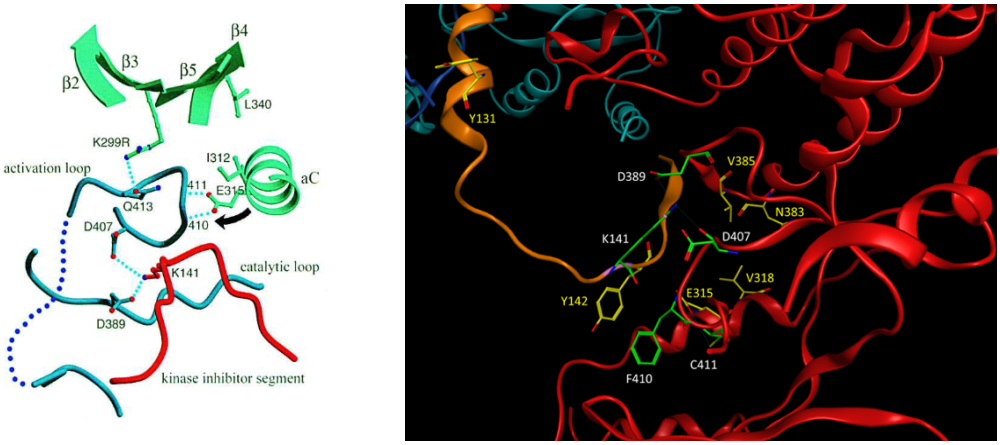

Figure 6.3.7 *Proposing mechanism of JB compounds' PAK1 activation.* **A)** Key residues involved in forming the interaction between the kinase inhibitory segment and the activation loop. The KI segment is thought to stabilize the activation loop's inhibitory conformation (Figure derived from Let et al., 2000). **B)** Modified residues from PAL probes are highlighted to show the interface between the KD and AID. Y131 may likely be position either near the KI interface or may also contribute through inhibiting the dimerization between PAK1 monomers.

Using the PAL-MS approach, we were able to elucidate the topology of the PAK1 binding site of PAL probe. The compound was shown to bind at the interface of the kinase domain and the autoregulatory region of PAK1 kinase inhibitory segment (KI segmnet). In the presence of CDC42, the KI segment of PAK1 was not photo-labelled by the PAL probe. This was probably the result of the PAK1 conformational change induced by CDC42 which withdrew the KI segment from the kinase cleft and released the activation loop. The PAL prob binding might break hydrogen bonds between K141 and D389 of the catalytic loop and D407 of the activation loop and those between E315 of Helix C and F410 and C411 of the activation loop. This might trigger a series of conformational changes allowing for the interaction between E315 (Helix C) and K299R to be restored and allow for the binding of an ATP. In other words, the shift in Helix C by PAL prob binding may trigger a series of conformational changes leading to the rearrangement of the kinase into a catalytically competent state. In the absence of CDC42, however, PAL probe binding may be less frequent on PAK1 as the conformational changes due to CDC42 was found to be significant for exposing the ligand binding site. This may explain why only five different modified peptides were observed for PAK MS, instead three peptides as seen from the PAK1-CDC42 MS analysis. Overall, the PAL-MS provided first proof of evidence on how PAK1 small-molecules are able to stimulate PAK1 activity, through interfering at the kinase inhibitory (KI) domain of the auto-inhibitory (AI) domain of PAK1.

6.4 Co-crystallography: Process update

Previous co-crystallography study was tried using two different constructs Full length PAK1 (FL-PAK1) and PAK1 (His a.a.70-149) + PAK1 (His a.a. 249-545). This project was a collaboration with Proteros, a biomedical company specialized in structural biology. Total of 1,600 different conditions set by Proteros protocol were tried in order to determine the optimal conditions required for crystallization. Despite successful protein purifications and crystallization, only the protein structure of PAK1 (His a.a.70-149) + PAK1 (His a.a. 249-545) could be detected through the x-ray co-crystallography. The ligand was unfortunately not able to be seen through the co-crystallography. To investigate for this cause, we had received the proteins and firstly checked for the protein activity. The protein activity was previously confirmed by Proteros that they were functional, but we were concerned about the quality of the purified protein. Hence, using our optimized RF-MS kinase assay, we tested for PAK1's response to both CDC42 and confirmed PAK1 activating JB compounds. The results of the RF-MS are shown below:

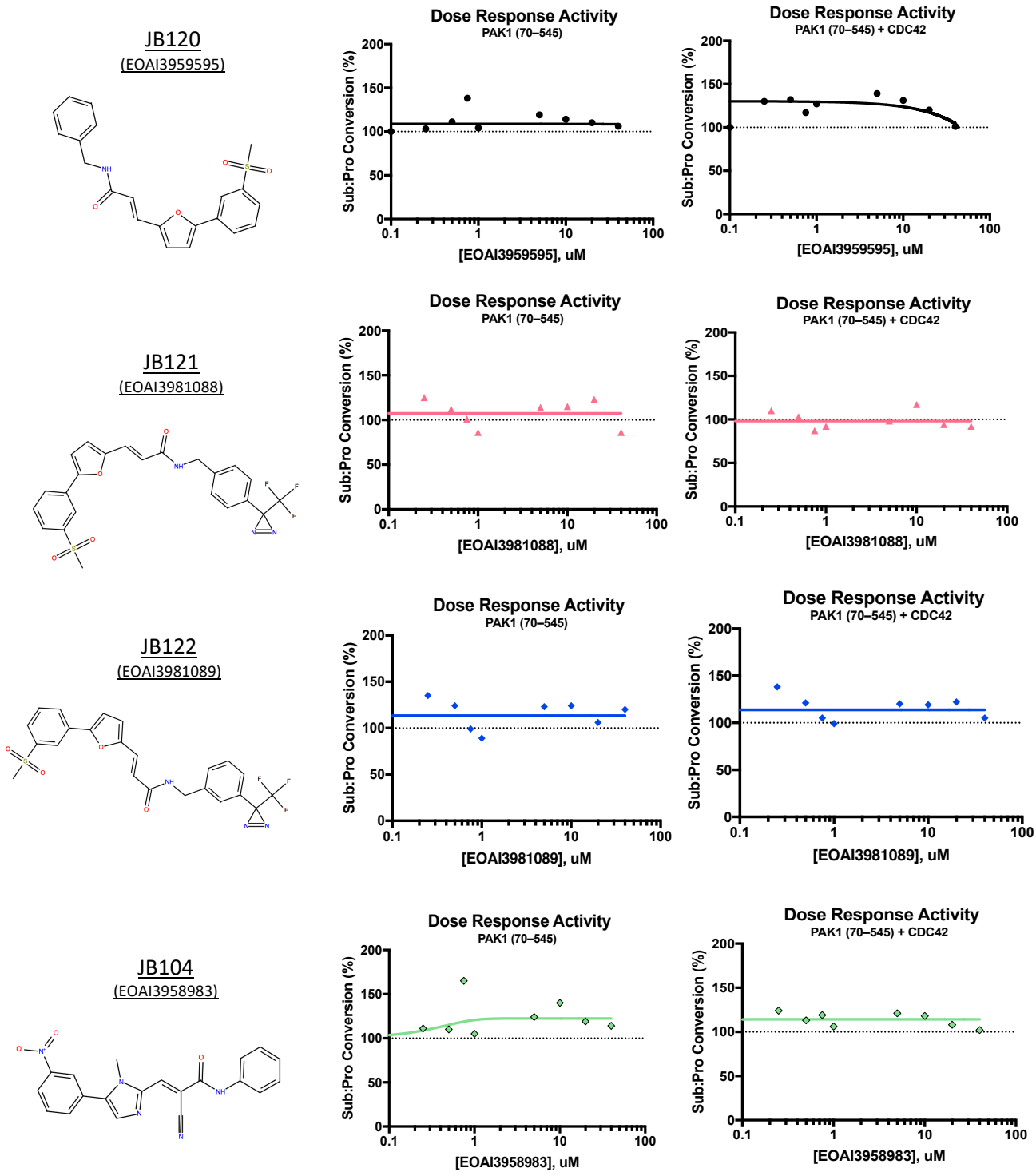

Figure 6.4.1: *Dose response test results of PAL probes measuring the activation of PAK1 (Proteros Ltd.).* Rapid-Fire mass spectrometry kinase assay was used to measure the activation effect of the designed PAL Probes under the presence of PAK1 alone or PAK1&CDC42. Activity was normalized based on the amount of generated phosphorylated substrate by the vehicle (DMSO) treated reaction. Incubation time was set at 30 minutes for all kinase assay. 9 different drug concentrations were examined (0, 0.25, 0.5, 0.75, 1, 5, 10, 20, 40uM) and their direct substrate phosphorylation were measured and plotted using best fit sigmoid curves.

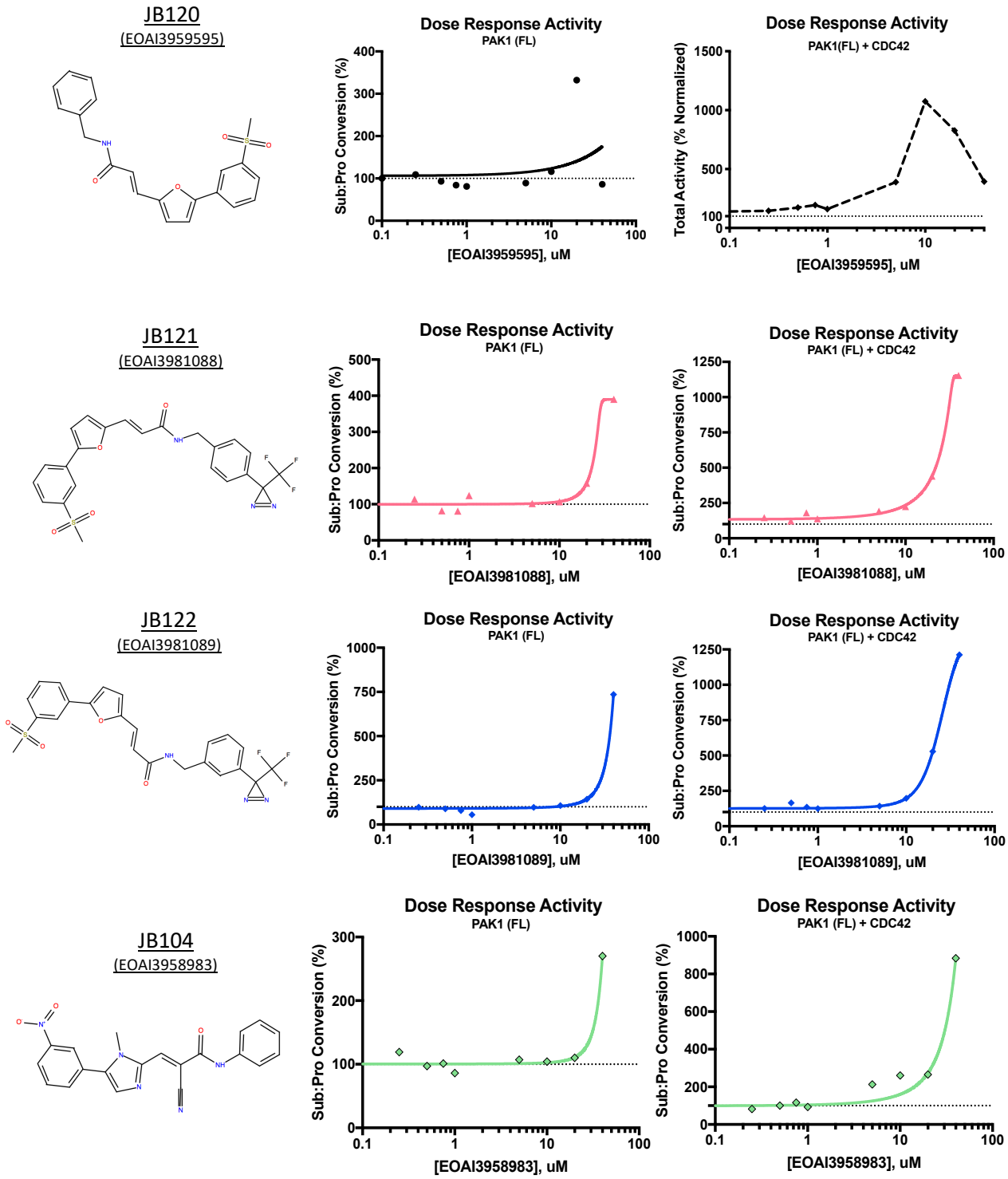

Figure 6.4.2: *Dose response test results of PAL probes measuring the activation of PAK1 (University of Oxford).* Rapid-Fire mass spectrometry kinase assay was used to measure the activation effect of the designed PAL Probes under the presence of PAK1 alone or PAK1&CDC42. Activity was normalized based on the amount of generated phosphorylated substrate by the vehicle (DMSO) treated reaction. Incubation time was set at 30 minutes for all kinase assay. 9 different drug concentrations were examined (0, 0.25, 0.5, 0.75, 1, 5, 10, 20, 40uM) and their direct substrate phosphorylation were measured and plotted using best fit sigmoid curves.

As observed from the RF-MS Kinase assay results, both CDC42 and compounds had no effect on the PAK1 received by Proteros. Through MS the molecular weight of the PAK1 were confirmed to be at its expected size (results not shown), but observing no responses to both CDC42 or JB compound raised concerns as to whether or not, these proteins were active. As a positive control, proteins (purified from Oxford) were tested in parallel conditions with the same conditions, and they exhibited predicted stimulatory effect; the compounds were shown to activate PAK1 activity, and presence of CDC42 had augmented effect of the compounds in PAK1 stimulations (see Figure 6.4.2). These results unfortunately confirmed that the proteins that had been purified from Proteros are not functional. Although these proteins could not be further utilized for other experimental studies, the results also indicate that the cause of not being able to observe the ligand in their co-crystallography was due to the protein's lack of functional activity. As previously indicated by structural studies and our PAL-MS results, the binding affinity of the PAK1 small molecules are highly dependent on the conformational changes that occur through protein activations. Without such protein activation and conformational changes, it is highly likely that the compounds binding site may have not been exposed and consequently not be able to bind to PAK1 with a strong affinity. Hence, we predicted that using functional PAK1 proteins, rather than non-active proteins, would increase our chances of achieving a successful crystallography.

Currently, another attempt at performing co-crystallography using newly purified PAK1 are being in place with the Evotec team. Two different constructs – Full length PAK1 (FL-PAK1) and PAK1 (His a.a.70-149) + PAK1 (His a.a. 249-545) – are currently being purified and tested for their functional activities. Recently, the newly purified FL-PAK1 from Evotec was confirmed to have kinase activity similar that of the FL-PAK1 proteins from Oxford. RF-MS kinase assay were used again to confirm the activity of the proteins (see Figure 6.4.3). PAK1 (His a.a.70-149) + PAK1 (His a.a. 249-545), on the other hand, is still in the process of purification, as the team is having difficulty in connecting the two protein domains together. Overall. three proteins FL-PAK1 (Oxford), Δ70-PAK1 (Oxford) & FL-PAK1 (Evotec) are currently available for the co-crystallization.

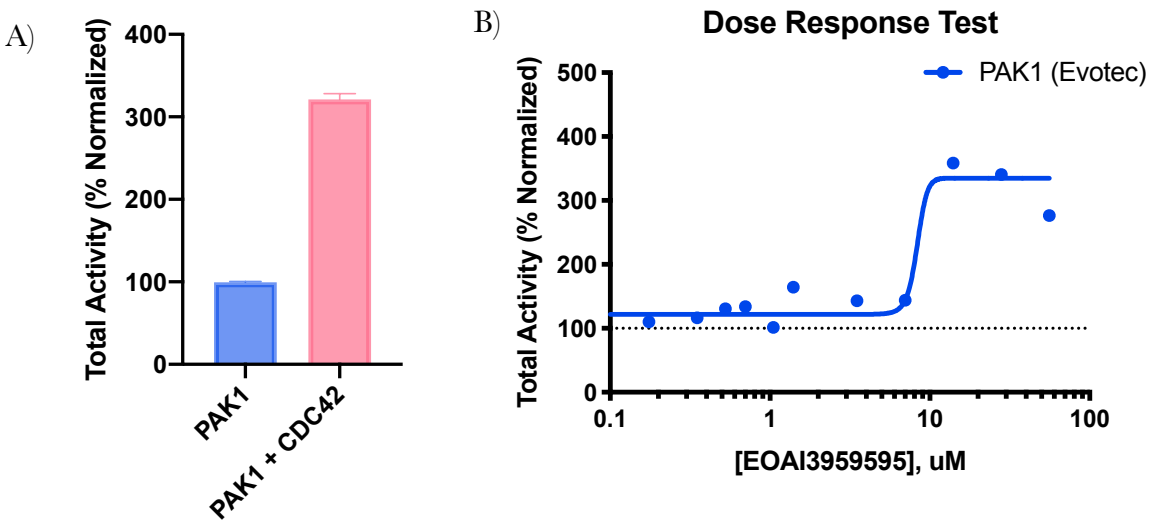

Figure 6.4.3 *Validation of FL-PAK1(Evotec) in response to CDC42 and JB120 compound* **A)** Rapid-Fire mass spectrometry kinase assay was used to measure the activity of PAK1. Total kinase activity was compared between PAK1 alone and PAK1 with CDC42 co-incubation. **B)** Dose response test of JB120 on PAK1 (Evotec) activity. Total activity was normalized based on the amount of generated phosphorylated substrate by the vehicle (DMSO) treated reaction. Incubation time was set at 30 minutes for all kinase assay. 9 different drug concentrations were examined (0, 0.25, 0.5, 0.75, 1, 5, 10, 20, 40uM) and their direct substrate phosphorylation were measured and plotted using best fit sigmoid curves.

6.5 Catecholaminergic polymorphic ventricular tachycardia (CPVT)

CPVT is an inherited arrhythmogenic disease characterized by cardiac electrical instability exacerbated by acute activation of the adrenergic nervous system. It is an autosomal dominant and recessive forms of a rare arrhythmogenic disorder characterized by adrenergic-induced bidirectional and polymorphic (Behere et al., 2016). If untreated, the disease is highly lethal, as approximately 30% of those affected experience at least one cardiac arrest and up to 80% one or more syncopal spells (Napolitano et al., 2016). The true prevalence of CPVT in populations is not known, but it is estimated to be around 1: 10,000 (Napolitano et al., 2016).

CPVT patients contains mutations at the cardiac ryanodine receptor gene (RYR2), an intracellular channel at the SR playing a major role in the regulation of Ca2+ homeostasis in the heart. There is also homozygous missense mutation in the cardiac calsequestrin gene called CASQ2 as the cause of this recessive form, however this form of CPVT is found to be rare (Leenhardt et al., 2012). These CPVT mutations were shown to contain cardiomyocytes that contains calcium leakage from the SR, leading to cytosolic calcium overload generating delayed afterdepolarizations and ventricular arrhythmias (Bhuiyan et al., 2007; Kushnir et al., 201). Genetically modified mice models with CPVT have demonstrated abnormal activity of their Purkinjie cells, leading to Purkinjie origin of the ventricular premature beats resembling those of the human disease (Cerrone et al., 2007). Cardiomyocytes isolated from the CASQ2-null (CASQ2−/−) mice were shown to have significantly increased volume of SR, increased gain of Ca^{2+}-induced SR Ca^{2+} release and increased diastolic SR Ca^{2+} leaks (Knollmann et al. 2006). Despite having understood the pathophysiology of the disease, asymptomatic clinical presentations, as well as lack of effective therapeutic management, make the CPVT patients hard to manage their disease. Patients with CPVT have the absence of either structural heart disease or prolonged QT interval, making it typically hard to detect with current diagnostic methods (Braidwood, & Fitzgerald, 1975). Even if the diagnosis was detected at an early stage, the current therapeutic treatment for CPVT is only β-blockers – with no other pharmacologic therapy, proven effective. Although β-blockers reduce the occurrence of ventricular tachycardia, 30% of patients treated with β-blockers still experience cardiac arrhythmias over

long term follow ups, eventually requiring implantable cardioverter defibrillator implantation to prevent cardiac arrest (Boule et al., 2016). It is also important to note that the concentration of β-blockers given to CPVT patients is at the maximal tolerated concentration. Hence these patients often report fatigue and poor quality in life styles due to significant reduction of cardiac activity. Given no current drugs are effective in providing protection against CPVT, designing a therapeutic drug that can maintain normal Ca^{2+} in CPVT patients may reduce the shock and improve the quality of these patients. If proven effective, PAK1 activator may have the potential to be the first line of therapeutic treatment for CPVT.

To examine whether current optimized small molecule PAK1 activators provide any anti-arrhythmogenesis effect in CPVT, we used similar optimized ex vivo whole heart assay to examine the effect of the lead compound JB131 on CPVT mice hearts. The CPVT mice model that was used for this experiment was the RyR2-V2475F+/+, which the mutation causes the heart to be more vulnerable towards cardiac stress. This mutation is also the same mutation found in actual human CPVT patients, making the experiment more translatable towards human therapeutic than those of animals. The isolated hearts from the CPVT mice were hung onto a Langendorff heart perfusion apparatus, where the oxygenated saline solutions had continuously perfused the heart. The control reading and the effect of acute β-adrenergic stimulations (through isoprenaline injection) are shown as below (see Figure 6.5.1):

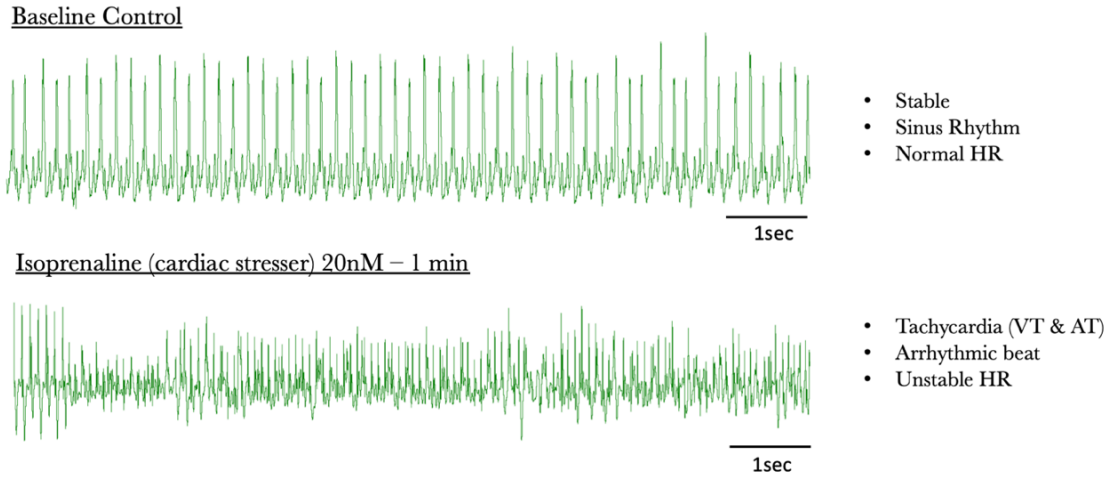

Figure 6.5.1 *Electrocardiography of ex vivo CPVT heart recording (without JB131).* **A)** baseline control with Krebs solution perfusion. Normal sinus rhythm and stable contractions were observed. **B)** Effect of isoprenaline in less than 1 minutes of drug administration. CPVT mice hearts were found to be more vulnerable towards tachycardia and arrhythmia in comparison to those of WT mice.

The baseline heart rate for the control recording was measured to be optimal (HR = 422 + 26). When isoprenaline was introduced to the saline solution, the β-adrenergic stimulation had raised the blood pressure to 600. Within less than a minute, tachycardia was observed, and ventricular arrhythmia were found (see Figure 6.5.1.B). Note that the time that it took for isoprenaline to cause tachycardia was less than 1 minute and at the concentration of isoprenaline was low, 20nM (significant lower concentration, in comparison to testing on the WT mice). The CPVT mice hearts were found to be significantly more vulnerable towards ISO-induced arrythmia in comparison to that of the WT mice. This was as expected as these CPVT mice hearts had mutations at the RyR receptors which provided less efficient mechanism of regulating calcium level in myocardium. After a few minutes of continuous arrhythmia, JB131 at 10uM was added into the saline and was perfused throughout the heart. Within 15 minutes after the drug injection, the arrhythmia had stopped, and the cardiac functions of the heart was found to be significantly improved. Despite the significant reduction in the heart rate from the previous β-adrenergic stress damage, the overall contractility of the heart was found to be very similar to those found at the baseline control. Throughout 25 minutes of drug perfusion, no re-occurrence of arrhythmia was found, and the contractility had continuously improved. After the heart had stabilized, another same dosage of isoprenaline – at the concentration in which it had previously caused arrhythmia – was given to the heart and the results were recorded (see Figure 6.5.2.A).

The ECG recording of the heart exhibited clear effect of the isoprenaline; the heart rate had increased from 250 to 510. However, even after continuous perfusion of the heart for three minutes with isoprenaline, no arrhythmogenesis could be observed in the heart. This was quite an astonishing result as the same heart – which had previously showed tachycardia, within less than a minute of isoprenaline administration – was now able to tolerate high concentrations of isoprenaline. Both the rate and the contractility of the heart were observed to be well and showed no signs of abnormal cardiac contractility. Previous study on anti-arrhythmia effect of JB compound was mainly focused on the prophylactic measurement, however this was the first experimental result to demonstrate functional recoveries of cardiac tissues.

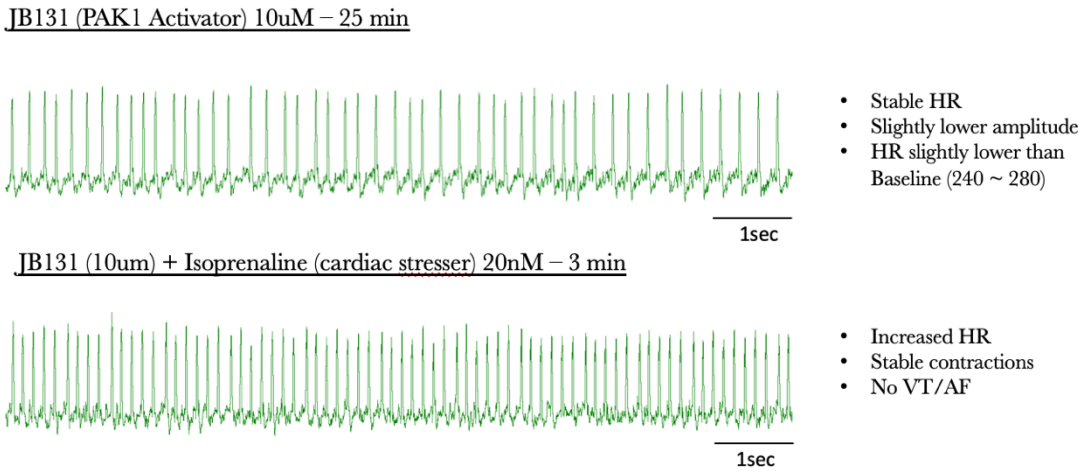

Figure 6.5.2 *Electrocardiography of ex vivo CPVT heart recording (with JB131).* **A)** Effect of JB131 exhibited stabilization of the isoprenaline induced arrhythmia and improved overall contractility of the heart. The same damaged heart which previously showed episodes of arrythmia were no longer visible, and the pace of the cardiac contraction were examined to be stable after having perfused with PAK1 activator for 25 minutes. **B)** *Effect of isoprenaline after three minutes of drug administration.* Co-treatment of isoprenaline and JB131 only demonstrated significant increase in heart rate, but no signs of previously indicated arrhythmia and tachycardia were observed. PAK1 activation in heart demonstrated potential improvement in calcium homeostasis and thereby providing cardioprotective mechanisms in cardiac tissue.

Functional recovery after damaging stimulation is something that is rarely found in cardiac tissues. As previously reported in calcium transient studies using isoprenaline, the effect of β-adrenergic stimulation was found to cause irreversible damage to the cardiomyocytes in which the recovery of normal calcium transient was difficult to observe even after prolong perfusion of PAK1 small molecule activators (See Chapter 4). The study was concluded that the PAK1 activators are able to provide preventable measurements against irregular calcium transients (pathological indications of arrhythmia), but not able to repair the effect of isoprenaline.

The *ex vivo* ECG recording results from above, however, shows promising therapeutic indication of reversible recovery from adrenergic damage and induce optimal cardiac functions. Possible explanation for this observation is due to PAK1's role in homeostatic functions of RyR2 (Ca^{2+} releasing channel in SR) via PP2A signalling (Ke et al., 2008). Studies have suggested that the phosphorylation of RyR2 is highly regulated by a macromolecular signaling complex that contains PKA, CaMKII and the phosphatases – PP1 and PP2A. RyR2 hyperphosphorylation by either PKA or CaMKII has been suggested to present a possible

mechanism for Ca^{2+}-dependent arrhythmia including CPVT and VTs associated with HF (DeSantiago et al., 2014). Based on our biochemical evidence, PAK1 activates PP2A through PP2A auto-dephosphorylation. We found that PAK1 cardiomyocyte deficiency ($Pak1^{CKO}$) mice showed increasing phosphorylation of RyR(S2808) and at the S2814 phosphorylation site under the adrenergic stress condition (isoprenaline treatment). Furthermore, phosphorylation of CaMKII (T287) was also increased in $PAK1^{cko}$ mouse heart tissue (Unpublished data). These implicate the intercommunications between PAK1 and CaMKII, and thereby RyR. Previous experimental evidence from JB79 also demonstrates the interplay amongst PAK1 downstream targets. Pak1 activator JB79 significantly attenuates ISO induced abnormal spontaneous Ca^{2+} transients/waves, illustrating PAK1' crucial role in in maintaining homeostatic RyR2 functions and calcium levels. These supporting evidences may account for the improved cardiac function in the CPVT heart, after having overstressed damage. Such proof-of-concept experiment suggests a potential application of Pak1 activating compounds in abnormal SR Ca^{2+} release related ventricular arrhythmias such as CPVT. Therefore, a larger study on the effect of JB131 on CPVT mice model are currently being investigated for further validation.

6.6 Summary & Concluding Remarks

After the validation of the small-molecule PAK1 activation and defining a hit series, we sought to gain a better understanding of the protein-ligand interactions. To this end, a triage optimization process was performed. This process frequently involves designing a maximally high number of analogues of the hit compounds and measuring their functional efficacy through an *in vitro* kinase assay. Performing this measurement based on the differences of the compounds in the functional groups, (e.g., electron withdrawing strength and positions) makes it possible to predict the chemical space of the active site for ligands with improved efficacy and affinity. In the present study, we further optimised the previous lead JB79 compound so that to obtain a better physiochemical profile and to enhance its efficacy in activating PAK1. Creating various analogues of JB79 helped us to visualise the chemical space within the active site. Functional moieties with the previous indication of having poor DMPK properties were replaced by the groups that exhibited more favorable physiochemical properties. The core group of JB79 compound was also substituted by a simple amide core, reducing the potential toxicity reported for acrylamide. Through the optimization process, three new compounds—namely, JB120, JB124, and JB130—were selected; these compounds contained the most favorable physiochemical properties with minimum indications of the PAINS score. These compounds also produced a significant increase in PAK1 activation, inducing direct and sufficient activation of PAK1 protein. Along with a relatively lower affinity (EC_{50} in a low micromolar range), the developed PAK1 activators exhibited favorable drug-like properties, suggesting a potentially high therapeutic value of PAK1 small molecules for CVDs indications.

In general, improvements in ligand affinity and selectivity can be achieved as a result of a comprehensive understanding of the ligand binding site. Other methods that have been demonstrated to be useful in some cases of hit to lead (H2L) optimization process include QSAR (ligand-based ligand optimization) or *in silico* optimization. However, until present, the preferred approach has been a structural study focusing on the protein-ligand interactions through either a cryo-EM or an X-ray crystallography, as this approach is more cost-efficient. For instance, co-crystallography between PAK1 and JB compounds would determine the binding site and the orientation in which these molecules bind to PAK1, making it possible to

directly identify the residues essential for creating the active site. Yet, the limitation of the co-crystallography method is that it requires additional resources and evidential proof of the occurrence of molecular interaction between PAK1 and JB compounds. Therefore, before conducting the full co-crystallography, we first performed the PAL-MS assay through adding a photoaffinity label to the lead compound JB120. This was followed by an examination of protein-ligand interactions. Upon further analysis, PAL probe was identified to bind to the KI domain section of the AID (specifically, at the asparagine and valine residues), where the removing of the KI domain is essential to expose the kinase domain for phosphorylation activation state. Our hypothesis is that the mechanism action of JB compound is that it inhibits the KI domain of PAK1, thereby interfering its *cis* inhibitory mechanism and causing a significant activation in PAK1. These findings were encouraging and provided foundation for our hypothesis in its mechanism of activation. As a next step, we plan to perform the X-ray crystallography to validate our previous results and to gain a deeper insight into the orientation in which these molecules bind.

Furthermore, several preliminary functional therapeutic applications of the newly developed small-molecule PAK1 activators were studied using catecholaminergic polymorphic ventricular tachycardia (CPVT). As PAK1 has been reported to be involved in preventing arrhythmia and improving calcium regulations in cardiac homeostasis, we sought to establish whether the newly developed PAK1 activator would provide an effective therapeutic means to prevent acute arrhythmia in the CPVT mice model. Considering that currently available drugs do not ensure complete protection from a sudden cardiac death, an anti-arrhythmic molecule like the PAK1 activator could serves as a potential medication to prevent cardiac arrest in CPVT patients. Exhibiting significant benefits through the PAK1 activator (JB124), the results of our CPVT mice model studies provided evidence in support of this possibility. Due to their mutation at RyR receptors, CPVT mice showed a greater sensitivity towards isoprenaline-induced arrhythmia as compared to normal mice; at 10nM ISO, CPVT mice already showed symptoms of ventricular arrhythmia. However, JB124 10uM heart-perfusion served as an effective prevention of arrhythmia and improved contractility of the heart. Even after another isoprenaline dosage was provided, the contractility rate was maintained, and no arrhythmia

was observed. Thus, although further characterization of the anti-arrhythmic effect of PAK1 activators would require confirmation in larger-scale future research, our preliminary results highlight potential benefits of stimulating the intrinsic PAK1 signalling and preventing maladaptive hypertrophic remodelling and heart failure progressions. To conclude, we hope that our research findings on the development of PAK1 activators will provide a solid foundation for future development of new treatment strategies and medications for HF and other CVD conditions.

CHAPTER 7

FUTURE STUDIES AND CONCLUSIONS

Summary Points

- Perspective plans for optimizing the PAK1 small molecule activators are currently in development.
- Further optimizations will be aimed to improve the affinity of the compounds towards PAK1 (reducing EC_{50} towards the nanomolar range). This would be greatly facilitated by the information derived from the co-crystallography on the protein-ligand interactions.
- New constructs for PAK1 proteins for co-crystallization are in discussion; AID and the KD will be linked by a short chain to keep both domains intact, but the flexible region (a.a. 189 – 245) will be removed to improve the likelihood of crystallization.
- Based on the newly optimized ligands, further clinical studies will be conducted to examine potential therapeutic benefits of the PAK1 activators.
- Inhibitory switch domain of PAK1-AID may be another allosteric site for regulating PAK1 enzymatic activity. This may be used therapeutically in order to explore other ligands.
- Final thoughts on the thesis are detailed in the conclusion.

7.1 Additional Functional Studies for Clinical Indication

Additional functional studies are currently being planned for testing CVD therapeutics of the small molecule PAK1 activators. The functional studies will entail using newly designed JB131 in order to validate whether or not the drugs can alleviate symptoms of CVDs. Although many of the clinical validation of PAK1 activators have been previously studied using JB79, the newly designed compounds contain different functional groups, which may translate to different therapeutic effect as well as different efficacy in PAK1activation.Therefore, it is imperative that we repeat the functional studies in order to affirm the previous findings. Currently, whole heart *ex vivo* heart perfusion studies are being carried out to assess the effect of PAK1 activation in CPVT. As previously discussed in Chapter 6, the preliminary results using JB131 treatment showed significant improvement of the CPVT myocardium, illustrating optimal contractility as well as higher threshold required for ISO-induced arrythmia. Observation of substantial anti-arrhythmic effect after the drug treatment on the whole hearts and improvement in calcium handling in isolated cardiomyocytes have provided potential therapeutic indication of small molecule PAK1 activators for alleviating CPVT complications. Currently there are no therapeutic drugs available to effectively treat CPVT patients. β-blockers are first-line of drugs used for symptomatic management; however, they have been shown to significantly impair quality life of patients. Novel innovative and effective measurements for managing CPVT are therefore urgently needed, and our PAK1 small molecule activators could be the solution to these problems.

Other collaborators from the U.S. – Dr. Ke and Dr. Solaros – are currently using the newly developed small molecule PAK1 activators to examine the compound's efficacy in protective effect in myocardium. Long-term effect of JB131 will be tested on IPSC differentiated cardiomyocytes to measure any consequences of PAK1 activation when given for a prolong time treatment. Immunohistochemistry (IHC) on cardiac slices will also be performed to detect any difference in the inflammatory markers – indicating for ischemic injury or TAC induced cardiac hypertrophy – between the control group and drug treated groups. Lastly, our other collaborators in Luzou, China, plan to conduct a large-scaled *in vivo* study to measure any acute benefit of PAK1 activators on CPVT mice models. If proven therapeutically useful, the small

molecule PAK1 activators could be the first targeted therapy for CPVT. In any cases, we will continue to communicate closely with our collaborators to ensure that the designed experiments are aimed to answer the intended questions with appropriate statistical methods for validations.

7.2 PAK1 Molecular Signaling Map

PAK1's cardioprotective signaling pathway have been extensively studied over the last two decades, validating to be a promising therapeutic target for providing effective treatment for cardiovascular diseases. Using JB79 small molecule PAK1 activator, we have shown that activation of PAK1 *in vitro* cell models, as well as in myocardium tissues, demonstrates noticeable functional improvements. One prominent activated PAK1 pathway in maintaining cardiac homeostasis within myocardium is thought through activating the protein phosphatase 2A (PP2A). This activation leads to reduction in the phosphorylation effect of protein kinase A (PKA) and reducing the activity of L-type Ca^{2+} and ryanodine receptor (RyR) (both PKA dependent). Ke et al. identified through immunoprecipitation of expressed CA-PAK1 in cardiomyocytes that showed the interaction between PAK1 and PP2A – forming a complex and inducing dephosphorylation of the Tyr-307 residue of the PP2A catalytic subunit. This result indicated that association with active PAK1 elicited auto-dephosphorylation of PP2A and an increase in dephosphorylation activity toward substrates (Ke et al, 2004). As current JB compounds have been confirmed to activate intracellular PAK1 directly and provide significant improvement in myocardium functions, additional molecular evidence for cardioprotective signaling pathway by PAK1 activation may be required for necessary validation. One suggestive assay is to use fluorescence resonance energy transfer (FRET) method to validate whether JB compounds promote higher frequency interaction between PP2A and PAK1. If the compound were to activate intracellular PAK1 in cardiomyocytes, the fluorescence from the FRET assay would be expected to be significantly higher in drug treated groups than those with vehicle treatments. Other western blot studies may also be useful for understanding which targets are essential for promoting cardioprotective mechanisms.

7.3 Ligand expansion search for small molecule PAK1 activators

Early indications of PAK1 regulation was observed in lipid studies where the certain lipid families of sphingosine were shown to noticeably stimulate PAK1 activity (Bokoch et al., 1998; Morreale et al., 2000). Dose response test using S1P was demonstrated to cause direct activation of PAK1 in a dose dependent manner, however, this was later confirmed to be an indirect activation through interacting with S1P receptors, which causes subsequent downstream activation of PAK1 signaling pathway (Egom et al., 2011; Cannavo et al., 2017; Wang et al., 2017). RF-MS kinase assay was used to verify whether or not S1P and FTY-720 could directly activate PAK1. Both S1P (<1mM) and FTY-720 (FDA approved analogues of S1P drug, <10uM) were confirmed not to exhibit any affect in regulating PAK1 activity. However, this does not mean that lipid pharmacophore groups were not drug design candidate for PAK1 activators. Among the list of our confirmed small molecule PAK1 activators, few of our JB compounds contains long carbene chains which also portrayed significant activation of PAK1. Examples of these compounds are JB120, JB124, JB131. These compounds contain lipid-like long chains of carbenes which are similar to those of S1P and have been confirmed to directly stimulate PAK1 activity. This was supported by Chong et al. who have reported that sphingosine at very high concentrations (>1mM) can directly activate PAK1 activity; there was a representative dose response activation of PAK1 by sphingosine, with maximum activity illustrated to be a four-fold increase in PAK1 activity on MBP phosphorylation (see Figure 7.3.1). Measurement of MBP phosphorylation (substrate) through western blot showed significant amount of phosphorylation in comparison to the control group (Chong et al., 2001). Therefore, the pharmacophore for designing small molecule PAK1 activators from sphingosine families may be one possibility for exploring other potential analogues.

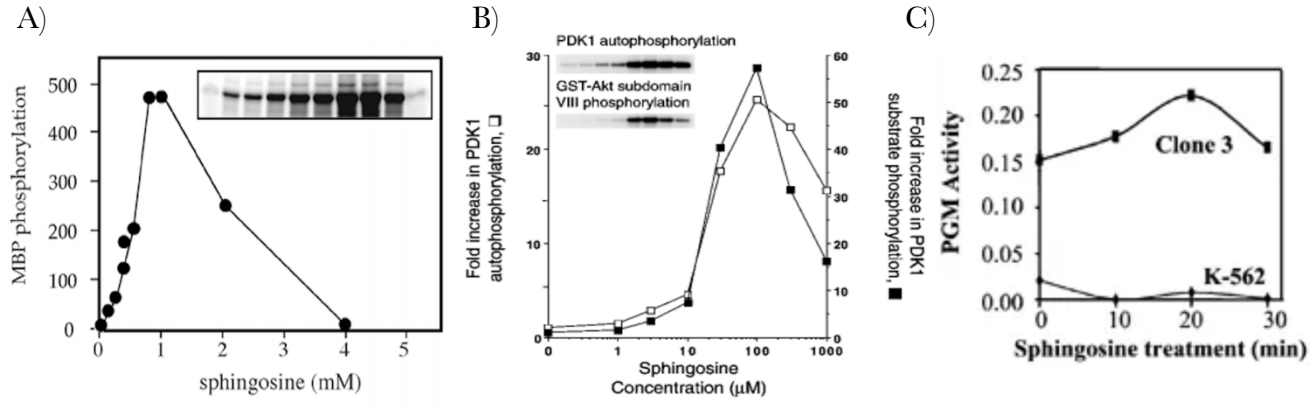

Figure 7.3.1 *Activation-inhibition pattern found in kinase activation by sphingosine.* **A)** Dose dependent activation of PAK by sphingosine. MBP substrate phosphorylation was measured as an indirect method of measuring the kinase activity using the autoradiography SDS-PAGE. **B)** Autophosphorylation of IP Myc-PDK1was measured in the presence of increasing sphingosine concentrations and 1 ug of GST-Akt kinase subdomain VIII by an in vitro kinase assay. **C)** PGM activity in parental K-562 cells and PGM-expressing-K-562 clone 3 was assayed after stimulation with sphingosine at different time intervals (Figures derived from Chong et al., 2001; King et al., 2000; Gururaj et al. 2004)

The purpose for the compound ligand expansions is to abolish the inhibitory effect of PAK1 activators at higher concentrations. Many of our current activators have been shown to have a certain therapeutic window where they demonstrated significant activation of PAK1 but found to inhibit at high concentrations. Interestingly, these patterns were also recognized by previous papers illustrating PAK1 activation using external ligands. In Chong et al. 2001, the activation curve of S1P on PAK1 resembled those of our PAK1 activators dose response tests. At therapeutic concentrations (in such case, 0 – 1.5mM), PAK1 was shown to significantly activate PAK1, however at higher concentrations (>1.5mM) the stimulatory effect of sphingosine was abolished and instead showed inhibitory mechanism. Other studies observing the effect of sphingosine in other enzyme activities also demonstrated similar pattern in which after the activation effect of the sphingosine, inhibitory effect was observed in the enzyme activity (King et al., 2000; Gururaj et al. 2004). As discussed in chapter 5, the cause of the inhibitory effect may be due to the possibility of non-specific binding at high concentrations. The over saturation of the ligand may interfere with the substrate binding at the active site and consequently reducing the enzymatic activity. Additional studies on the mechanism of inhibition, therefore, would allow for better design of compounds that does not lead to inhibition at high concentrations. Eliminating such potential adverse effect would enable wider therapeutic window and be essential for prospective drug discovery on small molecule kinase activators.

7.4. X-ray Co-crystallography

Following the failure to crystalize the FL-PAK1 as well as unable to observe the ligand from the crystallography work done by Proteros using the PAK1 construct – (Hs a.a.82-149) & PAK1 (Hs a.a. 249-545) – further investigation done to examine the causes of the negative results. It was discovered that the PAK1 that was purified by Proteros were not functional, yet they were attempted for crystallization with a protein without having confirmed the efficacy of compound on PAK1 activation. This was a crucial step in confirming whether the ligand was interacting with PAK1 or not; without having confirmed ligand-protein interaction, it was a risky step to move on to doing the x-ray crystallography. However, this has provided an explanation as to why the previous co-crystallography had failed. In attempt to reproduce the co-crystallography, new construct was expressed in bacteria and FL-PAK1 was purified by Evotec Team. These proteins have been tested for their functional activity using RF-MS kinase assay and were verified to be active and responding well to both CDC42 and JB compounds. Having confirmed FL-PAK1 activity, diffraction light scattering (DLS) was conducted to see whether the FL PAK1 was optimal for the crystallography or not (Figure 7.4.1).

A) FL-PAK1 (Eovtec)

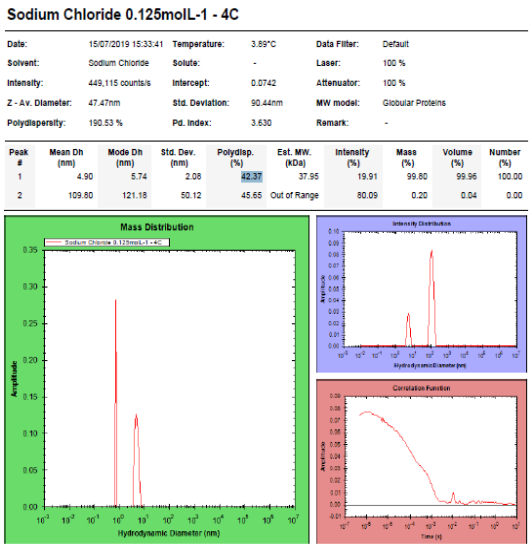

B) Δ70 - PAK1(OU)

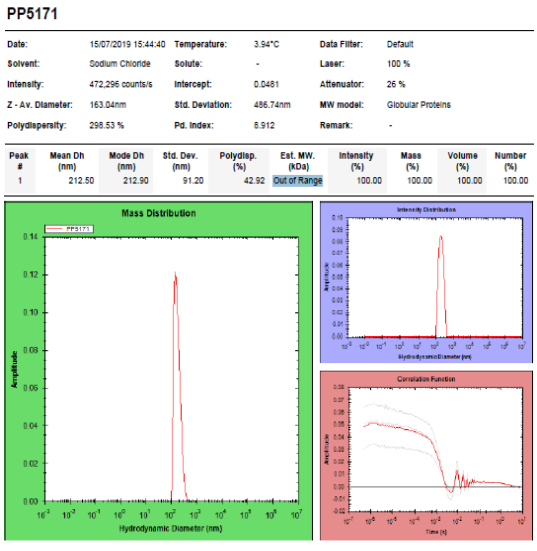

Figure 7.4.1 *DLS analysis of FL-PAK1 (Evotec) and PAK1 Δ70 (OU).* A) FL-PAK1 (Evotec) mass distribution at high concentration suggests two peaks, indicating small forms of aggregates. B) PAK1 Δ70 (OU) analysis shows multiple peaks at the correlation functions, which may suggest difficulty in analyzing its light scattering.

DLS was used as a technique to determine the size distribution profile of PAK1 in solution. The analysis includes mass distribution, polydispersity and correlation function which could interpret the likelihood of crystal formations. Unfortunately, for both PAK1-FL (purified from Evotec) and PAK1 Δ70 (purified from OU) samples showed forms small aggregates with polydispersity indicating a high value. These number suggest that the proteins are unlikely to be crystallize and that the risk of performing co-crystallization is likely to be less.

Due to the low chances of crystal formations, we are currently discussing whether to try purifying another PAK1 protein that is more simplified and easier to crystallize. The rationale is to remove flexible parts (C-terminus of KID) which may be interfering with the crystallization for current PAK1 construct – (Hs a.a.82-149) & PAK1 (Hs a.a. 249-545). The stabilization of the AID-KID interaction could be reinforced through providing a linker between the two domains, a short ~ 8 aa linker, to make PAK1 (Hs a.a.82-149)-$(GS)_4$-PAK1 (Hs a.a. 249-545) (see Figure 5.5.2). Such stability and reduction of flexible residues are thought to provide a better chance of detecting the ligand binding.

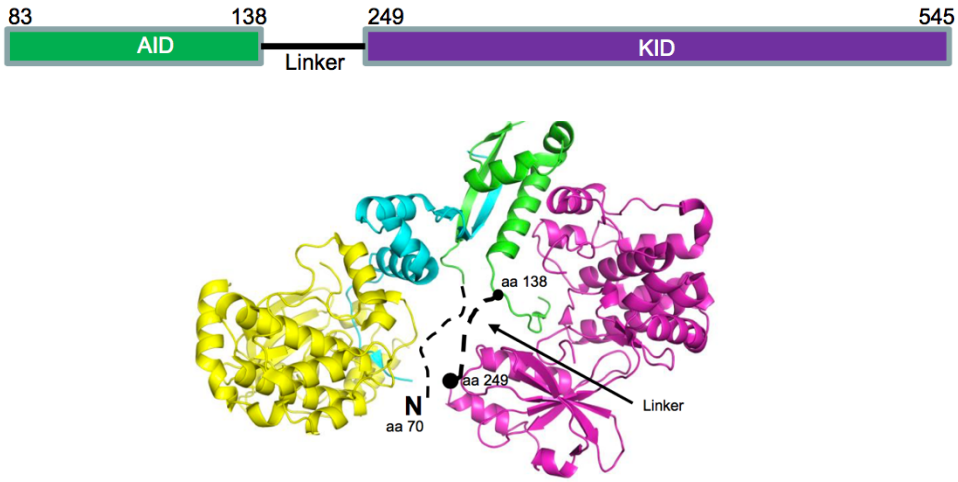

Figure 7.4.2 *Proposing PAK1 construct for co-crystallography*. Linker is introduced in between the AID and the KD domain in order to provide stabilization of interaction motifs. The linkage is also thought to make the purification easier as two separate expression and purification steps would not be necessary once the two proteins are linked. Both AID and the KD are maintained in order to keep the activity of PAK1 functional, while pertaining the regulatory mechanism.

Another alternative plan is to co-crystallize between PAK1 AID + CDC42 to see if the ligand may be acting as a stabilizer for linking the two proteins together. From our RF-MS kinase assay, we found that the compound does not stimulate the activity of the kinase if PAK1 does

not have the AID (Chapter 5.2), indicating that the binding site is likely to be outside of the KD domain. However, before planning on doing another co-crystallography, additional preliminary studies using SPR or ITC could be helpful for confirming the ligand interaction to AID. This has been scheduled in the next perspective study with Evotec.

7.5. IS: another potential allosteric site for PAK1 activators

One of the interesting observations from the dose response tests was that there seemed to be different levels of kinase activation that were measured by JB compounds. Majority of the compounds caused increased in PAK1 activity by a few fold (2 ~ 3x total activity). However, a few compounds exhibited exceptional high increase in PAK1 activity. For instance, JB131 compounds exhibits 20-fold increased in PAK1 activity when co-incubated with CDC42. Another compound JB127 showed the highest activation of PAK1 activity recorded so far, demonstrating 45 times higher in PAK1 activity at 40uM. Assuming that PAK1 activators bind to the same binding site – the interface between the kinase inhibitory domain and the kinase domain – the overall maximum activation effect should still be similar amongst the PAK1 activators. However, this was not the case with our JB compounds as some of their efficacy was measured to be extremely high. Potential explanations for such high activation could be due to an additional binding at the inhibitory switch (IS) of PAK1 AID. Through binding at another allosteric site of the AID, the JB compounds may confer additional level of activation to PAK1 – potentially through disrupting the dimerization mechanism on top of the interfering the *cis* inhibition mechanism. According to the crystallography structure of PAK1 (PDB: 1F3M), the PAL-labelled Y131 was identified to be quite distance from the rest of the identified residues; Y131 was positioned at the IS domain, rather than at the KI domain where majority of the covalently modified residues were. As 1F3M PAK1 is a truncated version of PAK1 which contains AID (a.a. 70 – 149) and KD (a.a. 245 – 545) and was missing a large segment between a.a. 149 – 245, we weren't sure whether the position of the Y131 is accurately represented. There is a possibility that the missing segment may cause conformation changes to the AID, where the Y131 may be positioned closely to the KI – KD interface. However, if Y131 position is truly located at the IS domain as indicated by our PAL-MS study, this may suggest a

secondary binding site where the compound may also work through to stimulate PAK1 activity. Compound that can bind to both the KI-KD interface, as well as the IS domain, would therefore confer higher activity as we have previously observed with JB127. To further investigate this, it would be interesting to look at the difference in the interacting site between compounds with significant difference in their maximal activation. Using thermal shift assay, for instance, we may be able to observe greater thermal changes on compounds that bind to both KI-KD interface and the IS, in comparison to another compound that only binds to the KI-KD interface. An alternative option is to repeat the PAL-MS study through designing another PAL probe based on the compounds that exhibit > x20 fold increase in PAK1 activity. Elucidating the difference in the total efficacy of these PAK1 activators may be crucial for understanding the compound's mechanism of action, as well as for prospective design of kinase activators.

7.6 Conclusions

Over two decades of research has demonstrated that PAK1 possess multiple cardioprotective mechanism through activating several pathways essential in maintaining cardiac homeostasis. PAK1 has been identified as the key regulatory in cardiac ion channels, calcium handling, as well as in cardiac contractility. These essentials roles of PAK1 in heart has been implicated in various physiological and pathological conditions. Anti-hypertrophic effect was observed in NVRM which had expressed constitutively active PAK1 genes; later confirmed to be through activating JNK pathways. Protective effect of PAK1 in cardiac ischemic injury was reported to stimulate AKT, another protein kinase that has been extensively validated to promote cardiomyocytes survivals (Fujio et al, 2000; Matsui et al., 2001; Zhu et al., 2006). Recent work by our group have also implicated the importance of PAK1 in anti-arrhythmic effects through usage of FTY-720, analogues of sphingosine-1-phospohate (S1P), which demonstrated indirect PAK1 activations and therefore, providing improved calcium handling in myocardium. These studies have indicated PAK1 as a key controller in maintaining cardio-protection. Through the regulation of calcium homeostasis and cellular remodeling, PAK1 exhibits a promising therapeutic target for the treatment for arrythmia and cardiomyopathy – common symptoms found during progression of heart failure patients.

From therapeutic validations, drug discovery effort was put to search for synthetic ligands that could directly stimulate PAK1 activity. Subsequently, PAK1-activating-peptide (PAP), which contained complementary sequence to the AID, was designed in order to disrupt PAK1 inhibitory dimerization. Having observed significant activation effect of PAP in PAK1 as well as preliminary indication of therapeutic benefits, such proof of concept was used to translate from the peptide ligand to small molecule. PAK1 small molecule activators were search through using computational *in silico* screening method. Using various applications of computational docking and screening software, libraries of virtual ligands were examined for their affinity towards the auto-inhibitory domain (AID) of PAK1. Compounds that exhibited strong affinity towards the AID were filtered and then synthesized for *in vitro* kinase assays. Two different types of *in vitro* kinase assays, – ADP-GLO and RF-MS Kinase assays – were utilized to assure the consistently in the effect on the kinase activity. Amongst the initial screened compounds, the

first identified small molecule PAK1 activator was called JB01 and it has been confirmed to cause significant stimulation on PAK1 activity. Since the discovery of JB01, small molecule PAK1 activators have gone through several rounds of optimization process. Structure activity relationship (SAR) was studied using the previous lead compound JB79 and replacing with various other functional groups. Through these group substitutions, we were able to obtain greater understanding of the ligand binding site and be able to improve the compounds' physiochemical profiles as well as its efficacy in PAK1 activation. Current lead compounds JB120, JB124, and JB131, displays significant improvements its overall chemical properties as well as maintain ~ 4 folds activation in PAK1 activity at low micromolar concentrations.

The mechanism of action of the small molecule PAK1 activators were further studied using biophysical assays and information from the previous SAR studies. Through photo-affinity labeling, coupled with mass-spectrometry (PAL-MS) studies, the compounds were identified to bind at the interface between AID and the kinase domain (KD). This region has been recognized as the kinase inhibitory segment where it prevents the kinase domain from being exposed for auto-phosphorylation at the T423 residue. Interfering at such AID segment through a small molecule thought to dysregulate the inhibitory mechanism and consequently promoting for PAK1 activation. Another potential allosteric site of PAK1 activators is the inhibitory switch (IS) motif of AID, where two monomers of PAK1 AID interact to dimerize. Dimerization process is an additional system in which PAK1 regulates its activity (dimer inhibition). Some preliminary evidences suggest that binding at the IS motif of AID can produce even more activation in PAK1 enzymatic activity. In addition to the PAL-MS studies, x-ray crystallography studies are currently in the process of preparation. The co-crystallography was previously attempted with Proteros, but the negative result was due to the lack of the enzymatic activity of the purified protein. Another effort to co-crystallize between PAK1 and the JB compounds is currently being planned for future studies. Recently, Evotec has purified a new batch of FL-PAK1 protein for the co-crystallography, and the proteins have been verified to be active with good response from both CDC42 and JB compound activations.

Finally, therapeutic validation of PAK1 stimulation were observed using various functional study models. Proof of anti-arrhythmic effect of JB79 was observed through measuring the

reduction of irregular calcium transients induced by isoprenaline in isolated cardiomyocytes. Using the human iPSC model, the derived human stem cells also demonstrated reduction in the adrenergic stimulation of calcium transient amplitudes after the drug treatment. PAK1 activation through the small molecule exhibited effective improvement in the cell's ability to handle intracellular calcium flows as well showed promising transability for human therapeutics. Another functional study examining at *ex vivo* whole heart model illustrated JB79's cardioprotective effect against programmed electrical stimulation (PES)-induced arrhythmia, specifically observing premature ventricular contractions (PVC) and ventricular fibrillation (VF). The results showed that sufficient activation of PAK1 signaling at 10mg/kg concentration had significant benefit in increasing threshold required for PES-induced VF and PVC, reducing the overall frequency of cardiac arrhythmia. Finally, using TAC-induced cardiac hypertrophy model, significant alleviation of pressure overload cardiac hypertrophy was observed upon prolong treatment of the PAK1 activator. These preliminary results demonstrate potential therapeutic applications for small molecule PAK1activators in providing both the treatment for and the prophylactic measurement against cardiovascular complications. This study explores the development of small molecule PAK1 activator and its promising cardio-protective effect.

In addition to the potential therapeutic benefits of the PAK1 small molecule activators, one of wider applications of our small molecule PAK1 activator is that it has provided a proof of concept in the novel mechanism of drug activation. Such conception of mechanism of kinase activation could be utilized as a blue-print to design other activators aimed at other therapeutic targets. Majority of current therapeutic drugs are focusing on inhibiting the pathological pathway to alleviate disease symptoms – little effort has been done to elevate the beneficial pathway to induce protection. Using the JB compounds as proof of concept, we have demonstrated for first time that kinase activity can be directly modulated through a small molecule. The mechanism of activation is hypothesized to bind at the auto-inhibitory domain of PAK1 and thereby inhibiting the inhibiting mechanisms. Currently, no therapeutic drugs have been shown to utilizes such mechanism of action to activate intracellular proteins. We hope that such application can be adopted by the scientific field as well as pharmaceutical companies to expand our horizons for therapeutic targeting.

References

Adabag AS, Luepker RV, Roger VL, Gersh BJ. Sudden cardiac death: epidemiology and risk factors. Nat Rev Cardiol. 2010;7(4):216-25.

Ahmed N, Linardi D, Muhammad N, et al. Sphingosine 1-Phosphate Receptor Modulator Fingolimod (FTY720) Attenuates Myocardial Fibrosis in Post-heterotopic Heart Transplantation. Front Pharmacol. 2017;8:645. Published 2017 Sep 15. doi:10.3389/fphar.2017.00645

Ajijola OA, Yagishita D, Patel KJ, et al. Focal myocardial infarction induces global remodeling of cardiac sympathetic innervation: neural remodeling in a spatial context. Am J Physiol Heart Circ Physiol. 2013;305(7):H1031-40.

Alamo L, Ware JS, Pinto A, et al. Effects of myosin variants on interacting-heads motif explain distinct hypertrophic and dilated cardiomyopathy phenotypes. Elife. 2017;6:e24634. Published 2017 Jun 13. doi:10.7554/eLife.24634

Andrikopoulos GK, Pastromas S, Tzeis S. Flecainide: Current status and perspectives in arrhythmia management. World J Cardiol. 2015;7(2):76-85.

Arias-Romero LE, Villamar-Cruz O, Pacheco A, et al. A Rac-Pak signaling pathway is essential for ErbB2-mediated transformation of human breast epithelial cancer cells. Oncogene. 2010;29(43):5839–5849. doi:10.1038/onc.2010.318

Baccarelli, A., & Ghosh, S. (2012). Environmental exposures, epigenetics and cardiovascular disease. Current opinion in clinical nutrition and metabolic care, 15(4), 323–329. doi:10.1097/MCO.0b013e328354bf5c

Bagheri-yarmand R, Mandal M, Taludker AH, et al. Etk/Bmx tyrosine kinase activates Pak1 and regulates tumorigenicity of breast cancer cells. J Biol Chem. 2001;276(31):29403-9.

Baher A, Valderrabano M. Management of ventricular tachycardia in heart failure. Methodist Debakey Cardiovasc J. 2013;9(1):20-5.

Balasenthil S, Sahin AA, Barnes CJ, et al. p21-activated kinase-1 signaling mediates cyclin D1 expression in mammary epithelial and cancer cells. J Biol Chem. 2004;279(2):1422-8.

Banerjee M, Worth D, Prowse DM, Nikolic M. Pak1 phosphorylation on t212 affects microtubules in cells undergoing mitosis. Curr Biol. 2002;12(14):1233-9.

Barf T, Covey T, Izumi R, et al. Acalabrutinib (ACP-196): A Covalent Bruton Tyrosine Kinase Inhibitor with a Differentiated Selectivity and In Vivo Potency Profile. J Pharmacol Exp Ther. 2017;363(2):240-252.

Barth AS, Tomaselli GF. Cardiac metabolism and arrhythmias. Circ Arrhythm Electrophysiol. 2009;2(3):327-35.

Bhatnagar P, Wickramasinghe K, Williams J, Rayner M, Townsend N. The epidemiology of cardiovascular disease in the UK 2014. Heart. 2015;101(15):1182-9.

Bhatnagar P, Wickramasinghe K, Wilkins E, Townsend N. Trends in the epidemiology of cardiovascular disease in the UK. Heart. 2016;102(24):1945-1952.

Bhuiyan ZA, Hamdan MA, Shamsi ET, et al. A novel early onset lethal form of catecholaminergic polymorphic ventricular tachycardia maps to chromosome 7p14-p22. J Cardiovasc Electrophysiol. 2007;18(10):1060-6.

Bleicher KH, Böhm HJ, Müller K, Alanine AI. Hit and lead generation: beyond high-throughput screening. Nat Rev Drug Discov. 2003;2(5):369-78.

Blumenthal JA, Emery CF, Madden DJ, et al. Cardiovascular and behavioral effects of aerobic exercise training in healthy older men and women. J Gerontol. 1989;44(5):M147-57.

Bisson WH, Koch DC, O'donnell EF, et al. Modeling of the aryl hydrocarbon receptor (AhR) ligand binding domain and its utility in virtual ligand screening to predict new AhR ligands. J Med Chem. 2009;52(18):5635-41.

Bokoch GM, Reilly AM, Daniels RH, et al. A GTPase-independent mechanism of p21-activated kinase activation. Regulation by sphingosine and other biologically active lipids. J Biol Chem. 1998;273(14):8137-44.

Borriello L, Montès M, Lepelletier Y, et al. Structure-based discovery of a small non-peptidic Neuropilins antagonist exerting in vitro and in vivo anti-tumor activity on breast cancer model. Cancer Lett. 2014;349(2):120-7.

Brinkmann V, Davis MD, Heise CE, et al. The immune modulator FTY720 targets sphingosine 1-phosphate receptors. J Biol Chem. 2002;277(24):21453-7.

Brown JL, Stowers L, Baer M, Trejo J, Coughlin S, Chant J. Human Ste20 homologue hPAK1 links GTPases to the JNK MAP kinase pathway. Curr Biol. 1996;6(5):598-605.

Brown MC, West KA, Turner CE. Paxillin-dependent paxillin kinase linker and p21-activated kinase localization to focal adhesions involves a multistep activation pathway. Mol Biol Cell. 2002;13(5):1550-65.

Bursulaya BD, Totrov M, Abagyan R, Brooks CL. Comparative study of several algorithms for flexible ligand docking. J Comput Aided Mol Des. 2003;17(11):755-63.

Cannavo A, Rengo G, Liccardo D, et al. β-Blockade Prevents Post-Ischemic Myocardial Decompensation Via βAR-Dependent Protective Sphingosine-1 Phosphate Signaling. J Am Coll Cardiol. 2017;70(2):182-192.

Cerrone M, Noujaim SF, Tolkacheva EG, et al. Arrhythmogenic mechanisms in a mouse model of catecholaminergic polymorphic ventricular tachycardia. Circ Res. 2007;101(10):1039–1048. doi:10.1161/CIRCRESAHA.107.148064

Chang CP, Bruneau BG. Epigenetics and cardiovascular development. Annu Rev Physiol. 2012;74:41-68.

Cheng C, Yan KK, Hwang W, et al. Construction and analysis of an integrated regulatory network derived from high-throughput sequencing data. PLoS Comput Biol. 2011;7(11):e1002190. doi:10.1371/journal.pcbi.1002190

Chen-scarabelli C, Saravolatz L, Hirsh B, Agrawal P, Scarabelli TM. Dilemmas in end-stage heart failure. J Geriatr Cardiol. 2015;12(1):57-65.

Chong C, Tan L, Lim L, Manser E. The mechanism of PAK activation. Autophosphorylation events in both regulatory and kinase domains control activity. J Biol Chem. 2001;276(20):17347-53.

Chow HY, Jubb AM, Koch JN, et al. p21-Activated kinase 1 is required for efficient tumor formation and progression in a Ras-mediated skin cancer model. Cancer Res. 2012;72(22):5966-75.

Coletta AP, Clark AL, Cleland JG. Clinical trials update from the Heart Failure Society of America and the American Heart Association meetings in 2008: SADHART-CHF, COMPARE, MOMENTUM, thyroid hormone analogue study, HF-ACTION, I-PRESERVE, beta-interferon study, BACH, and ATHENA. Eur J Heart Fail. 2009;11(2):214-9.

Congreve M, Murray CW, Blundell TL. Structural biology and drug discovery. Drug Discov Today. 2005;10(13):895-907.

Davies L, Jin J, Shen W, et al. Mkk4 is a negative regulator of the transforming growth factor beta 1 signaling associated with atrial remodeling and arrhythmogenesis with age. J Am Heart Assoc. 2014;3(2):e000340.

Denning C, Anderson D. Cardiomyocytes from human embryonic stem cells as predictors of cardiotoxicity. Drug Discov Today Ther Strateg. 2008;5:223–232.

Desantiago J, Bare DJ, Ke Y, Sheehan KA, Solaro RJ, Banach K. Functional integrity of the T-tubular system in cardiomyocytes depends on p21-activated kinase 1. J Mol Cell Cardiol. 2013;60:121-8.

Dick E, Rajamohan D, Ronksley J, Denning C. Evaluating the utility of cardiomyocytes from human pluripotent stem cells for drug screening. Biochem Soc Trans. 2010;38(4):1037-45.

Dimasi JA, Grabowski HG, Hansen RW. Innovation in the pharmaceutical industry: New estimates of R&D costs. J Health Econ. 2016;47:20-33.

Dummler B, Ohshiro K, Kumar R, Field J. Pak protein kinases and their role in cancer. Cancer Metastasis Rev. 2009;28(1-2):51-63.

Edwards DC, Sanders LC, Bokoch GM, Gill GN. Activation of LIM-kinase by Pak1 couples Rac/Cdc42 GTPase signalling to actin cytoskeletal dynamics. Nat Cell Biol. 1999;1(5):253-9.

Egom EE, Ke Y, Musa H, et al. FTY720 prevents ischemia/reperfusion injury-associated arrhythmias in an ex vivo rat heart model via activation of Pak1/Akt signaling. J Mol Cell Cardiol. 2010;48(2):406-14.

Egom EE, Ke Y, Solaro RJ, Lei M. Cardioprotection in ischemia/reperfusion injury: spotlight on sphingosine-1-phosphate and bradykinin signalling. Prog Biophys Mol Biol. 2010;103(1):142-7.

Egom EE, Mohamed TM, Mamas MA, et al. Activation of Pak1/Akt/eNOS signaling following sphingosine-1-phosphate release as part of a mechanism protecting cardiomyocytes against ischemic cell injury. Am J Physiol Heart Circ Physiol. 2011;301(4):H1487-95.

Egom EE, Mamas MA, Chacko S, et al. Serum sphingolipids level as a novel potential marker for early detection of human myocardial ischaemic injury. Front Physiol. 2013;4:130. Published 2013 Jun 13. doi:10.3389/fphys.2013.00130

Egom EE, Bae JS, Capel R, et al. Effect of sphingosine-1-phosphate on L-type calcium current and Ca(2+) transient in rat ventricular myocytes. Mol Cell Biochem. 2016;419(1-2):83-92.

Ferrara P, Gohlke H, Price DJ, Klebe G, Brooks CL. Assessing scoring functions for protein-ligand interactions. J Med Chem. 2004;47(12):3032-47.

Ferrari R, Fox K. Heart rate reduction in coronary artery disease and heart failure. Nat Rev Cardiol. 2016;13(8):493-501.

Flaherty EG, Thompson R, Dubowitz H, et al. Adverse childhood experiences and child health in early adolescence. JAMA Pediatr. 2013;167(7):622-9.

Fosgerau K, Hoffmann T. Peptide therapeutics: current status and future directions. Drug Discov Today. 2015;20(1):122-8.

Foty R. A simple hanging drop cell culture protocol for generation of 3D spheroids. J Vis Exp. 2011;(51)

Frey N, Olson EN. Cardiac hypertrophy: the good, the bad, and the ugly. Annu Rev Physiol. 2003;65:45-79.

Frost JA, Khokhlatchev A, Stippec S, White MA, Cobb MH. Differential effects of PAK1-activating mutations reveal activity-dependent and -independent effects on cytoskeletal regulation. J Biol Chem. 1998;273(43):28191-8.

Gatti A, Huang Z, Tuazon PT, Traugh JA. Multisite autophosphorylation of p21-activated protein kinase gamma-PAK as a function of activation. J Biol Chem. 1999;274(12):8022-8.

Giamas G, Stebbing J, Vorgias CE, Knippschild U. Protein kinases as targets for cancer treatment. Pharmacogenomics. 2007;8(8):1005-16.

Glaab E. Building a virtual ligand screening pipeline using free software: a survey. Brief Bioinformatics. 2016;17(2):352-66.

Goicoechea SM, Bednarski B, García-mata R, Prentice-dunn H, Kim HJ, Otey CA. Palladin contributes to invasive motility in human breast cancer cells. Oncogene. 2009;28(4):587-98.

Gordon LJ, Allen M, Artursson P, et al. Direct Measurement of Intracellular Compound Concentration by RapidFire Mass Spectrometry Offers Insights into Cell Permeability. J Biomol Screen. 2016;21(2):156-64.

Gross S, Rahal R, Stransky N, Lengauer C, Hoeflich KP. Targeting cancer with kinase inhibitors. J Clin Invest. 2015;125(5):1780-9.

Guo J, Macdonell KL, Giles WR. Effects of sphingosine 1-phosphate on pacemaker activity in rabbit sino-atrial node cells. Pflugers Arch. 1999;438(5):642-8.

Gururaj, A., Barnes, C. J., Vadlamudi, R. K., & Kumar, R. (2004). Regulation of phosphoglucomutase 1 phosphorylation and activity by a signaling kinase. Oncogene, 23(49), 8118–8127. http://doi.org/10.1038/sj.onc.1207969

Ha BH, Davis MJ, Chen C, et al. Type II p21-activated kinases (PAKs) are regulated by an autoinhibitory pseudosubstrate. Proc Natl Acad Sci USA. 2012;109(40):16107-12

Ha BH, Boggon TJ. CDC42 binds PAK4 via an extended GTPase-effector interface. Proc Natl Acad Sci USA. 2018;115(3):531-536.

Harms FL, Kloth K, Bley A, et al. Activating Mutations in PAK1, Encoding p21-Activated Kinase 1, Cause a Neurodevelopmental Disorder. Am J Hum Genet. 2018;103(4):579-591.

He H, Hirokawa Y, Gazit A, et al. The Tyr-kinase inhibitor AG879, that blocks the ETK-PAK1 interaction, suppresses the RAS-induced PAK1 activation and malignant transformation. Cancer Biol Ther. 2004;3(1):96-101.

Hecht D, Fogel GB. Computational intelligence methods for docking scores. Curr Comput-Aided Drug Des. 2009;5:56–68. doi: 10.2174/157340909787580863.

Heineke J, Molkentin JD. Regulation of cardiac hypertrophy by intracellular signalling pathways. Nat Rev Mol Cell Biol. 2006;7(8):589-600.

Higuchi M, Onishi K, Kikuchi C, Gotoh Y. Scaffolding function of PAK in the PDK1-Akt pathway. Nat Cell Biol. 2008;10(11):1356-64.

Huang SY, Grinter SZ, Zou X. Scoring functions and their evaluation methods for protein-ligand docking: recent advances and future directions. Phys Chem Chem Phys. 2010;12(40):12899-908.

Irwin JJ, Shoichet BK. ZINC--a free database of commercially available compounds for virtual screening. J Chem Inf Model. 2005;45(1):177-82.

Jackson LR, Ju C, Zettler M, et al. Outcomes of Patients With Acute Myocardial Infarction Undergoing Percutaneous Coronary Intervention Receiving an Oral Anticoagulant and Dual Antiplatelet Therapy: A Comparison of Clopidogrel Versus Prasugrel From the TRANSLATE-ACS Study. JACC Cardiovasc Interv. 2015;8(14):1880-9.

Jha RK, Wu YI, Zawistowski JS, Macnevin C, Hahn KM, Kuhlman B. Redesign of the PAK1 autoinhibitory domain for enhanced stability and affinity in biosensor applications. J Mol Biol. 2011;413(2):513-22.

Jin ZQ, Zhang J, Huang Y, Hoover HE, Vessey DA, Karliner JS. A sphingosine kinase 1 mutation sensitizes the myocardium to ischemia/reperfusion injury. Cardiovasc Res. 2007;76(1):41-50.

Johnson LN, Noble ME, Owen DJ. Active and inactive protein kinases: structural basis for regulation. Cell. 1996;85(2):149-58.

Jorgensen WL. The many roles of computation in drug discovery. Science. 2004;303(5665):1813-8.

Jorgensen WL, Thomas LL. Perspective on Free-Energy Perturbation Calculations for Chemical Equilibria. J Chem Theory Comput. 2008;4(6):869–876. doi:10.1021/ct800011m

Kaitin KI, Dimasi JA. Pharmaceutical innovation in the 21st century: new drug approvals in the first decade, 2000-2009. Clin Pharmacol Ther. 2011;89(2):183-8.

Ke Y, Wang L, Pyle WG, De tombe PP, Solaro RJ. Intracellular localization and functional effects of P21-activated kinase-1 (Pak1) in cardiac myocytes. Circ Res. 2004;94(2):194-200.

Ke Y, Lei M, Collins TP, et al. Regulation of L-type calcium channel and delayed rectifier potassium channel activity by p21-activated kinase-1 in guinea pig sinoatrial node pacemaker cells. Circ Res. 2007;100(9):1317-27.

Ke Y, Lei M, Solaro RJ. Regulation of cardiac excitation and contraction by p21 activated kinase-1. Prog Biophys Mol Biol. 2008;98(2-3):238-50.

Ke Y, Sheehan KA, Egom EE, Lei M, Solaro RJ. Novel bradykinin signaling in adult rat cardiac myocytes through activation of p21-activated kinase. Am J Physiol Heart Circ Physiol. 2010;298(4):H1283-9.

Ke Y, Lei M, Wang X, Solaro RJ. Novel roles of PAK1 in the heart. Cell Logist. 2012;2(2):89-94.

Ke Y, Lei M, Wang X, Solaro RJ. Unique catalytic activities and scaffolding of p21 activated kinase-1 in cardiovascular signaling. Front Pharmacol. 2013;4:116. Published 2013 Sep 27. doi:10.3389/fphar.2013.00116

Kichina JV, Goc A, Al-husein B, Somanath PR, Kandel ES. PAK1 as a therapeutic target. Expert Opin Ther Targets. 2010;14(7):703-25.

King CC, Gardiner EM, Zenke FT, et al. p21-activated kinase (PAK1) is phosphorylated and activated by 3-phosphoinositide-dependent kinase-1 (PDK1). J Biol Chem. 2000;275(52):41201-9.

Knaus UG, Bokoch GM. The p21Rac/Cdc42-activated kinases (PAKs). Int J Biochem Cell Biol. 1998;30(8):857-62.

Knollmann BC, Chopra N, Hlaing T, et al. Casq2 deletion causes sarcoplasmic reticulum volume increase, premature Ca2+ release, and catecholaminergic polymorphic ventricular tachycardia. J Clin Invest. 2006;116(9):2510-20.

. Kobayashi K, Hagiwara K. Epidermal growth factor receptor (EGFR) mutation and personalized therapy in advanced nonsmall cell lung cancer (NSCLC). Target Oncol. 2013;8(1):27-33.

Kumar R, Gururaj AE, Barnes CJ. p21-activated kinases in cancer. Nat Rev Cancer. 2006;6(6):459-71.

Kumar R, Li DQ. PAKs in Human Cancer Progression: From Inception to Cancer Therapeutic to Future Oncobiology. Adv Cancer Res. 2016;130:137-209.

Kushnir A, Marks AR. The ryanodine receptor in cardiac physiology and disease. Adv Pharmacol. 2010;59:1–30. doi:10.1016/S1054-3589(10)59001-X

Kwon YG, Min JK, Kim KM, Lee DJ, Billiar TR, Kim YM. Sphingosine 1-phosphate protects human umbilical vein endothelial cells from serum-deprived apoptosis by nitric oxide production. J Biol Chem. 2001;276(14):10627-33.

Langsdorf EF, Malikzay A, Lamarr WA, et al. Screening for antibacterial inhibitors of the UDP-3-O-(R-3-hydroxymyristoyl)-N-acetylglucosamine deacetylase (LpxC) using a high-throughput mass spectrometry assay. J Biomol Screen. 2010;15(1):52-61.

Leenhardt A, Denjoy I, Guicheney P. Catecholaminergic polymorphic ventricular tachycardia. Circ Arrhythm Electrophysiol. 2012;5(5):1044-52.

Leeson PD, Springthorpe B. The influence of drug-like concepts on decision-making in medicinal chemistry. Nat Rev Drug Discov. 2007;6(11):881-90.

Lei M, Lu W, Meng W, et al. Structure of PAK1 in an autoinhibited conformation reveals a multistage activation switch. Cell. 2000;102(3):387-97.

Lei M, Ke Y, Solaro RJ. Pak1: steps towards understanding the regulatory mechanisms of pacemaker function of the heart. Future Cardiol. 2007;3(5):473-6.

Lei M, Wang X, Ke Y, Solaro RJ. Regulation of Ca(2+) transient by PP2A in normal and failing heart. Front Physiol. 2015;6:13.

Lei M, Wu L, Terrar DA, Huang CL. Modernized Classification of Cardiac Antiarrhythmic Drugs. Circulation. 2018;138(17):1879-1896.

Li Z, Hannigan M, Mo Z, et al. Directional sensing requires G beta gamma-mediated PAK1 and PIX alpha-dependent activation of Cdc42. Cell. 2003;114(2):215-27.

Lipinski CA. Lead- and drug-like compounds: the rule-of-five revolution. Drug Discov Today Technol. 2004;1(4):337-41.

Liu J, Zhang C, Tao W, Liu M. Systematic review and meta-analysis of the efficacy of sphingosine-1-phosphate (S1P) receptor agonist FTY720 (fingolimod) in animal models of stroke. Int J Neurosci. 2013;123(3):163-9.

Liu W, Zi M, Chi H, et al. Deprivation of MKK7 in cardiomyocytes provokes heart failure in mice when exposed to pressure overload. J Mol Cell Cardiol. 2011;50(4):702-11.

Liu W, Zi M, Tsui H, et al. A novel immunomodulator, FTY-720 reverses existing cardiac hypertrophy and fibrosis from pressure overload by targeting NFAT (nuclear factor of activated T-cells) signaling and periostin. Circ Heart Fail. 2013;6(4):833-44.

Lonsdale R, Ward RA. Structure-based design of targeted covalent inhibitors. Chem Soc Rev. 2018;47(11):3816-3830.

Lu W, Katz S, Gupta R, Mayer BJ. Activation of Pak by membrane localization mediated by an SH3 domain from the adaptor protein Nck. Curr Biol. 1997;7(2):85-94.

Lu X, Wang L, Chen S, et al. Genome-wide association study in Han Chinese identifies four new susceptibility loci for coronary artery disease. Nat Genet. 2012;44(8):890-4.

Maksimoska J, Feng L, Harms K, et al. Targeting large kinase active site with rigid, bulky octahedral ruthenium complexes. J Am Chem Soc. 2008;130(47):15764-5.

Manser E, Huang HY, Loo TH, et al. Expression of constitutively active alpha-PAK reveals effects of the kinase on actin and focal complexes. Mol Cell Biol. 1997;17(3):1129-43.

Mao K, Kobayashi S, Jaffer ZM, et al. Regulation of Akt/PKB activity by P21-activated kinase in cardiomyocytes. J Mol Cell Cardiol. 2008;44(2):429-34.

Marti-Renom MA, Stuart AC, Fiser A, Sanchez R, Melo F, Sali A. Comparative protein structure modeling of genes and genomes. Annu. Rev. Biophys. Biomol. Struct. 2000;29:291–325.

Mayhew MW, Jeffery ED, Sherman NE, et al. Identification of phosphorylation sites in betaPIX and PAK1. J Cell Sci. 2007;120(Pt 22):3911–3918. doi:10.1242/jcs.008177

Mccoull W, Hennessy EJ, Blades K, et al. Optimization of Highly Kinase Selective Bis-anilino Pyrimidine PAK1 Inhibitors. ACS Med Chem Lett. 2016;7(12):1118-1123.

Mcgovern SL, Caselli E, Grigorieff N, Shoichet BK. A common mechanism underlying promiscuous inhibitors from virtual and high-throughput screening. J Med Chem. 2002;45(8):1712-22.

Mcgovern SL, Helfand BT, Feng B, Shoichet BK. A specific mechanism of nonspecific inhibition. J Med Chem. 2003;46(20):4265-72.

Mcnamara CW, Lee MC, Lim CS, et al. Targeting Plasmodium PI(4)K to eliminate malaria. Nature. 2013;504(7479):248-253.

Meng E. C., Shoichet B. K., Kuntz I. D. (1992). Automated docking with grid-based energy evaluation. J. Comput. Chem. 13 505–524. 10.1002/jcc.540130412

Messersmith WA, Ahnen DJ. Targeting EGFR in colorectal cancer. N Engl J Med. 2008;359(17):1834-6.

Miano JM, Long X, Fujiwara K. Serum response factor: master regulator of the actin cytoskeleton and contractile apparatus. Am J Physiol, Cell Physiol. 2007;292(1):C70-81

Molkentin JD. Calcineurin-NFAT signaling regulates the cardiac hypertrophic response in coordination with the MAPKs. Cardiovasc Res. 2004;63(3):467-75.

Morphy R. The influence of target family and functional activity on the physicochemical properties of pre-clinical compounds. J Med Chem. 2006;49(10):2969-78.

Morreale A, Venkatesan M, Mott HR, et al. Structure of Cdc42 bound to the GTPase binding domain of PAK. Nat Struct Biol. 2000;7(5):384-8.

Murray BW, Guo C, Piraino J, et al. Small-molecule p21-activated kinase inhibitor PF-3758309 is a potent inhibitor of oncogenic signaling and tumor growth. Proc Natl Acad Sci USA. 2010;107(20):9446-51.

Najm P, El-Sibai M. Palladin regulation of the actin structures needed for cancer invasion. Cell Adh Migr. 2014;8(1):29–35. doi:10.4161/cam.28024

Nakajima N, Cavalli AL, Biral D, et al. Expression and characterization of Edg-1 receptors in rat cardiomyocytes: calcium deregulation in response to sphingosine 1-phosphate. Eur J Biochem. 2000;267(18):5679-86.

Napoli C, Infante T, Casamassimi A. Maternal-foetal epigenetic interactions in the beginning of cardiovascular damage. Cardiovasc Res. 2011;92(3):367-74.

Napolitano C, Priori SG and Bloise R. Catecholaminergic polymorphic ventricular tachycardia. GeneReviews. NCBI/NIH. Initial posting 2004, last update 2009

Nassar MA, Stirling LC, Forlani G, et al. Nociceptor-specific gene deletion reveals a major role for Nav1.7 (PN1) in acute and inflammatory pain. Proc Natl Acad Sci USA. 2004;101(34):12706-11.

Navab M, Reddy ST, Van lenten BJ, Fogelman AM. HDL and cardiovascular disease: atherogenic and atheroprotective mechanisms. Nat Rev Cardiol. 2011;8(4):222-32.

Ndubaku CO, Crawford JJ, Drobnick J, et al. Design of Selective PAK1 Inhibitor G-5555: Improving Properties by Employing an Unorthodox Low-pK a Polar Moiety. ACS Med Chem Lett. 2015;6(12):1241–1246. Published 2015 Oct 31. doi:10.1021/acsmedchemlett.5b00398

Nelson CP, Goel A, Butterworth AS, et al. Association analyses based on false discovery rate implicate new loci for coronary artery disease. Nat Genet. 2017;49(9):1385-1391.

Nie J, Sun C, Faruque O, et al. Synapses of amphids defective (SAD-A) kinase promotes glucose-stimulated insulin secretion through activation of p21-activated kinase (PAK1) in pancreatic β-Cells. J Biol Chem. 2012;287(31):26435-44.

Nikpay M, Goel A, Won HH, et al. A comprehensive 1,000 Genomes-based genome-wide association meta-analysis of coronary artery disease. Nat Genet. 2015;47(10):1121-1130.

Niu G, Scherlag BJ, Lu Z, et al. An acute experimental model demonstrating 2 different forms of sustained atrial tachyarrhythmias. Circ Arrhythm Electrophysiol. 2009;2(4):384-92.

Niu Z, Yu W, Zhang SX, et al. Conditional mutagenesis of the murine serum response factor gene blocks cardiogenesis and the transcription of downstream gene targets. J Biol Chem. 2005;280(37):32531-8.

Ockene IS, Miller NH. Cigarette smoking, cardiovascular disease, and stroke: a statement for healthcare professionals from the American Heart Association. American Heart Association Task Force on Risk Reduction. Circulation. 1997;96(9):3243-7.

Ong CC, Jubb AM, Haverty PM, et al. Targeting p21-activated kinase 1 (PAK1) to induce apoptosis of tumor cells. Proc Natl Acad Sci USA. 2011;108(17):7177-82.

Outeiro TF, Kontopoulos E, Altmann SM, et al. Sirtuin 2 inhibitors rescue alpha-synuclein-mediated toxicity in models of Parkinson's disease. Science. 2007;317(5837):516-9.

Pando MP, Pinchak AB, Cermakian N, Sassone-corsi P. A cell-based system that recapitulates the dynamic light-dependent regulation of the vertebrate clock. Proc Natl Acad Sci USA. 2001;98(18):10178-83.

Papakonstanti EA, Stournaras C: Tumor necrosis factor-alpha promotes survival of opossum kidney via Cdc42-induced phospholipase C-gamma 1 activation and actin filament redistribution. Mol Biol Cell 15 : 1273 –1286, 2004

Parrini MC, Lei M, Harrison SC, Mayer BJ. Pak1 kinase homodimers are autoinhibited in trans and dissociated upon activation by Cdc42 and Rac1. Mol Cell. 2002;9(1):73-83.

Parrini MC, Matsuda M, De gunzburg J. Spatiotemporal regulation of the Pak1 kinase. Biochem Soc Trans. 2005;33(Pt 4):646-8.

Peng X, He Q, Li G, Ma J, Zhong TP. Rac1-PAK2 pathway is essential for zebrafish heart regeneration. Biochem Biophys Res Commun. 2016;472(4):637-42.

Peters SL, Alewijnse AE. Sphingosine-1-phosphate signaling in the cardiovascular system. Curr Opin Pharmacol. 2007;7(2):186-92.

Priori SG, Blomström-lundqvist C, Mazzanti A, et al. 2015 ESC Guidelines for the management of patients with ventricular arrhythmias and the prevention of sudden cardiac death: The Task Force for the Management of Patients with Ventricular Arrhythmias and the Prevention of Sudden Cardiac Death of the European Society of Cardiology (ESC). Endorsed by: Association for European Paediatric and Congenital Cardiology (AEPC). Eur Heart J. 2015;36(41):2793-2867.

Proudfoot JR. The evolution of synthetic oral drug properties. Bioorg Med Chem Lett. 2005;15(4):1087-90.

Qu Q, Russell PL, Sharom FJ. Stoichiometry and affinity of nucleotide binding to P-glycoprotein during the catalytic cycle. Biochemistry. 2003;42(4):1170-7.

Quercia AK, Lamarr WA, Myung J, Ozbal CC, Landro JA, Lumb KJ. High-throughput screening by mass spectrometry: comparison with the scintillation proximity assay with a focused-file screen of AKT1/PKB alpha. J Biomol Screen. 2007;12(4):473-80.

Radu M, Semenova G, Kosoff R, Chernoff J. PAK signalling during the development and progression of cancer. Nat Rev Cancer. 2014;14(1):13-25.

Reid BG, Stratton MS, Bowers S, et al. Discovery of novel small molecule inhibitors of cardiac hypertrophy using high throughput, high content imaging. J Mol Cell Cardiol. 2016;97:106-13.

Reid DS, Tynan M, Braidwood L, Fitzgerald GR. Bidirectional tachycardia in a child. A study using His bundle electrography. Br Heart J. 1975;37(3):339-44.

Renkema GH, Pulkkinen K, Saksela K. Cdc42/Rac1-mediated activation primes PAK2 for superactivation by tyrosine phosphorylation. Mol Cell Biol. 2002;22(19):6719-25.

Rider L, Shatrova A, Feener EP, Webb L, Diakonova M. JAK2 tyrosine kinase phosphorylates PAK1 and regulates PAK1 activity and functions. J Biol Chem. 2007;282(42):30985-96.

Ripphausen P, Nisius B, Peltason L, Bajorath J. Quo vadis, virtual screening? A comprehensive survey of prospective applications. J Med Chem. 2010;53(24):8461-7.

Roerecke M, Rehm J. Irregular heavy drinking occasions and risk of ischemic heart disease: a systematic review and meta-analysis. Am J Epidemiol. 2010;171(6):633-44

Rognan D. The impact of in silico screening in the discovery of novel and safer drug candidates. Pharmacol Ther. 2017;175:47-66.

Ronksley PE, Brien SE, Turner BJ, Mukamal KJ, Ghali WA. Association of alcohol consumption with selected cardiovascular disease outcomes: a systematic review and meta-analysis. BMJ. 2011;342:d671.

Rosado-muñoz A, Martínez-martínez JM, Escandell-montero P, Soria-olivas E. Visual data mining with self-organising maps for ventricular fibrillation analysis. Comput Methods Programs Biomed. 2013;111(2):269-79.

Rose BA, Force T, Wang Y. Mitogen-activated protein kinase signaling in the heart: angels versus demons in a heart-breaking tale. Physiol Rev. 2010;90(4):1507-46.

Ross R. Atherosclerosis--an inflammatory disease. N Engl J Med. 1999;340(2):115-26.

Rosso R, Kalman JM, Rogowski O, et al. Calcium channel blockers and beta-blockers versus beta-blockers alone for preventing exercise-induced arrhythmias in catecholaminergic polymorphic ventricular tachycardia. Heart Rhythm. 2007;4(9):1149-54.

Roth GA, Huffman MD, Moran AE, et al. Global and regional patterns in cardiovascular mortality from 1990 to 2013. Circulation. 2015;132(17):1667-78.

Schunkert H, König IR, Kathiresan S, et al. Large-scale association analysis identifies 13 new susceptibility loci for coronary artery disease. Nat Genet. 2011;43(4):333-8.

Sells MA, Knaus UG, Bagrodia S, Ambrose DM, Bokoch GM, Chernoff J. Human p21-activated kinase (Pak1) regulates actin organization in mammalian cells. Curr Biol. 1997;7(3):202-10.

Sheehan KA, Ke Y, Wolska BM, Solaro RJ. Expression of active p21-activated kinase-1 induces Ca2+ flux modification with altered regulatory protein phosphorylation in cardiac myocytes. Am J Physiol, Cell Physiol. 2009;296(1):C47-58.

Sim DS, Kauser K. In Vivo Target Validation Using Biological Molecules in Drug Development. Handb Exp Pharmacol. 2016;232:59-70.

Singhal R, Kandel ES. The response to PAK1 inhibitor IPA3 distinguishes between cancer cells with mutations in BRAF and Ras oncogenes. Oncotarget. 2012;3(7):700–708. doi:10.18632/oncotarget.587

Slack-davis JK, Eblen ST, Zecevic M, et al. PAK1 phosphorylation of MEK1 regulates fibronectin-stimulated MAPK activation. J Cell Biol. 2003;162(2):281-91.

Snir M, Kehat I, Gepstein A, et al. Assessment of the ultrastructural and proliferative properties of human embryonic stem cell-derived cardiomyocytes. Am J Physiol Heart Circ Physiol. 2003;285(6):H2355-63.

Sousa SF, Fernandes PA, Ramos MJ. Protein-ligand docking: current status and future challenges. Proteins. 2006;65(1):15-26.

Spiegel S, Milstien S. Sphingosine-1-phosphate: an enigmatic signalling lipid. Nat Rev Mol Cell Biol. 2003;4(5):397-407.

Staben ST, Feng JA, Lyle K, et al. Back pocket flexibility provides group II p21-activated kinase (PAK) selectivity for type I 1/2 kinase inhibitors. J Med Chem. 2014;57(3):1033-45.

Stelzer AC, Frank AT, Kratz JD, et al. Discovery of selective bioactive small molecules by targeting an RNA dynamic ensemble. Nat Chem Biol. 2011;7(8):553-9.

Sterling T, Irwin JJ. ZINC 15--Ligand Discovery for Everyone. J Chem Inf Model. 2015;55(11):2324-37.

Still W. C., Tempczyk A., Hawley R. C., Hendrickson T. (1990). Semianalytical treatment of solvation for molecular mechanics and dynamics. J. Am. Chem. Soc. 112 6127–6129. 10.1021/ja00172a038

Sun L, Zong G, Pan A, et al. Elevated plasma ferritin is associated with increased incidence of type 2 diabetes in middle-aged and elderly Chinese adults. J Nutr. 2013;143(9):1459-65.

Taglieri DM, Monasky MM, Knezevic I, et al. Ablation of p21-activated kinase-1 in mice promotes isoproterenol-induced cardiac hypertrophy in association with activation of Erk1/2 and inhibition of protein phosphatase 2A. J Mol Cell Cardiol. 2011;51(6):988-96.

Tao J, Oladimeji P, Rider L, Diakonova M. PAK1-Nck regulates cyclin D1 promoter activity in response to prolactin. Mol Endocrinol. 2011;25(9):1565-78.

Totrov M, Abagyan R. Flexible ligand docking to multiple receptor conformations: a practical alternative. Curr Opin Struct Biol. 2008;18(2):178–184. doi:10.1016/j.sbi.2008.01.004

Trott O, Olson AJ. AutoDock Vina: improving the speed and accuracy of docking with a new scoring function, efficient optimization, and multithreading. J Comput Chem. 2010;31(2):455–461. doi:10.1002/jcc.21334.

Tu H, Wigler M. Genetic evidence for Pak1 autoinhibition and its release by Cdc42. Mol Cell Biol. 1999;19(1):602-11.

Van der Horst IC, Voors AA, van Veldhuisen DJ. Treatment of heart failure with ACE inhibitors and beta-blockers: what is next? Aldosterone receptor antagonists?. Clin Res Cardiol. 2007;96(4):193–195. doi:10.1007/s00392-007-0487-y

Veber DF, Johnson SR, Cheng HY, Smith BR, Ward KW, Kopple KD. Molecular properties that influence the oral bioavailability of drug candidates. J Med Chem. 2002;45(12):2615-23.

Vessey DA, Kelley M, Li L, Huang Y. Sphingosine protects aging hearts from ischemia/reperfusion injury: Superiority to sphingosine 1-phosphate and ischemic pre- and post-conditioning. Oxid Med Cell Longev. 2009;2(3):146-51.

Vieth M, Siegel MG, Higgs RE, et al. Characteristic physical properties and structural fragments of marketed oral drugs. J Med Chem. 2004;47(1):224-32.

Vlieghe P, Lisowski V, Martinez J, Khrestchatisky M. Synthetic therapeutic peptides: science and market. Drug Discov Today. 2010;15(1-2):40-56.

Vogelstein B, Papadopoulos N, Velculescu VE, Zhou S, Diaz LA, Kinzler KW. Cancer genome landscapes. Science. 2013;339(6127):1546-58.

Wang H, Ngwenyama N, Liu Y, Walker JC, Zhang S. Stomatal development and patterning are regulated by environmentally responsive mitogen-activated protein kinases in Arabidopsis. Plant Cell. 2007;19(1):63-73.

Wang J, Wu JW, Wang ZX. Structural insights into the autoactivation mechanism of p21-activated protein kinase. Structure. 2011;19(12):1752-61.

Wang R, Lu Y, Fang X, Wang S. An extensive test of 14 scoring functions using the PDBbind refined set of 800 protein-ligand complexes. J Chem Inf Comput Sci. 2004;44(6):2114-25.

Wang R, Wang Y, Lin WK, et al. Inhibition of angiotensin II-induced cardiac hypertrophy and associated ventricular arrhythmias by a p21 activated kinase 1 bioactive peptide. PLoS ONE. 2014;9(7):e101974.

Wang Y, Tsui H, Bolton EL, et al. Novel insights into mechanisms for Pak1-mediated regulation of cardiac Ca(2+) homeostasis. Front Physiol. 2015;6:76.

Wang Z, Ma L, Su M, et al. Baicalin induces cellular senescence in human colon cancer cells via upregulation of DEPP and the activation of Ras/Raf/MEK/ERK signaling. Cell Death Dis. 2018;9(2):217.

Warren GL, Andrews CW, Capelli AM, et al. A critical assessment of docking programs and scoring functions. J Med Chem. 2006;49(20):5912-31.

Wenlock MC, Austin RP, Barton P, Davis AM, Leeson PD. A comparison of physiochemical property profiles of development and marketed oral drugs. J Med Chem. 2003;46(7):1250-6.

WHO. Int, Cardiovascular Disease (CVDs). N.P. 2018

Woolfolk EA, Eguchi S, Ohtsu H, et al. Angiotensin II-induced activation of p21-activated kinase 1 requires Ca2+ and protein kinase C{delta} in vascular smooth muscle cells. Am J Physiol, Cell Physiol. 2005;289(5):C1286-94.

Wu X, Wang J, Tan L, et al. In vitro ADME profiling using high-throughput rapidfire mass spectrometry: cytochrome p450 inhibition and metabolic stability assays. J Biomol Screen. 2012;17(6):761-72.

Yu J, Zhang Y, Mcilroy J, Rordorf-nikolic T, Orr GA, Backer JM. Regulation of the p85/p110 phosphatidylinositol 3'-kinase: stabilization and inhibition of the p110alpha catalytic subunit by the p85 regulatory subunit. Mol Cell Biol. 1998;18(3):1379-87.

Zenke FT, King CC, Bohl BP, Bokoch GM. Identification of a central phosphorylation site in p21-activated kinase regulating autoinhibition and kinase activity. J Biol Chem. 1999;274(46):32565-73.

Zhang J, Zhang F, Ebert D, Cobb MH, Goldsmith EJ. Activity of the MAP kinase ERK2 is controlled by a flexible surface loop. Structure. 1995;3(3):299-307.

Zhao ZS, Manser E, Chen XQ, Chong C, Leung T, Lim L. A conserved negative regulatory region in alphaPAK: inhibition of PAK kinases reveals their morphological roles downstream of Cdc42 and Rac1. Mol Cell Biol. 1998;18(4):2153-63.

Zhao ZS, Manser E. PAK family kinases: Physiological roles and regulation. Cell Logist. 2012;2(2):59-68.

Zhong HJ, Liu LJ, Chong CM, et al. Discovery of a natural product-like iNOS inhibitor by molecular docking with potential neuroprotective effects in vivo. PLoS ONE. 2014;9(4):e92905.

Zhou GL, Zhuo Y, King CC, Fryer BH, Bokoch GM, Field J. Akt phosphorylation of serine 21 on Pak1 modulates Nck binding and cell migration. Mol Cell Biol. 2003;23(22):8058-69.

Zhou K, Wang Y, Gorski JL, Nomura N, Collard J, Bokoch GM. Guanine nucleotide exchange factors regulate specificity of downstream signaling from Rac and Cdc42. J Biol Chem. 1998;273(27):16782-6.

APPENDIX

- Appendix 1. *Experimental Methods*
- Appendix 2. *In silico* Virtual Ligand Screening Software
- Appendix 3. *JB Compounds Overview*
- Appendix 4. *Physiochemical Properties* & *Efficacies of JB Compounds*
- Appendix 5. *Co-Crystallography Result Report (prepared by Proteros)*

Appendix 1: Experimental Methods

A.1.1 In silico studies of PAK1 Activating Peptides

Partial PAK1 crystal structures were obtained from the Protein Data Bank (PDB), accession code no. 2b8l. After the water molecules and inhibitor were removed from the whole structure, the autodocking VINA program was used to predict the binding affinity of the ligands. In this study, autodocking parameters used for the x- y- z-dimension were 96, 126, and 126, respectively. The center grid box x- y- z-centers were 6.94, 49.889, and 55.72, respectively. The highest calculated affinity was used to predict the binding site of the peptide. Plymol program was used to produce the images and for structural analysis.

A.1.2 ADP-GLO Kinase Assay

A.1.2.1 Kinase Assay Conditions

All kinase reactions were performed using the ADP-Glo™ kinase assay kit from Promega Corporation. Kinase reactions were performed in Reaction Buffer A (40 mM Tris, pH 7.5, 20 mM MgCl2, 2mM DTT and 0.1 mg/mL BSA), GTP Solution (250um) and ATP Assay solution (250uM ATP) at 30 °C for 90 minutes. An ATP-ADP standard conversion curve was generated to assess the linearity of the assay and to correlate specific activities of the kinase based on the amount of ADP produced.

A.1.2.2 Kinase Assay Procedures

The kinase assays were performed using a standard technique described in the Promega ADP-Glo™ Kinase Assay Technical Manual. Initial reaction volumes of 20ul – containing 5ul of diluted active kinase (100ng) with the drug of interest, 5ul of 0.5mM GTP solution, 5ul 2x reaction buffer A and 5ul of 250um ATP Assay solution – were prepared and incubated at 30°C for 90 minutes. After the incubation period, 25µL ADP-Glo™ reagent was added to the reaction to quench up the left over ATP and to prevent further reactions. The plate was incubated at room temperature for 40 minutes. Finally, 50 µL of kinase detection reagent was added at room temperature for 60 minutes. Luminescence was recorded and EC_{50}/IC_{50} values were determined.

A.1.2.3 Luminescence Measurements

Final reactions were transferred to a 96-well reaction plate (Corning® 96-well clear-bottom plates, CLS3603 SIGMA) and luminescence was recorded using POLARstar OPTIMA. An ATP-ADP standard curve was used to predict the amount of ATP conversion and to calculate the kinase-specific activity.

A.1.3 Rapid-Fire™ Mass spectrometry Kinase Assay (Dose-Response Test)

All kinase assays were performed on 96 Target Well Plates, 500 ul, Round Bottom plates. Assays were prepared at room temperature using a reaction buffer (Abcam kinase assay buffer 1, ab189135) containing 25 mM MOPS, pH7.2, 12.5 mM ß-glycerol-phosphate, 25 mM MgCl2, 5 mM EGTA and 2 mM EDTA. PAK1 and CDC42 were added to a final concentration of 20 nM and 0.5μM, respectively to the buffer solution – protein buffer volume constituting 80uL. Compounds dissolved in 1uL DMSO were diluted in the of assay buffer (final DMSO concentration 1%). The reaction was initiated by adding 20uL substrate solutions, containing PAKtide (30 µM final concentration) and adenosine triphosphate (100 µM final concentration). The total reaction volume was 100 µL. The optimal kinase reaction time at RT is considered to be 25~30 minutes.

Assay plates were transferred to a RapidFire365 integrated autosampler/SPE system coupled with 6530 QTOF (Agilent Technologies). Samples were aspirated from each well for 500 ms, and 10 µL was loaded directly onto a RapidFire micro-scale SPE C4 (type C) cartridge. Solvent A, used for sample loading and washing, was water containing 0.1% (v/v) formic acid. Solvent B, used for sample elution, was acetonitrile (v/v) containing 0.1% (v/v) formic acid. The 10 µL of sample was loaded onto the C4 cartridge and washed for 3 s with Solvent A to remove any non-organic components. Analytes were then eluted into the mass spectrometer, in a 3 s elution cycle, using Solvent B, and the cartridge was then equilibrated by washing with Solvent A for 500 ms.

Agilent RapidFire 4.0 and Agilent MassHunter B.07.00 software was used for instrument acquisition and data processing. Quantitative analysis was performed for each analyte of interest by calculating the ratio of the area of the most abundant ion with respect to the area of the internal standard. The ratio of peptide substrate and phosphorylated product were analyzed masses at 1921.1 (substrate) and 2006.1 (product) to measure their quantity

A.1.4 Rapid-Fire™ Mass spectrometry Kinase Assay (Kinetic Assay)

All kinase assays were performed on 1.1mL polystyrene 96-well deep well plates. Assays were prepared at room temperature using a reaction buffer (abcam kinase assay buffer 1, ab189135) containing 25 mM MOPS, pH7.2, 12.5 mM ß-glycerol-phosphate, 25 mM MgCl2, 5 mM EGTA and 2 mM EDTA. PAK1 and CDC42 were added to a final concentration of 20 nM and 0.5μM, respectively to the buffer solution – protein buffer solution volume constituting 795uL. Compounds dissolved in 5uL DMSO were diluted in 800 µL of assay buffer (final DMSO concentration 0.5%). The reaction was initiated by adding 200uL substrate solutions, containing PAKtide (30 µM final concentration) and adenosine triphosphate (100 µM final concentration). The total reaction volume was 1000 µL.

Assay plates were transferred to a RapidFire365 integrated autosampler/SPE system coupled with 6530 QTOF (Agilent Technologies). Samples were aspirated from each well for 500 ms, and 10 µL was loaded directly onto a RapidFire micro-scale SPE C4 (type C) cartridge. Solvent A, used for sample loading and washing, was water containing 0.1% (v/v) formic acid. Solvent B, used for sample elution, was acetonitrile (v/v) containing 0.1% (v/v) formic acid. The 10 µL of sample was loaded onto the C4 cartridge and washed for 3 s with Solvent A to remove any non-organic components. Analytes were then eluted into the mass spectrometer, in a 3 s elution cycle, using Solvent B, and the cartridge was then equilibrated by washing with Solvent A for 500 ms. In kinetic assays, the sample readouts are repeated at different time intervals in order to ensure that enough data points are acquired in plotting a kinetic response of PAK1 activity.

Agilent RapidFire 4.0 and Agilent MassHunter B.07.00 software was used for instrument acquisition and data processing. Quantitative analysis was performed for each analyte of interest by calculating the ratio of the area of the most abundant ion with respect to the area of the internal standard. The ratio of peptide substrate and phosphorylated product were analyzed masses at 1921.1 (substrate) and 2006.1 (product) to measure their quantity

A.1.5 Preparation of Isolated Cardiac Myocytes

Isolated myocytes were isolated from the ventricles of male Sprague-Dawley rats (300-325g) using enzymatic digestion and mechanical dispersion. Animals were sacrificed by

stunning followed by cervical dislocation. The heart was rapidly removed and rinsed in isolation solution composed of (in $mmol.l^{-1}$):NaCl, 120; KCl, 4; $MgCl_2$, 1.2 ; glucose, 11; HEPES, 10; NaH_2PO_4, 2; pyruvic acid, 2.5; pH 7.4 at 37°C; supplemented with heparin sodium ($5U.l^{-1}$). The heart was mounted onto a Langendorff perfusion apparatus with a peristaltic pump (flow approximately $7ml.min^{-1}$). The heart was perfused with heparinised isolation solution until fully cleared of blood before being perfused with isolation solution containing collagenase type 2 ($0.9mg.ml^{-1}$, Worthington) and protease type XIV ($0.09mg.ml^{-1}$, Sigma) for 10 mins. The heart was removed and cut into pieces. Cells were dispersed by trituration before being filtered through a 250µM nylon mesh. The remaining tissue was incubated in the enzyme solution for a further 15 mins at 37°C prior to trituration and filtering. Collected cells were stored at room temperature in isolation solution containing 1mM Ca^{2+} until required.

A.1.6 Single Cell Calcium Trainsient Protocol

To measure the drug effect on calcium transients, Krebs solutions containing the following reagents were prepared and perfused over the cells: Solvent 1 (Krebs solution), Solvent 2 (Isoprenaline, 5nM), Solvent 3 (S1P, 25nM), and Solvent 4 (ISO 5nM + S1P 25nM). All protocols involved 5 minutes of buffer perfusion at first, followed by perfusion of other solvents. All recordings were made after 5 minutes of perfusion.

A.1.6.1 Effects of Isoprenaline on Calcium Transient

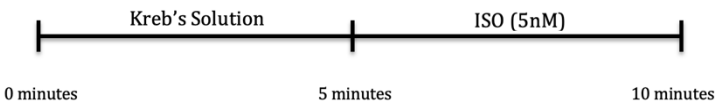

A.1.6.2 Prophylactic effect of JB79 on ISO-induced Calcium Transient

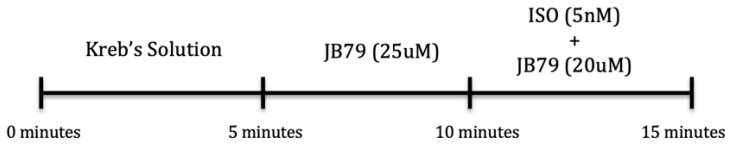

A.1.6.3 Therapeutic effect of JB79 on ISO-induced Calcium Transient

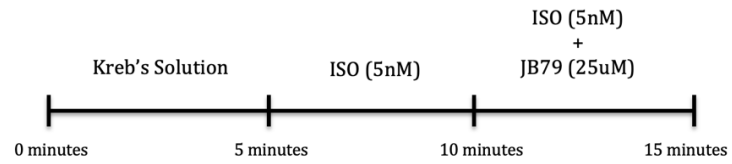

A.1.7 Loading of cells with Fluo-4 AM and Internal Perfusion

Prepared isolated cardiac myocytes in Krebs-Henseleit solution were treated with 5uM of Fluo-4AM and incubated at 32°C for 15 minutes (Appendix A). After having absorbed the calcium fluorescence dye, cells were transferred to a Perspex 30 x 15 x 5 mm chamber on the stage of a Leica (model no. DMIRM) microscope, 40x magnification. The glass cover slips were first treated with poly-DL-alanine to increase the spontaneous attachment of the myocytes. After 5 minutes of settling the cell to the bottom plate, the cells were superfused with Krebs solution at the rate of 1.8 to 3 ml/min. The medium was preheated to maintain the cells at body temperature, 37.5 °C. The cells were stimulated at 1.5 x threshold, with a pulse width of 100ms. The cells were recorded from underneath the chamber, and part of the fluorescent light (wavelength 490nm) was diverted to a Watec (model no. WAT902B) video camera sided-mounted on the microscope. The image of the cell was projected on a 9 in high-grade monitor (SANYO, model no. VM6612P) and the calcium transients were measured using the software Axon pCLMAP™ 10.

A.1.8 Transverse Aortic Constriction (TAC)

All mice operated were male between the ages of 8-10 weeks. Mice were anaesthetised by a mixture of ketamine hydrochloride (FORD Dodge Animal Health Ltd, 50 mg/kg) and xylazine (Bayer Healthcare, 10 mg/kg), administered through intra-peritoneal (i.p.) injection. Hair was subsequently removed from the operating site and sterilised prior to endotracheal intubation with a catheter, which was subsequently connected to a rodent ventilator (Harvard Apparatus). The chest cavity was exposed through a small incision and a constriction was created on the transverse aorta using a 7-0 prolene suture (Ethicon Inc) ligated against a 27-gauge needle, which the latter was subsequently removed to generate a stenosis. Following surgery mice were i.p. injected with analgesia, buprenorphine (Alstoe Animal Health Care Ltd, 10 mg/kg). The chest was closed by suturing both the muscle and skin layer using 6-0 prolene suture (Ethicon Inc). Control groups, known as sham groups, were subjected to exact same procedures but without a ligation on the transverse aorta. For the drug treatment, JB79 (5mg/kg or 10mg/kg) were given intraperitoneally for two weeks, once a day.

A.1.9 Ex vivo ECG and MAP recordings

Animals were killed by cervical dislocation and the heart was quickly removed, cannulated and perfused via a Langendorff system. The heart was perfused with Krebs–Ringer solution with a constant flow rate of 4 ml min−1 at 37°C to allow good circulation of the coronary artery system. After cannulation of the aorta, a metal clip was used to clamp the aorta to the cannula. The excess tissues and lungs were removed, and a thread was used to tie the aorta just below the clip to maintain constant pressure to the heart. To obtain stabilized and reliable recordings, the heart was left on the Langendorff system for 15 min to allow it to reach a steady state before recording started. The two ECG electrodes were placed opposite each other on the left atrium and ventricle apex; the MAP electrode was placed on the right atrium. ECG and MAP recordings were performed simultaneously. The positions of the electrodes were optimized to be consistent between different hearts. Noise was minimized by grounding the devices and set-ups to the earth. The ECG and MAP recordings were made by LabChart 5 software (ADInstruments, Oxford, UK). The onset of the QT interval was taken to correspond either to the Q wave deflection or, if this was absent, the base of the R wave. The end of the QT interval was taken as the time point after the T wave peak when the first derivative of the voltage trace (dV/dt) became zero. When undershoots were present, the end of the QT interval was estimated from the minimum value of the undershoot. The QT interval was also corrected for heart rate (HR) using the following formula: $QTc = QT/(RR/100)^{1/2}$, where QTc is the corrected QT interval and RR is the R–R interval (Wang et al., 2017; Mitchell et al. 1998).

A.1.10 Programmed electrical stimulation

A pair of bipolar pacing electrodes (custom-made) were placed on the atrial septum and the PES, controlled by Spike2 software (Cambridge Electronic Design, Cambridge, UK) was applied. Propensity to atrial arrhythmias in Langendorff-perfused hearts was assessed by PES. Pacing trains of eight stimuli (S1) delivered at a basic cycle length of 100 ms were followed by a single premature extra stimulus (S2) introduced at S1–S2 intervals progressively shortened with successive stimulus cycles repeated until arrhythmia was induced or the atrial refractory period was reached. A burst-pacing protocol applied atrial pacing in trains of 20 S1 stimuli at progressively shorter intervals from an initial cycle length of 100 ms until an arrhythmia was induced or a cycle length of 30 ms was reached. Arrhythmia was defined as three or more consecutive premature atrial waveforms.

Tachycardia showing regular waveforms was defined as atrial tachycardia (AT), whereas irregular fibrillating waveforms were considered to represent atrial fibrillation (AF) (Wang et al., 2017)

A.1.11 Spheroids invasion in 3D collagen matrix

Multicellular tumor spheroids were generated by using the hanging-drop method In brief, HOP92 and MDA-MB-231 cancer cells were detached with EDTA (1mM) and trypsin (0.025%, Invitrogen), re-suspended in medium supplemented with methylcellulose (20%; Sigma-Aldrich) and Matrigel (1%) (BD Biosciences, Growth factor reduced), and incubated as droplets (25 µl) containing 1000 cells for 48 h to ensure multicellular aggregation. HOP92 and MDA-MB-231 spheroids were washed with medium and mixed with a solution of rat tail collagen (SERVA Electrophoresis) (2.0 mg/ml), which was pipetted as a drop-matrix, polymerized at 37°C, and replaced with medium with or without JB79. Spheroids were examined for invasive features 15 hours after seeding in 3-dimensional collagen matrix.

A.1.12 Boyden chamber Invasion Assays

HOP92 and MBA-MB-231 cells (1×10^5) were cultured with or without JB79 in the upper wells (in triplicate) of Transwell Matrigel Boyden chambers (BD Biosciences) and allowed to invade and migrate toward 10% FBS in the bottom wells. After 6 and 15 hours of incubation, invading cells were stained with 0.1% crystal violet, imaged, and counted manually using Adobe Photoshop software.

A.1.13 Wound Healing scratch assay

For scratch assays, HOP92 and MDA-MB-231 cells were cultured to confluence, scratched with a pipette tip and treated with or without JB79. Wound healing was monitored after 24 hours. The scratches were analyzed by ImageJ at the beginning (time=0 hour) and 24 hours after for areas with migrated cells and normalized to the original open area according to: normalized area = (area at 0 h−area at 24 h)/area at 0 h × 100.ound healing assay.

A.1.14 Resazurin Proliferation Assay

HOP92 and MDA-MB-231 cells (in triplicate) were seeded in opaque-walled 96-well plate containing a final volume of 100µl per well with or without JB79 (drug was changing every second day). After 6 days, 200 µl Resasurin solution was added into cells and incubated for 2 hours at 37°C. Fluorescence was recorded using a 560nm excitation/590nm emission filter set presented as relative resazurin fluorescence.

A.1.15 Immunocytochemistry of NRCMs

NRCMs were plated onto laminin coated coverslips at a concentration of 0.4 x 106 cells per well and treatment was applied accordingly. Medium was removed and cells washed three times in ice cold PBS. Cells were fixed in 4% w/v PFA for 30 minutes at 4oC, and subsequently washed in PBS for 5 minutes, twice. Permeabilization was achieved through incubation in 0.1% v/v triton X-100 for 10 minutes prior to blocking in 0.5% w/v bovine serum albumin (BSA, Sigma Aldrich; 0.5 g of BSA in 100 ml of PBS) for an hour at RT. Primary antibody (diluted accordingly in 0.5% w/v BSA) was added to each coverslip and incubated overnight at 4oC. Coverslips were washed in PBS for 5 minutes, 3 times, prior to addition of the appropriate secondary antibody (diluted accordingly in 0.5% w/v BSA) and incubated for an hour at RT. Coverslips were washed twice in PBS for 5 minutes, and subsequently subjected to 4' 6-diamidino-2-phenylindole dihydrochloride (DAPI, Life Technologies; diluted at 1:1000 in 0.5% w/v BSA) for 5 minutes. The coverslips were further washed in PBS for 5 minutes, twice, prior to application of fluorescent images were viewed using an Olympus BX51 microscope.

A.1.16 Statistical Analysis

All figures are reproduced using Graph Pad Prism 8 Software. Data were expressed as means ± S.E.M of n experiments. *Student's t-tests* for unpaired data were used for statistical analysis; values of $p<0.05$ were considered significant.

.

Appendix 2: *In Silico* VLS Software

Program	Year Published	Organisation	Description	Webservice	License
DOCK	1988	University of California-San Francisco	Based on Geometric Matching Algorithm	No	Freeware for academic use
AutoDock	1990	The Scripps Research Institute	Automated docking of ligand to macromolecule by Lamarckian Genetic Algorithm and Empirical Free Energy Scoring Function	No	Freeware
SOFTDocking	1991	University of California, Berkeley	Matching of molecular surface cubes	No	Academic
DockVision	1992	DockVision	Based on Monte Carlo, genetic algorithm, and database screening docking algorithms	No	Commercial
ADAM	1994	IMMD Inc.	Prediction of stable binding mode of flexible ligand molecule to target macromolecule	No	Commercial
DIVALI	1995	University of California-San Francisco	Based on AMBER-type potential function and genetic algorithm	No	Freeware
GOLD	1995	Collaboration between the University of Sheffield, GlaxoSmithKline plc and CCDC	Genetic algorithm based, flexible ligand, partial flexibility for protein	No	Commercial
LIGIN	1996	Weizmann Institute of Science	Molecular docking using surface complementarity	No	Commercial
FTDOCK	1997	Biomolecular Modelling Laboratory	Based on Katchalski-Katzir algorithm. It discretises the two molecules onto orthogonal grids and performs a global scan of translational and rotational space	No	Freeware
ICM-Dock	1997	MolSoft	Docking program based on pseudo-Brownian sampling and local minimization	No	Commercial
QXP	1997	Novartis Pharmaceuticals Corporation	Monte Carlo perturbation with energy minimization in Cartesian space	No	Academic
SANDOCK	1998	University of Edinburgh	Guided matching algorithm	No	Academic
LPCCSU	1999	Weizmann Institute of Science	Based on a detailed analysis of interatomic contacts and interface complementarity	Available	Freeware
MCDOCK	1999	Georgetown University Medical Center	Based on a non-conventional Monte Carlo simulation technique	No	Academic
PRODOCK	1999	Cornell University	Based on Monte Carlo method plus energy minimization	No	Academic
DARWIN	2000	The Wistar Institute	Prediction of the interaction between a protein and another biological molecule by genetic algorithm	No	Freeware
EUDOC	2001	Mayo Clinic Cancer Center	Program for identification of drug interaction sites in macromolecules and drug leads from chemical databases	No	Academic
FlexX	2001	BioSolveIT	Incremental build based docking program	No	Commercial

PatchDock	2002	Tel Aviv University	The algorithm carries out rigid docking, with surface variability/flexibility implicitly addressed through liberal intermolecular penetration	Available	Freeware
FDS	2003	University of Southampton	Flexible ligand and receptor docking with a continuum solvent model and soft-core energy function	No	Academic
FRED	2003	OpenEye Scientific	Systematic, exhaustive, nonstochastic examination of all possible poses within the protein active site combined with scoring Function	No	Free for academic use
HADDOCK	2003	Centre Bijvoet Center for Biomolecular Research	Makes use of biochemical and/or biophysical interaction data such as chemical shift perturbation data resulting from NMR titration experiments, mutagenesis data or bioinformatic predictions. Developed for protein-protein docking, but can also be applied to protein-ligand docking.	Available	Freeware
LigandFit	2003	BioVia	CHARMm based docking program	No	Commercial
Surflex-Dock	2003	Tripos	Based on an idealized active site ligand (a protomol)	No	Commercial
GEMDOCK	2004	National Chiao Tung University	Generic Evolutionary Method for molecular docking	No	Freeware
Glide	2004	Schrödinger	Exhaustive search based docking program	No	Commercial
Score	2004	Alessandro Pedretti & Giulio Vistoli	The Score service allows to calculate some different docking scores of ligand-receptor complex	Available	Freeware
Docking Study with HyperChem	2006	Motonori Tsuji	Biomacromolecule- and ligand-flexible docking using combination between the predicted structure-based pharmacophores and ligand-based pharmacophores	No	Commercial
eHiTS	2006	SymBioSys Inc	Exhausted search algorithm	No	Commercial
MolDock	2006	Molegro ApS	Based on a new heuristic search algorithm that combines differential evolution with a cavity prediction algorithm	No	Academic
PSI-DOCK	2006	Peking University	Pose-Sensitive Inclined (PSI)-DOCK	No	Academic
EADock	2007	Swiss Institute of Bioinformatics	Based on evolutionary algorithms	Available	Freeware
FLIPDock	2007	Scripps Research Institute	Genetic algorithm based docking program using FlexTree data structures to represent a protein-ligand complex	No	Free for academic use
MEDock	2007	SIGMBI	Maximum-Entropy based Docking web server is aimed at providing an efficient utility for prediction of ligand binding site	Available	Freeware
ParDOCK	2007	Indian Institute of Technology	All-atom energy based Monte Carlo, rigid protein ligand docking	Available	Freeware
PSO@AUTO DOCK	2007	University of Leipzig	Particle Swarm Optimization (PSO) algorithms varCPSO and varCPSO-ls are suited for rapid docking of highly flexible ligands	No	Academic
SODOCK	2007	Feng Chia University (Taiwan)	Swarm optimization for highly flexible protein-ligand docking	No	Academic
Lead finder	2008	MolTech	Program for molecular docking, virtual screening and quantitative evaluation of ligand binding and biological activity	No	Commercial
Molecular Operating Environment (MOE)	2008	Chemical Computing Group	Docking application within MOE; choice of placement methods (including alpha sphere methods) and scoring functions (including London dG)	No	Commercial

MS-DOCK	2008	INSERM	Multi-stage docking/scoring protocol	No	Academic
PLATINUM	2008	Moscow Institute of Physics and Technology (State University)	Analysis and visualization of hydrophobic/hydrophilic properties of biomolecules supplied as 3D-structures	Available	Freeware
Q-Dock	2008	Georgia Institute of Technology	Low-resolution flexible ligand docking with pocket-specific threading restraints	No	Freeware
Blaster	2009	University of California San Francisco	Combines ZINC databases with DOCK to find ligand for target protein	Available	Freeware
DockingServer	2009	Virtua Drug Ltd	Integrates a number of computational chemistry software	Available	Commercial
AutoDock Vina	2010	The Scripps Research Institute	New generation of AutoDock	No	Open source
Fitted	2010	Molecular Forecaster Inc.	Docking program with flexibility, covalent, metalloenzyme, displaceable water considerations	Available	Free for academic use
FlexPepDock	2010	The Hebrew University	Modeling of peptide-protein complexes, implemented within the Rosetta framework	Available	Freeware
1-Click Docking	2011	Mcule	Docking predicts the binding orientation and affinity of a ligand to a target	Available	Basic free version
AADS	2011	Indian Institute of Technology	Automated active site detection, docking, and scoring(AADS) protocol for proteins with known structures based on Monte Carlo Method	Available	Free to use Webservice
BetaDock	2011	Hanyang University	Based on Voroni Diagram	No	Freeware
iScreen	2011	China Medical University	Based on a cloud-computing system for TCM intelligent screening system	Available	Freeware
LigDockCSA	2011	Seoul National University	Protein-ligand docking using conformational space annealing	No	Academic
PythDock	2011	Hanyang University	Heuristic docking program that uses Python programming language with a simple scoring function and a population based search engine	No	Academic
SwissDock	2011	Swiss Institute of Bioinformatics	Webservice to predict interaction between a protein and a small molecule ligand	Available	Free webservice for academic use
VoteDock	2011	University of Warsaw	Consensus docking method for prediction of protein-ligand interactions	No	Academic
BSP-SLIM	2012	University of Michigan	A new method for ligand-protein blind docking using low-resolution protein structures	Available	Freeware
GPCRautomodel	2012	INRA	Automates the homology modeling of mammalian olfactory receptors (ORs) based on the six three-dimensional (3D) structures of G protein-coupled receptors (GPCRs) available so far and performs the docking of odorants on these models	Available	Free for academic use
idTarget	2012	National Taiwan University	Predicts possible binding targets of a small chemical molecule via a divide-and-conquer docking approach	Available	Freeware
rDock	2013	University of York/ Open source project	HTVS of small molecules against proteins and nucleic acids	No	Open source
DOLINA	2014	University of Basel	Pharmacophore-based aligment, local combinatorial induced-fit	No	Academic
FlexAID	2015	University of Sherbrooke	Target side-chain flexibility and soft scoring function, based on surface complementarity	No	Open source
MOLS 2.0	2016	University of Madras	Rigid protein-small-molecule docking,Flexible protein-peptide docking	No	Open Source

Appendix 3: JB Compounds

JB01

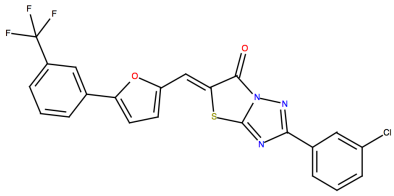

JB02

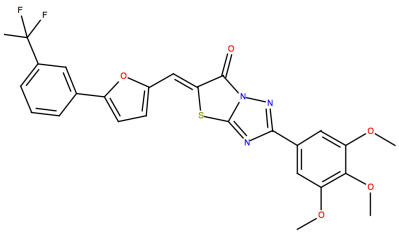

JB03

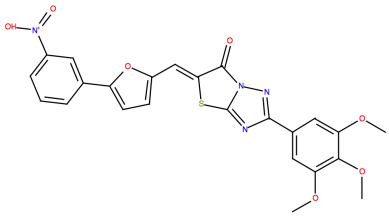

JB04

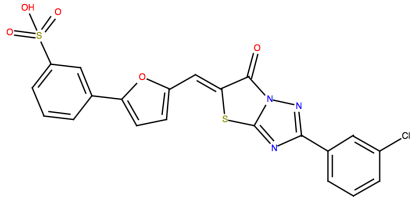

JB05

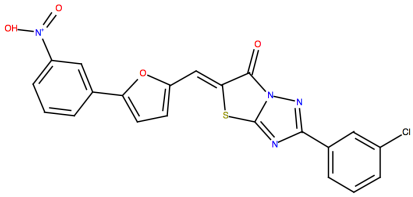

JB06

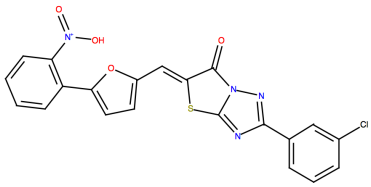

JB07

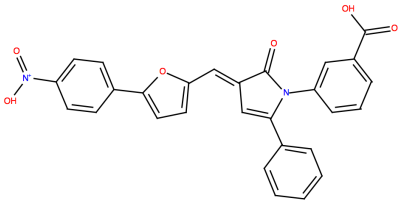

JB08

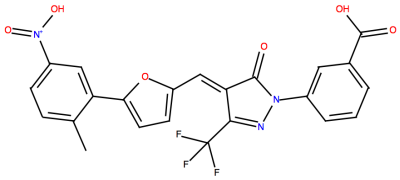

JB09

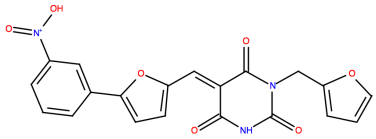

JB10

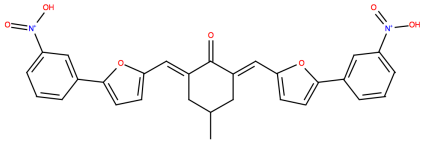

JB11

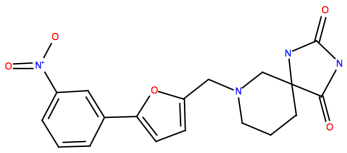

JB12

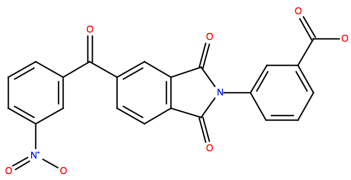

JB13

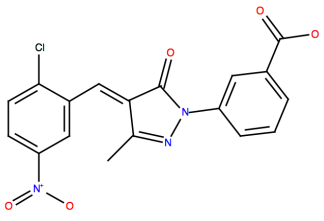

JB14

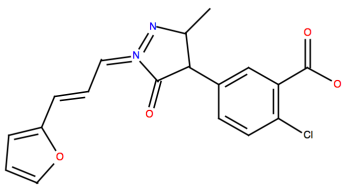

JB15

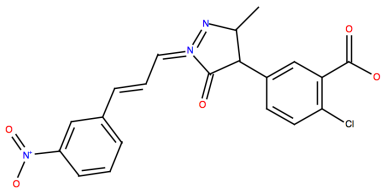

JB16

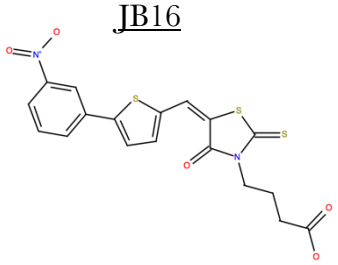

JB17

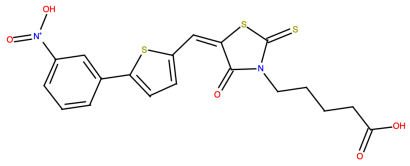

JB18

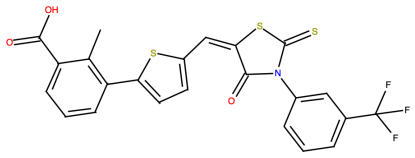

JB19

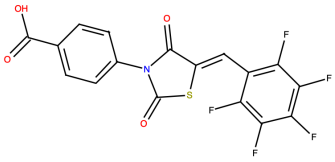

JB20

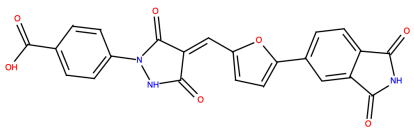

JB21

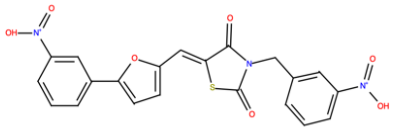

JB22

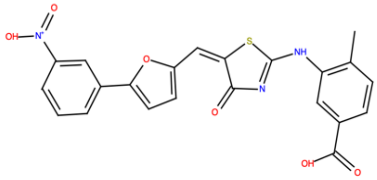

JB23

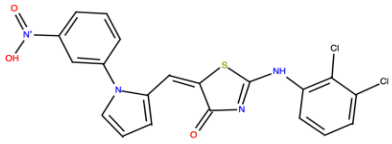

JB24

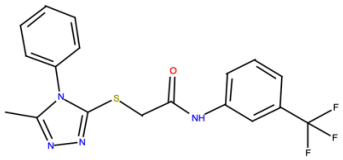

JB25

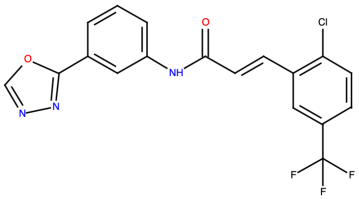

JB26

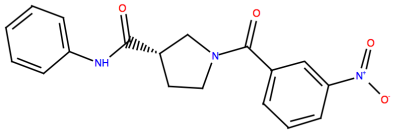

JB27

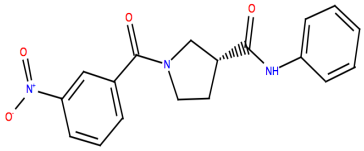

JB28

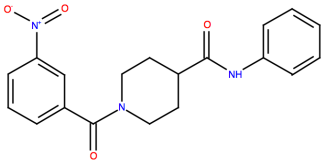

JB29

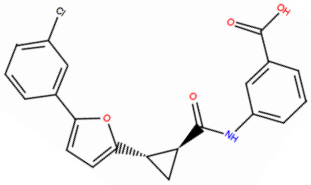

JB30

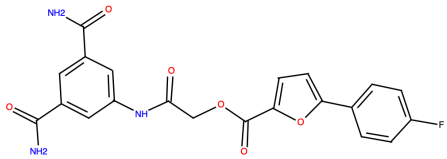

JB31

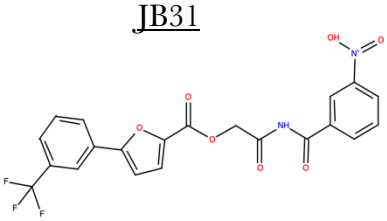

JB32

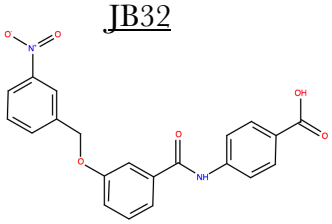

JB33

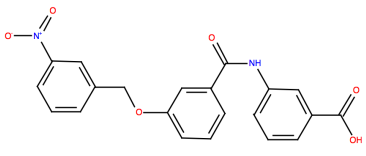

JB34

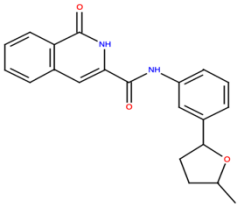

JB35

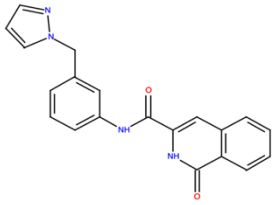

JB36

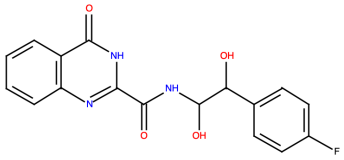

JB37

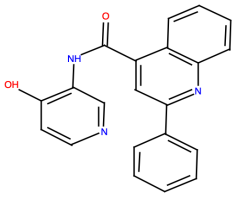

JB38

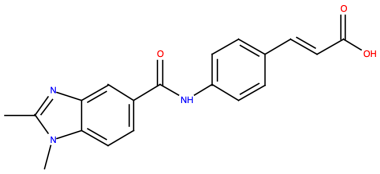

JB39

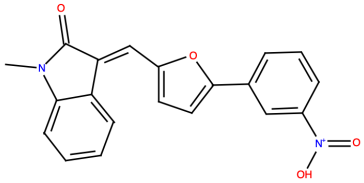

JB40

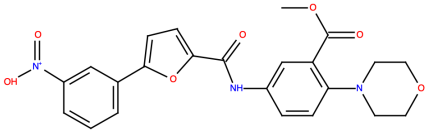

JB41

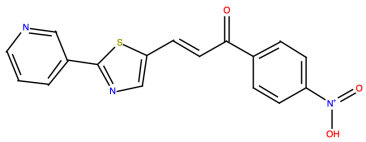

JB42

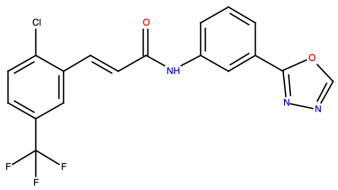

JB43

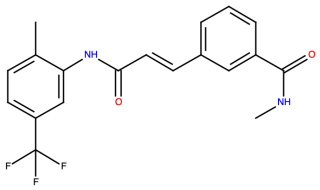

JB44

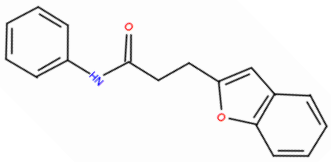

JB45

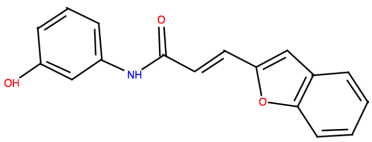

JB46

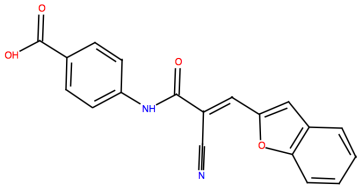

JB47

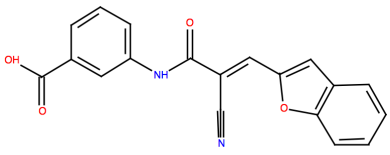

JB48

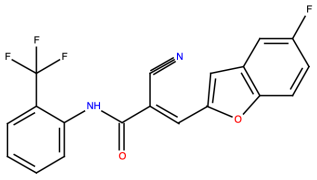

JB49

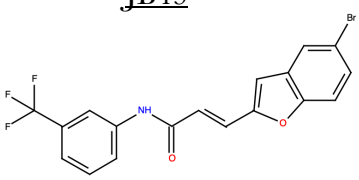

JB50

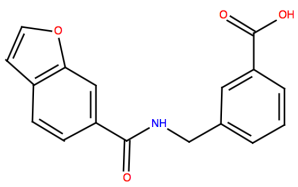

JB51

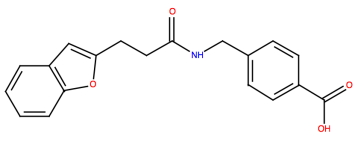

JB52

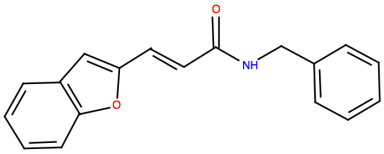

JB53

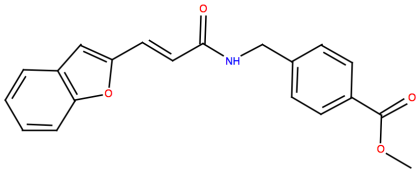

JB54

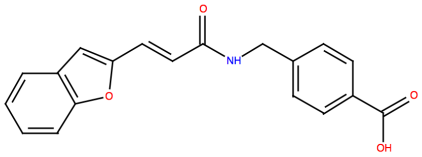

JB55

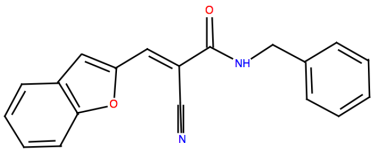

JB56

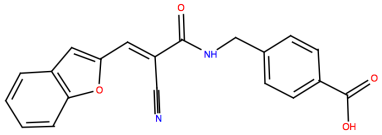

JB57

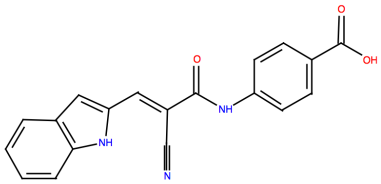

JB58

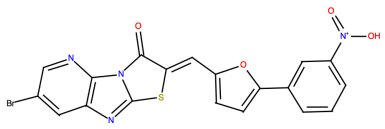

JB59

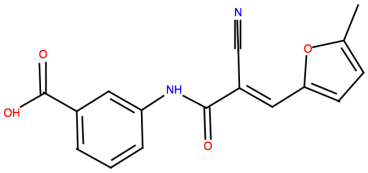

JB60

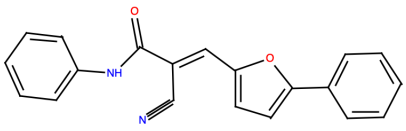

JB61

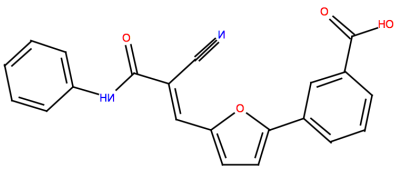

JB62

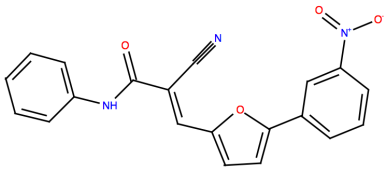

JB63

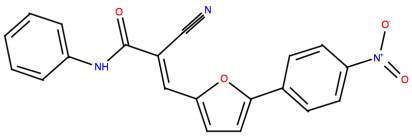

JB64

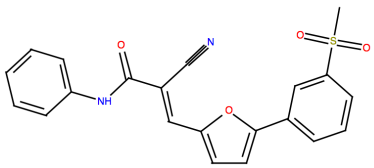

JB65

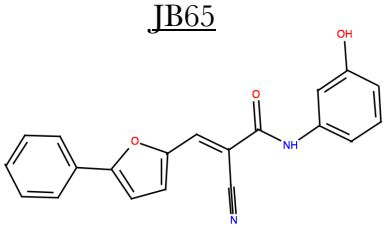

JB66

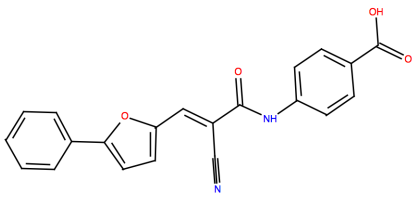

JB67

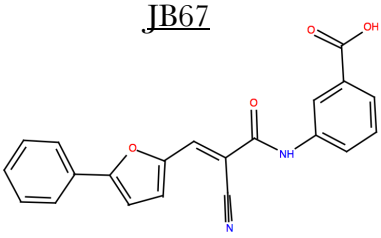

JB68

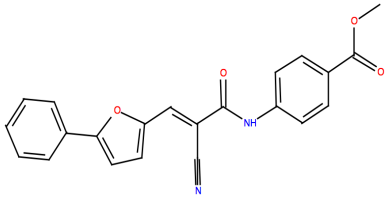

JB69

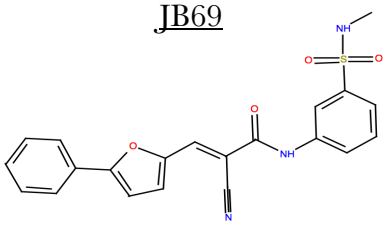

JB70

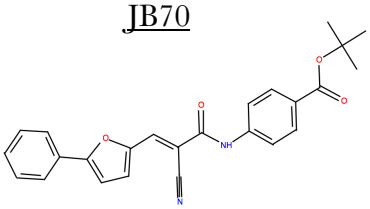

JB71

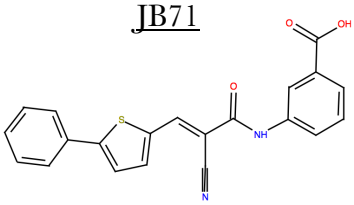

JB72

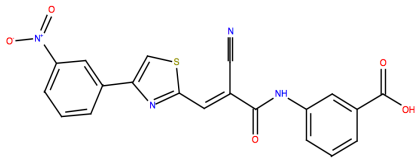

JB73

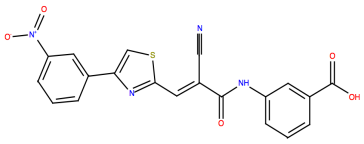

JB74

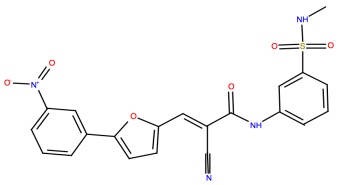

JB75

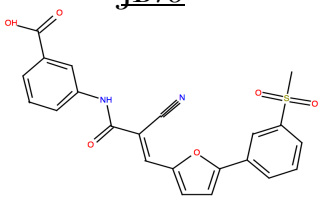

JB76

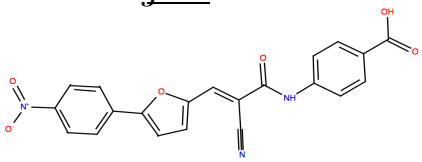

JB77

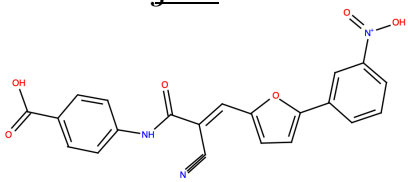

JB78

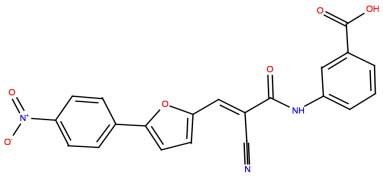

JB79

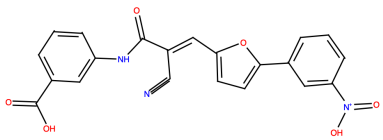

JB80

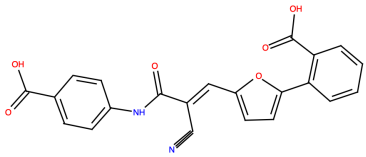

JB81

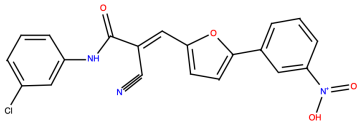

JB82

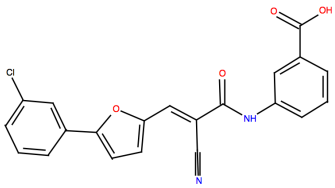

JB83

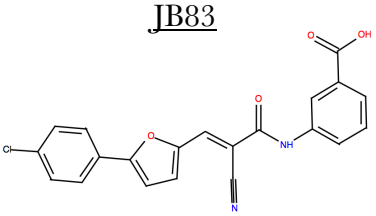

JB84

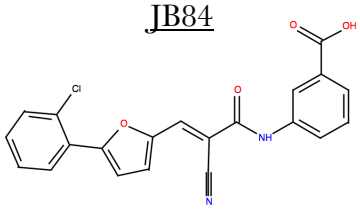

JB85

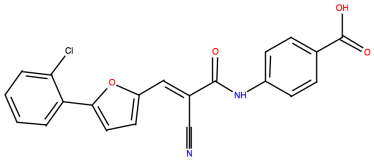

JB86

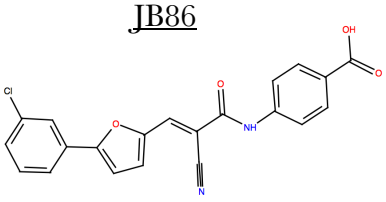

JB87

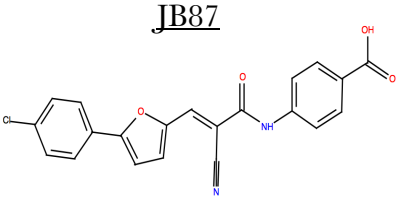

JB88

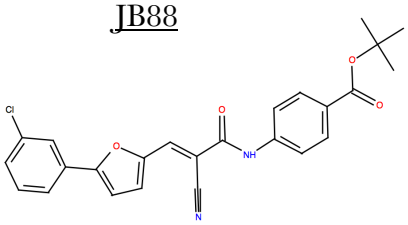

JB89

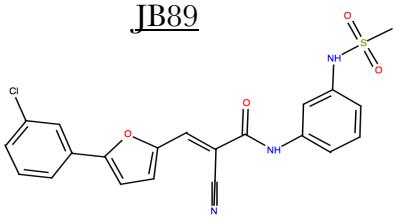

JB90

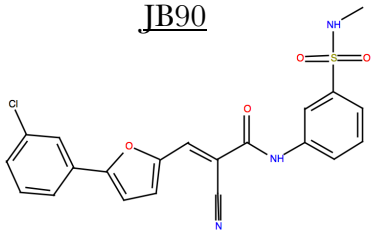

JB91

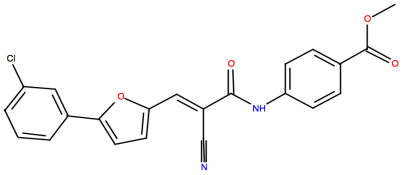

JB92

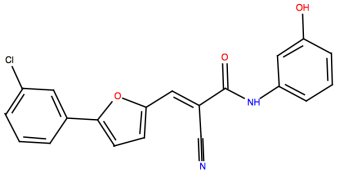

JB93

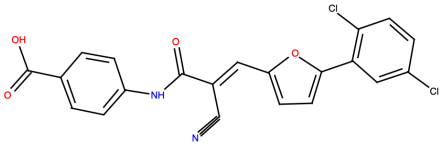

JB94

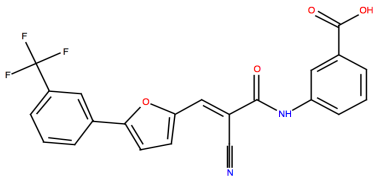

JB95

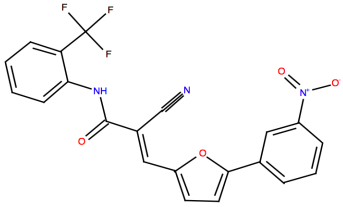

JB96

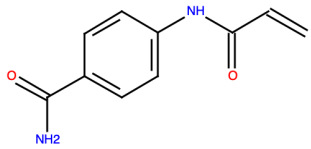

JB97

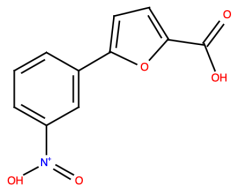

JB98

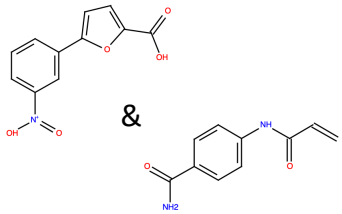

JB99

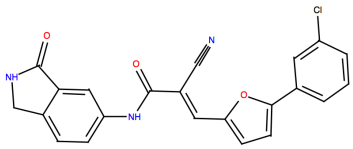

JB100

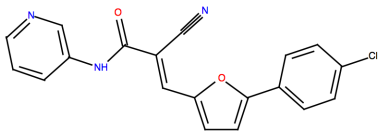

JB101

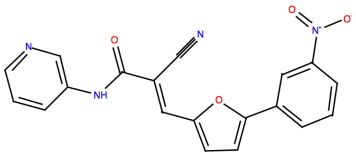

JB102

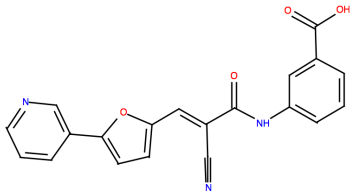

JB103

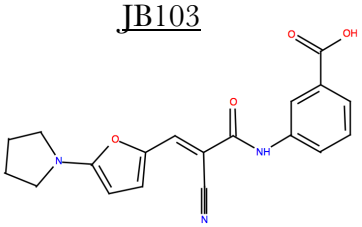

JB104

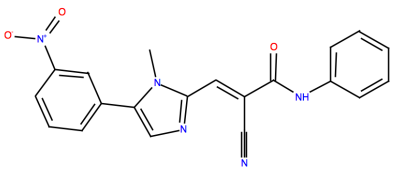

JB105

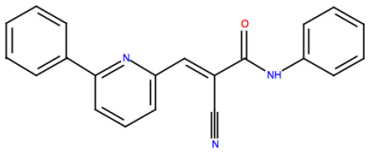

JB106

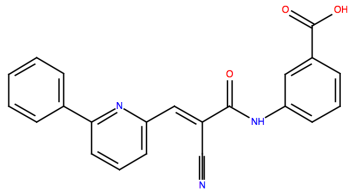

JB107

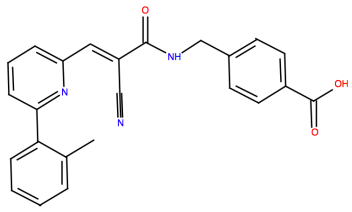

JB108

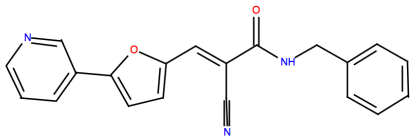

JB109

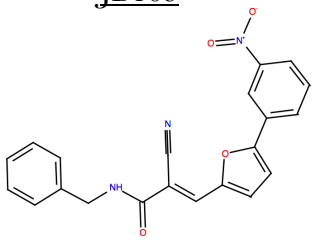

JB110

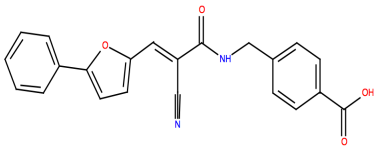

JB111

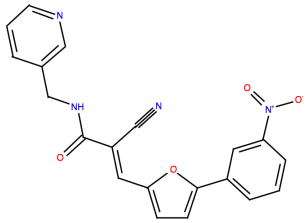

JB112

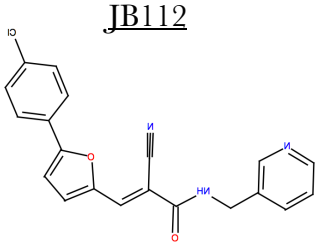

JB113

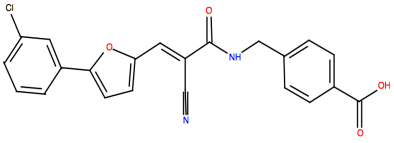

JB114

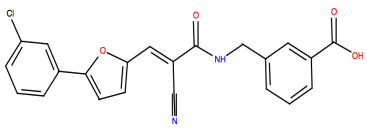

JB115

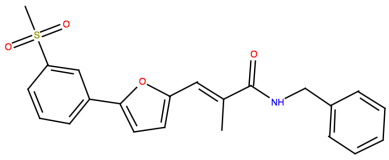

JB116

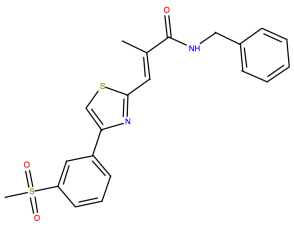

JB117

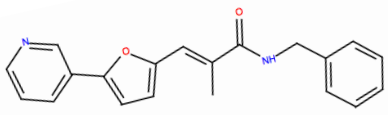

JB118

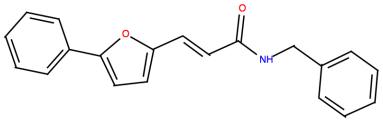

JB119

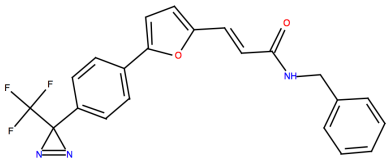

JB120

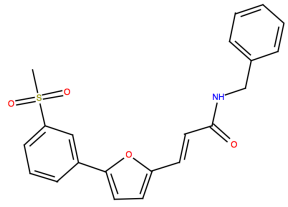

JB121

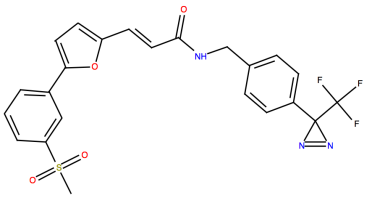

JB122

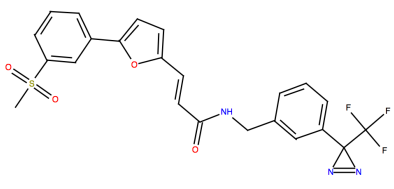

JB123

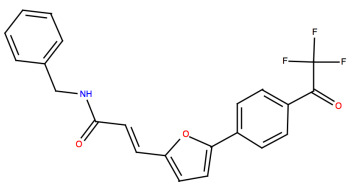

JB124

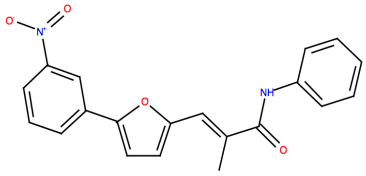

JB125

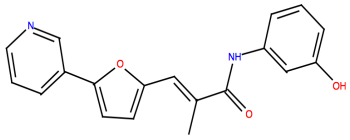

JB126

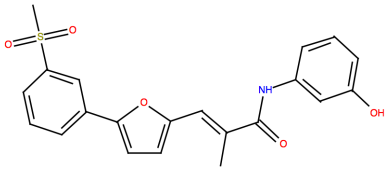

JB127

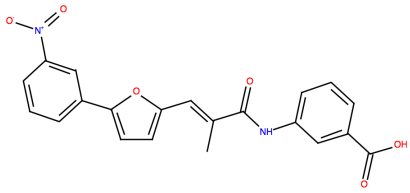

JB128

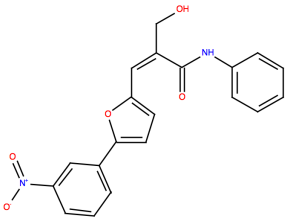

JB129

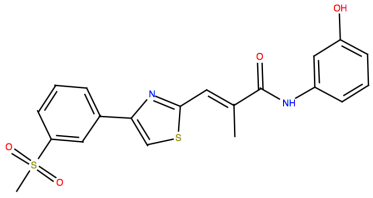

JB130

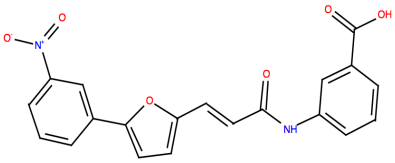

JB131

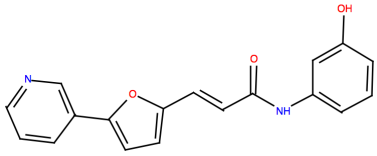

JB132

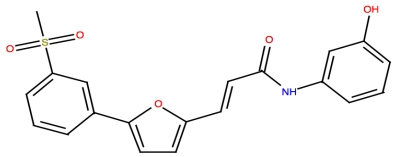

JB133

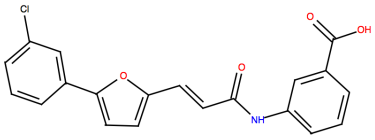

JB134

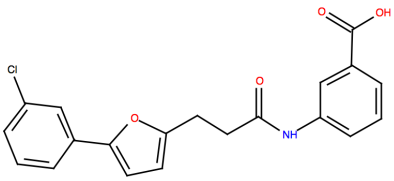

JB135

